

University of Warwick institutional repository: <http://go.warwick.ac.uk/wrap>

A Thesis Submitted for the Degree of PhD at the University of Warwick

<http://go.warwick.ac.uk/wrap/2342>

This thesis is made available online and is protected by original copyright.

Please scroll down to view the document itself.

Please refer to the repository record for this item for information to help you to cite it. Our policy information is available from the repository home page.

Methods for Reducing the
Cost of Cementitious
Building Components in
Developing Countries, with
Particular Reference to
Rainwater Harvesting

Gwilym T. Still



*This report is submitted as partial fulfilment
of the requirements for the PhD Programme of the
School of Engineering
The University of Warwick*

2007

© Copyright 2007

by

Gwilym T. Still

School of Engineering

The University of Warwick

Abstract

Cementitious¹ building components, although widely used in low-income countries, are too expensive for many applications related to low-income housing. This thesis explores three options for reducing component cost:

1. Use of local fine aggregates, often with clay contamination, instead of low-fines sands transported from a distance.
2. Improved designs, to achieve better material economy.
3. Change of production environment, from on-site to component prefabrication followed by transport to site.

Water storage tanks for rainwater harvesting were used as the example for component design, and as a case-study for considering the effect of changing the production environment. The work showed that:

- In some cases, use of local aggregates will give a cost saving of around 10%.
- Improved design can give significant reduction in materials usage, of up to 40%.
- Off-site prefabrication of components, followed by on-site assembly to produce the desired product, does not seem preferable to the prevalent practice of entirely on-site production from raw materials. However, factory-based manufacture of complete products, followed by transport to site, has a number of attractions over entirely on-site production.

Out of the three options examined, improved component design offers the greatest benefits for the case study considered.

Keywords: Rainwater harvesting, cement, tank, clay-contamination, developing countries.

¹Cementitious: Material containing cement as the primary strength-providing component

Acknowledgements

I would like to thank: Terry Thomas, Mim, Mum, Dad, Huw, Alyn, Colin Banks, and the workshop technicians, Vicky Fernandes, Mark Evernden, Brett Martinson, Phil Purnell, Colin Oram, Novak Elliot, Martin Judge, Joe Peel, Neil Evans, Liz Aldridge, Louise Ruthven, Paul Dunkley, Phil Banfill, John Hattersley, and Gordon Rennie.

Contents

Abstract	iii
Acknowledgements	iv
Contents	xii
Tables	xiv
Figures	xix
Nomenclature and Terms	8
 I Problem Definition and Background	 9
1 Introduction	10
1.1 Global housing demand	10
1.2 Overview: production of goods in Developing Countries	10
1.2.1 Production technologies	11
1.2.2 Research and Development	12
1.2.3 Capital-labour cost ratio	12
1.2.4 Cementitious building components	12
1.2.5 Infrastructure and transport	13
1.3 Strategies for reducing component cost	14
1.4 Scope of this thesis	14
 II Materials choice and proportioning	 17
Cementitious Building Materials: Experimental Work and Publications	18
Cementitious Building Materials: Overview	19

2	Cementitious Building Materials: Introduction and Literature Review	21
2.1	Introduction	21
2.1.1	Failure scenarios	23
2.1.2	Aggregate choice	23
2.1.3	Properties of interest	24
2.1.4	Materials	24
2.1.5	Mix composition	25
2.2	Tensile and compressive strength relationship	25
2.3	Abrams' Law	27
2.4	Clay structure and effect of clay contamination	30
2.5	Workability, rheology and vibration compaction	32
2.5.1	Rheology and workability	32
2.5.2	Compaction	34
2.6	Calculating water demand	35
2.7	Sand-cement ratio and strength	39
2.8	Curing conditions	40
2.9	Workability aids	41
2.10	Further research required	42
	Tensile-compressive strength relationship	43
	Abrams' law	43
	Sand-cement ratio and optimum strength	43
	Young's modulus	44
	Effect of sand quality	44
3	Cementitious Building Materials: Experimental Work	45
3.1	Experimental methodology: mortars in tension	45
3.1.1	Choice of materials	46
3.1.2	Experimental method: casting and curing of mortar	48
3.1.3	Experimental method: testing of mortar	49
	Tests on mortar components	49
	Tests on fresh mortar	49
	Tests on hardened, cured samples	50
3.2	Mortar and materials: results and analysis	51
3.2.1	Strength relationships	52
	Splitting tensile and flexural tensile strength	52
	Compressive and splitting tensile strength	52
3.2.2	Strength and water-cement ratio	55
3.2.3	Effect of sand type	55
	Abrams' law	55
	Effect on workability	58
	Effect on peak strength developed	60
3.2.4	Curing Conditions	61

3.2.5	Young's Modulus	62
3.2.6	Optimising water-cement ratio	64
	Reduction in strength arising from selecting non-optimum water-cement ratio	64
	Methods for obtaining optimum water-cement ratio	66
	Water-cement ratio optimisation strategy 2: constant moisture content	66
	Water-cement ratio optimisation strategy 3: maximum density	70
	Water-cement ratio optimisation strategy 4: constant workability measure	74
	Summary of strategies	74
3.2.7	Cement	74
	Particle size distribution	75
	Strength developed	76
3.2.8	Sieve analysis of some building sands from LEDCs	76
3.2.9	Admixtures to enhance workability	76
3.2.10	Economic Optima: Sand-cement ratio selection	79
3.2.11	Selection of most economical sand type	84
	Cementitious Building Materials: Summary of Findings	89
	III Component Design	92
	Component Design: Overview	93
4	Component Design: Tank Classification and Theory	95
4.1	Production and design of cementitious components in LEDCs . . .	95
4.2	Rainwater harvesting	96
4.3	Current designs classified by location and by geometric complexity	97
4.3.1	0-dimensional curvature: prismatic cisterns built with flat panels	97
4.3.2	1-dimensional curvature: cylindrical structures	98
4.3.3	2-dimensional curvature	99
4.4	Materials usage of current designs	99
4.5	Specification for DRWH cisterns	101
4.6	Theory and Numerical Tools	103
4.6.1	Plate theory	103
4.6.2	Shell theory	104
4.6.3	Finite Element Analysis	104

5	Component Design: Datum Tank Design and Performance Measure	106
5.1	Performance measure	106
5.2	Datum Tank Design	107
5.3	Analysis of datum design: Cylindrical tanks with constant wall thickness	107
5.3.1	Shell theory: Cylinders of constant wall thickness, no lid .	111
5.3.2	Shell theory: Cylinders of constant wall thickness, encastered lid	113
5.3.3	Location of peak stress	114
5.3.4	Implications and possible generalisations from analysis of cylindrical tanks	115
	Effect of lid on peak stress	115
	Variation in peak stress with wall thickness	115
	Choice of sand type for datum configuration	117
	Location of wall-base joint	118
5.3.5	Optimisation of uniform thickness cylindrical tanks	118
	Generating the datum design	120
5.4	Modifications to improve the Relative Cement Index of cylindrical tanks	120
5.4.1	FEA modelling of cylindrical tanks	122
	Model generation	122
	Mesh generation	124
	Convergence criteria	125
	Validation	126
5.4.2	Radial fillet at joint between tank wall and base	128
	Approach: thickness to satisfy membrane constraint	129
5.4.3	Linear wall thickness variation with height	131
5.4.4	Fillet at base and linearly varying wall thickness with height	132
5.5	Summary	133
5.5.1	Relative Cement Indices for cylindrical tanks	133
5.5.2	General implications for tank designs	133
6	Component Design: Optimising Tank Designs	135
6.1	0D curvature: flat plates	135
6.2	2D Curvature	139
6.2.1	Variation of peak stress with wall thickness	140
6.2.2	Analysis of existing designs	142
	Thai jar	142
	Sri Lankan pumpkin tank	143
	Summary of existing designs with 2D curvature	144
6.2.3	Profile selection: constant wall thickness	145

6.2.4	Optimisation of membrane action tanks	149
6.3	Summary	150
7	Component Design: Tank Prototype Design, Manufacture and Testing	151
7.1	Design	152
7.1.1	Geometry	152
7.1.2	Materials and mix	152
7.2	Method: Tank production	152
7.2.1	Wooden mould construction	154
7.2.2	Mould preparation: mud coating	154
7.2.3	Application of mortar	156
7.2.4	Joining tank lid and base	156
7.2.5	Curing	157
7.3	Method: Tank strain and strength testing	157
7.3.1	Instrumentation	157
	Video recording	157
	Strain measurements	158
7.3.2	Loading process	159
7.4	Results and Analysis	162
7.4.1	FEA results	162
7.4.2	Visual observations	165
7.4.3	Video recording	165
7.4.4	Post-failure material samples	171
	Joint between lid and base	171
	Variable wall thickness	171
	Poor bonding	172
	Summary of post-failure samples	172
7.4.5	Demec readings	174
7.4.6	Strain gauge readings	174
	Variation between meridians	176
	Strain at failure	176
7.4.7	Discrepancies between instrumentation and modelling . . .	176
7.5	Conclusions	178
	Component Design: Summary	179
IV	Production Environment	181
	Production Environment: Overview	182

8	Production Environment: Prefabrication Concepts and Scenarios	183
8.1	Introduction	183
8.2	Trends and current situation in housing	183
8.2.1	Industrialised Countries	184
8.2.2	Developing countries	184
8.3	Generic pros and cons for prefabrication	184
8.4	Production scenarios	187
8.5	Arguments specific to LEDCS	187
8.6	Summary	189
9	Production Environment: Production Process	190
9.1	On-site production of water tanks	190
9.2	“Knock-down” production	191
9.3	Factory-based production	192
9.3.1	Alternative production method: external moulds	194
	Choice of mould type	197
	Results from testing: Base joint	197
	Results from testing: demoulding	197
	Results from production: mud coating and surface finish	198
	Results from production: batch size	198
	Results from production: thickness control	199
	Results from production: pre-sale testing	200
9.3.2	Evaluation of factory-based production	200
	Production Environment: Summary	202
V	Conclusions and Further Work	203
10	Conclusions	204
10.1	Overview	204
10.2	Material selection	205
10.3	Component Design	206
10.4	Production environment	207
10.5	Summary	208
11	Further Work	210
11.1	Materials	210
11.1.1	Plasticisers	210
11.1.2	Sand analysis	210
11.1.3	Shrinkage and creep	211
11.1.4	Vibration compaction	211
11.1.5	Curing conditions and strength	211

11.1.6	Young's Modulus	211
11.2	Component Design	212
11.2.1	Prototype testing	212
11.2.2	Geometry optimisation using shell theory	212
11.2.3	Membrane action panel tanks	212
11.2.4	Effect of imperfections	213
11.2.5	Stepwise thickness changes	214
11.2.6	Automation of design optimisation	214
11.3	Production Environment and Process	215
11.3.1	Post-construction testing of materials	215
11.3.2	Improved methods of quality control	215
11.3.3	Batch size and production	215
11.3.4	Alternative methods for producing external moulds	215
VI	Bibliography, Appendices and Index	216
	Bibliography	217
A	Materials Choice and Proportioning	227
A.1	Publications arising from materials research ratio	227
A.2	Relationships between strength and sand-cement ratio	274
A.3	Curing and Strength	275
A.3.1	Data from Kim et al.	275
A.3.2	Data from Cebeci	277
A.4	Workability	278
A.5	Optimum moisture content	279
A.6	Workability Data from Aldridge	280
A.7	Optimal sand-cement ratios	282
A.7.1	Example calculations toward determining optimum sand-cement ratio	282
A.7.2	Example of optimum sand-cement ratio for membrane loading	285
B	Component Design	286
B.1	FEA software used	286
B.2	Analytical Solution: Effect of Roof	287
B.3	FEA Validation	288
B.4	Tank configurations for 2D tank optimisation	288
B.5	Wooden mould construction	291
B.6	Configuration of instrumentation for strain gauge testing	296

C Automating Component Design: Genetic Algorithm Optimisation of Tank Designs 297

C.1 Overview 297

C.2 Introduction 298

 C.2.1 Genetic Algorithms 298

 Basic principles 298

 C.2.2 Problem description and suitability of GAs 298

C.3 Implementation 299

 C.3.1 Interfacing with Finite Element Analysis program 299

 C.3.2 PySGA: Python Simple Genetic Algorithm 300

D Electronic Data 302

D.1 Material Selection: Mortar results 302

D.2 Material Selection: Sand-cement ratio and component thickness . 302

D.3 Component Design: Cylindrical tank optimisation 303

D.4 Component Design: Membrane tank optimisation 303

D.5 Component Design: Tank prototyping—FEA models 303

D.6 Component Design: Tank protoyping—Video recording 303

D.7 Component Design: Tank prototyping—Demec readings 303

D.8 Component Design: Tank prototyping—Strain gauge readings . . 303

D.9 Component Design: Automating Tank Optimisation—Genetic Algorithms and FEA 303

Index 304

List of Tables

2.1	Typical values of parameters in Abrams' law	27
2.2	Conditions required for concretes to be considered "comparable" .	29
2.3	Structure and property of clays	31
3.1	Abrams' constants for the three sand types, for compression and tension	56
3.2	Peak Strengths (MPa).	60
3.3	Effect of curing on compressive strength	61
3.4	Young's moduli of 3:1 and 10:1 mortar samples using sand S, at optimum water contents	62
3.5	Strength as percentage of peak when mix designed using constant optimum moisture content	69
3.6	Densities of mortar components	70
3.7	Strength as percentage of peak when mix designed to give peak density	72
3.8	Compressive strength of small cubes made with different cements	77
3.9	Assumptions for selection of most economic sand-cement ratio . .	81
4.1	Material usage of some representative tanks	101
5.1	Cylinder configurations used to test that peak stress in cylindrical tanks occurs at wall-base joint	115
5.2	Datum design configuration	122
5.3	Criteria and settings used for FEA models	126
5.4	Relative Cement Indices for cylindrical tanks of increasing thickness complexity	134

7.1 Filling process for tank testing 161

7.2 Relative Cement Indices of tank designs of increasing complexity . 179

8.1 Factors affecting the extent of off-site fabrication 185

8.2 Methods of production 188

8.3 Comparison of “on-site” and “knock-down” manufacture 188

9.1 Pros and cons of external moulds for rainwater tanks 195

A.1 Aggregate properties for mixes produced by
Kim, Han & Song (2002) 275

A.2 Proportions for mixes produced by Kim *et al.* (2002) 275

A.3 Compressive and tensile strengths of concretes cured at different
temperatures 276

A.4 Strength of mortars cured in lime-saturated water 277

B.1 Data obtained in validation of FEA software 288

B.2 Tank configurations for constant thickness shape optimisation . . 290

List of Figures

2.1	Relationship between compressive and flexural strength of mortars	26
2.2	Abrams' Law and the effect of poor compaction	28
2.3	"Building blocks" for clays: tetrahedral and octahedral sheets . .	30
2.4	Effect of changing mix conditions and components on Bingham constants	34
2.5	Vibro-profiling system	35
2.6	Relationship between water demand of sand to give constant workability, and apparent dry density	37
2.7	Cement-sand ratio and flexural strength	39
3.1	Grading of chosen sand for experimental work, and limits from British Standard 882	47
3.2	Method for conducting the slump test on fresh mortar	50
3.3	Method for conducting the Vebe test on fresh mortar	50
3.4	Brazilian test for tensile strength	51
3.5	Relationship between splitting tensile (cylinder) and flexural tensile (beam) strengths	53
3.6	Relation between compressive and splitting tensile strengths . . .	54
3.7	Compressive strength and water-cement ratios for all mixes using sand S	56
3.8	Fitted tensile Abrams' curves for the three sand types	57
3.9	Vebe time variation with moisture content	59
3.10	Measurement of Young's modulus, and effects of non-linearity . .	63

3.11	Variation in strength relative to peak strength with water-cement ratio around optimum water-cement ratio	65
3.12	Optimum water-cement ratio with sand-cement ratio	67
3.13	Moisture content at optimum strength	68
3.14	Density and strength variation with water-cement ratio for 5:1 sand series S	71
3.15	Comparison of w/c to give peak density, and that to give peak strength	73
3.16	Particle size distributions of cement samples	75
3.17	Sand gradings for building sands: Developing Country samples . .	78
3.18	Sand-cement optimisation process	80
3.19	Economic optimum sand-cement ratio for bending load (Note: shaded area indicates typical cost ratios in LEDCs; between 20 and 70)	82
3.20	Cost penalty with bending loading for constant sand-cement ratio	83
3.21	Cost comparison of optimal mix designs using sand S and K, for membrane loading	85
3.22	Cost comparison of optimal mix designs using sand S and K, for bending loading	86
3.23	Cost comparison of optimal mix designs using sand S and M, for membrane loading	87
3.24	Cost comparison of optimal mix designs using sand S and M, for bending loading	88
4.1	Example rainwater harvesting system	97
4.2	Example of a flat panel tank, taken from Paramasivam & Nathan (1984)	98
4.3	Example of a cylindrical tank, in use in Bangladesh	99
4.4	Thai Jar water tank	100
4.5	Sri Lankan pumpkin tank	100

5.1	Membrane deformation of cylindrical tank under hydrostatic loading	108
5.2	Wall deformation of uniform wall thickness cylindrical tank under hydrostatic loading	112
5.3	Peak stress with height for cylindrical tank	113
5.4	Bending moment with height for cylindrical tank with encastered lid	114
5.5	Peak stress with wall thickness for cylindrical tank	117
5.6	Cross-section of cylindrical tank to show proposed joint location .	119
5.7	Effect of changing lid and base thickness on optimum height of cylinders	121
5.8	FEA model of cylindrical tank in SolidWorks, showing loads and restraints	123
5.9	Mesh applied to FEA model of section of a cylindrical tank	124
5.10	Section of mesh applied to cylindrical tank, showing increase in mesh resolution at “control”	125
5.11	Example of FEA validation using cylindrical tank	127
5.12	Cross section of wall-base joint of a cylindrical tank, showing radial fillet at joint	128
5.13	Section of FEA model showing mesh around radial fillet	129
5.14	Variation in peak stress with radial fillet size for cylindrical tank .	130
6.1	OD curvature tank section with and without radial fillets	136
6.2	Variation in peak stress with wall thickness for flat panel tank . .	137
6.3	Effect of edge fillets on the peak stress in a flat sided tank	138
6.4	Peak stress with wall thickness for a variety of tank profiles	141
6.5	Examples of 2D profile types	141
6.6	Thai jar profile	142
6.7	Variation in peak stress with height within Thai jar	143
6.8	Profile of Sri Lankan Pumpkin tank, showing smooth wall-base joint, and extra layer of mortar at base	144

6.9	Example model for tank with 2D curvature	145
6.10	Example FEA model and mesh for tank with 2D curvature	146
6.11	Selected profiles for tank shape optimisation	147
6.12	Example stress profiles for 2D curvature tanks	148
7.1	Profile selected for 2000l water tank	153
7.2	Stages in Wooden frame construction	155
7.3	Application of mud coating to wooden tank mould	156
7.4	Joining lid section to base tank section	157
7.5	Orientation of Demec and strain gauges on the tank surface . . .	158
7.6	Sample video image, showing location of strain gauge meridians .	160
7.7	FEA results showing maximum principal stresses alongside the tank design used for the prototype	162
7.8	Predicted meridional and hoop strains within tank during filling .	163
7.9	External surface of the tank during filling, with dark damp patches indicating locations of leaks	165
7.10	Frames from video footage of tank failure	167
7.11	Section of tank showing joint debonding	171
7.12	Section of prototype tank showing thin wall section	172
7.13	Tank section with flaw due to poor plastering	173
7.14	Summary of demec readings taken during tank testing	175
7.15	Strain gauge readings, showing several approaching material limit	177
9.1	Applying mortar to the mesh and rebar formwork of the Pumpkin tank	191
9.2	Alternative joint location for hexagonal prismatic tank	193
9.3	Comparison of bases of two failed tanks	198
9.4	Section from broken tank in Uganda, indicating variable wall thickness produced by plastering	199
11.1	Examples of predicted membrane action panel shapes	213
A.1	Variation in slump distance with moisture content for sands S, K and M	278

- A.2 Optimum sand-cement ratio for membrane loading 285
- B.1 Example profile of 2D curvature tank, with locations of 4 defining
radii 289
- B.2 Wooden template forming semicircular profile of tank 291
- B.3 Single frame of wooden mould (1/2 bottom section of mould) . . . 292
- B.4 Complete frame (assembled) 293
- B.5 Frame section, with ply strips attached 294
- B.6 Assembled frame, with two coats of varnish applied 295
- B.7 Configuration of instrumentation on tank 296

Nomenclature

- a Radius of a cylindrical tank, see equation (5.7), page 110
- A, B Constants in Abrams' law. A gives some indication of the general strength of the mix, whilst B indicates how sensitive that strength will be to variations in water-cement ratio, see equation (2.7), page 27
- E Young's modulus, see equation (3.2), page 62
- f Strength of concrete, see equation (2.7), page 27
- f_c Compressive strength, see equation (2.6), page 25
- f_t Tensile strength, see equation (2.6), page 25
- h Height of a component, such as cylindrical water tank, see equation (5.13), page 111
- I Second moment of area, page 21
- M Bending moment, page 21
- m , Fineness modulus: A derived grading property, obtained from a sieve analysis of an aggregate. It is computed as the sum of the cumulative percentages retained on a standard series of sieves. In general, the higher the modulus, the coarser the aggregate. It has been shown (Neville, 1995) that the fineness modulus corresponds to the logarithmic average of the PSD of the aggregate. Fineness modulus does not give a full description of the

aggregate: even amongst particles of identical aspect ratios and general shape, an infinite number of different gradings could give the same modulus. However, it does give an indication of the probable behaviour of concrete mixes with aggregate of a particular grading. , page 38

- m_c The mass of cement in a given mix, see equation (2.10), page 37
- M_e The bending moment at the wall-base joint of a cylinder, see equation (5.13), page 111
- m_s The mass of sand in a given mix, see equation (2.10), page 37
- m_w The mass of water required to give desired workability, for given mix quantities and compaction method, see equation (2.10), page 37
- mc Moisture content, see equation (3.3), page 67
- $owcr$ The optimum water-cement ratio, leading to peak strength for a given mix and method of compaction., page 28
- s Specific surface: the surface area per unit mass of material, page 38
- s/c Sand-cement ratio, by mass, page 19
- t Component thickness, page 20
- w/c Water-cement ratio, measured by mass, see equation (2.6), page 27
- w_c Water demand of cement - the fractional amount of water required due to the presence of cement in a mix, to give the desired level of workability, see equation (2.10), page 37
- w_s Water demand of sand - the fractional amount of water required due to the presence of sand in a mix, to give the desired level of workability, see equation (2.10), page 37
- y Distance from neutral axis, page 21

- β A derived property used in shell theory to analyse shapes such as cylindrical tanks, see equation (5.13), page 111
- γ Water loading term, equal to the product of water density (ρ_w) and the gravitational constant, g , see equation (5.6), page 110
- μ Plastic viscosity of a Bingham fluid, see equation (2.8), page 32
- σ Stress, page 21
- σ_p The peak stress in a component from a given loading, page 20
- τ_o Yield stress of a Bingham fluid, below which no flow develops, see equation (2.8), page 32
- ν Poisson's ratio, see equation (5.7), page 110
- 0D curvature tanks: Those tanks made with flat panels, generally forming a prismatic structure, page 97
- 1D curvature tanks: Cylindrical tanks, generally used with a vertical axis, page 98
- 2D curvature tanks: Tanks with curvature in two dimensions, giving axisymmetric structures, including "vase-like" tanks, page 99
- Abrams' law: A relationship between strength and water-cement ratio of a concrete/mortar, stating that strength varies inversely with water-cement ratio. Note that a number of caveats apply to this relationship, see equation (2.7), page 27
- Apparent dry density: The density of a material, including voids, obtained by placing it in a container of known volume in some method (e.g. pouring), and measuring the mass of the full container, page 36
- Artisans: Workers producing goods in LEDCs, skilled in a craft but with little or no formal academic training, page 12

Base exchange, or cation exchange: The ability of a clay or mineral to exchange cations within its structure for other cations, measured in milli-equivalents per 100 grams of dry soil, page 31

Bingham fluid: A model for non-Newtonian fluids, which includes a yield shear stress (τ_o), below which the material behaves pseudo-elastically, and no permanent deformation occurs. At shear stresses above the yield value, shear strain rate ($\dot{\gamma}$) varies linearly with shear stress, the rate depending on the plastic viscosity (μ), see equation (2.8), page 32

Brazilian test: A test for the splitting tensile strength of a concrete/mortar, involving inducing tensile stress indirectly by diametric loading of a cylindrical test specimen, page 50

Cement Intensity: The mass of cement used to produce a particular design of component; rainwater harvesting tanks in this thesis. This gives some indication of the performance of the design, page 107

Cementitious: Material containing cement as the primary strength-providing component, page iii

Characteristic strength: The value of strength below which 5% of all test results are expected to fall, page 102

Compressive-membrane: A loading situation leading to failure in compression, with peak stress proportional to $1/t$, page 23

Curing conditions: The environment in which cementitious components are stored until their use, described by factors including temperature and humidity, page 40

Design reserve: A factor, sometimes termed safety factor, representing the capability of a system over the requirements it will experience. This factor can be arrived at by combining a number of factors, including, cost of failure,

statistical variation in material, effects of imperfection in construction etc.,
page 102

Developing countries: Generally refers to low-income countries. See LEDCs,
page 10

Domestic Roofwater Harvesting: A subcategory of Rainwater Harvesting (RWH),
operating at a household level, and involving the collection of rainwater
from roofs, normally those covering the household, rather than custom-
made covers, page 96

Finite Element Analysis (FEA): A computer simulation technique used for en-
gineering applications, including structural analysis. It uses a numerical
technique called the Finite Element Method, involving discretisation of a
geometry into individual elements forming a mesh, and using equations of
equilibrium and physical considerations to generate a set of simultaneous
equations. Whilst these solutions are, to some degree, approximations,
sufficient accuracy can be achieved by mesh refinement or higher-order
interpolation of values within elements, page 103

Lean mix: A mix with a high sand-cement ratio. Lean mixes generally achieve
low strengths, as they require relatively large amounts of water to become
workable, page 25

LEDCs, Less Economically Developed Countries: A term used to describe what
were previously called “third-world” countries. LEDCs does not have the
implications of lower status associated with this term, page 11

MEDCs, More Economically Developed Countries: A term used for industrialised
or “Western” nations, to contrast with LEDCs, page 11

Modulus of rupture test: A test to measure the modulus of rupture, or flexural
strength, of a mortar/concrete, by loading a beam to give bending stresses,
page 51

Moisture Content: The water content of a mix as a mass fraction of the total solids in the mix, page 39

Nelder-Mead simplex algorithm: A commonly used optimisation algorithm for smoothly-varying functions, that generates a new combination of parameters by extrapolating from previous results using simplexes (polytopes of $n + 1$ dimensions for n parameters, e.g. a line for $n = 1$, and a triangle for $n = 2$), page 284

OPC: Ordinary Portland Cement, page 46

Optimum moisture content: The moisture content that gives peak achievable strength for a given mix (sand type and sand-cement ratio) and method of compaction, page 66

Particle Size Distribution, PSD: The size distribution of a component, be it a sand or clay. Measured in various ways, including sieve analysis and laser diffractometry, page 49

PySGA, Python Simple Genetic Algorithm: An implementation of a simple genetic algorithm in the object-oriented language Python, with the novel feature of a dictionary of previous evaluations to minimise computational effort, page 300

Rainwater harvesting: The collection of rainwater from a capture surface, normally a building roof, followed by its storage and use, page 15

Relative Cement Intensity (RCI): A relative measure of component performance. Relative cement intensity compares the amount of cement used in a design with that used in a datum design, both designs storing the same volume of water. A $RCI < 1$ indicates a design that makes better use of materials than the datum, whilst an $RCI > 1$ indicates a design that makes worse use of materials than the datum., see equation (5.1), page 107

Relative specific surface: the surface area per unit mass of sand, page 36

Rheology: The study of the flow and deformation of matter, page 32

Rich mix: A mix with a low sand-cement ratio, and hence high cement content.

Rich mixes generally achieve high strengths, as they require relatively little water to become workable, page 25

Sand M: A synthetic sand produced to represent local, clay-contaminated sands in LEDCs, made by contaminating Sand S to 20% by mass montmorillonite clay, page 46

Sand K: A synthetic sand produced to represent local, clay-contaminated sands in LEDCs, made by contaminating Sand S to 20% by mass kaolin clay, page 46

Sand S: A sand considered broadly representative of those available in LEDCs, with no clay contamination, page 46

Sieve analysis A test to establish the grading, or particle size distribution of a sand or coarser aggregate. The test involves passing a known mass of sand through a series of representative sieves of decreasing size, and measuring the mass retained on each one, page 49

Slump test: A common test for workability of a fresh concrete mix, measuring the distance by which a truncated cone subsides on removal of a containing mould, page 33

Stabilised soil: Soil with an additional low cement content, to give improved performance for use as a load-bearing construction material, page 13

Tensile-bending: A loading situation leading to failure in tension, with peak stress proportional to $1/t^2$, page 23

Tensile-membrane: A loading situation leading to failure in compression, with peak stress proportional to $1/t$, page 23

Vebe test: A test to measure the workability of a fresh mix. Measures the time taken for a truncated cone of mortar/concrete, produced by the slump test, to form a flat-topped cylinder when excited in a container, page 49

Vibro-profiling: A production technique for mortar components. Moves a vibrating mould piece (the “profile”) over mortar laid on the opposite mould part, to give mechanised compaction to the required form, page 34

Water demand: The amount of water required in a given mix to achieve a desired level of workability, page 35

PART I

Problem Definition and Background

CHAPTER 1

Introduction

This Chapter provides an overview of the thesis, detailing the reasons for examining cement-based building components, and the methods considered for reducing their cost.

1.1 Global housing demand

Current estimates place the number of slum dwellers worldwide at around 1 billion, plus approximately 100 million homeless (Erguden, 2001). Predictions hold that this figure will rise threefold by the year 2050. These daunting figures give an indication of the global housing shortage; both the current demand of those without adequate shelter, and the continuing growth of this situation. Whilst many organisations have clear objectives for addressing the political and social aspects of this situation, provision of acceptable technologies to lower the economic cost of providing housing remains an important issue.

1.2 Overview: production of goods in Developing Countries

Whilst the local variations in conditions in Developing Countries¹ make all generalisations on this subject inaccurate to some degree, sources including existing

¹Developing countries: Generally refers to low-income countries. See LEDCs

literature, personal experience and consultation with those in the field allow some generalisations, described in this section.

1.2.1 Production technologies

Historically, we may characterise the development of industrialised countries as the move towards less labour-intensive and more capital-intensive methods of production as technologies changed (Todaro, 2000; Meier & Rauch, 2000). We might then expect to see the same trend apply to the continued evolution of so-called “developing countries” (referred to from this point on as Less Economically Developed Countries, or LEDCs, and contrasted with More Economically Developed Countries², also termed industrialised countries) and anticipate that the introduction of capital-intensive technologies would further economic development. Such introductions have, however, often proved unsuccessful, leading to movements advocating “intermediate technology”, i.e. the use of technologies that offer a less labour-intensive solution than existing practices, but without the prohibitive entry costs of western technologies. In addition to this, we cannot expect LEDCs to pass through identical changes to those historically experienced in industrialised countries, mainly because LEDCs do not exist independent of other (industrialised) nations, but interact and trade with them, making various tools and materials available for their use.

This situation leads many to believe that development may best be aided by the introduction of new “appropriate” technologies; those that alter existing practice in a manner tailored to the specific situation.

²MEDCs, More Economically Developed Countries: A term used for industrialised or “Western” nations, to contrast with LEDCs

1.2.2 Research and Development

The production situation in these countries is such that most improvement in housing will have to be delivered by artisans,³ rather than through self-build, or work by contractors large enough to employ engineers. This group generally has neither the training nor resources to perform engineering analyses, but can copy designs produced by specialists. The availability of such specialists is limited, as reflected by the limited literature targeted at LEDC/artisanal production.

1.2.3 Capital-labour cost ratio

In general, labour costs much less relative to capital in LEDCs than in industrialised countries (Todaro, 2000). This has numerous implications, one of the most obvious being for the selection of an appropriate technology: the highly capital-intensive techniques mentioned above may prove economically successful in the west, but fail to repeat this success when applied to a less industrialised country. Even in rich countries, however, the building industry has proved somewhat resistant to labour replacement or mass-production (Gibb, 1999).

1.2.4 Cementitious building components

Within the building industry, cementitious products continue to rise in popularity. As hydraulic cements have become readily available throughout LEDCs, and high consumption depletes alternative resources (local natural materials), demand for cementitious (cement-based) building materials will rise.⁴ This situation suggests that cementitious building components will continue to prove economically attractive in the future. Such components were therefore chosen as the focus of this thesis. Cement-based building elements of interest include:

³Artisans: Workers producing goods in LEDCs, skilled in a craft but with little or no formal academic training

⁴As shown by cases in India where ferrocement doors have become economically attractive due to a shortage of wood (Building Materials and Technology Promotion Council, 2001).

- Water storage tanks
- Lintels
- Ring beams
- Foundations
- Suspended floors
- Roofs

Extensive literature covers the use of cement in building components, from concrete to stabilised soil.⁵ In these cases the material is generally subject only to compressive forces. For cases where loading leads to the development of significant tensile stresses, conventional practice includes some steel reinforcement. For low-cost building this reinforcement may be unattractive for financial reasons, or for technical reasons, particularly in water-saturated structures. For these reasons, this thesis gives primary attention to the use of unreinforced mortars.

1.2.5 Infrastructure and transport

Builders in industrialised countries do not experience prohibitive costs when sourcing materials from geographically dispersed locations (i.e. over 60km). However the situation is different in LEDCS. For the case of small enterprises at or near the artisan level of production, transport costs may be very significant in the case of building materials, and there is a consequent high cost on using non-local materials. There are significant cost and organisational benefits to using on-site materials if possible for low-cost housing, as indicated by the popularity of clamp-firing bricks 'on-site' in LEDCs wherever firewood is not too costly; for example, clamp-fired bricks in Uganda cost about USh60 (60 Ugandan Shillings) each if

⁵Stabilised soil: Soil with an additional low cement content, to give improved performance for use as a load-bearing construction material

suitable soil is available on-site, but US\$ 40 more to transport over 4km (Thomas, 2007).

1.3 Strategies for reducing component cost

This thesis considers the following three strategies for reducing component cost:

Materials selection. As mentioned above, using non-local materials may incur a significant transport penalty. Local materials are often, or are often perceived as being, of lower quality. However, selection of appropriate local materials, along with suitable ways of employing them (in terms of proportions and quantity) may make their use attractive.

Component design. Production of many components takes place at an artisanal level, which therefore involves no formal design analysis. However, a more rigorous treatment, using relevant theory and modelling tools (e.g. finite element analysis) may produce designs with more efficient materials usage.

Production environment. Production of building elements may take place on-site, in a factory environment followed by transport to site, or via a hybrid of the two, with production of components in a factory, followed by assembly on-site. The processes used to make the component may also vary. Consideration of the production method and tools, with associated issues including quality control, productivity, cost of tooling etc. may allow reduction in component cost.

1.4 Scope of this thesis

Within the context of housing in LEDCs, this thesis will examine the potential for the three methods above to reduce component cost. It will use as its central

case-study the production of water tanks for rainwater harvesting,⁶ as:

- Current research indicates a significant demand for adequate quality water and rainwater harvesting provides an appropriate solution in many cases (Gould & Nissen-Petersen, 1999). It is, in consequence, growing rapidly in popularity, but is constrained by the current high cost of water storage structures.
- Whilst some literature on prefabricated tanks exists (Paramasivam & Nathan, 1984; Khan, 1983; Kumar, Sharma & Robles-Austriaco, 1984; Sharma, 2005; Kumar *et al.*, 1984; Naaman, 2000), little of this work has made its way into the field.

This thesis consists of six parts:

Part I: Introduction and Background. Contains this introduction, giving a brief background and outlining the scope of the thesis, but without a review of the literature.

Part II: Materials selection and proportioning. Covers the choice of raw materials and their proportioning to achieve better economy. In particular, it examines:

- The effect of clay-contamination of aggregates on the performance of mortars/concretes made from such aggregates.
- The behaviour of unreinforced mortars in tension.
- Selection of sand-cement ratio to minimise cost under different loading conditions.

Part III: Component Design. Examines the potential for better component designs to achieve greater economy, taking rainwater harvesting tanks as a

⁶Rainwater harvesting: The collection of rainwater from a capture surface, normally a building roof, followed by its storage and use

case study. It covers a review of relevant theory, a description and analysis of existing tank designs, giving an assessment of the material efficiency possible at different levels of geometric complexity. Part III also includes a description of the manufacture and testing of a prototype tank, using a new design generated by this work.

Part IV: Production Environment. Examines the potential for alternative production methods to reduce the cost of production. This includes a report and discussion of an alternative production method for producing rainwater tanks, namely plastering on to an external mould.

Part V: Conclusions. Contains the conclusions, including a brief comparison of the three cost-reduction strategies proposed.

Part VI: Back Matter. Contains references, appendices, and an index.

PART II

Materials choice and proportioning

Cementitious Building Materials in Developing Countries: Experimental Work and Publications

The author conducted the bulk of the experimental work in this Part with another PhD student, V. Fernandes. This research formed the basis of the following publications:

1. An article published in “Advances in Applied Ceramics” (Still & Thomas, 2006).
2. An additional paper, accepted for publication by “Cement and Concrete Research” (Fernandes, Purnell, Still & Thomas, 2006), covering the experimental work and other research examining the chemistry of cement-clay interactions.
3. Two papers presented at the 24th and 25th Cement and Concrete Science Conferences (Still & Thomas, 2004; 2005).
4. An article submitted to “Building Research and Information” (Still, Thomas, Fernandes & Purnell, 2006).

Section A.1 of Appendix A contains copies of the papers in items 1 and 2 above.

Cementitious building materials in LEDCs: Overview

Chapter 1 gave several reasons for an interest in reducing the cost of cementitious building components in LEDCs. This Part presents:

- A review of existing literature (Chapter 2), identifying what new empirical materials data would assist the design of building components (Section 2.10 on page 42).
- A description of experimental work to obtain this data (Section 3.1 on pages on pages 45–51).
- Results obtained from the experimental program, analysis of these results, and their practical implications (Section 3.2 on pages on pages 51–87).
- A brief summary of the findings (on pages 89–91).

In particular, the experimental work considers the use of clay-contaminated sands for building, and selection of the most economical sand-cement ratio (s/c) for ⁷ construction, for those cases in which component thickness may vary to compensate for changes in material strength. The work considers unreinforced mortars both in tension and compression.

⁷ s/c : Sand-cement ratio, by mass

The results indicate that, for the case of loading where peak stress (σ_p) varies inversely with the square of wall thickness, t ($\sigma_p \propto 1/t^2$), e.g. bending loading of beams, a standard sand-cement ratio of around 7:1 gives good economic performance for practical situations.

With this stress-thickness relationship, a local, cheaper sand with clay content of 20% by mass kaolin is, in most cases, economically preferable to an imported, more expensive, uncontaminated sand. However, for the same stress-thickness relationship, a local, cheaper sand with clay content of 20% by mass montmorillonite, rarely proves economically acceptable when compared with the alternative of an imported, more expensive, uncontaminated sand.

For cases where peak stress varies inversely with wall thickness ($\sigma_p \propto 1/t$), the recommended sand-cement ratio falls to around 3:1 by mass. With this stress-thickness relationship, a local, cheaper sand with clay content of 20% by mass kaolin proves economically acceptable when compared with an imported, more expensive, uncontaminated sand. For the same stress-thickness relationship, a local, cheaper sand with clay content of 20% by mass montmorillonite, incurs an unacceptable cost penalty when compared with the alternative of an imported, more expensive, uncontaminated sand.

In all cases it appears that, for identical water-cement ratio, and with full compaction, the presence of kaolin or montmorillonite does not have a significant effect on strength. However, the two clays do impact workability, with montmorillonite being more detrimental than kaolin, and this has an effect on the strength achievable under a given compaction regime, if water-cement ratio may be chosen to maximise strength. It is this behaviour that differentiates the performance of the two clays, leading to kaolin-contaminated sand often proving an economically viable choice, whilst montmorillonite-contaminated clay incurs an unacceptable cost penalty.

CHAPTER 2

Cementitious building materials in developing countries:

Introduction and Literature review

2.1 Introduction

Cement-based materials have proved useful in construction in industrialised countries for many years. They see increasing use in LEDCs, in a variety of components, including those listed on page 13 of Chapter 1.

The following section briefly describes a number of these components, and details expected peak stress-thickness relationships.

For a suspended beam, whether simply supported or encastered at both ends, if the dominant loading is due to external loads, the maximum stress will arise from the beam acting in bending to resist the load. This stress will occur at the surfaces of the beam. In this case, stress (σ) will vary with moment (M), second moment of area (I), and distance from the neutral axis (y):

$$\sigma = \frac{My}{I} \quad (2.1)$$

Taking the example of a rectangular beam of constant width (b) and thickness

(t), the peak stress will occur at the surface ($y = t/2$), as the neutral axis runs through the mid-depth of the beam. The second moment of area is given by:

$$I = \frac{bt^3}{12} \quad (2.2)$$

So in this case, the maximum stress, σ_p is given by:

$$\sigma_p = \frac{Mt/2}{bt^3/12} = \frac{6M}{b} \frac{1}{t^2} \quad (2.3)$$

With M and b fixed (the moment arising from the applied loading and support conditions, which are constant and the width from the geometric constraint of the space the beam must fit within), they may be treated as a constant, k , giving:

$$\sigma_p = k \frac{1}{t^2} \rightarrow \sigma_p \propto \frac{1}{t^2} \quad (2.4)$$

This situation is also analogous to the design of a wall to resist wind loading: the wind acts as an external load which does not vary with component thickness.

For a similar case of a spanning beam, but in this case with the dominant loading arising from the weight of the beam, the load, and hence the moment will be proportional to the thickness of the beam (holding the width of the beam and density of the materials constant). In this case, $M = k_l t$, so, substituting in Equation 2.3 gives:

$$\sigma_p = \frac{Mt/2}{bt^3/12} = \frac{k_l t t/2}{bt^3/12} = \frac{6k_l}{b} \frac{1}{t} \quad (2.5)$$

So in this case, $\sigma_p \propto \frac{1}{t}$. This situation is also similar to that of a wall designed to resist lateral earthquake loading: the acceleration of the ground will lead to inertia loads. As the magnitude of this inertial load will be proportional to the mass of the wall, and the mass is also proportional to the thickness (providing other dimensions do not change), this again gives the situation where load is proportional to thickness.

For a final example case of a wall supporting a roof and floors, the load can be considered as axially compressive. In this case, as the load arises from external

sources (the weight of the roof and floors), it is independent of wall thickness, giving the case of peak stress inversely proportional to wall thickness ($\sigma_p \propto 1/t$).

2.1.1 Failure scenarios

Although cementitious mortars can find use in many applications, several general scenarios will cover most applications:

Compressive-membrane Loading in which failure occurs owing to a compressive force, with the peak stress varying inversely with component thickness:
 $\sigma_p \propto 1/t$.

Tensile-membrane: Loading in which failure occurs in tension, with the peak stress varying in the same way as for compressive-membrane.

Tensile-bending: Loading in which failure occurs in tension, with the peak stress varying inversely with the square of component thickness¹: $\sigma_p \propto 1/t^2$

2.1.2 Aggregate choice

Masons often face the choice between using cheap, locally-available sand, with high fines content, or more expensive sand, transported over some distance, with associated increased cost. Whilst conventional wisdom in concreting holds that clay has a detrimental effect (Yool, Lees & Fried, 1998; Gullered & Cramer, 2002), some research suggests that this does not always apply in situations prevalent in LEDCs (Fernandes, 2002).

Scenarios of interest thus include situations in which the worker can choose sand type, component thickness and sand-cement ratio to achieve the best economic performance.

¹As noted in section 2.1.3, concretes exhibit significantly lower strengths in tension than compression. Pure bending usually leads to equal maximum compressive and tensile stresses, so failure will occur through tension, and we need not consider compressive-bending failure.

2.1.3 Properties of interest

The properties of main interest are compressive and tensile strengths.² Concrete exhibits significantly lower strengths in tension than compression (by a factor of 5 to 10). Generally the design of RWH storage tanks leads to tensile and compressive stresses of equal magnitude developing under loading, so *tensile* failure forms the limiting design criteria for those scenarios. Young's modulus affects the distribution of stresses in structures, so is also of interest.

2.1.4 Materials

In addition to the focus on tensile rather than compressive strength, our applications differ from those covered by the majority of concreting literature, in that the materials of interest come from developing countries. Though aggregates in industrialised countries have to conform to certain standards, such constraints commonly do not apply in LEDCs. Similarly, lack of quality control checks may lead to wide variation in cement quality, as demonstrated by some experimental research (Walker, 2002). Whilst a large body of literature covers the behaviour of concrete, determining the constants for relationships still requires empirical data.

Relative component costs may differ from location to location. In industrialised countries, sand-cement *cost* ratios typically take values of around 1:6 (Bailey Buildbase, 2006). However, data from LEDCs suggests larger ratios, from 1:20 to 1:70, based on field data obtained from Martinson (2005) and Kintingu (2005), and data in the literature (DTU, 2006b;a).

²Whilst water-tanks do have to retain stored liquid, building practice generally uses an additional waterproofing agent, either in the form of a coat of neat cement slurry, or a leak-seal compound mixed into the mortar and thus the permeability of the concrete is not of primary interest.

2.1.5 Mix composition

Cement-based mortars have seen extensive use in the field, generally using rich (low sand-cement ratio) mixes. Currently many rainwater storage tank designs use sand-cement ratios of around 3:1, and building blocks use ratios of 4:1 and 8:1 for hollow and solid components respectively. Whilst areas of the literature cover the properties of lean (high sand-cement ratio) mixes (Thanh, 1991; Montgomery, 2002b), no work was found on approaches to obtain the most economical design of such mixes for LEDCs. Lean mixes might offer an economic advantage, substituting greater quantities of lower cost materials for the more expensive cement. In addition, peak bending moment stress may vary inversely with the square of the section thickness ($\sigma \propto 1/t^2$), so it may become economically advantageous to use a thicker section made of a weaker material.

2.2 Tensile and compressive strength relationship

As mentioned in section 2.1.3, cementitious materials generally exhibit significantly lower strengths in tension than compression. Neville (1995) quotes several relationships between tensile and compressive strengths, of the form:

$$f_t = k(f_c)^n \quad (2.6)$$

Where f_t and f_c represent tensile and compressive strengths respectively, and k and n constants. n typically takes values of between 1/2 and 3/4. For experimental data obtained using mortars (Thanh, 1991), a power law relationship seems to give a good fit between compressive and flexural strength, as shown by Figure 2.1. This data set gives n from Equation 2.6 as 0.66, within the typical range. Using a linear fit gives flexural strength as around 24% of compressive strength.

We can note several points from this:

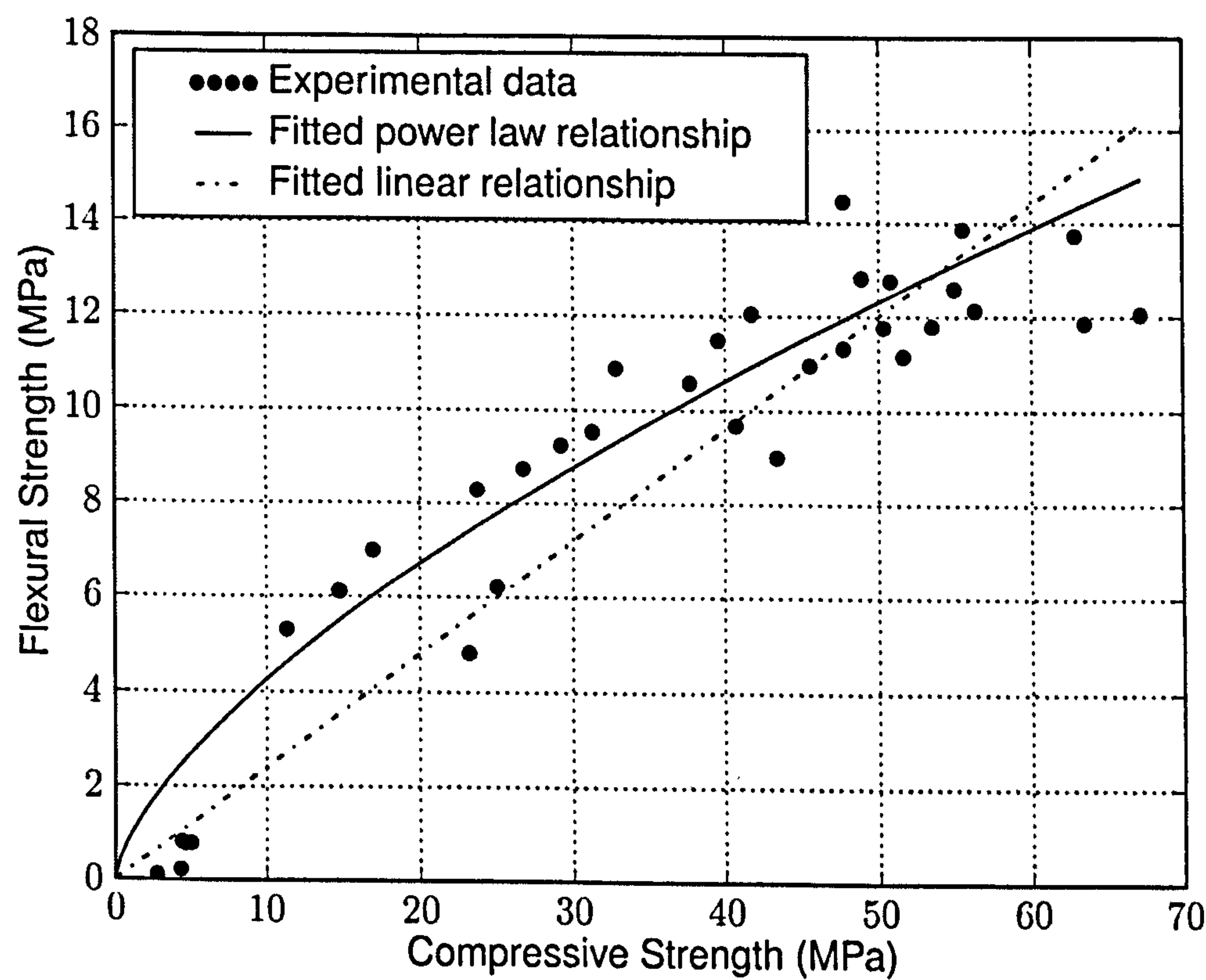


Figure 2.1: Relationship between compressive and flexural strength of mortars, as water-cement ratio is varied, from Thanh (1991) data

- The power relationship makes it difficult to achieve flexural strengths above 13 MPa.
- At low strengths, suitable for applications such as housing, both the power law and linear relationship overestimate the flexural strength: materials with compressive strength under 4 MPa may have negligible tensile strength.

2.3 Abrams’ Law

Abrams’ law holds that the strength of a concrete varies inversely³ with its water/cement ratio, as expressed in Equation 2.7, where f represents strength, A and B constants, and w/c the water-cement ratio (by mass).

$$f = \frac{A}{B^{w/c}} \tag{2.7}$$

Table 2.1 shows values of constants for Abrams’ law in compression and tension respectively, taken from literature (Popovics, 1998), and from fitting to existing data (Rao, 2001; Thanh, 1991).

Table 2.1: Typical tensile and compressive values of parameters in Abrams’ Law

Parameter	Source and Value		
	Thanh (1991)	Rao (2001)	Popovics (1998)
Tensile A (MPa)	26 (flexural)	3.6	20
Tensile B	5.6 (flexural)	2.8	7
Compressive A (MPa)	187	84	
Compressive B	19	5.5	

The physics underlying Abrams’ law for well-compacted concrete is that a fresh mix contains more water than could react in the hydration of the cement.

³“inversely” in the sense that increasing water-cement ratio leads to decreasing strength, rather than $strength = \frac{k}{w/c}$

This additional water acts as a lubricant, allowing placement of the mix without trapping air. As the mix hardens, the unreacted water trapped within it forms voids throughout the structure, which act to weaken the set material.

There are other factors that affect the strength developed. Popovics (1998) presents a list of conditions that must hold for concretes to be considered “comparable”, as shown in Table 2.2.

If the water-cement ratio is too low to allow for full compaction, air voids will also be present, which have a deleterious effect on strength, causing it to fall below that predicted by Abrams’ law. This effect leads to each mix having an optimum water-cement ratio (*owcr*). Decreasing water content gives increasing strength, following Abrams’ law (see section 2.3, page 27). As water content drops, so does workability, leading to air voids remaining within the material, reducing strength. For a given method of compaction, the optimum water content defines the water content at which strength peaks—increasing water content gives a reduction in strength from Abrams’ law behaviour, whilst reducing water content gives a reduction in strength from the deleterious effect of air voids created. This optimum ratio falls with improving compaction methods, leading to higher peak strengths, as shown in Figure 2.2.

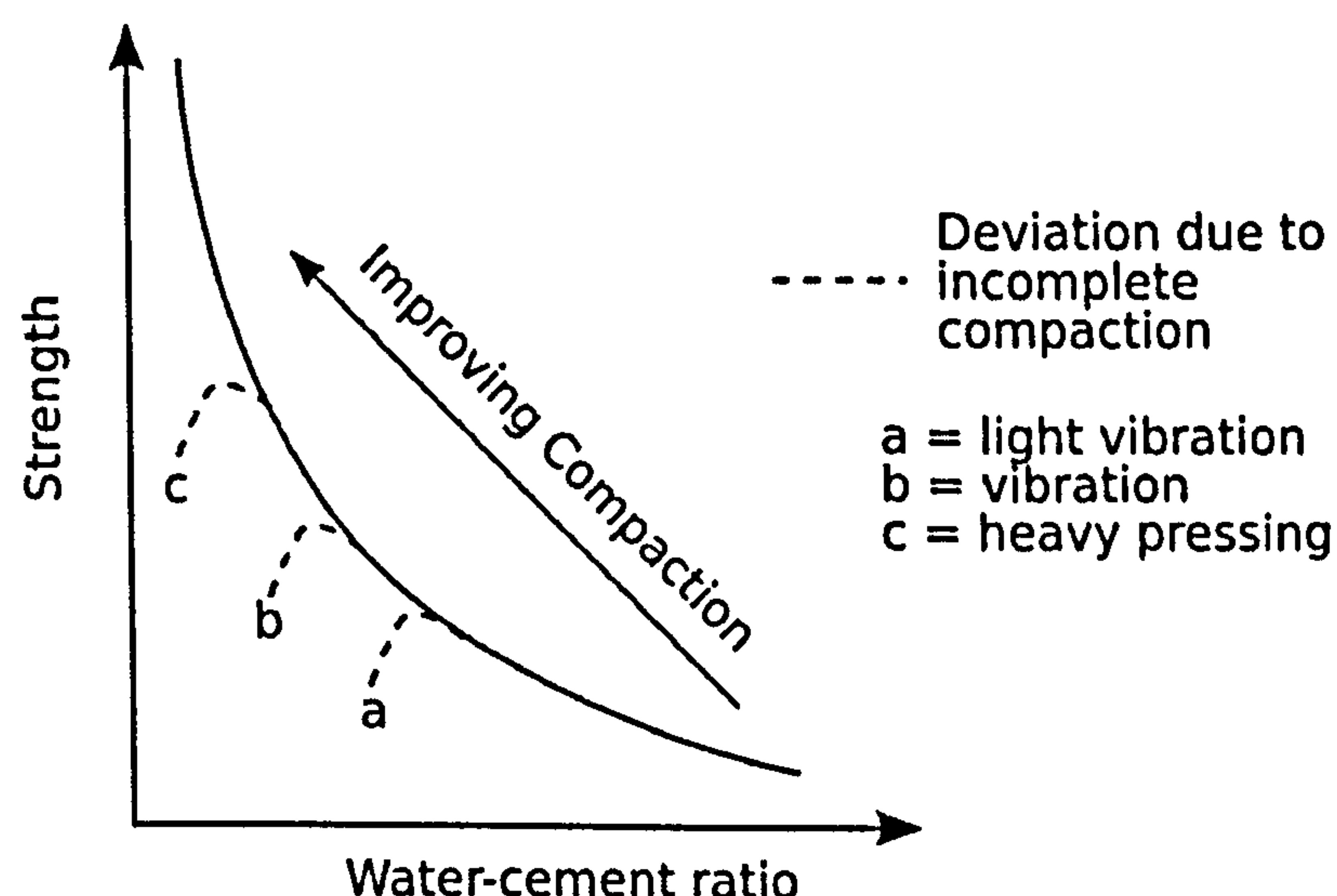


Figure 2.2: Abrams’ Law and the effect of poor compaction

Table 2.2: Conditions required for concretes to be considered “comparable” (Popovics, 1998)

The strength-developing capabilities of the cements used are identical.

The quantities and strength-influencing effects of the admixtures used are identical.

The concrete specimens are prepared, cured and tested under the same conditions.

The concrete ingredients (cement, water, aggregate particles, admixtures) are distributed uniformly in the concrete.

The air contents are the same in the concretes, the air voids are distributed uniformly in the concrete, and none of the voids is too large for the size of the specimens.

The aggregate particles are stronger than the matrix; that is, the fracture propagates more in the matrix than in the particles.

The bond between the aggregate surfaces and matrix is equally strong in the concretes compared and is strong enough to transfer the major portion of stresses in the matrix to the aggregate before the concrete is crushed by the load.

The strength-affecting physical and/or chemical processes in the concretes (drying, aggregate reactivity, etc), beyond the cement hydration, are not overwhelming (cracking, etc.) and are the same.

The nonhomogeneity or composite nature of concrete, the origin of which is in the differing characteristics of matrix and aggregate particles, affects the strength of the compared concretes to the same extent.

The contribution of the aggregate skeleton, resulting from interlocking of the aggregate particles during loading, to the concrete strength, is the same in the various concretes.

2.4 Clay structure and effect of clay contamination

Two clays that have been considered to give a broadly representative sample of clays in LEDCs are kaolin and montmorillonite (Fernandes, 2002). Both consist of stacked 2D sheets, of two types:

Silicon-oxygen tetrahedral layer: Tetrahedral SiO_4 groups linked together, with composition Si_2O_5 or, with attached hydrogen, $\text{Si}_2\text{O}_3(\text{OH})_2$.

Octahedral layer: A metal ion, either aluminium or magnesium, inside a group of six hydroxyls, arranged at the corners of an octahedron. Adjoining octahedra are linked by sharing hydroxyls, giving a composition of $\text{Al}_2(\text{OH})_6$ or $\text{Mg}_3(\text{OH})_6$. Metal ion substitution is also possible, with Fe^{3+} replacing Al^{3+} , or Fe^{2+} replacing Mg^{2+} .

Kaolin has a 1:1 structure; it consists of “building blocks”, shown in Figure 2.3, containing one tetrahedral sheet, and one octahedral sheet. Montmorillonite contains an octahedral sheet between two tetrahedral sheets (Blyth & de Freitas, 2006).

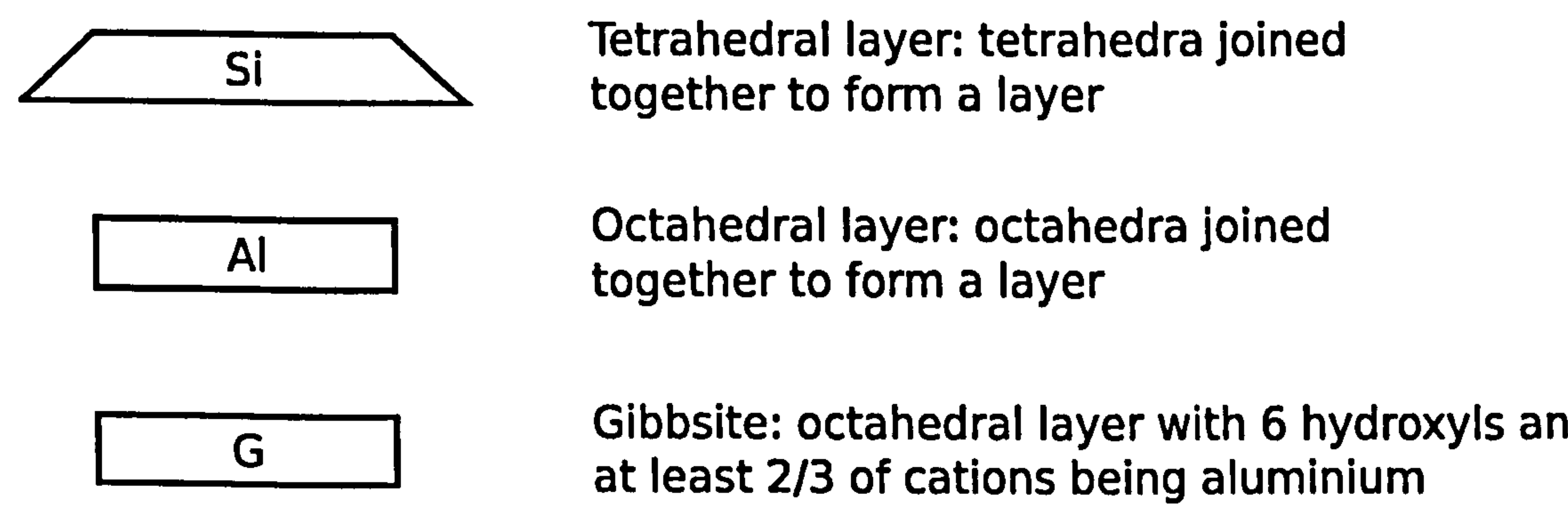
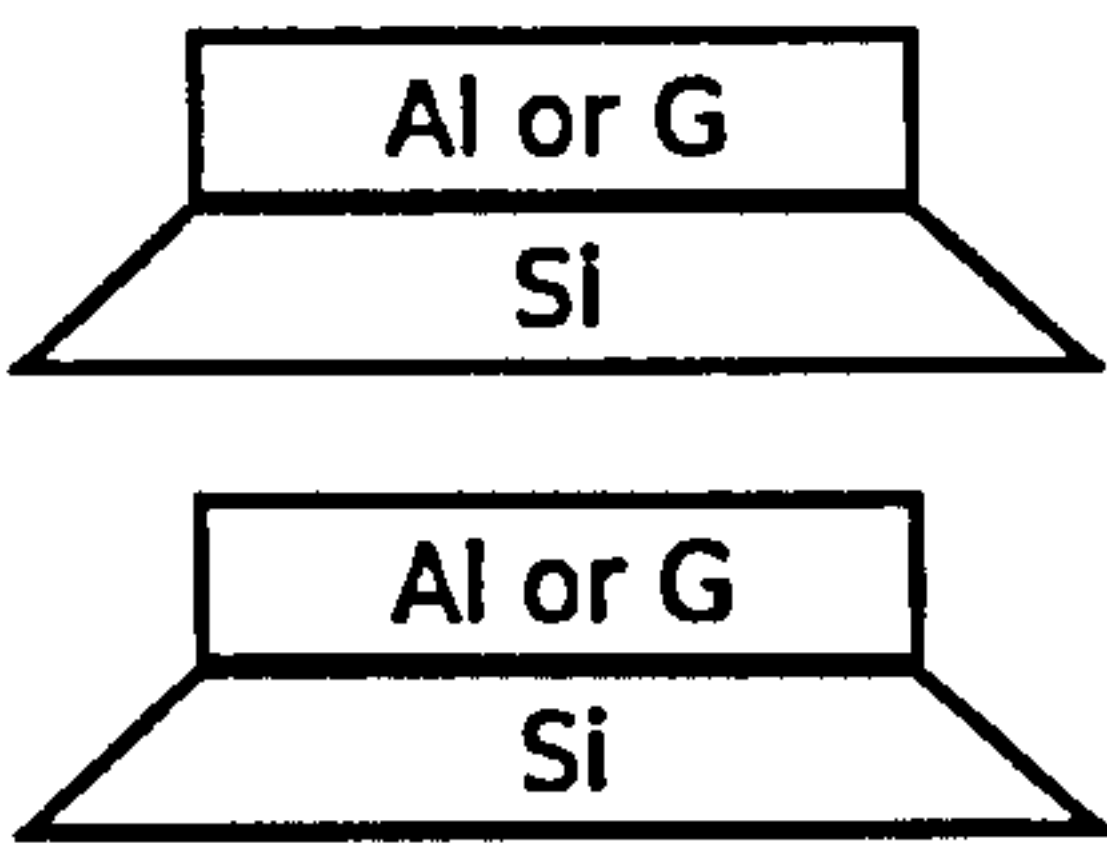
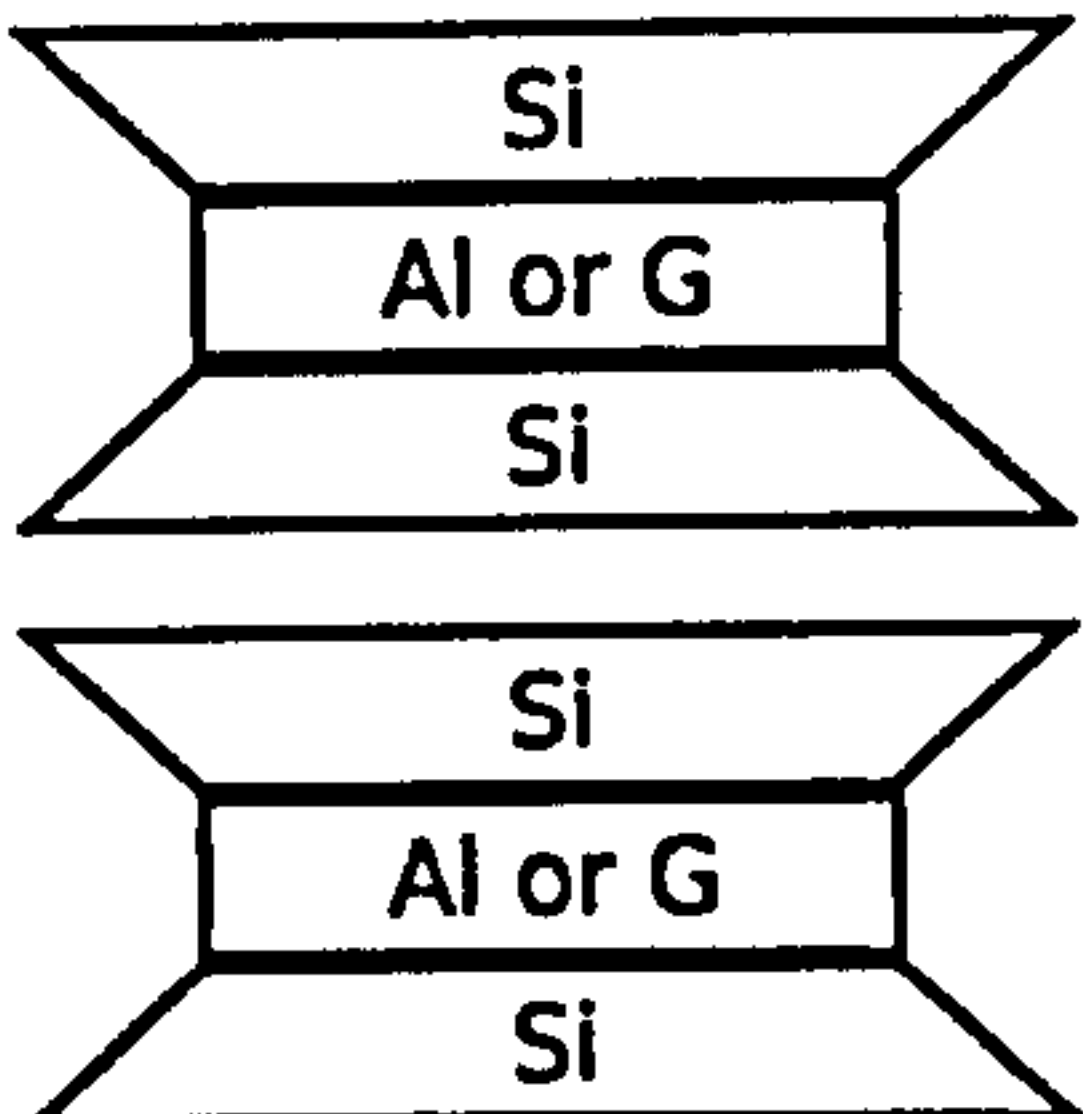


Figure 2.3: “Building blocks” for clays: tetrahedral and octahedral sheets

Table 2.3 provides a comparison between the structure and properties of the two clays. Both the clays adsorb water to their surface, giving high water uptake, and effectively competing with cement for water during hydration. The weaker inter-layer bonds in montmorillonite allow water molecules and exchangeable

Table 2.3: Structure and property of clays, compiled from Barnes (2000)

Property	Kaolin	Montmorillonite
Layer structure	1:1	2:1
Stack structure		
Bonding between layers	Hydrogen bonds (strong)	van der Waal's forces (weak)
Base exchange capacity (me/100g) ^a	3-15	80-140
Surface area (m ² /g)	10-70	800

^aBase exchange, or cation exchange: The ability of a clay or mineral to exchange cations within its structure for other cations, measured in milli-equivalents per 100 grams of dry soil

ions to enter between the layers; this capability of absorbing water between the layers, as well as adsorbing it onto the surface, makes montmorillonite more susceptible to expansion, swelling and shrinkage (Barnes, 2000). As the discussion above, and Table 2.3 show, the two clays have significantly different properties, ranging from surface area exposed per unit mass, to ability to absorb water within their structure. The combination of these give montmorillonite a greater swelling capacity, and hence greater water demand when present in aggregates.

2.5 Workability, rheology and vibration compaction

2.5.1 Rheology and workability

Rheology is the study of the flow and deformation of matter, which has applications in concrete and mortar. A full understanding of the flow of cement pastes has not developed yet (Banfill, 2003). Even numerical models able to qualitatively reproduce phenomena seen in fresh mixes require measurement of a large number of properties to characterise the material (Chandler & Macphee, 2003).

The rheology of cementitious composites appears less complex than that of cement pastes; mortars and concretes behave as Bingham fluids (Tattersall & Banfill, 1983; Hu & de Larrard, 1996). Bingham fluids have a yield shear stress (τ_o) below which the material is pseudo-elastic and no permanent deformation occurs, and above which shear strain rate ($\dot{\gamma}$) varies linearly with shear stress (τ), the rate depending on the viscosity, (μ), as shown in Equation 2.8.

$$\dot{\gamma} = \begin{cases} (\tau - \tau_o) \mu & \text{for } \tau > \tau_o \\ 0 & \text{for } \tau \leq \tau_o \end{cases} \quad (2.8)$$

There are other models for non-Newtonian fluids, some of which are used in modelling the flow of cement. These include power-law fluids, which can capture shear-thinning or shear-thickening behaviour. The Bingham model has the virtues of capturing the finite yield stress observed with concretes, and requires two parameters: the minimum number for a model more complex than a Newtonian fluid. Modifications to this include the Herschel-Bulkley fluid model (Cyr, Legrand & Mouret, 2000) given in Equation 2.9, with k and n as constants. Which has the potential of capturing shear-thinning and shear-thickening behaviour, but at the expense of increased complexity.

$$\tau = \tau_o + k\dot{\gamma}^n \quad (2.9)$$

Typical tests measure one property of mortar/concrete—for example, the slump test⁴ gives an indication of yield stress, but not of viscosity (Saak, Jennings & Surenda, 2004). An ideal field test should operate as simply as possible, measuring a single property of the material, and from this determine the optimum water-cement ratio etc. To characterise the behaviour of a Bingham fluid, however, requires two parameters: the yield stress (τ_o) and the viscosity (μ). In laboratory conditions these are often measured by apparatus using concentric cylinders, or helical impeller arrangements (Banfill, 2005). Shear strain rate is recorded for a number of applied torques (which allow calculation of shear stress), from which the yield stress and viscosity may be determined.

A plot of μ with τ_o can show the effect of different parameters on the behaviour of concretes and mortars, as shown in Figure 2.4. The addition of clay gives a reduction in plastic viscosity, but an increase in yield stress. As Banfill (2005) states that yield stress dominates workability, this suggests that the addition of clay will reduce workability.

Vibratory excitation increases the fluidity of concrete, often allowing it to flow under its own weight. Hu & de Larrard (1996) showed that vibration reduced the effective yield stress of high-performance concretes considerably, whilst some vibration regimes appear to give a zero effective yield stress (Tattersall & Banfill, 1983; Tattersall, 1992). Work by Tattersall (1992) suggests peak velocity as the parameter determining fluidity, with rising peak velocity causing an increase in fluidity until the point of zero effective yield stress is reached, above which fluidity will not increase (Banfill, Yongmo & Domone, 1999). Some experimental work with roller-compacted concrete (i.e. lean, dry mixes) suggests that peak acceleration determines the degree of final compaction (Kokobu, Cabrera & Ueno, 1996).

Rheology relates to vibration compaction, a topic of interest for the off-site production we wish to consider. In particular, an indication as to the optimum

⁴Slump test: A common test for workability of a fresh concrete mix, measuring the distance by which a truncated cone subsides on removal of a containing mould

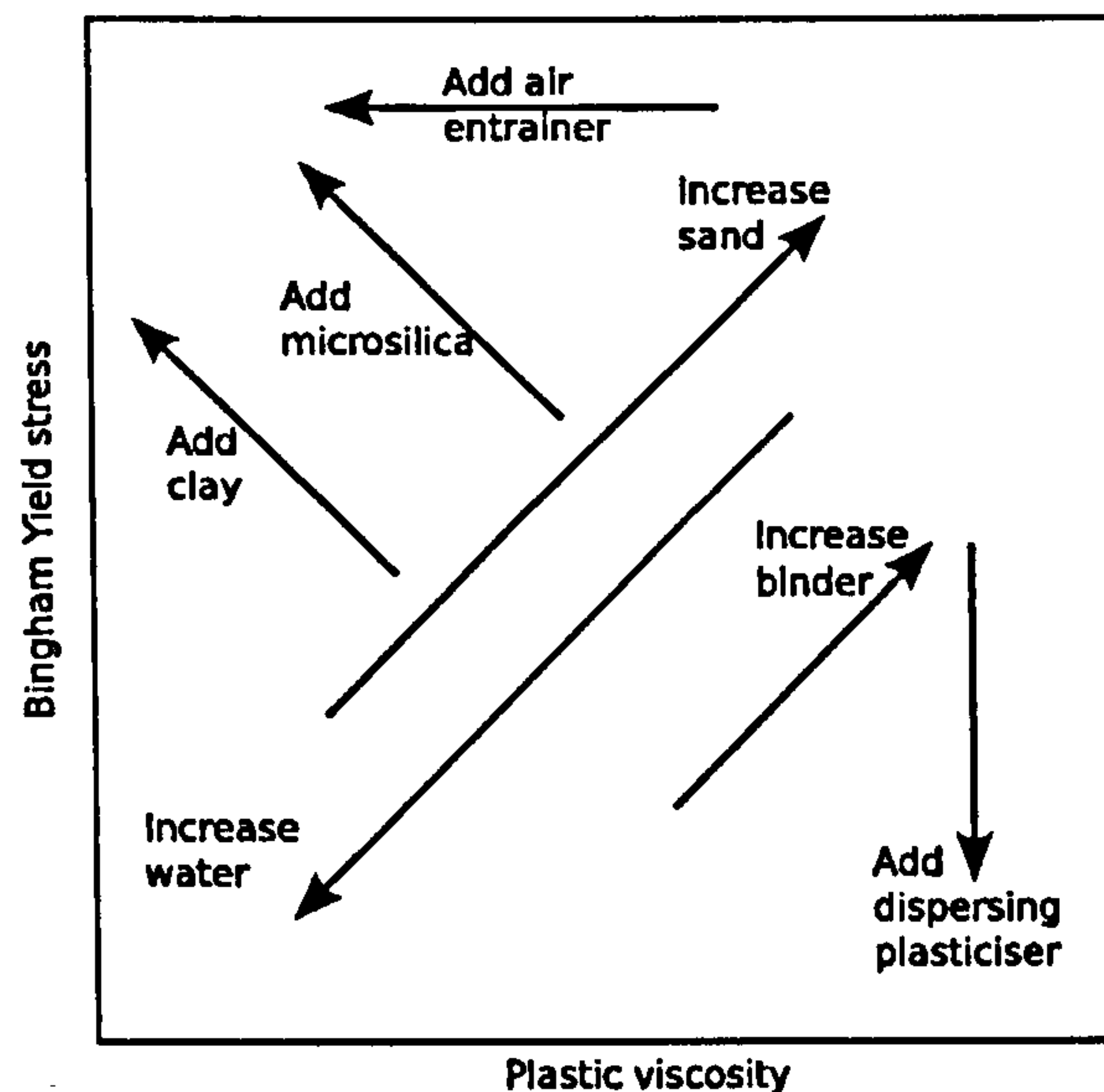


Figure 2.4: Effect of changing mix conditions and components on Bingham constants, taken from Banfill (2005)

combination of vibration frequency and amplitude would give useful information for producing designs. Previous work has produced and tested machines to compact thin-section cementitious composites (Sharma, 1983; Walkus & Malek, 1986), but reports only empirical success, without identifying any theoretical method of establishing an optimum combination of parameters.

2.5.2 Compaction

Given the deleterious effect on strength of excess water required to give sufficient workability for hand compaction, concreting practice often uses mechanical means to ensure placement of the material without trapping air. Compaction can use quasi-static pressure, dynamic applied loading, or a combination of the two. Given the large surface area of components, machinery to apply a high pressure over the entire surface would prove costly to produce. Previous research has examined the use of “vibro-profiling” devices, particularly in ferrocement applications, to compact fresh mortar (Sharma, 1983; Walkus & Malek, 1986). Vibro-profiling involves traversing a vibrating top plate over mortar, and com-

pacting it between the top plate and a base mould, as shown in Figure 2.5.

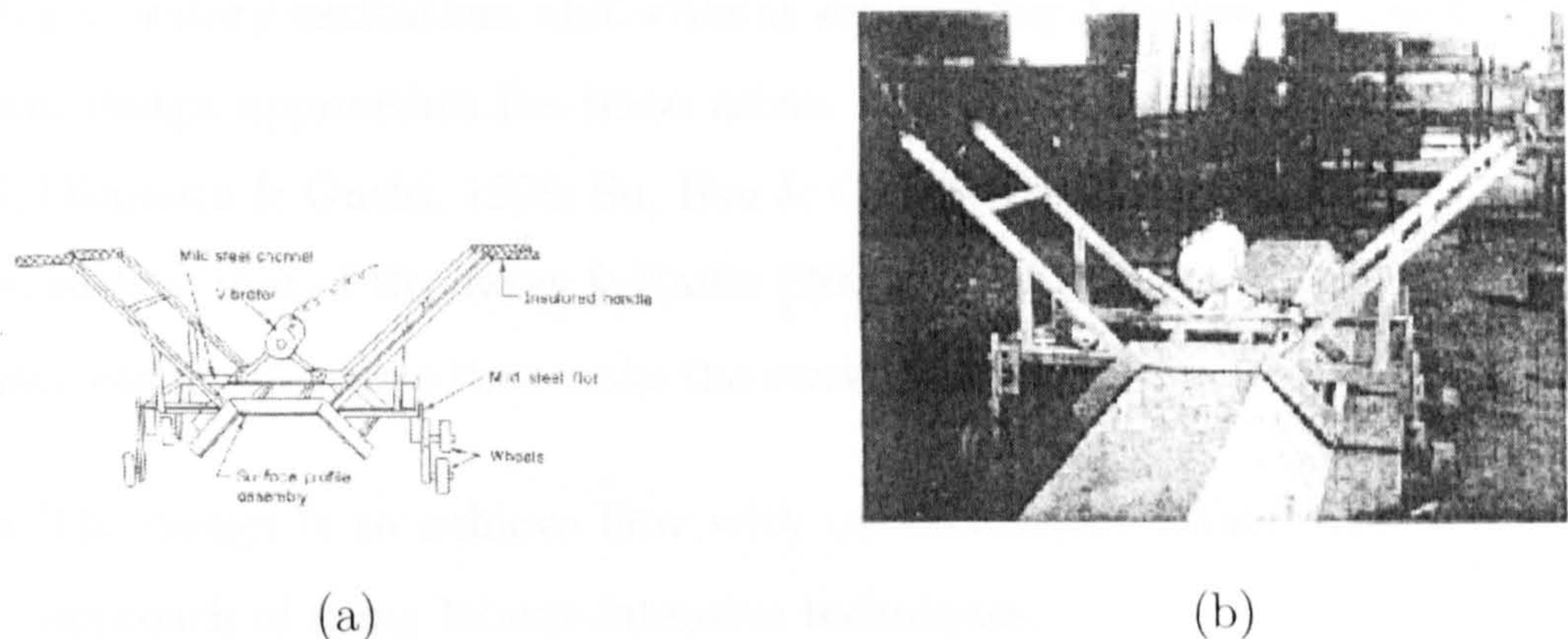


Figure 2.5: Vibro-profiling system, showing system components (a), and complete system in use (b)

These accounts indicate successful application of the technique, and some report a 20% increase in strength achieved (Sharma, 1983). However, they offer little help in choice of parameters, or exploring the water-reducing, and hence strength-enhancing, possibilities offered by the technology; they do not define the maximum possible benefit from using mechanised compaction.

2.6 Calculating water demand

Researchers have suggested various relationships between sand properties and water content required for a given workability⁵ (De Schutter & Poppe, 2004; Thanh, 1991). Standard testing of sands involves establishing a particle size distribution (grading) through sieving. Whilst giving useful information for the comparison of aggregates, sieving does not distinguish between particles of identical smallest dimension but different larger dimensions and/or geometry.

Areas of existing literature that address relationships between grading and workability include self-compacting concrete (SSC), developed in 1988. SCCs are

⁵Water demand: The amount of water required in a given mix to achieve a desired level of workability

designed to be sufficiently fluid to flow into place around reinforcing without requiring vibratory excitation, and without segregating (Okamura & Ouchi, 1998). Several design approaches for these mixes have developed (Brouwers & Radix, 2005; Okamura & Ouchi, 1998; Su, Hsu & Chai, 2001; Su & Miao, 2003). Whilst some, such as that of Brouwers & Radix (2005) even specify a grading curve, they all have distinct features that make the work inapplicable for LEDC applications:

- The design is to achieve flow with no excitation, rather than the LEDC approach of using labour-intensive techniques.
- The designs make use of superplasticisers, which are not appropriate for LEDC application for reasons of availability and cost.
- Design of the mixes is often to achieve a design strength (Su & Miao, 2003). Whilst this is acceptable in some cases in LEDCs, for many components achieving a higher strength will allow reduced materials usage, and is thus desirable.

The points above, and the distinct difference in applications, mean that the literature on SCC design will not prove useful in mix design for mortars in LEDCs. Whilst, for the applications of interest, the literature does not describe a direct relationship between aggregate grading and workability, derivative measures have shown some correlation to workability. De Schutter & Poppe (2004) found relative specific surface,⁶ calculated from gradings, shows a good correlation with water demand for a desired workability, providing the sands contain particles of a particular geometry type (smooth rather than angular). Interestingly, De Schutter found the most useful indicator of water requirement to be the apparent dry density obtained by pouring the sand from a low height (< 50mm) into a container of known volume, and measuring the mass of the full container. Figure 2.6 shows the strong correlation between water demand of various sands to give a desired workability, and their apparent dry densities. Although not commented

⁶Relative specific surface: the surface area per unit mass of sand

on in the text, provided that absolute sand density does not vary significantly, this measure should have equivalence to the voids content of the sand, a measure used in computer modelling of concrete mixtures (Dewar, 1999).

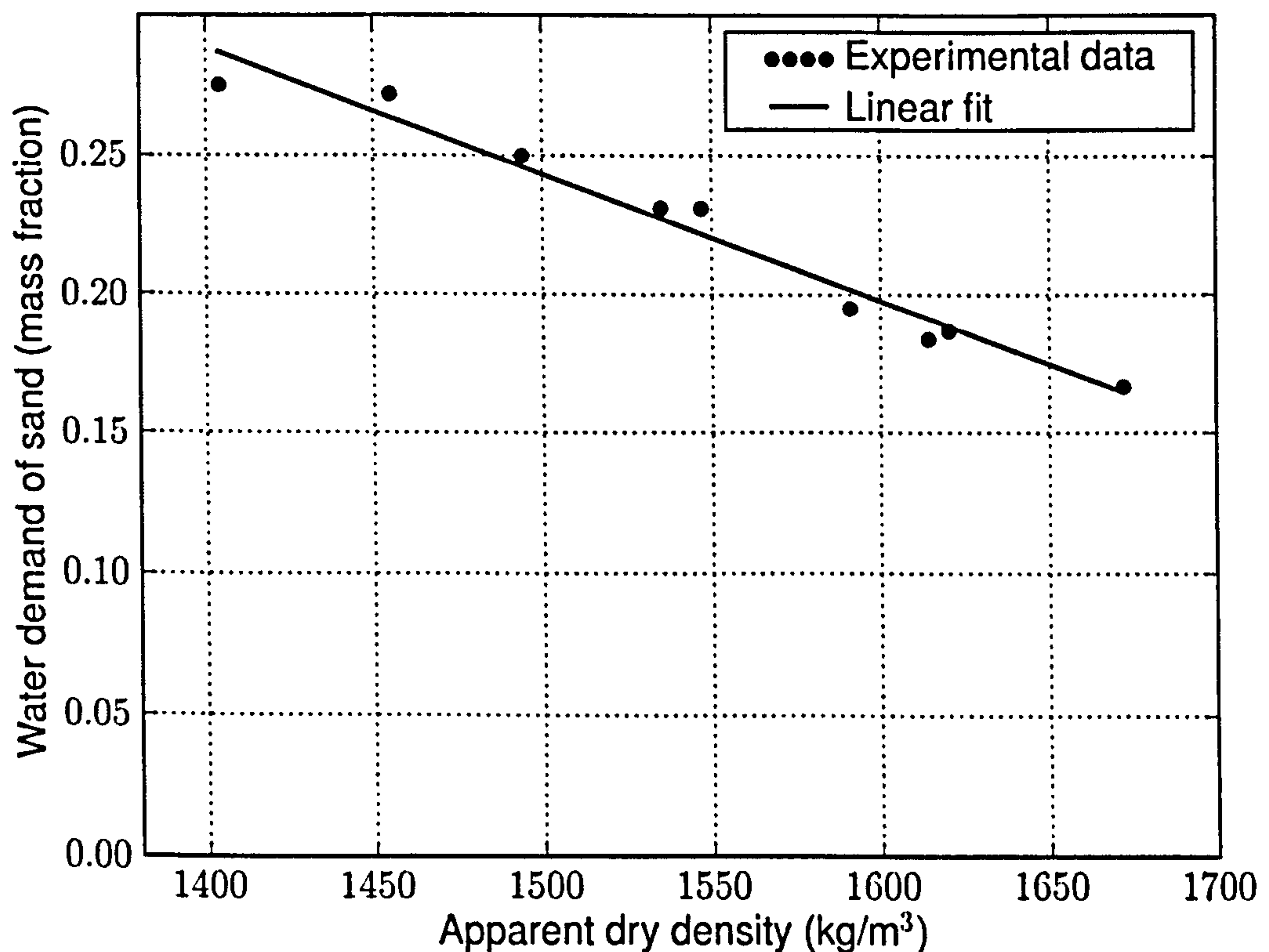


Figure 2.6: Relationship between water demand of sand and apparent dry density for 0.5 w/c mortars made with varying sand-cement ratio to give constant workability (De Schutter & Poppe, 2004)

Thanh (1991) quotes several relationships intended to determine the water content for a desired workability (effectively the optimum water content mentioned above in 2.3) such as those shown in Equations 2.10, 2.11 and 2.12. The total water demand (m_w in Equation 2.10) consists of a quantity determined by the amount of cement present ($m_c w_c$), plus a second amount related to the amount of sand present ($m_s w_s$).

$$m_w = m_s w_s + m_c w_c \quad (2.10)$$

m_w , m_s and m_c represent masses of water, sand and cement respectively, and w_s and w_c the corresponding water demands (dimensionless quantities). The expression in Equation 2.11 for m_s uses specific surface,⁷ s , with k and w_o constants.

$$w_s = k\sqrt{s} + w_o \quad (2.11)$$

This shows that, the finer the mix, the greater the water required to achieve the desired workability⁸.

Expression 2.12 uses fineness modulus,⁹ m , with a and b constants.

$$w_s = a \exp(-bm) \quad (2.12)$$

Again this has the expected feature that water demand increases with decreasing sand size.

Expressing the mass of sand in terms of mass of cement and sand-cement ratio ($m_s = m_c(s/c)$), and rearranging Equation 2.10 for water-cement ratio (m_w/m_c), gives a linear relationship between water-cement ratio and sand-cement ratio, as shown in Equation 2.13.

$$(w/c) = \frac{m_w}{m_c} = (s/c)w_s + w_c \quad (2.13)$$

⁷Specific surface measures the exposed area per unit mass of the material in question.

⁸If we consider the specific surface proportional to the square of a characteristic radius r , then $w_s = k.r + w_o$, so water content should vary linearly with representative radius for constant geometry.

⁹Fineness modulus is a derived grading property, obtained from a sieve analysis of an aggregate. It is computed as the sum of the cumulative percentages retained on a standard series of sieves. In general, the higher the modulus, the coarser the aggregate. It has been shown (Neville, 1995) that the fineness modulus corresponds to the logarithmic average of the PSD of the aggregate. Fineness modulus does not give a full description of the aggregate: even amongst particles of identical aspect ratios and general shape, an infinite number of different gradings could give the same modulus. However, it does give an indication of the probable behaviour of concrete mixes with aggregate of a particular grading.

In a similar vein, Lydon (1982) states that for lean mixes (high sand-cement ratios), moisture content ($m_w/(m_s+m_c)$) becomes more useful than water-cement ratio for determining the water content to give a desired workability.

2.7 Sand-cement ratio and strength

Other data from Thanh (1991) covers a series of mortar mixes, designed for constant workability, with varying sand type and varying sand-cement ratio. The results in tension, given in Figure 2.7 show an exponential type relationship between cement-sand ratio and flexural strength, suggesting little strength benefit in using richer mixes above 0.5 cement-sand ratio (2:1 sand-cement).

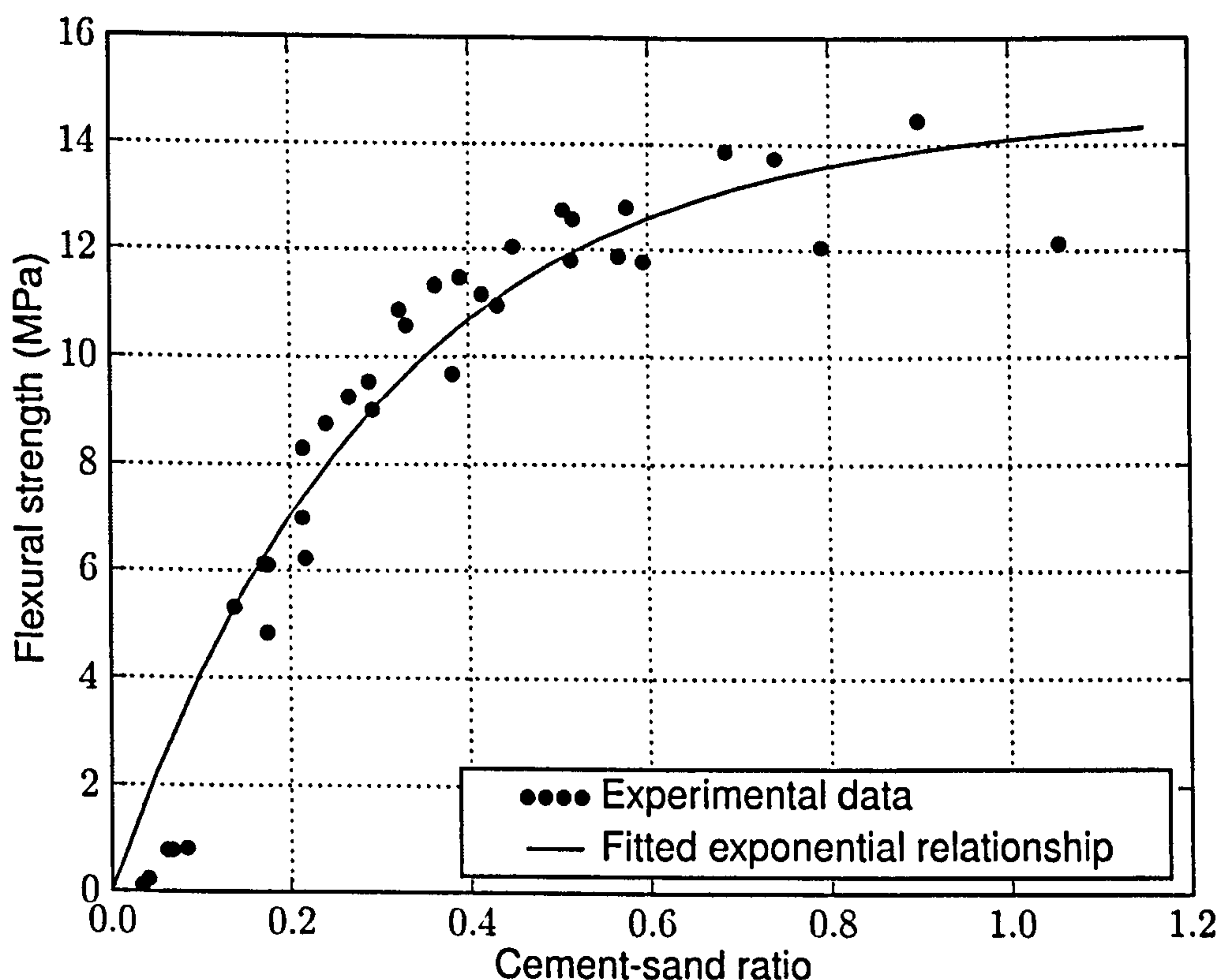


Figure 2.7: Cement-sand ratio and flexural strength, using Thanh (1991) data (water content chosen to achieve constant workability)

The relationship between optimum strength and sand-cement ratio has impli-

cations for efficient materials usage. Simple modelling using a linear fit between sand-cement ratio and strength (accurate for sand-cement ratios between 2:1 and 10:1) with the data from Thanh suggests an economic optimum sand-cement ratio of around 6:1. However, a log relationship, which better fits the high sand-cement ratio values, suggests a higher optimum, with greater sensitivity to sand-cement cost ratio.

If the relationship from Thanh (1991) holds, and peak strength equals a constant fraction (e.g. 90%) of the predicted Abrams' law strength for that water-cement ratio, then peak strength should vary in a similar form with sand-cement ratio, as shown in Equation 2.14:

$$f_t = \frac{k_1}{k_2^{w_s(s/c)}} \quad (2.14)$$

with k_1 and k_2 constants, and w_s as before. Section A.2 of Appendix A shows this.

2.8 Curing conditions

Curing conditions can have an effect on strength developed. Low humidity can act through two mechanisms:

- Insufficient water impedes the hydration reaction;
- Shrinkage cracking: drying at the surface combined with higher water content deeper inside the material can lead to differential shrinkage, with the interior material acting as a restraint, leading to crack development at the surface.

Curing conditions commonly cover temperature and humidity. Curing at high temperatures generally leads to high early strength gain, but lower long-term strength (Neville, 1995). Testing with concretes, varying the temperature

from 5 to 50°C showed strength differences of up to 10% at 28 days¹⁰ (Kim *et al.*, 2002). (Table A.4 in Appendix A shows the data.)

Research simulating the curing of cement-stabilised blocks in developing countries suggests that strength can vary by a factor of six with curing conditions (Kerali & Thomas, 2002). By contrast, Hotta & Takiguchi (1995), experimenting with rich mortars, found that only curing history immediately prior to testing had a significant effect on strength, but that the strength of a sample dried before testing could drop to 1/3 of an identical sample kept moist until testing. Testing by Cebeci, Al-Noury & Mirza (1989), using rich mortars, agrees with that of Kerali & Thomas (2002), suggesting that low humidity curing causes reduction in strength, but that the humidity prior to testing has a significant effect that can mask this. Samples cured and tested at low humidity show significantly greater strength than those cured at the same humidity, and then brought to a saturated state before testing. Section A.3 of Appendix A gives more details of this, along with relevant data from the article.

2.9 Workability aids

Common practice in industrialised countries uses chemical admixtures to improve the behaviour of mortars and concretes. Such admixtures have two problems within the context of low-income countries: cost and availability. Whilst most plasticisers are produced using by-products from the paper industry, some research has examined the potential of making plasticisers from other waste products, including soda pulping and straw pulp waste liquor (Kumar, Irshad, Agarwal & Kumar, 1995; Chang & Chan, 1995; Nadif, Hunkeler & Käuper, 2002), and the results suggest some potential, including the possibility of utilising waste materials from processes related to the processing of sugar.

¹⁰This value is probably conservative: the 10% difference comes from the lower tensile strengths, at which experimental noise will have a more significant effect

2.10 Further research required

We see from the preceding sections that:

- A number of factors influence the strength of cement-based mortars.
- Of these factors, many cannot be controlled by artisans producing building components.
- Of those that can be controlled, some will lead to simple recommendations, such as “provide moist curing conditions for components”.
- This leaves the following as factors an artisan has some control over:
 - Water-cement ratio.
 - Compaction regime.
 - Sand type
 - Sand-cement ratio.
- For a given compaction regime, sand type, and sand-cement ratio, there will be a water-cement ratio that optimises strength.
- For a given form of compaction, that optimum water-cement ratio might be re-expressed as “the water-cement ratio to give optimum workability”, which in turn is a function of sand-cement ratio and sand type.

However, the complexity of cementitious composites means no accurate model exists for determining their behaviour (dependent variables e.g. strength) from measuring inputs (independent variables e.g. sand-cement ratio); even advanced computer models require several empirical data to calibrate predicted strengths (Bentz, 1999). To produce useful results requires research of two types:

- Calibrating existing expressions obtained using industrialised country materials to mortars representative of developing countries
- Establishing new relationships not present in the literature

Tensile-compressive strength relationship

The literature provides well-documented relationships between the two, as noted in section 2.2.

Experimental work need only calibrate this relationship for materials of interest.

Abrams' law

The two papers quoted (Rao, 2001; Thanh, 1991) give data for Abrams' law with mortars using relatively high quality sands. For developing country applications the results from these superior quality materials may overestimate material performance.

Again, experimental work should establish the parameter values.

Sand-cement ratio and optimum strength

As noted in section 2.3, Abrams' law has limitations at water-cement ratios for which the compaction method does not remove all air from the material. For a given compaction method a relationship should exist between the maximum strength obtainable and water-cement ratio. The data from Thanh suggests a relationship between w/c and s/c will have the form $w/c = w_s(s/c) + w_c$, but does not link this to strength. The data leave some ambiguity, for two reasons:

1. The experiments did not vary water cement ratio to confirm a peak in strength for given workability, or even test workability to ensure the mix design method held it constant,
2. The strength variation with sand-cement ratio has considerable scatter at high sand-cement ratios.

The form and values of the relationship between sand-cement ratio and peak strength can have a significant effect on the most economic mortar mix for use.

Experimental work should establish the relationship between sand-cement ratio and strength for a representative compaction regime.

Young's modulus

Modelling deformations, stresses and strains under loading requires some knowledge of material properties other than strength, primarily Young's modulus and Poisson's ratio.

Experimental work should determine whether Young's modulus varies significantly over the range of mortars of interest. If substantial variation occurs, it should then calibrate the standard expressions to the specific materials of interest.

Effect of sand quality

Obtaining higher quality sand can entail greater cost than employing locally available sand of lower quality, due to the expense of the former's extraction, removal of contaminants, or transport.

To allow comparison of these two options experimental work should determine the peak strengths, obtained for representative materials and compaction methods, over a range of sand-cement ratios.

CHAPTER 3

Cementitious building materials in developing countries: Experimental Work

3.1 Experimental methodology: mortars in tension

Our primary interest (in materials) is to know the strength of mortars made from fine aggregates representative of those available to people producing cementitious building components in developing countries. For each of three representative aggregates we want to know the maximum strength attainable (by suitable choice of water-cement ratio) for a variety of sand-cement ratios. We therefore examined, for these materials, the empirical relationship between such measures as strength, workability, density, moisture content, and sand-cement ratio.

When describing the amount of water present in a mix, two measures will be used:

1. Water-cement ratio: the mass ratio of water to cement
2. Moisture content: the mass ratio of water to solids (cement and sand)

3.1.1 Choice of materials

The behaviour of materials used in the laboratory must represent that of those used in the field for the results to have validity. For producing mortar test pieces, obvious problems arise in the difficulty in obtaining sufficient quantities of sand and cement from the field. To overcome this problem, laboratory work used a Type 1 OPC and a fine sand considered representative (Montgomery, 2002a). As mentioned in section 2.1.1, sands in developing countries can have a high fines content (Fernandes, 2002), so two other composite sands were used, giving the following three:

1. “Pure” representative sand — sand S.
2. Sand 1 above, contaminated to 20% by mass kaolin, referred to as sand K.
3. Sand 1 above, contaminated to 20% by mass montmorillonite, referred to as sand M.

Figure 3.1 shows the grading of sand S (type 1 above), along with the grading limits for a concreting sand from BS 882: 1992 (BSI, 1992). As the grading shows, the sand, whilst having a fine grading, conforms to the limits of the standard. Sands K and M were chosen on the basis of previous work (Fernandes, 2002). The level of clay present is similar to that in other research involving mortars and clay: Venkatarama Reddy & Gupta (2005) used “soils” including clay contents of 8, 16 and 24% by mass. Both the clays used have the ability to adsorb water molecules; in addition to this, montmorillonite can absorb water into its microstructure. The two clays have different structures, and this is reflected in their specific surface areas: approximately 10–20m²/kg for kaolin, and 800m²/kg for montmorillonite (Akroyd, 1962).

Section 3.2.8 on page 76 covers a comparison of these materials with samples obtained from developing countries.

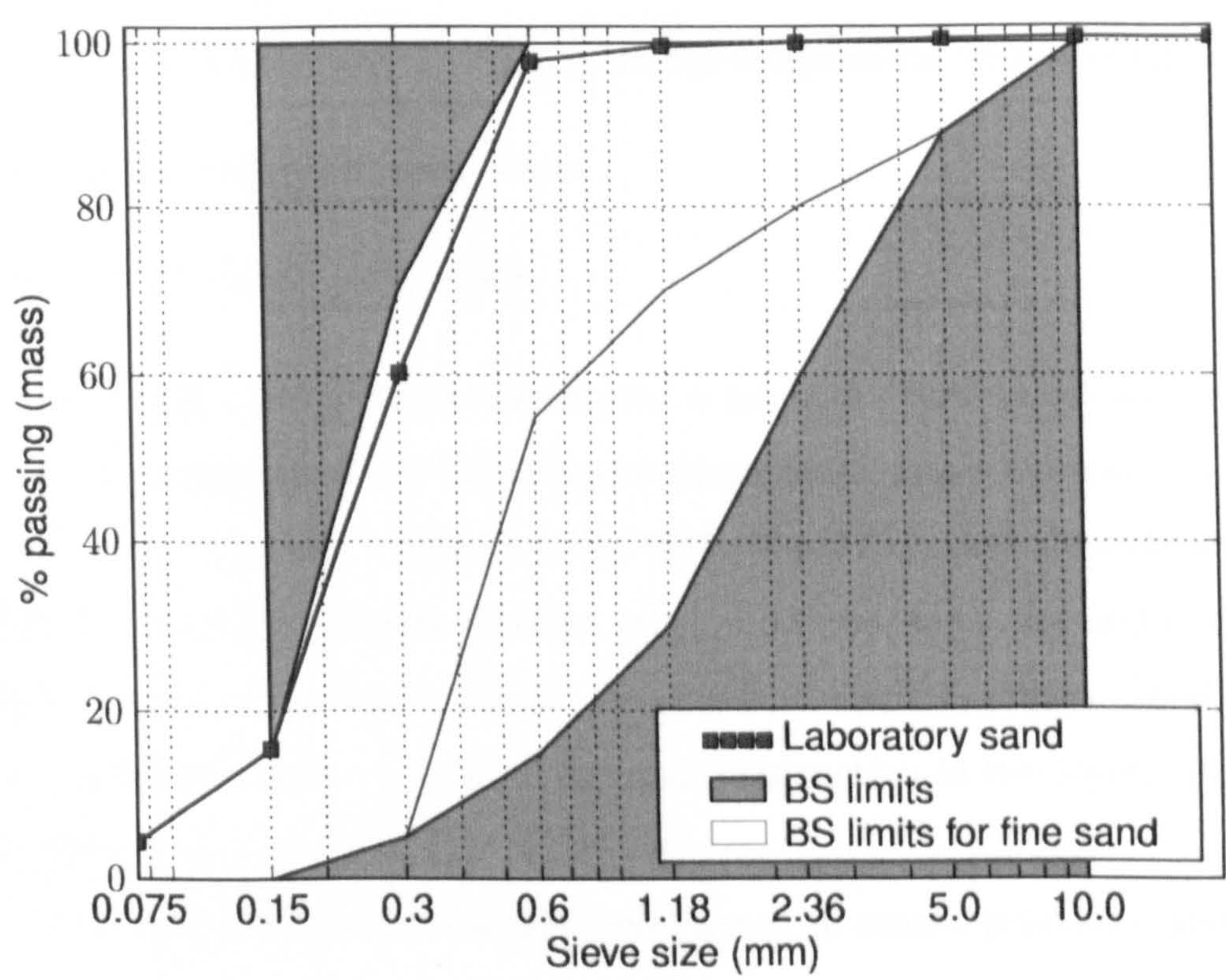


Figure 3.1: Grading of chosen sand for experimental work, and limits from British Standard 882

3.1.2 Experimental method: casting and curing of mortar

Sets of six 100mm mortar cubes were made using each of sands S, K and M, for a range of sand-cement ratios (3,5,7 and 10), and water-cement ratios to determine peak strength. Corresponding sets of three 100mm diameter, 200mm length cylinders were also cast.

The mixing process was:

- Place sand, and clay (when used) in pan mixer.
- If sand and clay were used, mix as dry components until homogeneous.
- Add the mix water, and remix.
- Add the cement, and remix.

The average mixing time was around 5 minutes. Both cubes and cylinders were cast in lubricated steel moulds, and compacted using vibration, according to BS 1881: Part108: 1983 and BS 1881: Part110: 1983 respectively (BSI, 1983c;d). In addition, beam samples, when produced, were cast and vibrated in similar fashion, according to BS1881: Part 109: 1983 (BSI, 1983b). Small (25mm side length) cubes were produced, by hand compaction in two layers, 16 strokes per layer, with a small, square-nosed bar¹.

After demoulding, the samples were stored in sealed polythene sacks until testing at 28 days, to simulate best available curing conditions.

¹It should be noted that there is a size effect on measured strengths with concrete: increasing specimen size is generally associated with a reduction in measured strength (Neville, 1995). The small cubes were intended for comparison between identically-sized cubes, rather than comparison with cubes of other sizes.

3.1.3 Experimental method: testing of mortar

Tests on mortar components

A number of tests exist to characterise the properties of components used in making mortar. Several of these measure size distributions, whilst others cover chemical content etc:

Particle Size Distribution (PSD) Measures the diffraction of an incident laser beam on cement powder suspended in a non-reactive liquid (isopropylalcohol), to give particle sizes, in the range of 1-200nm, and the frequency of their occurrence.

Sieve analysis A known mass of sand passes through a series of sieves of decreasing size. The masses retained on each sieve measure the size distribution of the sand.

Apparent dry density Sand is poured in to a container of known volume, and the mass taken to fill the container measured, giving the bulk, or apparent dry density, of the sand.

Tests on fresh mortar

Several tests were used to measure the workability of the mortar immediately after mixing:

Slump test: measures the distance by which a truncated cone of mortar subsides upon removal of a containing mould. Figure 3.2 shows the general steps for this test, detailed in BS EN 12350-2 (BSI, 2000b).

Vebe test: measures the time for a truncated cone (produced by the slump cone method above) takes to form a flat-topped cylinder when excited in a container. Figure 3.3 shows the general steps for this tested, detailed in BS EN 12350-3 (BSI, 2000d).

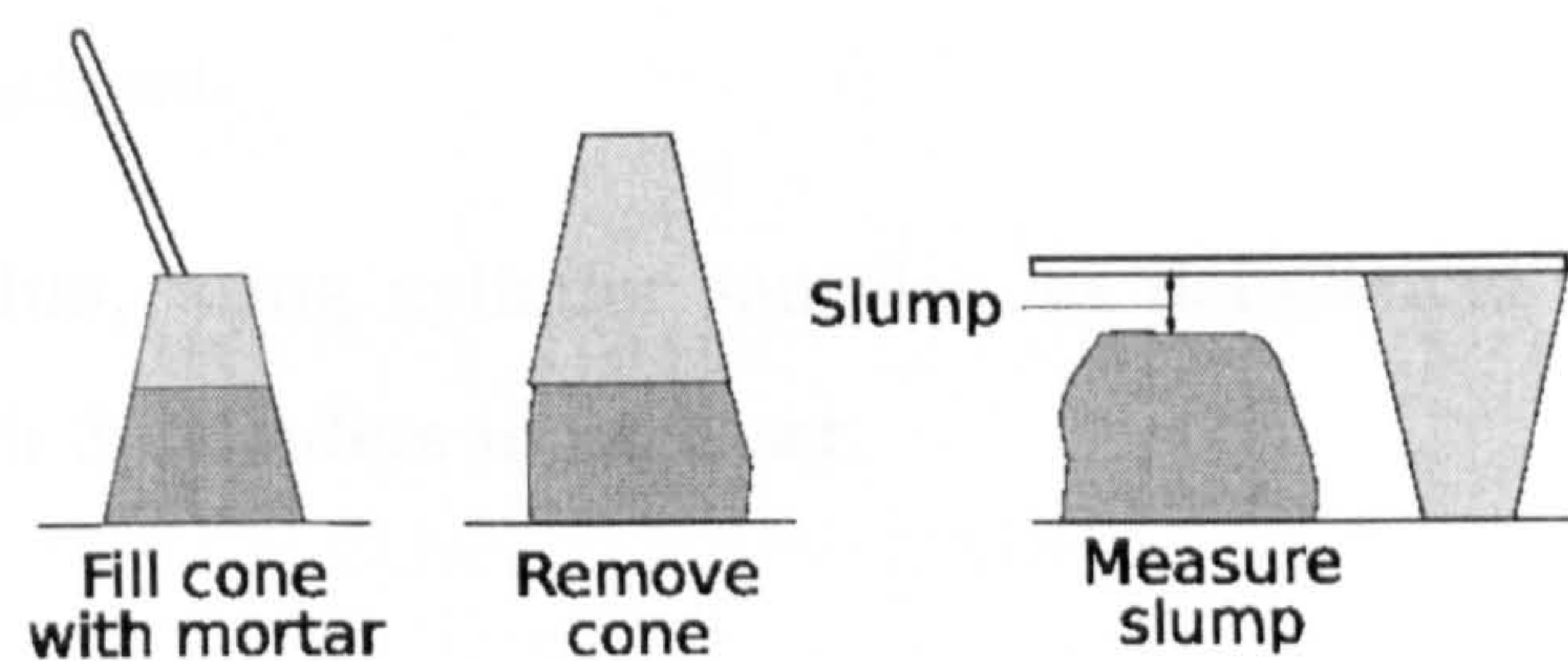


Figure 3.2: Method for conducting the slump test on fresh mortar

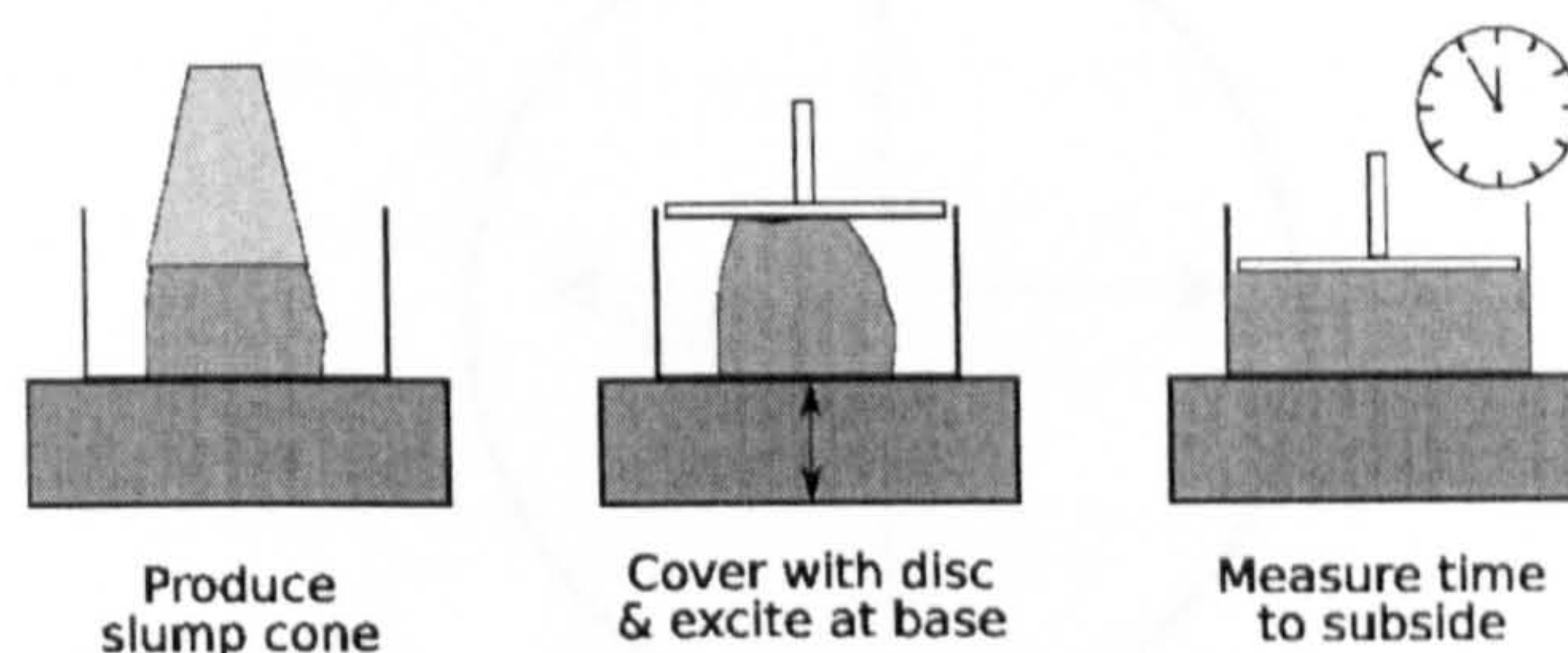


Figure 3.3: Method for conducting the Vebe test on fresh mortar

Tests on hardened, cured samples

A further set of tests were used to measure the properties of the hardened mortar:

Mass, measured prior to strength testing, gave a measure of density.

Compressive strength, measured by crushing cubes to failure. This used standard 100mm cubes for the majority of testing, with small 25mm cubes for testing limited samples obtained from developing countries. In both cases, each set comprised 6 cubes. BS EN 12398-3 (BSI, 2002) gives the details of this test.

Splitting tensile strength, as measured by the Brazilian testing method shown in Figure 3.1.3, and detailed in BS EN 12390-6 (BSI, 2000c), with 3 cylinders in each set.

Tensile flexural strength, or modulus of rupture, using beam samples loaded in four-point bending, detailed in BS EN 12390-5 (BSI, 2000a), with 4

beams in each set.

Young's Modulus, using cylinder samples, as detailed in BS 1881:121 (BSI, 1983a), with 3 cylinders in each set.

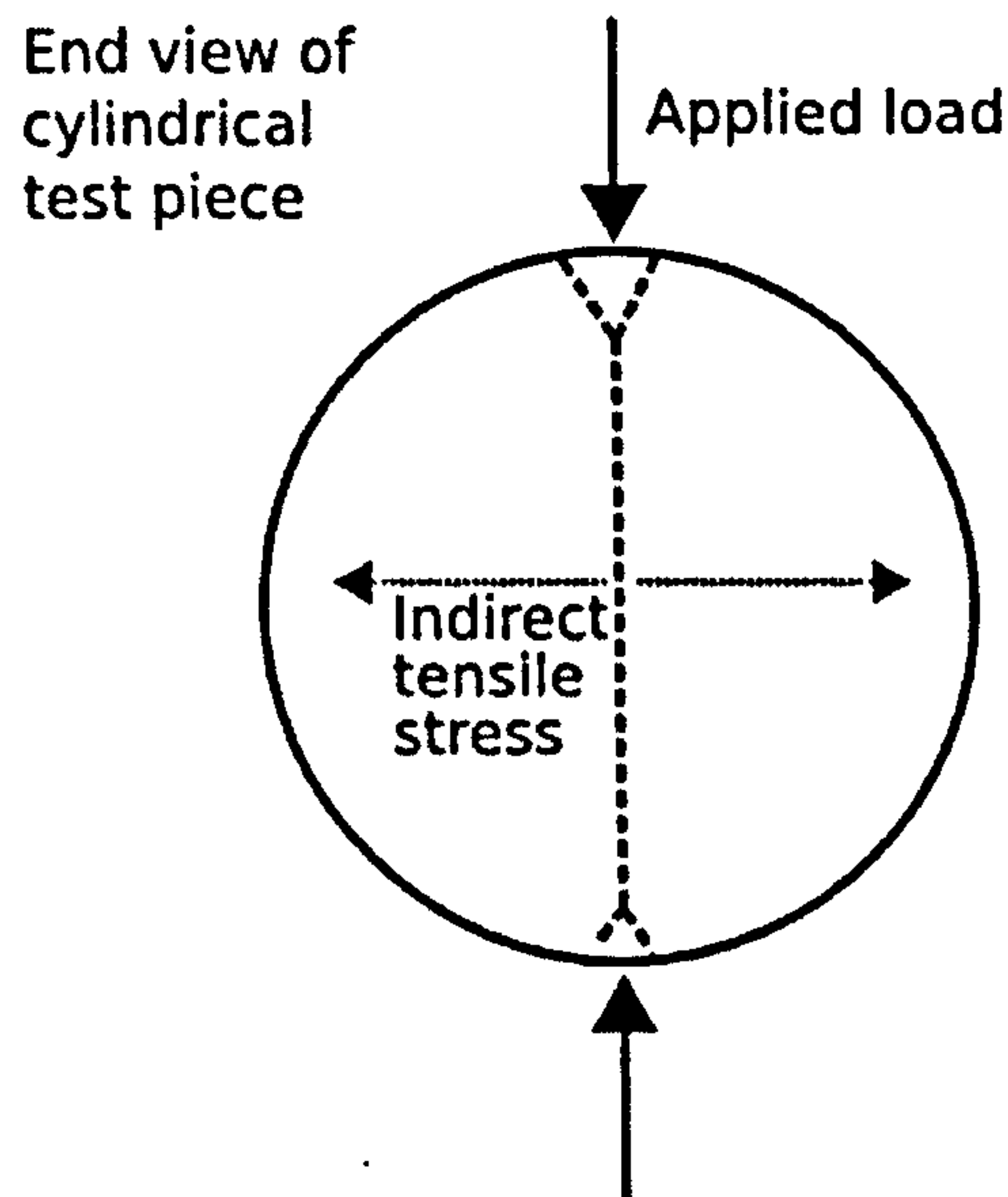


Figure 3.4: Brazilian test for measuring splitting tensile strength of mortar (BSI, 2000c)

Strength and Young's modulus testing took place on a Denison 7231 3000kN hydraulic servo-controlled compression testing machine. For compression testing of the 100mm cubes the load rate was 200kN/min, and for tensile testing of the cylinders 56kN/min.

3.2 Mortar and materials: results and analysis

Unless otherwise stated, all the data in the remaining sections of this Chapter was obtained from experiments conducted by the author, the majority of which were performed with V. Fernandes.

Section D.1 of Appendix D contains Excel spreadsheets with the full experimental data.

3.2.1 Strength relationships

Splitting tensile and flexural tensile strength

Limits on experimental equipment favoured the use of the Brazilian cylinder test for tensile strength. As the structural analysis in Chapter 6 will show, bending loads often dominate the stresses developed in water tanks and similar building elements.

The bending load is more closely approximated in a modulus of rupture test than in a cylinder test, so a smaller sample of beam rupture tests was conducted to measure the strength under this loading. (Neville, 1995) notes that tensile strength as measured through flexure is generally greater than that found from splitting tensile testing, and that data from Melis, Meyer & Fowler (1985) suggests a linear relationship holds between the two for mixes of a given age. Figure 3.5 shows the relationship between rupture (beam) and splitting tensile (cylinder) strengths.

All the beam strengths lie above the line of equality, indicating that splitting tensile strength gives a conservative estimate of flexural strength. Additionally, a linear relationship appears to fit the data well (with an R^2 value of 0.92), with $f_{beam} = 0.6 + 0.94f_{cylinder}$ (all strengths in MPa).

Tensile splitting and flexural strength

For cement-based mortars of interest, splitting tensile strength will give a safe (conservative) estimate of flexural strength.

Compressive and splitting tensile strength

Figure 3.6 shows the strong correlation between tensile and compressive strengths. The data set includes the whole range of sand types, sand-cement and water-cement ratios, and suggests that one may accurately predict the compressive

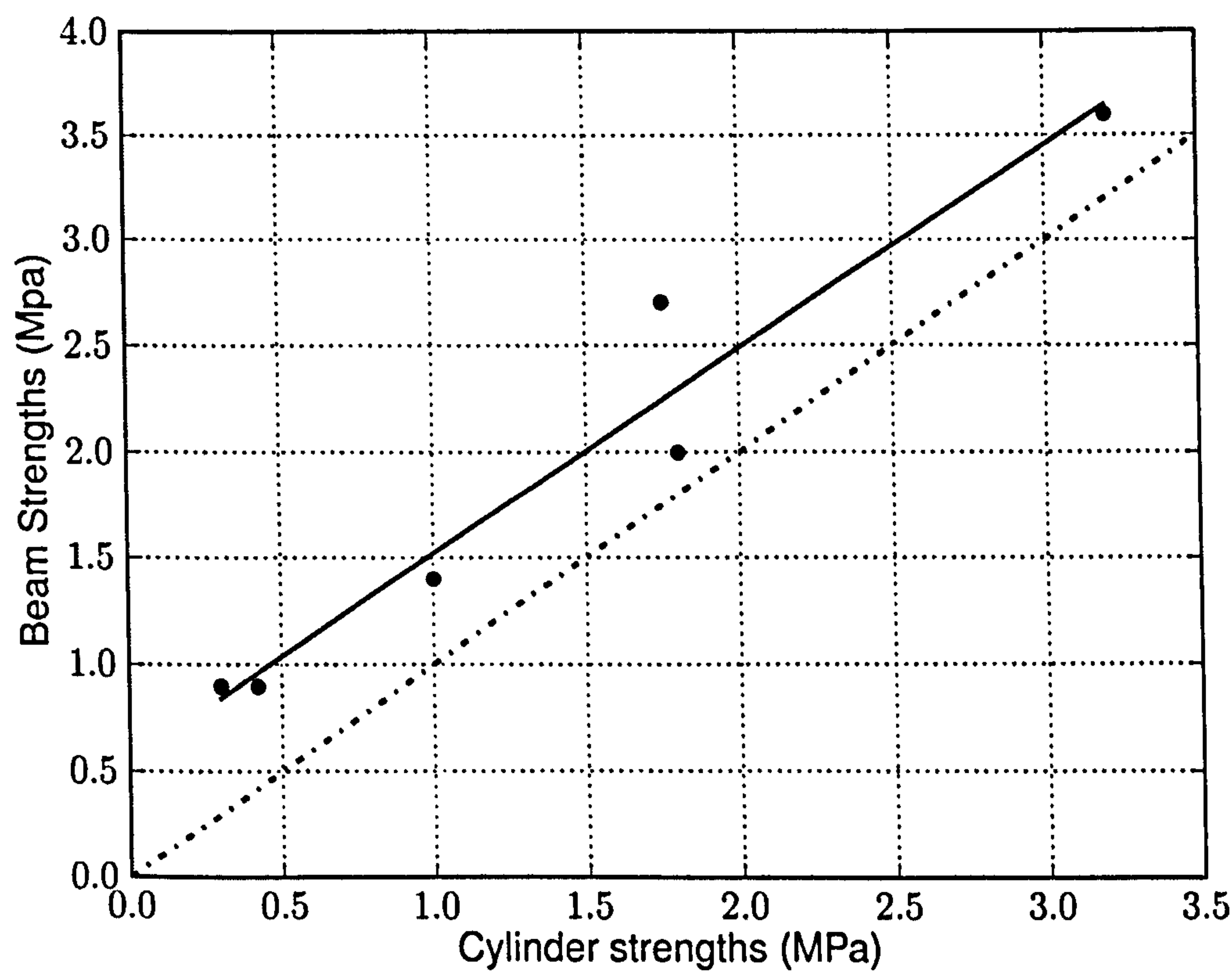


Figure 3.5: Relationship between splitting tensile (cylinder) and flexural tensile (beam) strengths

strength based only on the tensile strength, and vice versa. The power law fit suggested in section 2.2 matches the data reasonably ($R^2 = 0.79$ for raw data, and 0.87 with the four outlier points (2.64,1.34), (3.83,1.78), (11.52,0.65) and (14.15,0.8) removed), with $f_t = 0.17(f_c)^{0.85}$. A simpler, linear fit gives a better approximation ($R^2 = 0.87$ for the raw data, and 0.95 with the same four outlier points removed), with tensile strength 11% of the compressive strength.

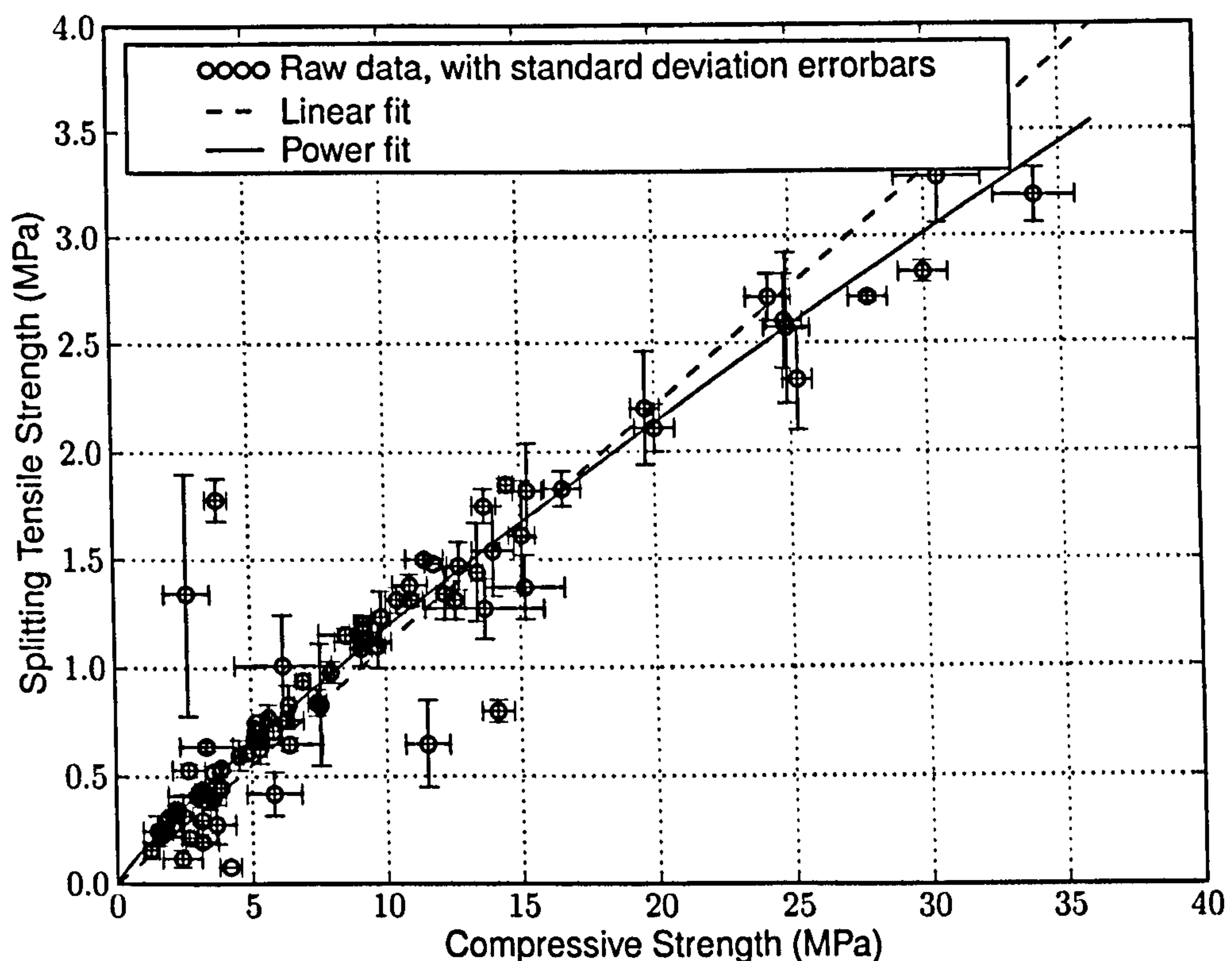


Figure 3.6: Relation between compressive and splitting tensile strengths

This also appears significantly different to the parameters obtained from fitting to the data in Thanh, which gave flexural tensile strength as approximately 24% of compressive. This is still significant despite the difference that the data from Thanh using flexural instead of splitting strength, as the previous section showed the two to give very similar values for mortars of interest.

Tensile and compressive strength

For general use, splitting tensile strength of sand-cement mortars may be estimated as 11% of compressive strength.

The relationship in the box above was chosen as it gives a better fit to the data than the power law relationship, and it is easier to calibrate for a different material by further experimental work.

3.2.2 Strength and water-cement ratio

Figure 3.7 shows a representative sample of the data obtained.

The figure shows expected features:

1. In general, water-cement ratio appears to dominate strength developed, irrespective of sand-cement ratio.
2. However, sand-cement ratio influences the water-cement ratio at which the mix diverges from Abrams' law behaviour, and hence the maximum strength obtainable for a given sand-cement ratio.

3.2.3 Effect of sand type

Abrams' law

Discarding the points that may diverge from Abrams' law behaviour, it remains possible to compare aggregate performance by fitting Abrams' curves through them. Figure 3.8 shows an Abrams' law curve fit for tensile strength. Table 3.1 gives Abrams' constants for compression and tension respectively.

The constants for Abrams' law ($f = \frac{A}{B^{w/c}}$) differ from those obtained in the literature. Both A and B have lower values than those from the literature,² with a more significant difference for A .

² B determines sensitivity of strength to water-cement ratio, as: $s_{s \rightarrow w/c} = \frac{df}{d(w/c)} / \frac{f}{(w/c)} = - (w/c) \ln(B)$

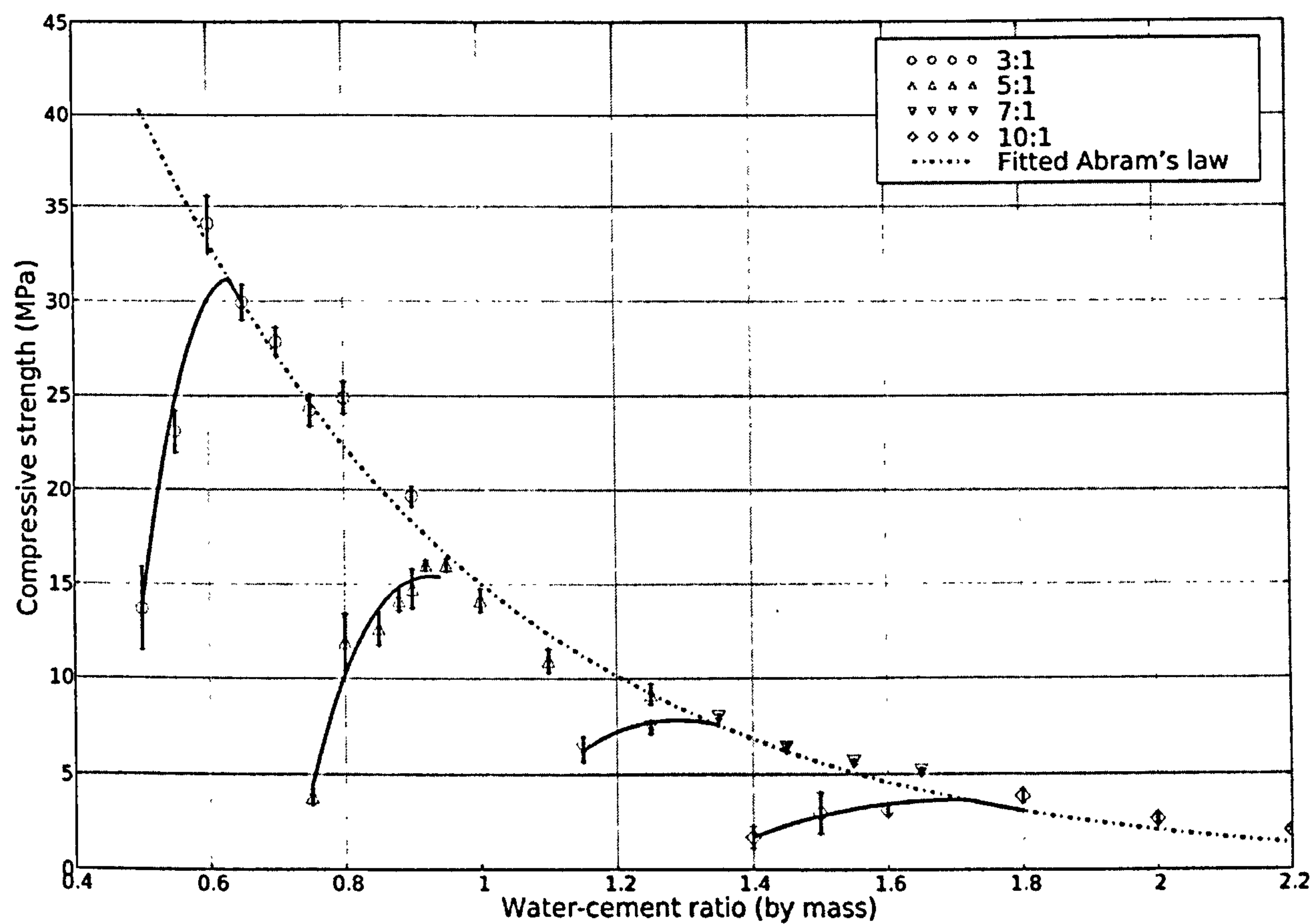


Figure 3.7: Compressive strength data for vibrated mixes using sand S, of varying sand-cement ratios

Table 3.1: Abrams' constants for the three sand types, for compression and tension

Sand type	Compression		Tension	
	A	B	A	B
S	108	7.2	8.2	4.8
K	83	4.9	7.1	3.7
M	46	3.3	4.1	2.8

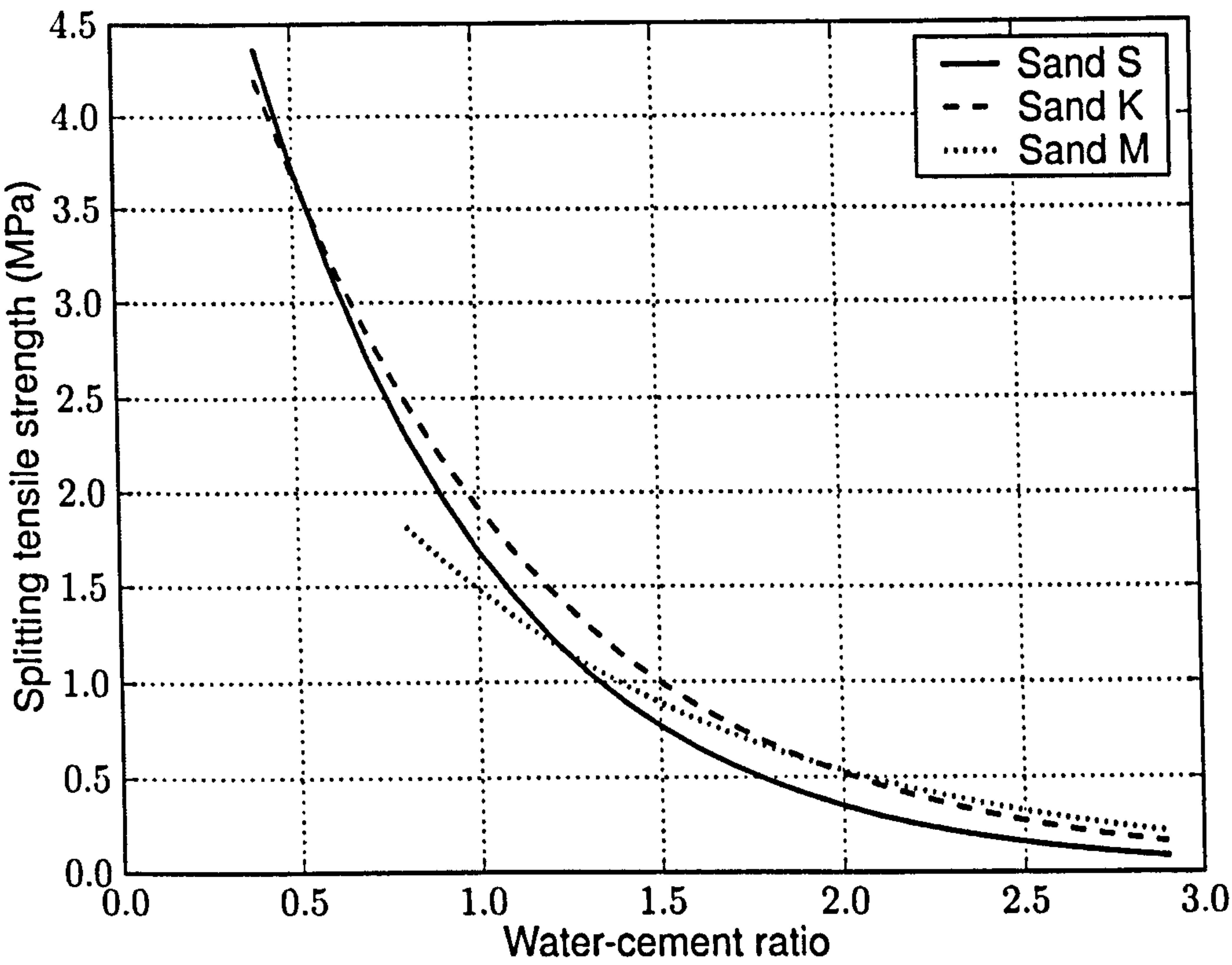


Figure 3.8: Fitted tensile Abrams' curves for the three sand types, for sand-cement ratios of 3:1, 5:1, 7:1 and 10:1

Effect on workability

As expected, increasing the amount of water present in a mix increases its workability. For constant water-cement ratio and sand type, increasing sand-cement ratio reduces the workability.

As mentioned in section 2, some workers have proposed using moisture content rather than water-cement ratio to proportion mixes, particularly in the case of lean concretes. Figure 3.9 shows the variation in Vebe time with moisture content (Figure A.1 in Appendix A shows the corresponding slump data). The increase in moisture content required to achieve the same workability indicates the reduction in workability that the two clays cause compared to the “pure” sand for a given moisture content. It also shows a strongly exponential relationship between Vebe time (t_{vb}) and moisture content (w_{mc}), as shown in Equation 3.1:

$$t_{vb} = a \exp(-bw_{mc}) \quad (3.1)$$

Where a and b represent constants.

The results in Figure 3.9 suggest that:

1. Knowing moisture content allows the prediction of workability, regardless of sand-cement ratio, for a given sand type
2. As the lines appear parallel to each other, this suggests that only constant “ a ” in Equation 3.1 varies with sand type, so measuring the workability of a single mix should suffice to characterise the workability of all mortars made with that sand.

Workability and aggregate type

The presence of clay reduces the workability of mortars, as measured by both slump and Vebe tests. Workability has a strong correlation with moisture content for a given aggregate, irrespective of sand-cement ratio.

Effect on peak strength developed

Table 3.2 shows the peak compressive and splitting tensile strengths for the three sand types and four sand-cement ratios.

Table 3.2: Peak Strengths (MPa)

Sand-cement ratio	Sand S	Sand K	Sand M
0.5	1.2	1.1	1.0
1.0	2.5	2.4	2.3
1.5	3.8	3.7	3.6
2.0	5.1	5.0	4.9

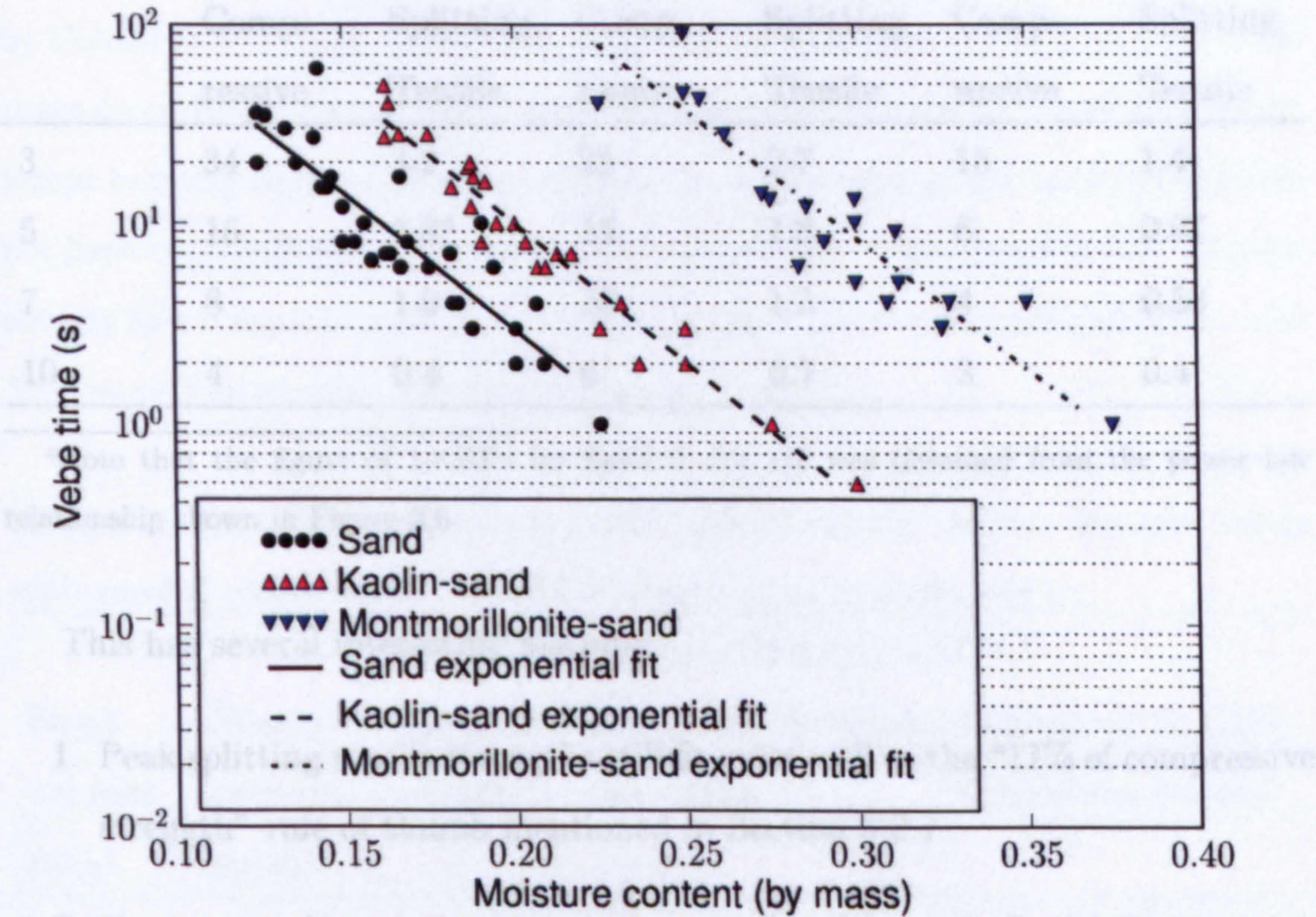


Figure 3.9: Vebe time variation with moisture content

Effect on peak strength developed

Table 3.2 shows the peak compressive and splitting tensile strengths for the three sand types and four sand-cement ratios.

Table 3.2: Peak Strengths (MPa).						
Sand-cement ratio	Sand S		Sand K		Sand M	
	Comp-ressive	Splitting Tensile	Comp-ressive	Splitting Tensile	Comp-ressive	Splitting Tensile
3	34	3.2	25	2.7	15	1.4
5	16	1.8 ^a	15	1.8	6	0.67
7	8	1.0	10	1.3	4	0.58
10	4	0.4	6	0.7	3	0.4

^aNote that the figure of 1.8MPa for Sand S, 5:1 s/c was obtained from the power law relationship shown in Figure 3.6

This has several interesting features:

1. Peak splitting tensile strengths still fit quite well to the “11% of compressive strength” rule of thumb mentioned in Section 3.2.1
2. For low sand-cement ratios mortars made with sands S and K give peak compressive and tensile strengths at least 90% greater than those made with sand M. Mortars made with sand S are 20% stronger than those made with sand K at a sand-cement ratio of 3:1, but are not stronger at sand-cement ratios of 5:1 and above.
3. With increasing sand-cement ratio, the performance of sand S drops relative to both sand K and sand M. Indeed sand K performs better than sand S at sand-cement ratios greater than 5.

3.2.4 Curing Conditions

Several sets of blocks were cured underwater, with drying prior to testing in compression. Table 3.3 shows the results obtained. The data indicates a general reduction in strength from using underwater curing. A students t-distribution comparison between the two samples indicates a significant difference at 95% confidence level for all but the last sample. This seems counter-intuitive: increasing the quantity of water present for curing should have either a neutral or beneficial effect on strength. The results may reflect the masking effect noted by Cebeci *et al.* (1989). Prior to testing, both the samples cured underwater and those cured in polythene sacks rested in the ambient laboratory conditions, to attempt to bring them to identical conditions. The length of this resting time may not have been sufficient to achieve identical degrees of saturation in the samples, leading to a comparison between wet strength of underwater-cured samples, with dry strength of samples cured in polythene bags.

Table 3.3: Effect on compressive strength of curing mortar samples made with sand S either under standard conditions, or underwater

Sand-cement ratio	Water-cement ratio	Compressive Strength (MPa)				
		Standard curing	Standard deviation	Saturated	Standard deviation	% Difference
5	0.9	14.8	1.0	12.3	0.70	-19
5	0.95	16.0	0.3	12.6	0.54	-22
5	1	14.2	0.59	10.8	0.53	-23
3	0.55	23.1	1.1	26.5	0.30	15
3	0.6	34.1	1.5	31.3	1.22	-8
3	0.65	30.0	0.9	29.5	0.50	-1

3.2.5 Young’s Modulus

Two sets of cylinders were cast, using sand-cement ratios of 3:1 and 10:1, and their respective optimum water-cement ratios. Table 3.4 gives the values of Young’s modulus obtained by testing according to BSI (1983a), compared with those predicted by the relationship in Equation 3.2, taken from (Neville, 1995), with E representing Young’s modulus, in GPa, and f_c compressive strength in MPa.

$$E = 4.73(f_c)^{0.5} \tag{3.2}$$

Table 3.4: Young’s moduli of 3:1 and 10:1 mortar samples using sand S, at optimum water contents

Sand-cement ratio	Measured Young’s Modulus (E) (GPa)	Coefficient of Variation	Predicted Young’s Modulus (GPa)
3	12	0.03	26
10	2	0.75	10

The table indicates that in both cases the commonly used relationships significantly overestimate the Young’s modulus. The difference in Young’s modulus measured could arise from several sources:

1. A degree of non-linearity in the stress-strain behaviour of the mortar. Figure 3.10 shows this behaviour, and how it could lead to an underestimate of Young’s modulus.
2. Increasing sensitivity to errors in experimental measurements. The standard used required loading to a specified base stress level, and then to 1/3 of the material strength. In the case of weak mortars, such as the 10:1 mix, there is little difference between these two stress levels, so errors in

readings may become more significant; the high variation coefficient for the weak sample indicates this.

3. The particular materials in question behave differently from the established relationships.

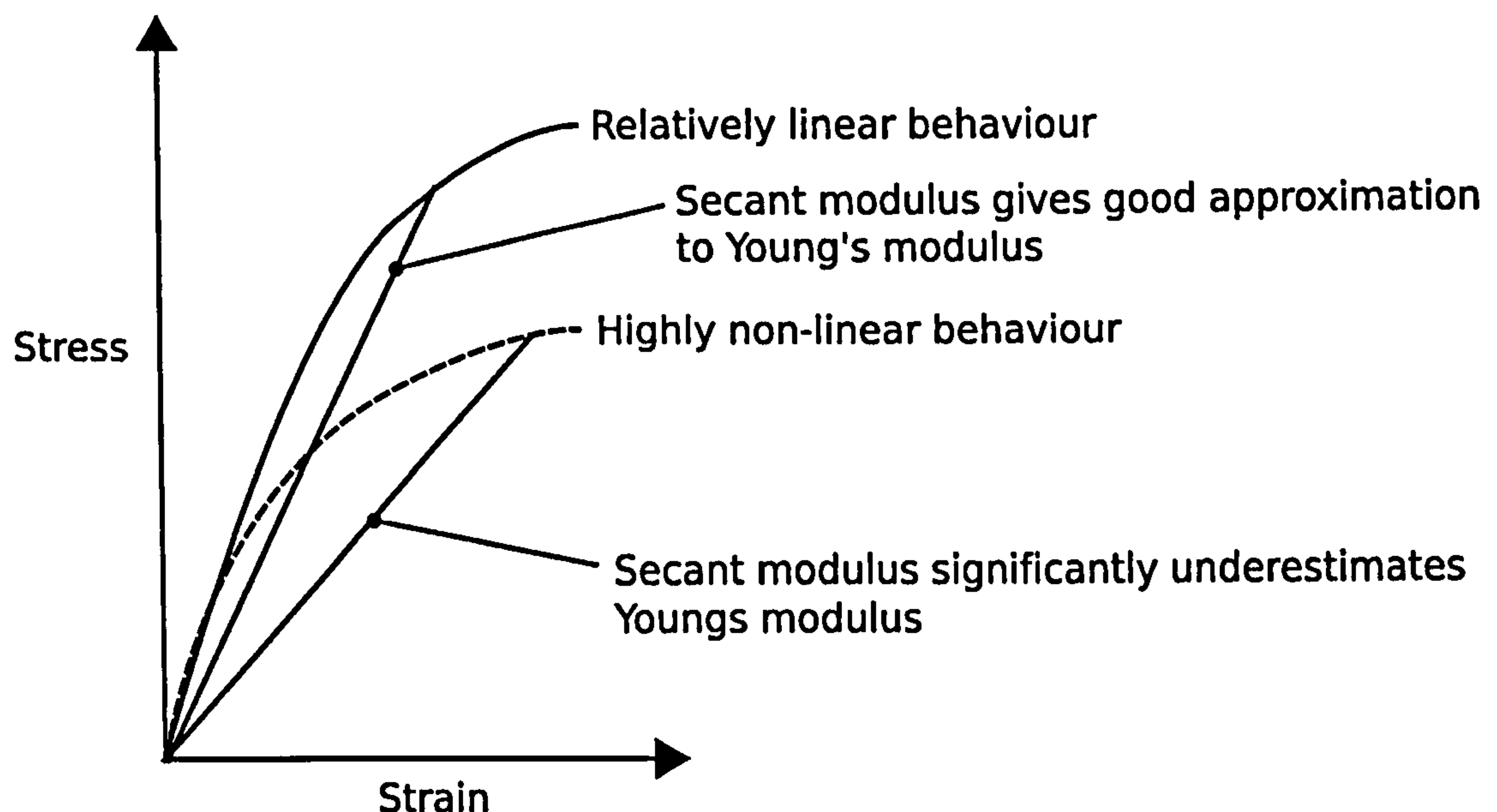


Figure 3.10: Measurement of Young's modulus, and effects of non-linearity

The experiments performed did not record a range of stress-strain data, and so do not allow for testing of hypothesis 1 above. Hypothesis 2 could be addressed by repeated experimentation, but again cannot be addressed by analysing the current small data set. Further experimental work is required before any definitive statement can be made on the matter.

Given the high error on the first sample, it seems more sensible to use a relationship of the form $E = k\sqrt{f_c}$ (with E Young's modulus, k a constant, and f_c the compressive strength), with k calculated from the 3:1 sample. In this case we obtain two values of k for tension and compression of 6.7 and 2.1 respectively, when f_c is measured in MPa, and E in GPa. Although the test to determine Young's modulus uses compressive loading, Neville (1995) states that there is

relatively little literature concerning Young's modulus of mortar in tension, and the data available indicates that, broadly, Young's modulus in tension is equal to that in compression.

3.2.6 Optimising water-cement ratio

As shown in section 3.2.2, strength varies with water-cement ratio for a given mix, rising and then falling with increasing water-cement ratio. Some incentive therefore exists for choosing the water-cement ratio to give peak strength.

Reduction in strength arising from selecting non-optimum water-cement ratio

To quantify the cost of choosing a non-optimal water-cement ratio we take two sand-cement ratios: a rich (3:1) and lean (10:1) mix. For each of these, and for the three sand types used, we compare strengths at 80, 90, 100, 110 and 120% of the optimum water-cement ratio, with peak strength. Figure 3.11 shows the results for this, averaged over the sand types.

The figure shows that, if one is attempting to use the optimum water-cement ratio for a mix, and has the choice between using slightly ($< 10\%$) excess or deficient amounts, it is generally preferable to use excess, as this results in strengths closer to the maximum possible, particularly in the case of rich mixes (the 3:1 mix results shown).

Excess or deficient water-cement ratio

In general it is preferable to use a water-cement ratio slightly greater than the *owcr* than slightly less than it, as this will have a smaller strength penalty, give a more workable mix, and tolerate better any water loss due to evaporation during the casting cycle.

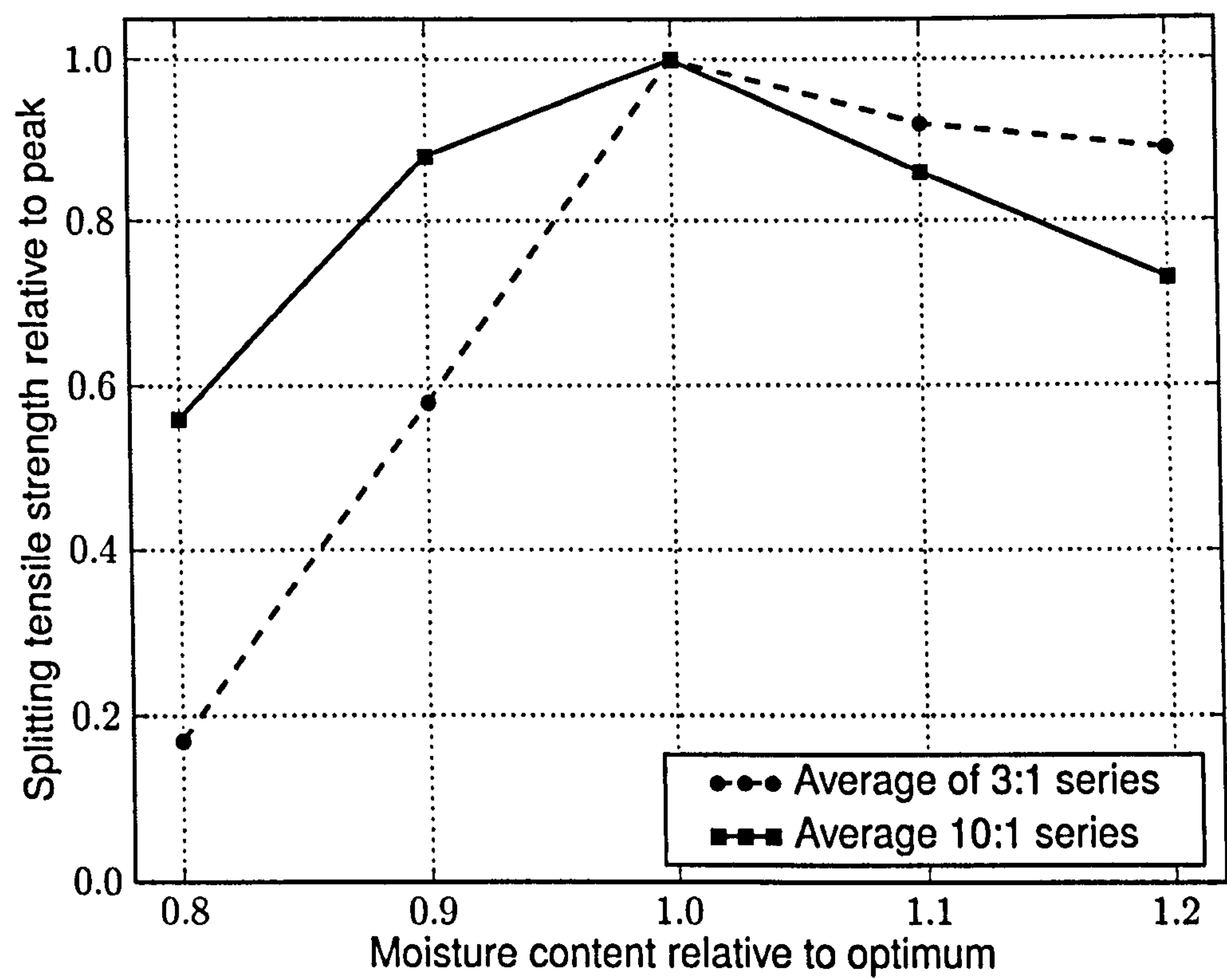


Figure 3.11: Variation in strength relative to peak strength with water-cement ratio around optimum water-cement ratio

Methods for obtaining optimum water-cement ratio

A number of methods might serve to determine the optimum water-cement ratio for a mix. These include:

1. Perform an exhaustive series of tests for every sand-cement ratio and sand type.
2. Determine the optimum moisture content³ experimentally for a realistic mortar (a typical sand-cement ratio), and then use this moisture content to determine the water-cement ratio for all mixes (all sand-cement ratios) made with that sand.
3. Measure density and determine the moisture content to maximise it. Use this moisture content, combined with an universal correction factor to give the water-cement ratio.
4. Measure the workability at optimum water-cement ratio for one sand type, and sand-cement ratio, and, either experimentally or using relationships such as those developed in section 3.2.3 determine the moisture content required to give this workability for any sand-cement ratio.

Method 1 guarantees determination of the optimum water-cement ratio, but requires extensive experimental work. A less labour-intensive method of determining the water-cement ratio therefore becomes desirable. The following sections explain the rationale behind three such methods (2, 3 and 4 above), and evaluate their accuracy.

Water-cement ratio optimisation strategy 2: constant moisture content

We can characterise the peak strength mix for each sand-cement ratio and sand type by a water-cement ratio. Figure 3.12 shows a good linear fit to the relation-

³Optimum moisture content: The moisture content that gives peak achievable strength for a given mix (sand type and sand-cement ratio) and method of compaction

ship between this optimum water-cement ratio and sand-cement ratio.

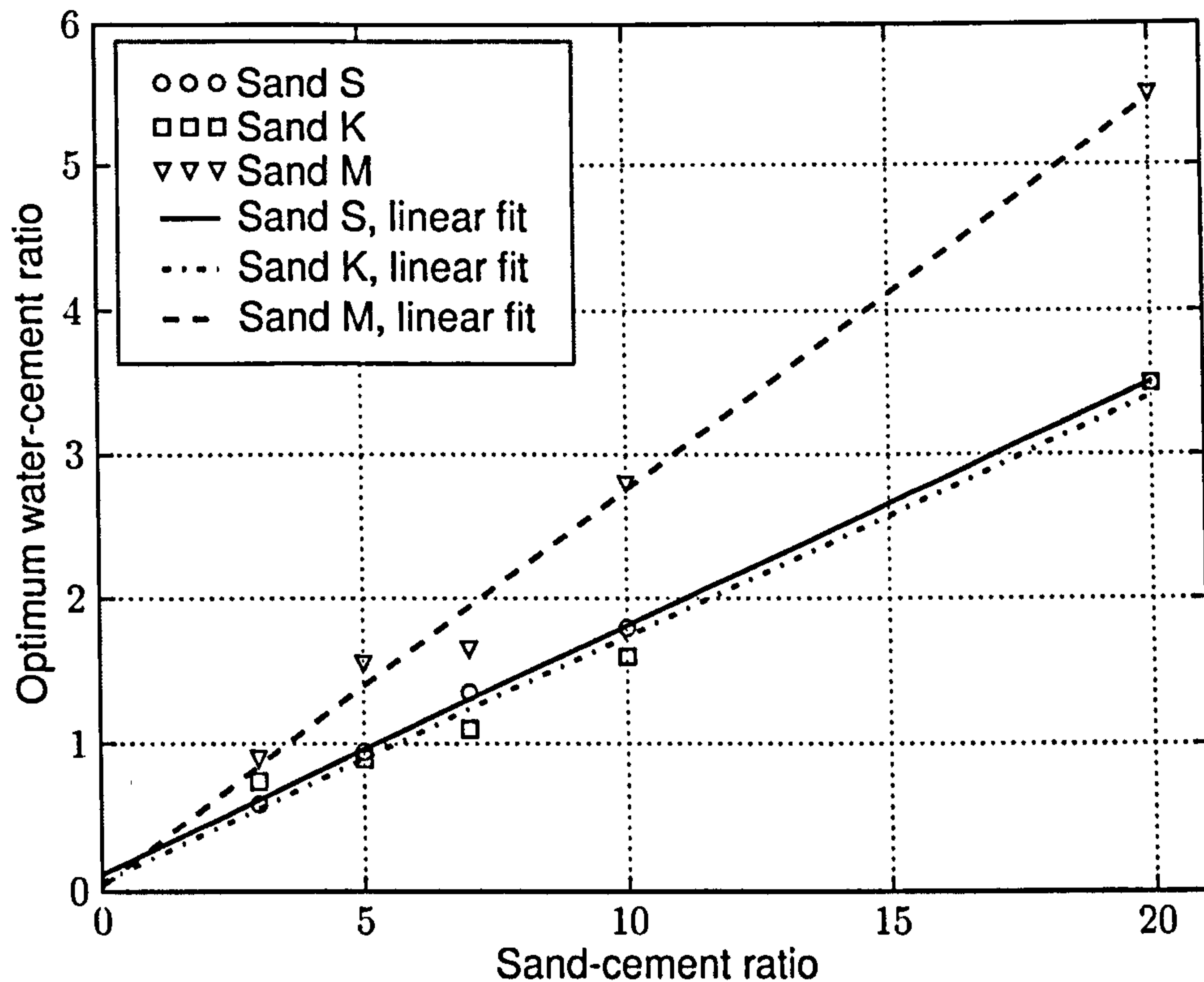


Figure 3.12: Optimum water-cement ratio with sand-cement ratio

Moisture content has a simple relationship to water-cement ratio and sand-cement ratio, shown in Equation 3.3.

$$mc = \frac{w/c}{1 + s/c} \quad (3.3)$$

Where mc represents moisture content, w/c water-cement ratio and s/c sand-cement ratio, all by mass.

As we observe a linear fit between water-cement ratio and sand-cement ratio, $w/c = C + D(s/c)$. If $C \simeq D$ or $D(s/c) \gg C$ and $s/c \gg 1$ then substituting in to Equation 3.3 gives the optimum moisture content⁴ as a constant, dependent only

⁴In soil mechanics literature, optimum moisture content refers to the water content that

on the sand type and compaction method (section A.5 of Appendix A shows this). As section 3.2.3 showed, workability measures such as Vebe time correlate strongly with moisture content, giving another reason to expect optimum moisture content to be constant over a range of sand-cement ratios. Figure 3.13 shows the optimum moisture content for the different sand-cement ratios tested, normalised to the 3:1 *omc* of each set (by aggregate type) and shows broadly constant values, with slightly higher *omcs* for lean mixes.

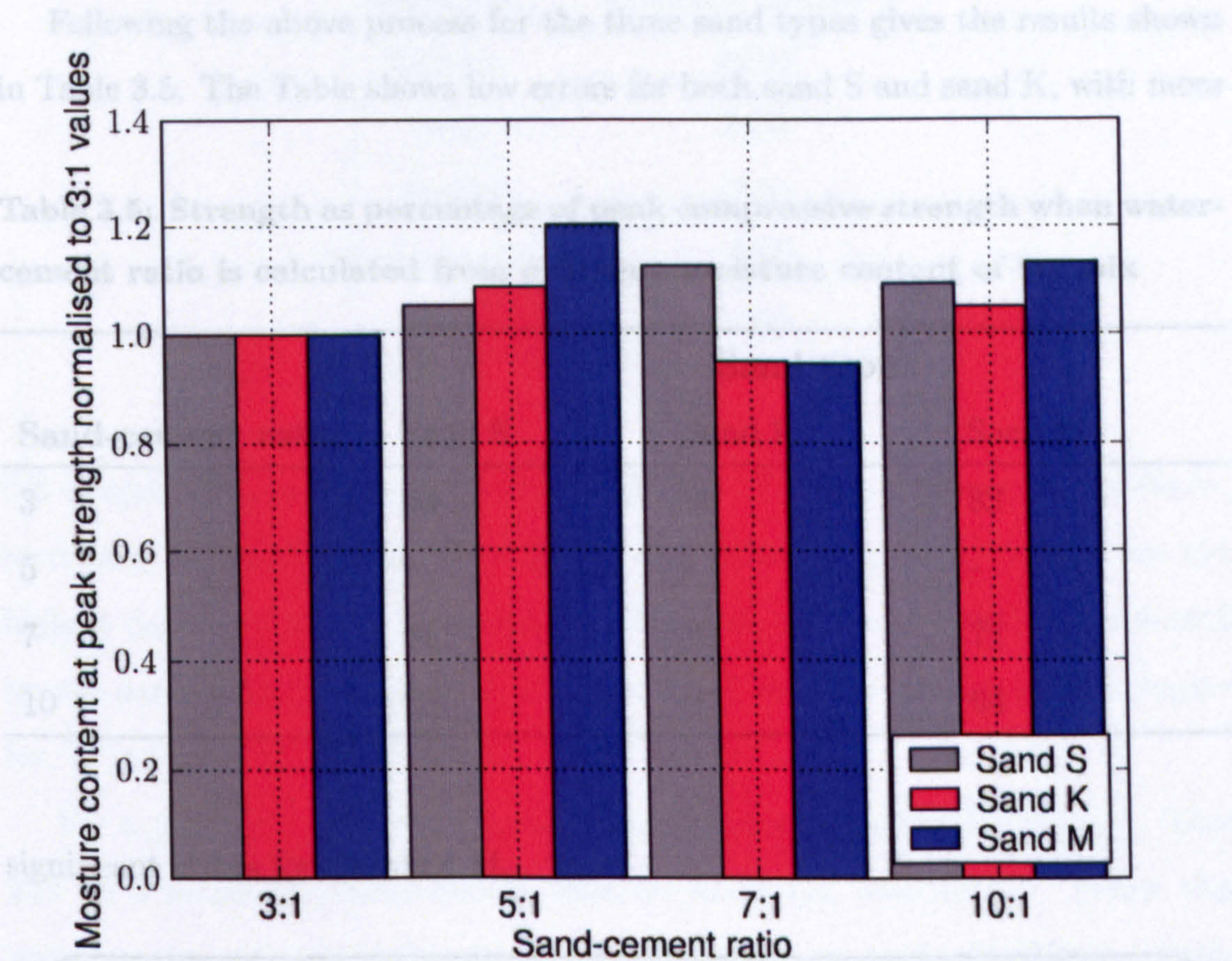


Figure 3.13: Moisture content at optimum strength

If this relationship does hold for a range of sand types, it implies that a single measure characterises the optimum moisture content of mortars, depending only on sand type and compaction method. We might quantify the error in estimating the optimum moisture content by:

maximises density. In this case we use optimum moisture content to indicate the water content giving optimum strength for a given compaction method.

1. Determining the optimum moisture content (*omc*) for a single sand-cement ratio, such as 5:1.
2. Employing the same *omc* for each of the other sand-cement ratios and finding, from experimental data, the strength developed at those ratios.
3. Finding the errors in strength by comparing each strength with the peak value for that sand-cement series.

Following the above process for the three sand types gives the results shown in Table 3.5. The Table shows low errors for both sand S and sand K, with more

Table 3.5: Strength as percentage of peak compressive strength when water-cement ratio is calculated from optimum moisture content of 5:1 mix

Sand-cement ratio	Sand type		
	Sand S	Sand K	Sand M
3	93	90	82
5	-	-	-
7	95	94	71
10	95	97	94

significant errors for the sand M.

Water-cement ratio selection strategy: Constant moisture content

Using the optimum moisture content at a sand-cement ratio of 5:1 to predict the optimum water-cement ratios of mixes of other sand-cement ratios, will give little ($\leq 10\%$) strength penalty for mixes using sands S or K.

Water-cement ratio optimisation strategy 3:
maximum density

All the mixes produced have several components of differing densities, as shown in Table 3.6. Increasing the water-cement ratio should reduce density (providing

Table 3.6: Densities of mortar components

Material	Density (kg/m ³)
Cement	3200
Sand	2300
Kaolin	2600
Montmorillonite	2600 ⁵
Water	1000

full compaction), as water has the lowest density of all the components. Similarly, increasing the sand-cement ratio should also reduce density, as cement has the highest density of all the components. This leads to the expectation, confirmed by the data, that the density of a block cannot serve on its own as a surrogate for, or indicator of, strength.

For a given mix (sand-type, sand-cement ratio and compaction regime), there will be a minimum water-cement ratio to allow full compaction. Below this water-cement ratio, the air voids in the mix will increase significantly, and this will reduce the density. Above this water-cement ratio, there will be no decrease in air content with increasing water-cement ratio, but the overall density will drop, as the mix will contain a higher fraction of water, which is less dense than the cement and sand. In this case, measuring the density of freshly cast blocks might give an indirect method of identifying whether optimum water content had been achieved for that mix and compaction method. Figure 3.14 shows these variations for the 5:1 sand mix.

Using the raw data, a Simple Peak approach gave the results shown in Table 3.7. In all cases calculating the optimum water-cement ratio on the basis of maximising density after curing would give a value less than or equal to the peak strength. In the case of sand K, the optimum water-cement ratio correctly identifying the optimum water-cement ratio, the fourth case having an error of only 6%.

Table 3.7: Strength as percentage of peak compressive strength when water-cement ratio is chosen as that giving peak density

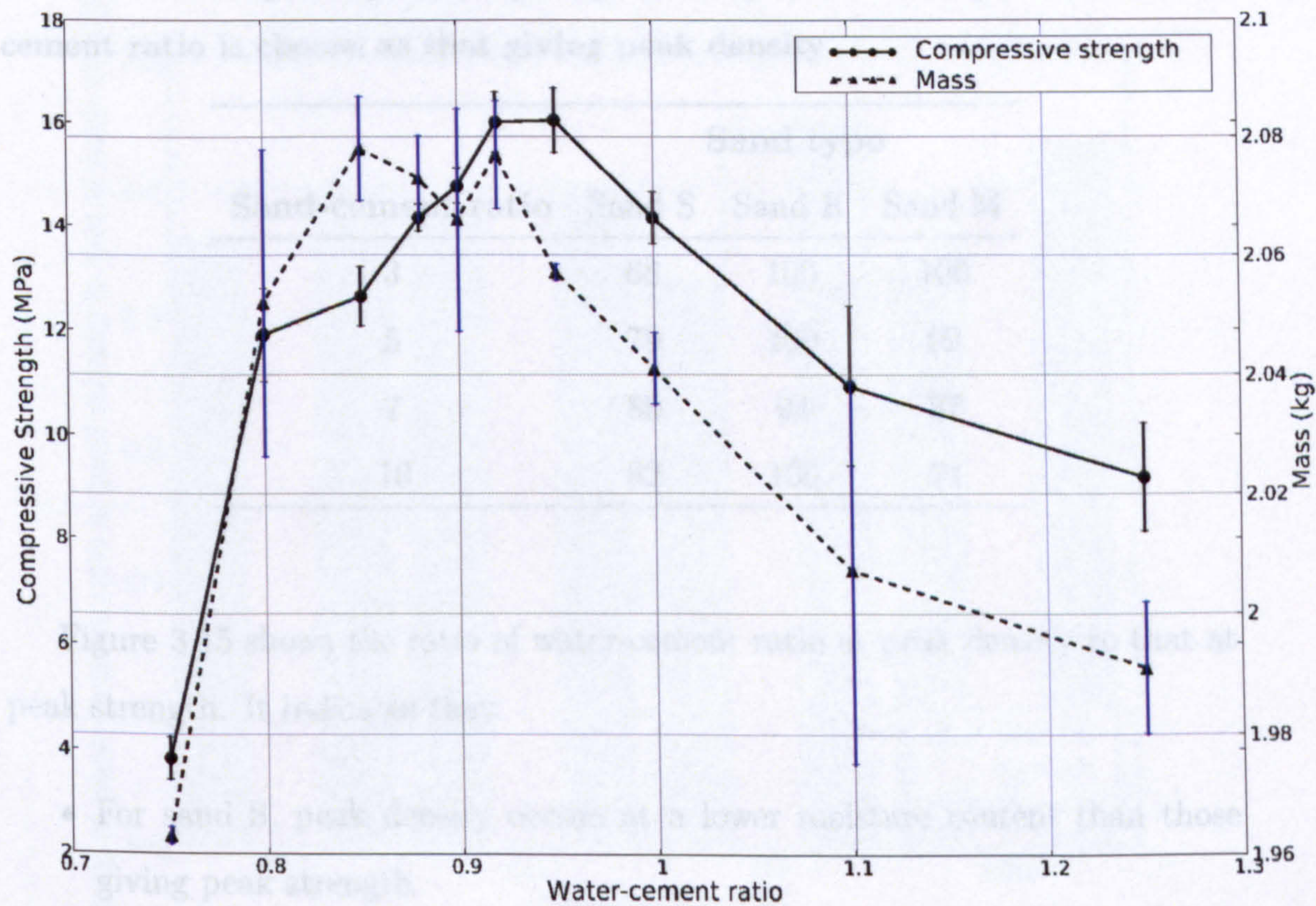


Figure 3.14: Density and strength variation with water-cement ratio for 5:1 sand series S

Using the raw data, a simple lookup approach gave the results shown in Table 3.7. In all cases estimating the optimum water-cement ratio on the basis of maximising densities after curing would give strengths less than or equal to the peak strength. In the case of sand K the estimations seem accurate: in three cases correctly identifying the optimum water-cement ratio, the fourth case having an error of only 6%.

Table 3.7: Strength as percentage of peak compressive strength when water-cement ratio is chosen as that giving peak density

Sand-cement ratio	Sand type		
	Sand S	Sand K	Sand M
3	68	100	100
5	79	100	92
7	80	94	87
10	82	100	71

Figure 3.15 shows the ratio of water-cement ratio at peak density to that at peak strength. It indicates that:

- For sand S, peak density occurs at a lower moisture content than those giving peak strength.
- For sand K, peak density and peak strength occur at similar water contents
- For sand M, peak density occurs at higher moisture contents than those giving peak strength.

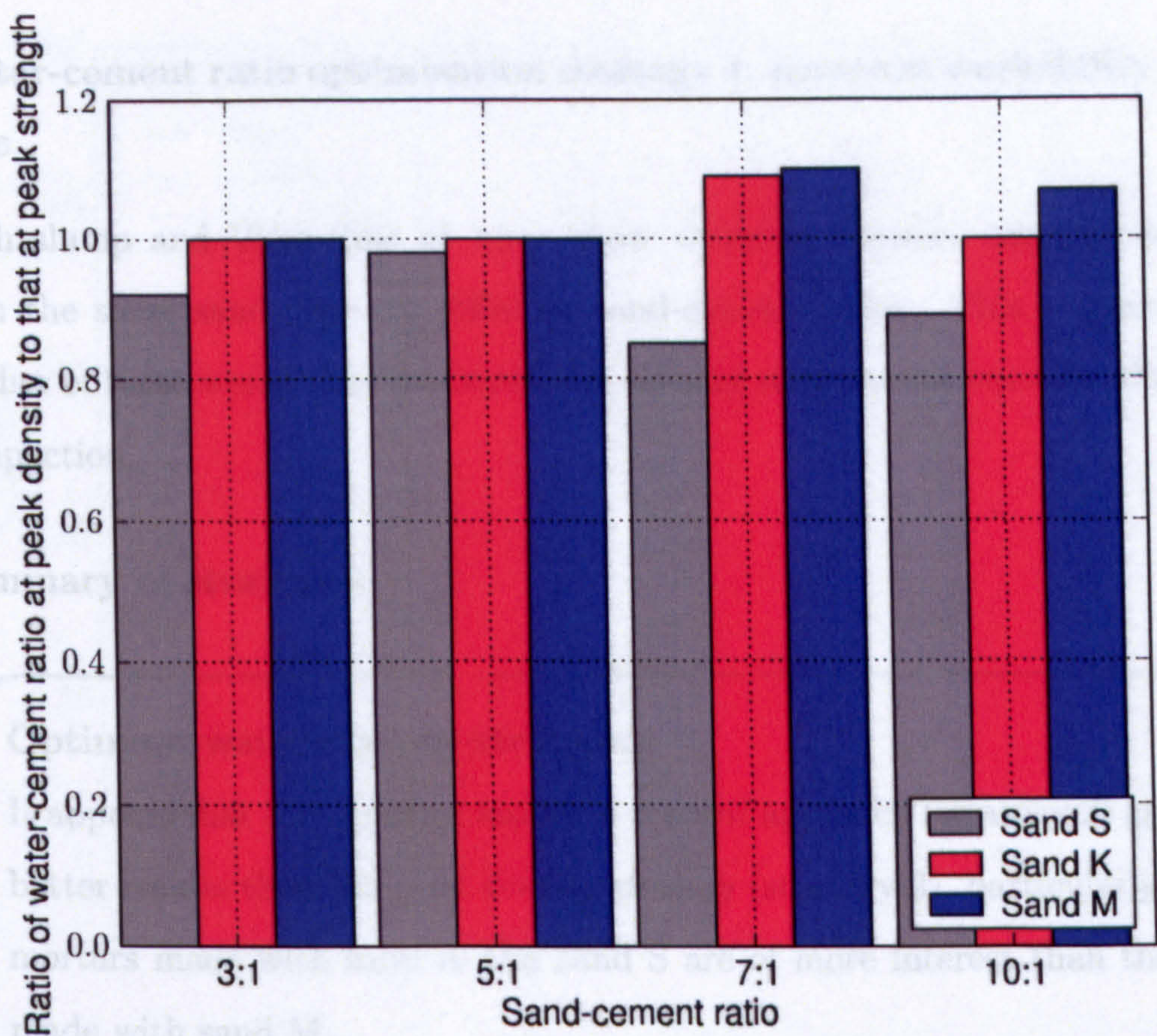


Figure 3.15: Comparison of water-cement ratio to give peak density, and that to give peak strength for 3 sand types and 4 sand-cement ratios

3.2.7 Cement

To fully assess the performance of cements found locally in LEDCs would form a thesis in itself. For this work we considered it sufficient to examine a few characteristics, namely:

- Particle size distribution

Water-cement ratio selection strategy: peak density

In the case of mixes using sand K, using water-cement ratio leading to peak density to predict optimum water-cement ratio will give little ($\leq 10\%$) penalty in strength. Both sand S and sand M have significant errors using this approach.

Water-cement ratio optimisation strategy 4: constant workability measure

Both slump and Vebe time at *owcr* show variation between sand types, and with the same sand type for different sand-cement ratios. This suggests that neither of these workability measures can reliably indicate the *owcr* for vibration compaction.

Summary of strategies**Optimum water-cement strategies**

It appears that the *constant moisture content* approach (strategy 2) gives better results than the *peak density strategy* (strategy 3), particularly as mortars made with sand K and sand S are of more interest than those made with sand M.

3.2.7 Cement

To fully assess the performance of cements found locally in LEDCs would form a thesis in itself. For this work we considered it sufficient to examine a few characteristics, namely:

- Particle size distribution

- Strength developed

Particle size distribution

Figure 3.16 shows the results obtained from a laser diffraction test on a number of cement samples, intended to compare the Type I OPC used in experimental work with cements from developing countries.

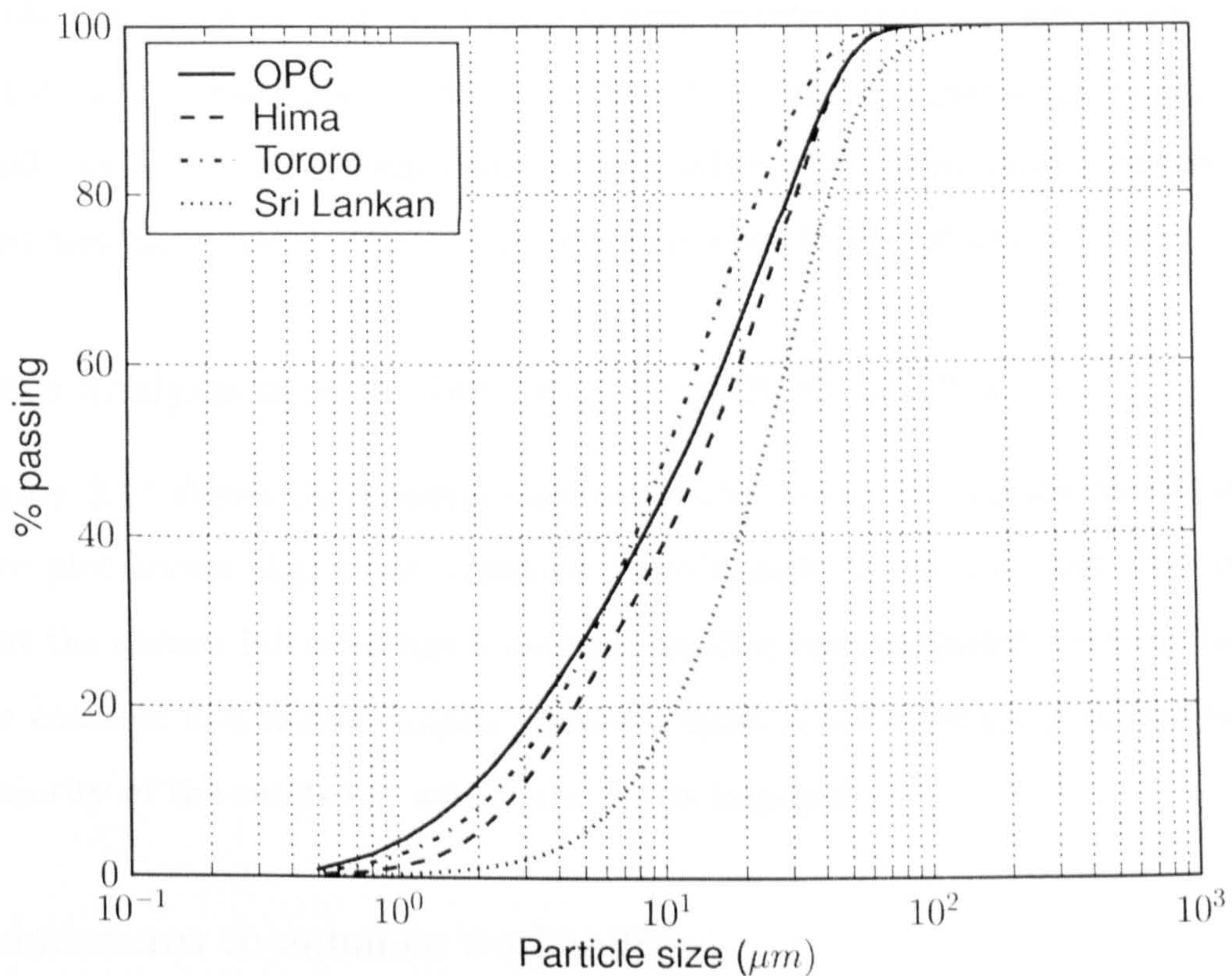


Figure 3.16: Particle size distributions of cement samples

PSD constitutes an area in which LDC cements might differ from those available, with coarser cement costing less to produce. However, the results indicate no significant difference in gradings between the OPC and the Ugandan samples (“Hima” and “Tororo”). The Sri Lankan cement does appear coarser, having about 1/3 the surface area of the OPC. However, this sample was delivered from the supplier in a non-protective (newspaper) container, and stored in this during transport through the country and to the UK, whilst the other samples were all

sealed in plastic bags within containers until testing. This leaves the possibility that changes in size distribution were due to storage conditions in transit, rather than a difference experienced by the user on purchase.

Strength developed

Ruthven (2005) produced a series of small cubes, made with four cement types, using samples obtained from Sri Lanka and Uganda. The data, summarised in Table 3.8, suggests that the local cements develop their strength more slowly, but do give similar long-term strengths. This small sample suggests that some small correction for strength might be needed when using local cements, or at least test pieces produced, as tank use will start before 28 days of curing.

3.2.8 Sieve analysis of some building sands from LEDCs

Figure 3.17 shows the grading curves obtained from sieving the sand samples. The plot shows significant variation from sample to sample, but also suggest that the chosen lab sand has a medium grading approximately midway between the coarsest and finest samples obtained from three developing countries. The majority of the sands fall within the limits imposed.

3.2.9 Admixtures to enhance workability

In general, plasticisers are used as water-reducing admixtures. They are adsorbed on the surface of cement particles, and the negative charge they give results in repulsion between the particles, and their deflocculation. As the particles become more mobile, this frees some water that would otherwise have been restrained by the flocculated system. This freed water acts to lubricate the mix, increasing workability.

Testing conducted in parallel with this project investigated the action of several plasticisers on a 5:1 mix using sand K (Aldridge, 2005). Testing used three plasticisers:

Table 3.8: Compressive strength of small (25mm) cubes, made with cements from Uganda, Sri Lanka, and a Type I OPC (Ruthven, 2005)

^a

Cement type	Temperature			
	23°C		38°C	
	Compressive Strength (MPa)	% of OPC Strength	Compressive Strength (MPa)	% of OPC Strength
28 days				
Sri Lankan	4.63	99	4.73	66
Hima	2.83	60	7	97
Tororo	3.95	84	7.01	97
Type I OPC	4.7	100	7.2	100
100 days				
Sri Lankan	0.83	99	1.06	83
Hima	0.66	79	1.27	99
Tororo	0.77	92	1.08	84
Type I OPC	0.84	100	1.28	100

^aThe table shows the strengths at two times of testing, under two different temperatures of curing, and for four different cements. For each combination of age and temperature the results are also listed as percentages of the strength achieved with the OPC

Superplasticiser Coupler 2P21 from Yansu.

Plasticiser Coupler P211 from Yansu.

Low-cost plasticiser Waplogap 501, Sinochem 130 from Foshan Petrochem.

The results (Table A.5 in Appendix A) indicated that all three of the plasticisers used increased workability as measured by slump and flow test. This fortunately allowed for a better comparison of the results to be derived from Abrams' law to give some idea of the degree to which the admixtures enhance the flow of concrete.

For the concrete made with the three plasticisers, the results of the tests showed that the concrete made with the plasticiser Coupler 2P21 from Yansu had the greatest strength, followed by the concrete made with the plasticiser Coupler P211 from Yansu, and the concrete made with the plasticiser Waplogap 501, Sinochem 130 from Foshan Petrochem. The results of the tests also showed that the concrete made with the plasticiser Coupler 2P21 from Yansu had the lowest water-cement ratio, followed by the concrete made with the plasticiser Coupler P211 from Yansu, and the concrete made with the plasticiser Waplogap 501, Sinochem 130 from Foshan Petrochem. The results of the tests also showed that the concrete made with the plasticiser Coupler 2P21 from Yansu had the highest compressive strength, followed by the concrete made with the plasticiser Coupler P211 from Yansu, and the concrete made with the plasticiser Waplogap 501, Sinochem 130 from Foshan Petrochem.

Figure 3.17: Sand gradings for building sands: Developing Country samples

A simple model for bedding load calculation, based on the assumptions given in Table 3.9, and following the process shown in the flow-chart in Figure 3.15, Section A.7.1 gives an example calculation, while Section D.2 in Appendix D gives the source code for the model.

For a given sand type the relationships established earlier in this chapter allow calculation of the peak strength and water-cement ratio giving this strength, based on water-cement ratio and sand type. For a given design stress and geometry, the required thickness can be calculated. Knowing the mass ratios of components in the mix and their respective densities, the quantities of each

Superplasticiser Conplast SP430 from Fosroc.

Plasticiser Conplast P211 from Fosroc.

Low-cost plasticiser Washing-up liquid Savona D20 from Premiere Products.

The results (Table A.6 in Appendix A) indicated that all three of the plasticisers used increased workability as measured by slump and Vebe test. Unfortunately Aldridge did not reduce water-cement ratio sufficiently to diverge from Abrams' law behaviour and establish the degree by which the admixtures enhanced the strength of the mortar.

For the same water-cement ratio, the increased exposed area of cement, and greater quantity of freed water may raise the rate of hydration in the early stages, leading to higher strengths. As a counter to this, some plasticisers act as air-entraining agents. Whilst this improves workability, the increased air voids content in the mix acts to reduce strength. The data from Aldridge appears to show a strength reduction with the addition of each of the plasticisers, combined with lower densities. This suggests that this air-entraining behaviour may be outweighing any effect the plasticisers have to increase the rate of hydration, for the samples produced.

3.2.10 Economic Optima: Sand-cement ratio selection

A simple model for bending loading was implemented, (based on the assumptions given in Table 3.9, and following the process shown in the flow-chart in Figure 3.18) Section A.7.1 gives an example calculation, while Section D.2 in Appendix D gives the source code for the model.

For a given sand type the relationships established earlier in this chapter allow calculation of the peak strength and water-cement ratio giving this strength, based on sand-cement ratio and sand type. For a given design stress and geometry, the required thickness can be calculated. Knowing the mass ratios of components in the mix, and their respective densities, the quantities of each

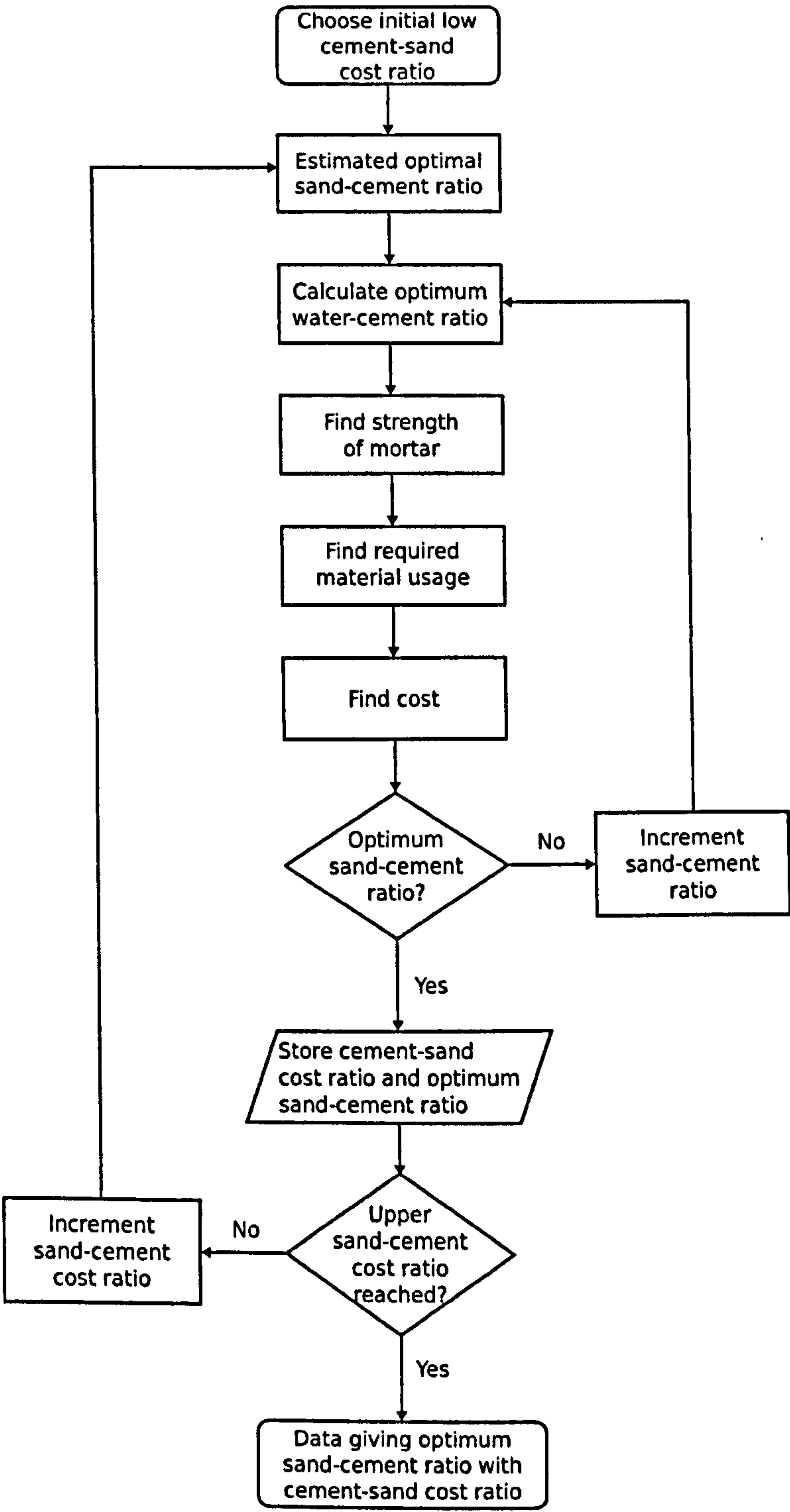


Figure 3.18: Sand-cement optimisation process

Table 3.9: Assumptions for selection of most economic sand-cement ratio

Optimum tensile strength and water-cement ratio can accurately be predicted from sand-cement ratio and sand type
Labour has a negligible cost compared to materials
Water has no cost relative to sand and cement, and so water-cement ratio may be adjusted to give optimum strength with no penalty

component present can be calculated. From the component quantities and their unit costs, the total materials cost can be determined. This allows for determination of materials cost from loading regime, cement-sand cost ratio, sand type and sand-cement ratio. Holding the first three of these constant allows for minimisation of cost with respect to sand-cement ratio, leading to an optimum sand-cement ratio. Repeating this process for a range of cement-sand cost ratios (using the range of 20:1 to 70:1 mentioned in Section 2.1.4) gives a characteristic curve for the sand type. Figure 3.19 shows the results for all three sand types; an optimum sand-cement ratio of around 6 for both sand S and sand M, over a wide range of sand-cement cost ratios, whilst the sand K mixes have a higher optimum sand-cement ratio, ranging from around 7.5 to 9.5.

This changes significantly in the case of membrane action (direct loading), with the optimum sand-cement ratios falling to around 3 for sands S and M, and around 4.5 for sand K (Figure A.2 in Section A.7.2 of Appendix A shows this graphically).

Whilst the optimum sand-cement ratio does change appreciably with cement-sand cost ratio, over the range of interest it varies by only around 1 for each sand type. This suggests that one might take a more convenient approach of using a single, constant, sand-cement ratio for each sand type, or even for all sand types. The average of sand-cement ratios over the typical cost range seems a sensible value to use. For the data shown in Figure 3.19 this gives values of 5.8, 8.7 and 7.5 for sands S, K and M respectively, with an overall average of 7.3.

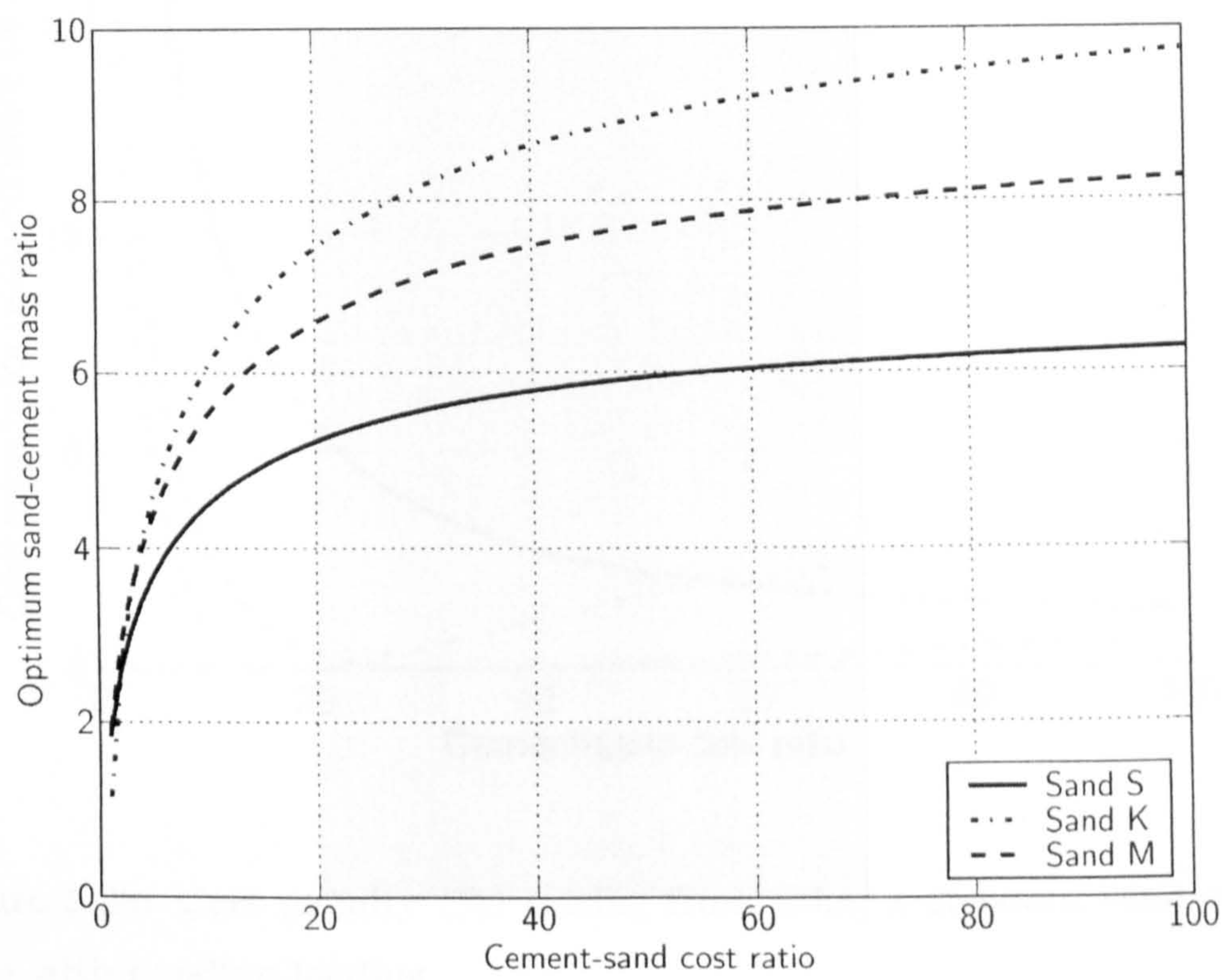


Figure 3.19: Economic optimum sand-cement ratio for bending load
(Note: shaded area indicates typical cost ratios in LEDCs; between 20 and 70)

Figure 3.20 shows the cost penalty, as a percentage of the optimal (minimum) cost, arising from using this mean sand-cement ratio for all sand types, over a range of cement-sand cost ratios.

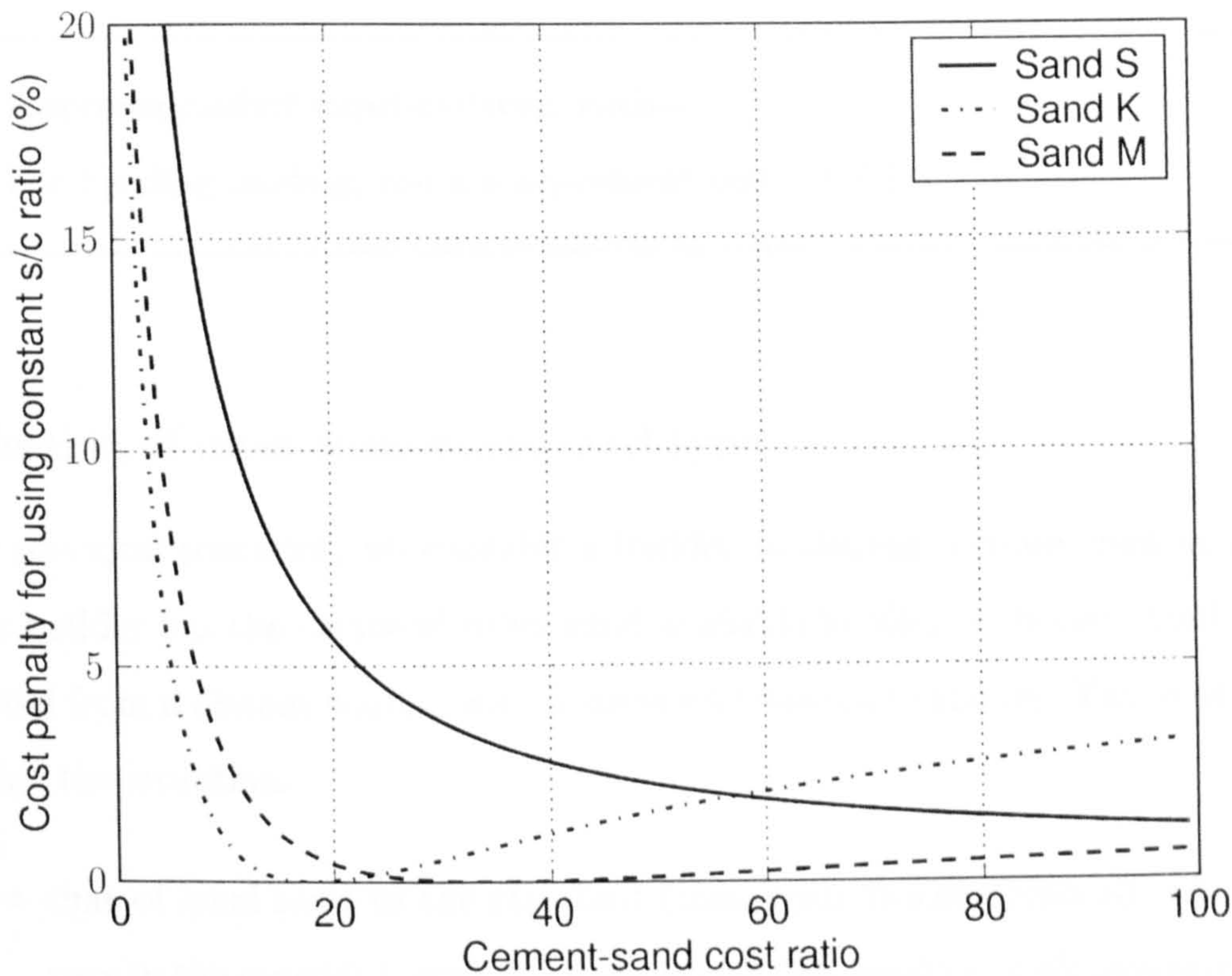


Figure 3.20: Cost penalty (%) arising from using a constant sand-cement ratio with bending loading

This clearly shows that at extremely low cement-sand cost ratios, using the mean sand-cement ratio incurs a significant cost penalty. However, this penalty rapidly diminishes with increasing cement-sand cost ratio, falling to around 10% at cement-sand cost ratios of 10:1. This suggests that, for typical cement:sand cost ratios, using a constant sand-cement ratio will not incur a large cost penalty, compared to using the optimal sand-cement ratio.

Applying the same analysis to loadings where maximum stress varies inversely with thickness (tanks where membrane/hoop stresses dominate, or building slabs under self load) gives similar results.

The most useful practical result would be one of suggesting an optimum sand-cement ratio, irrespective of loading type, sand type and cement-sand cost ratio. To obtain this value we might first try taking the mean of optimal sand-cement ratios for the different sand types under bending and membrane loads.

Recommended sand-cement ratios

For bending loading, use a sand-cement ratio of 7:1.

3.2.11 Selection of most economical sand type

For practical scenarios, we consider a builder producing a component at a site. The builder has the choice of using sand available locally, or ‘better’ sand transported from a distant source, with associated transport expense. Two cost ratios define the situation:

- that of local sand to the standard (transported) sand (cls:cts), which will vary in the range 0-1, with 0 reflecting cost-less sand i.e. with zero extraction cost from a site immediately adjacent to use, and 1 representing a situation in which the difficulty of extracting the local sand outweighs transport costs for the sand brought from a distance.
- that of cement (also transported) to the local sand (cc:cls). For each combination of these cost ratios we have calculated the ratio of cost using local sand to cost using transported sand. Values <1 indicate the local sand incurs a lower cost, whilst values >1 suggest the standard sand would give a cheaper component.

Figures 3.21 and 3.22 give a comparison between sands S and K for bending and membrane loading. The Figures indicate that, for bending loading there is an economic advantage to using sand K, of around 20% over typical cost ratios,

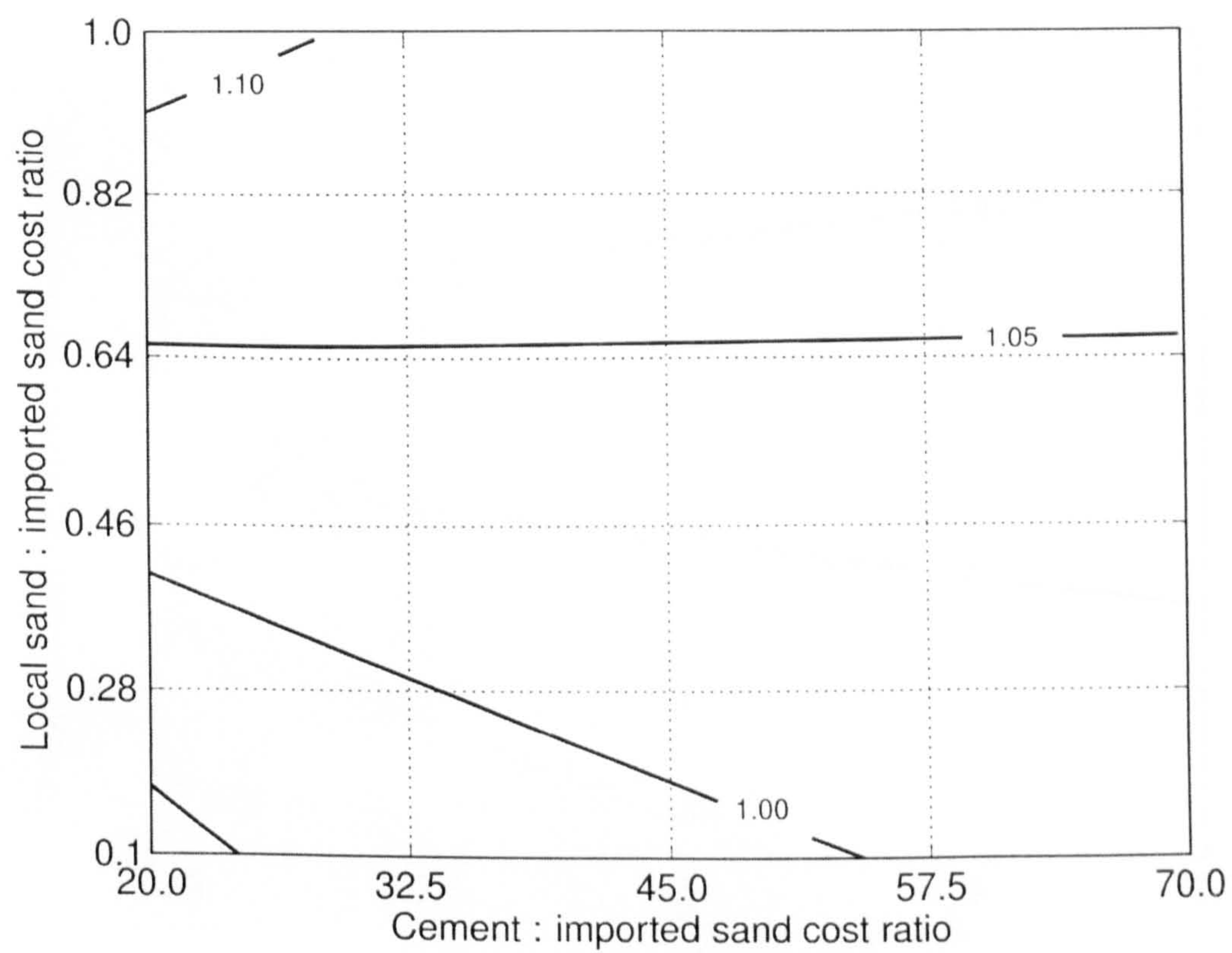


Figure 3.21: Ratio of cost using mix with sand K, to cost using mix with sand S, for membrane (direct) loading. Values <1 indicate using sand K costs less than using sand S

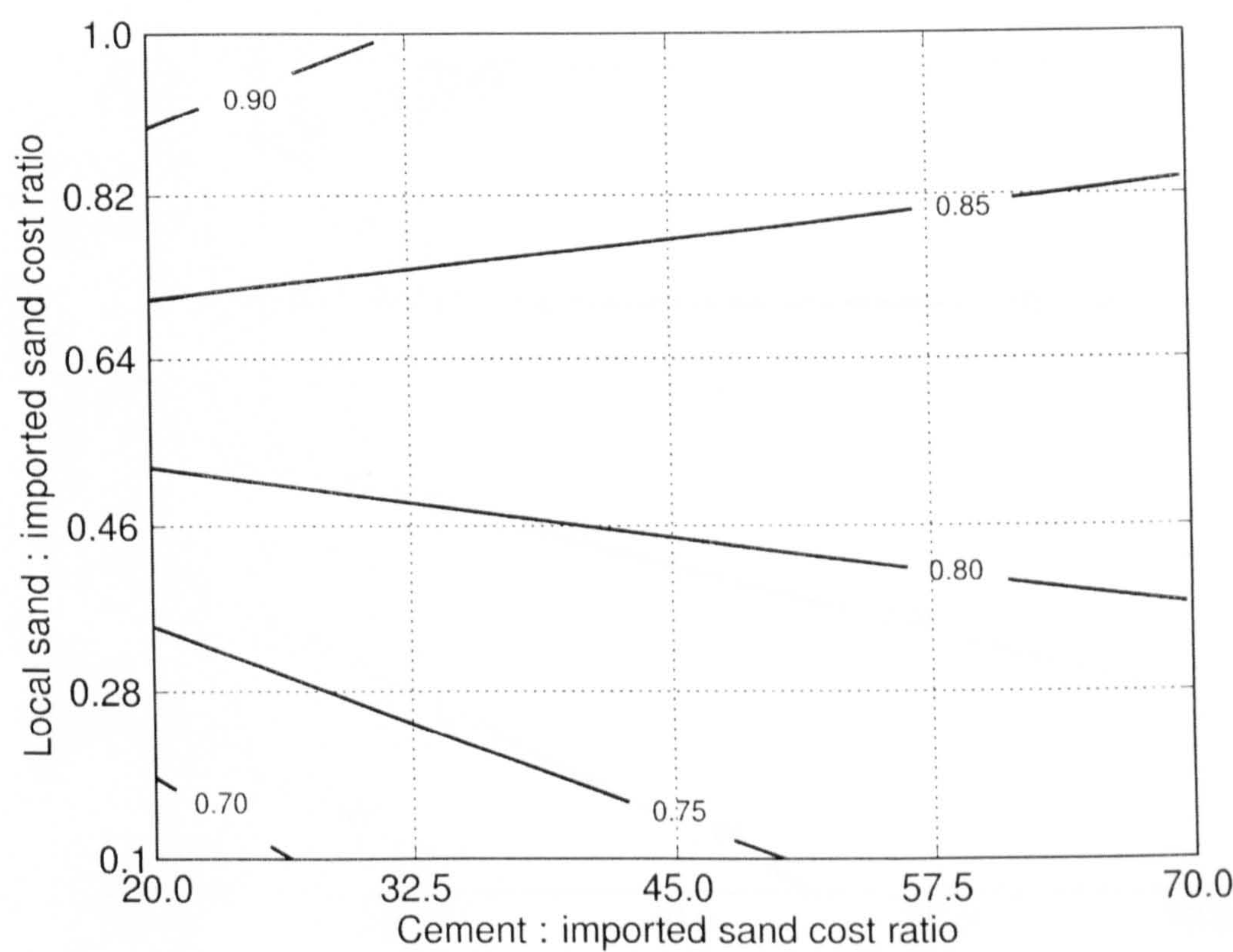


Figure 3.22: Ratio of cost using mix with sand K, to cost using mix with sand S, for bending loading. Values <1 indicate using sand K costs less than using sand S

whilst for membrane (direct) loading, using sand K incurs a cost penalty of around 5%.

By contrast, Figures 3.23 and 3.24 show the same comparisons, this time between sands M and S. These figures indicate that in both cases using sand M incurs a cost penalty, of around 70% for bending loading, and 100% for membrane loading.

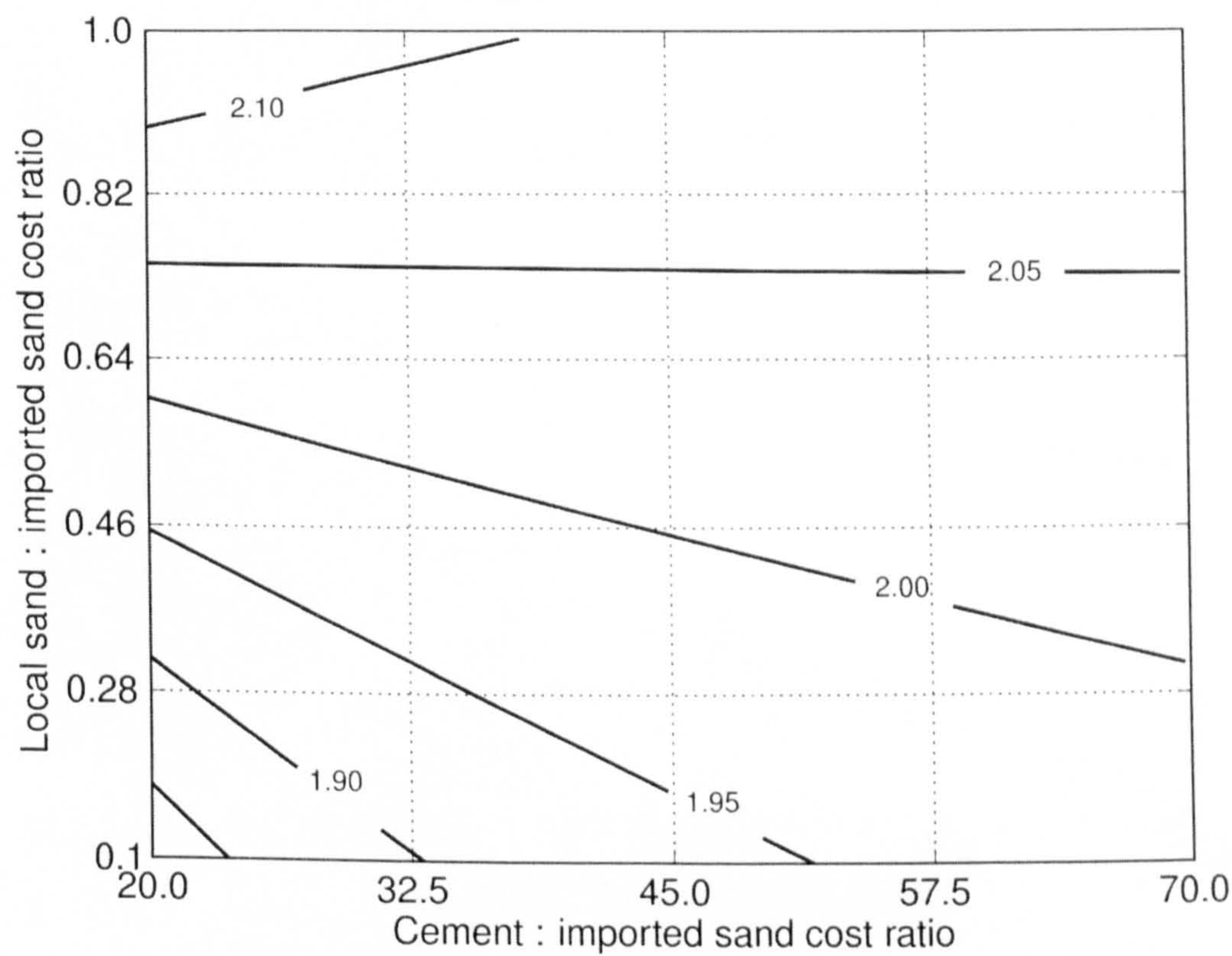


Figure 3.23: Ratio of cost using mix with sand M, to cost using mix with sand S, for membrane (direct) loading. Values <1 indicate using sand M costs less than using sand S

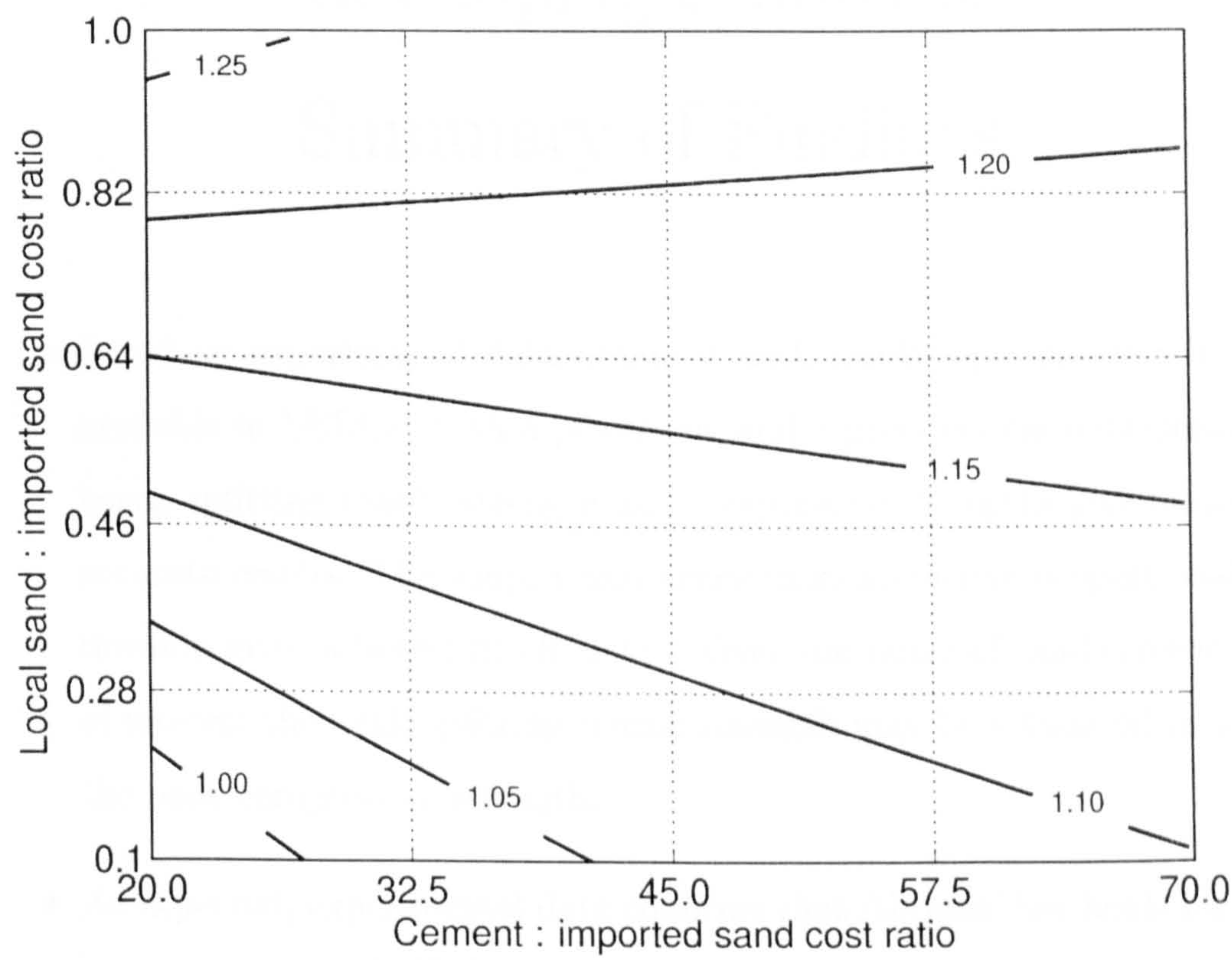


Figure 3.24: Ratio of cost using mix with sand M, to cost using mix with sand S, for bending loading. Values <1 indicate using sand M costs less than using sand S

Cementitious building materials in developing countries: Summary of Findings

- Based on experimental data obtained with sands representative of those available in LEDCs, both a power law and a proportional relationship between splitting tensile strength and compressive strengths give reasonably accurate results. The simpler and hence more attractive proportional relationship gives a better fit ($R^2 \simeq 0.9$). Over the range of sand-cement ratios of interest the peak splitting tensile strength may be estimated as 11% of the peak compressive strength.
- As expected, experimental data confirms that Abrams' law holds for sands representative of LEDCs, in both tension and compression. The strength-w/c relationship is, again as expected, independent of sand-cement ratio, but the Abrams' law parameters do vary slightly with sand type.
- The mechanical testing conducted does not allow for analysis or detection of cement-clay chemical interactions, beyond inference from the effects on strength and workability. The similar values of Abrams' law parameters for the three aggregates used does, however, indicate that any such reaction has relatively little effect on strength, providing full compaction is achieved. In this case, the presence of clays increases the optimum water-cement ratio,

and thus reduces optimal strength primarily by affecting workability and required water-cement ratio. In terms of the effect of clay on strength, statistical analysis of a comparable data set (Fernandes *et al.*, 2006), suggests that, using a different relationship for strength (based on pore content), the presence of kaolin does not affect strength, but montmorillonite does have a detrimental effect.

- As expected, optimum water-cement ratio increases linearly with sand-cement ratio. Analysis of documented relationships between sand-cement ratio and water required to give desired workability suggested optimum moisture content would be constant for a range of sand-cement ratios. This was confirmed, with the value of this constant depending on the aggregate in question.
- Peak density of a mix series serves as a good ($< 10\%$ strength penalty) indicator of optimum water-cement ratio for some sands (sand K in this work), but incurs a considerable ($\simeq 30\%$) strength penalty for others.
- The presence of (e.g. 20%) kaolin in sand reduces the peak strength at lower sand-cement ratios compared to that achievable with uncontaminated sand, but gives similar or better high sand-cement strengths. Hence, compared to the uncontaminated sand, there is a lower strength penalty associated with increasing sand-cement ratio of this kaolin-contaminated sand. An increase in this sand-cement ratio will give the same benefit in terms of reduced material cost per unit volume of mortar. Hence, the optimal sand-cement ratio for a kaolin-contaminated sand becomes higher than an uncontaminated sand.
- The presence of (e.g. 20%) montmorillonite clay substantially increases the water content to achieve peak tensile or compressive strengths. These peak strength mixes, requiring so much more water, and hence with significantly greater water-filled voids within the cement matrix, are much below that

of mortars made with uncontaminated sand except for very lean mortar mixes.

- For components where peak stress varies with thickness, and the thickness and sand-cement ratio may be varied to achieve best economy, there is a trade-off between using thicker, weaker and cheaper mixes, and using thinner, stronger and more expensive mixes. For loading where the peak stress varies inversely with the square of wall thickness ($\sigma_p \propto 1/t^2$), this favours a sand-cement ratio of around 7:1, whilst situations where peak stress varies inversely with thickness ($\sigma_p \propto 1/t$) favour lower sand-cement ratios of around 3:1.
- The presence of (e.g. 20%) kaolin clay gives mixes that, with the high optimal sand-cement ratio for $\sigma_p \propto 1/t$, give better economic performance (by about 20%) than a more expensive imported sand. With the lower sand-cement ratios for $\sigma_p \propto 1/t$, the same clay gives a small (around 5%) penalty.
- For both of the loading cases above, the high strength penalty incurred by using a local sand with (e.g. 20%) montmorillonite clay outweighs any benefits of lower cost associated with less transport, and always leads to a significant cost penalty.

PART III

Component Design

Component Design:

Overview

Part II considered the use of locally available materials to reduce component cost. This part examines an alternative cost-reduction strategy: improving component design. To do this it uses the case-study of water storage tanks for rainwater harvesting.

Chapter 4:

- Recaps the context of production in LEDCs.
- Gives a brief overview of rainwater harvesting.
- Presents current designs, and develops a geometric classification system.
- Gives a general specification for rainwater tanks.
- Reviews theoretical tools applicable to tank designs: shell and plate theory.

Chapter 5 addresses the datum design: cylindrical tanks with uniform wall thickness, chosen as representing a popular design choice. The Chapter:

- Applies relevant theory to analysing and optimising the datum case.
- Defines a performance measure, Relative Cement Index, to allow comparison between different tank designs.
- Evaluates modifications in the wall thickness of cylindrical tanks to improve their material economy, and hence reduce their cost.

Chapter 6 follows a similar approach to Chapter 5, applying analytical and numerical tools to other tank geometries, namely:

- Flat panelled tanks (0D curvature).
- Axisymmetric jar tanks (2D curvature).

Chapter 7 covers the production of a prototype tank, intended to provide:

- Confirmation that the designs developed in Chapter 6 perform as expected.
- Validation of the numerical packages used.

The part concludes with the brief summary on pages 179–180.

CHAPTER 4

Component Design: Tank Classification and Theory

The sections within this chapter:

- Briefly summarise the production situation as it relates to component design, and give an overview of rainwater harvesting systems as commonly used at a domestic level.
- List current RWH tank designs, categorised by geometry.
- Give a general specification for a tank, in terms of limits common to all manufacturing processes considered, and functions the tank must perform.
- Detail the areas of theory suitable for analysing tanks.

4.1 Production and design of cementitious components in LEDCs

LEDCs generally have lower labour costs relative to materials than industrialised nations. In addition, imported materials such as cement and reinforcing mesh will cost more, compared to local materials, than in high-income countries. However, OPC is widely available in LEDCs, and cementitious materials are rapidly replacing more traditional materials, even including clamp-fired ceramics.

Cementitious components are increasingly found in LEDC housing, a sector characterised by artisanal practice rather than engineering analysis. Such components fall into the categories of ‘massive’ (such as floors, wall foundations and walling blocks) and ‘thin-walled’ (roof structures, water tanks). Because the latter gives rise to possible *tensile* stresses, and these stresses often form the limiting design criterion, they lend themselves to obtaining significant material savings via better geometric design.

4.2 Rainwater harvesting

This Part considers cisterns for domestic roofwater harvesting (DRWH), a technique which provides householders with an autonomous supply of potable water (Gould & Nissen-Petersen, 1999), and which is growing rapidly in popularity. Figure 4.1 shows a typical system, which normally includes:

Catchment surface: typically a roof, though custom structures are occasionally used.

Conveyance: Guttering, or other devices to transport the water from the catchment surface to the storage inlet.

Filter: not always present in a system, acts to remove suspended contaminants from the water.

Storage: a tank of some form that retains the water until required.

Water access: e.g. a tap or pump.

The storage tank is invariably the most expensive component in the system, giving the strongest incentive for reducing its cost.



Figure 4.1: Example rainwater harvesting system

4.3 Current designs classified by location and by geometric complexity

Practitioners employ a large number of designs at present (for a more detailed set of case-studies, see DTU (2005)). The three main cistern types are:

1. Above ground.
2. Partially below ground.
3. Below ground.

Types 2 and 3 above perform well only in areas with suitable soil that will provide support; this Part considers the design of the more common above-ground tanks. Above-ground tanks fall into several general ‘geometric’ categories, presented below with examples. These designs are most commonly made with uniform wall thickness for ease of manufacture.

4.3.1 0-dimensional curvature: prismatic cisterns built with flat panels

Flat panels appear best suited to prefabrication, rather than on-site manufacture, and have seen some limited use (Paramasivam & Nathan, 1984; Khan, 1983;

Kumar *et al.*, 1984). These cases use four side panels, which reduces problems with forming joints, but does not give an efficient shape, with high stresses at the joints between panels. Figure 4.2 shows an example tank.

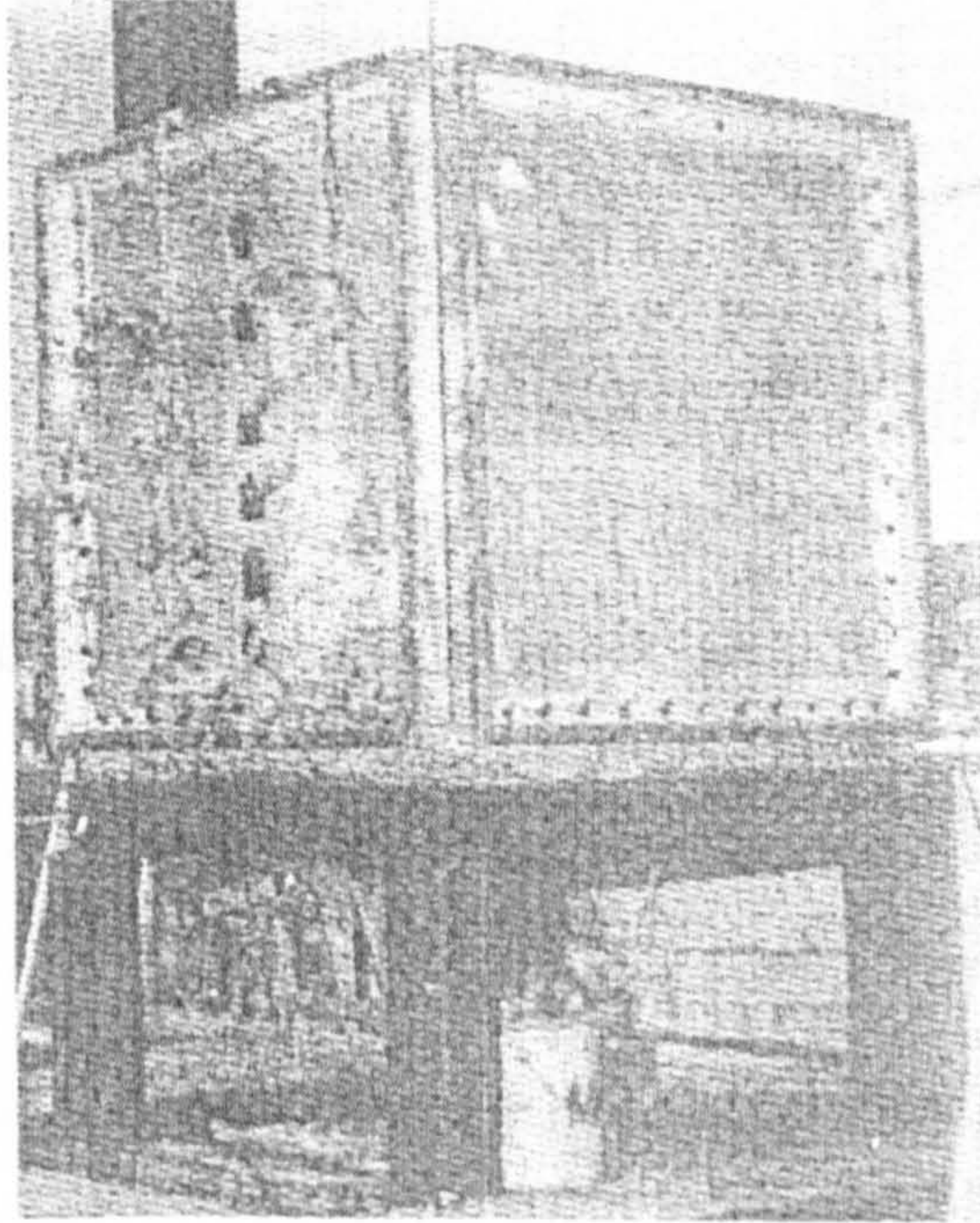


Figure 4.2: Example of a flat panel tank, taken from Paramasivam & Nathan (1984)

4.3.2 1-dimensional curvature: cylindrical structures

Cylindrical tanks suit both prefabrication (Sharma, 2005; Kumar *et al.*, 1984; Naaman, 2000) and on-site manufacture (Moita, de Las Casas, Carrasco & Bonifacio, 2003; Tarran, 1984; Watt, 1978; Paramasivam, Ong, Tan & Lee, 1990; Gould & Nissen-Petersen, 1999). Some related panel-based tanks have used barrel vaults (de Hanai, Martinelli, Montanari & Debs, 1984; Meek, 1982), but no reports cover their use for rainwater harvesting.

Cylindrical tanks are often cited as an efficient shape, particularly for resisting hoop stresses. However, they have several disadvantages:



Figure 4.3: Example of a cylindrical tank, in use in Bangladesh

- They require a separate technique for creating a cover, e.g. a ferrocement dome;
- A large bending moment develops at the wall-base joint.

4.3.3 2-dimensional curvature

A number of designs have curvature in two dimensions, including the popular Thai jar design, shown in Figure 4.4, with a storage capacity of up to 2m^3 , and the Sri Lankan pumpkin tank, shown in Figure 4.5, with a storage capacity of up to 5m^3 . Whilst having more complex shapes, these tanks have the advantages of efficient materials use, and a narrow opening at the top, which can have a small, simple and cheap cover over it.

4.4 Materials usage of current designs

The Thai jar and Sri Lankan pumpkin tank represent current “best of breed” designs. Table 4.1 shows the current materials usage of some representative tanks:

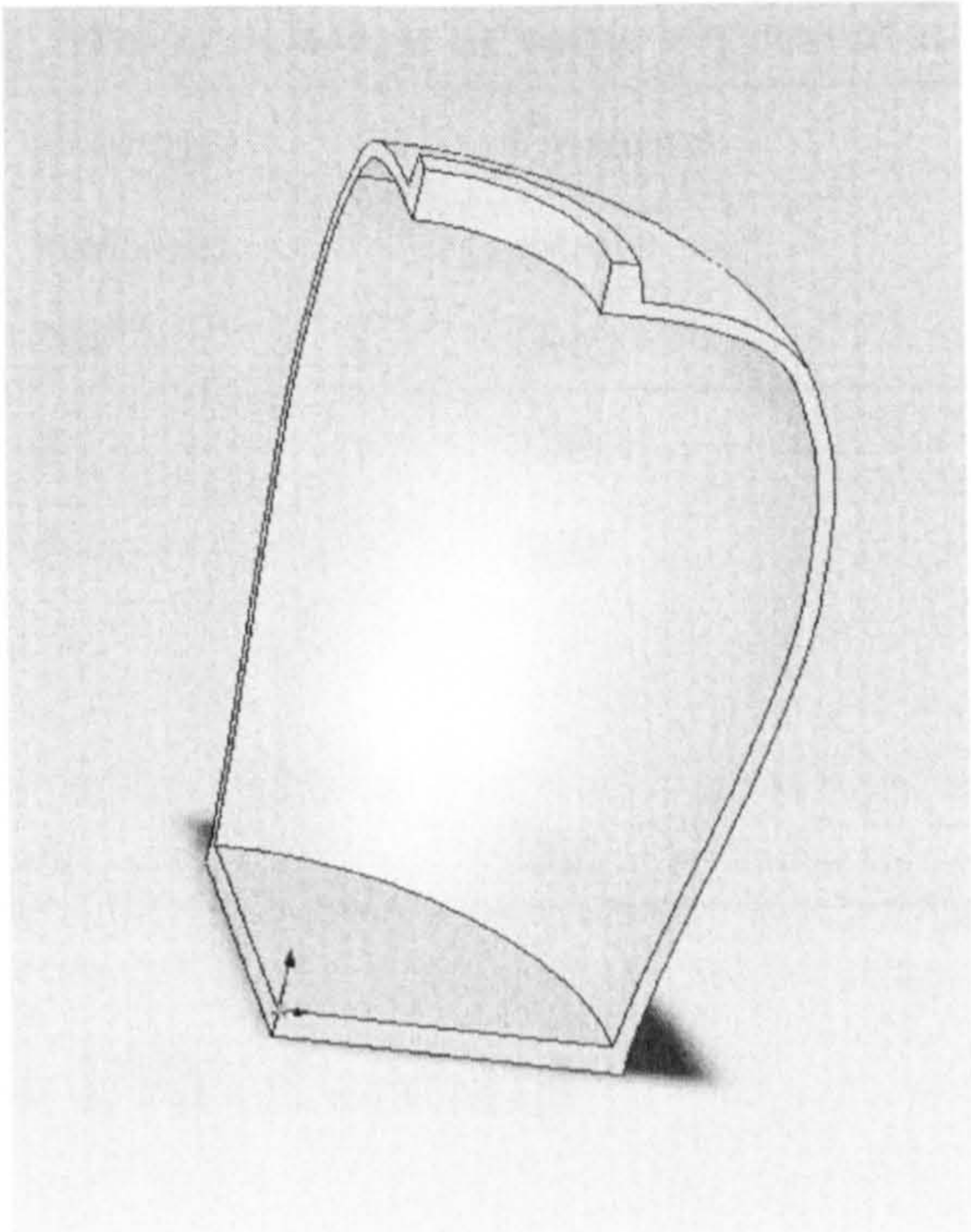


Figure 4.4: Thai Jar water tank

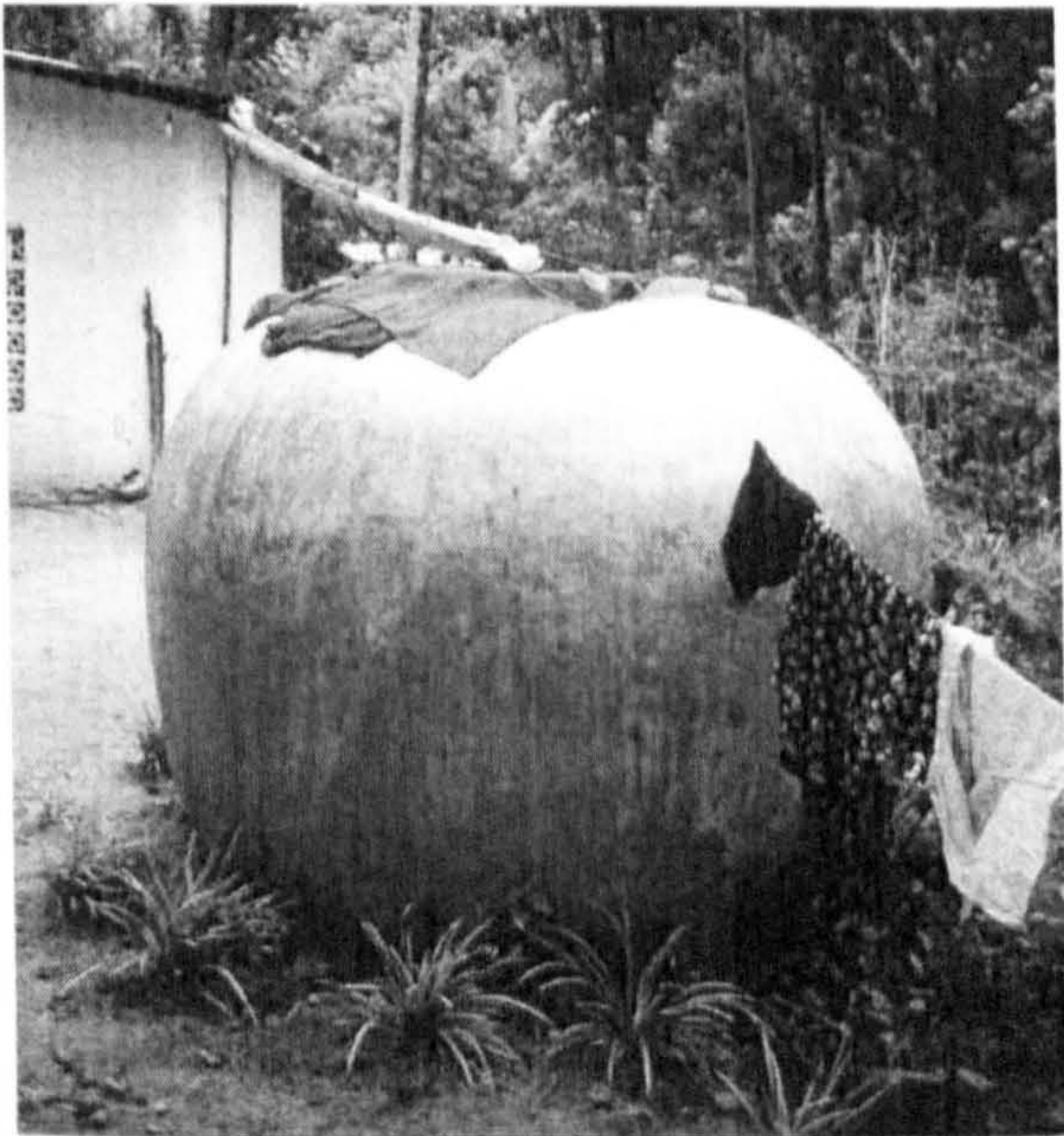


Figure 4.5: Sri Lankan pumpkin tank

Table 4.1: Material usage of some representative tanks

Design name	Storage volume (m ³)	Cement usage (kg)	Mortar volume (m ³)
Thai jar	2	120	0.27
“Jumbo jar” (adapted from Thai jar)	3	300	0.42
Pumpkin tank	5	350	0.81

4.5 Specification for DRWH cisterns

The shape of rainwater jars is constrained in various ways:

Storage: Tank storage capacities of 1.5-2 and 6 m³ give a reasonable range for RWH tanks

Height: The top of the tank should be below the outlet from the conveyance, otherwise the tank will have some “dead volume”. As many domestic structures are single-storey, this gives a maximum tank height of around 2m.

Stability: Reducing the base diameter will have the desirable effect of lowering the amount of material in the plinth, at the cost of stability.

Top aperture: Should be as small as possible consistent with allowing entry for cleaning: $\simeq 0.5\text{m}$.

Weight: Transport of the tank to its place of use gives an upper limit of around 300kg for each component being moved.

Water-tightness: Whilst the tank must retain water, common construction practises either include a leak-seal compound with the mortar, or apply a

Table 4.1: Material usage of some representative tanks

Design name	Storage volume (m ³)	Cement usage (kg)	Mortar volume (m ³)
Thai jar	2	120	0.27
“Jumbo jar” (adapted from Thai jar)	3	300	0.42
Pumpkin tank	5	350	0.81

4.5 Specification for DRWH cisterns

The shape of rainwater jars is constrained in various ways:

Storage: Tank storage capacities of 1.5-2 and 6 m³ give a reasonable range for RWH tanks

Height: The top of the tank should be below the outlet from the conveyance, otherwise the tank will have some “dead volume”. As many domestic structures are single-storey, this gives a maximum tank height of around 2m.

Stability: Reducing the base diameter will have the desirable effect of lowering the amount of material in the plinth, at the cost of stability.

Top aperture: Should be as small as possible consistent with allowing entry for cleaning: $\simeq 0.5\text{m}$.

Weight: Transport of the tank to its place of use gives an upper limit of around 300kg for each component being moved.

Water-tightness: Whilst the tank must retain water, common construction practises either include a leak-seal compound with the mortar, or apply a

neat cement slurry to the inside surface after manufacture. Thus porosity of the material being used to make the tank is not a concern: the problems of peak stress and water-tightness may be considered independently of each other.

Foundation: The foundation should be thick enough to withstand the effects of differential settlement without cracking.

Aesthetics: Whilst not a functional requirement, experience in the field, and care taken with other rainwater production methods, suggest customers attach considerable importance to the finished appearance of the tank. Though difficult to quantify, this suggests the tank should have:

- Good external surface finish.
- No significant discontinuities in the profile, or large imperfections.

Stress: As the tank material is relatively brittle, maximum principal tensile stress may be used as a design criterion. For a representative 3:1 mortar, with a mean tensile strength of around 3.2 MPa, and standard deviation of 0.13MPa, this gives a characteristic strength¹ of 3.0MPa. For this characteristic strength, the peak stress should not rise above 1MPa, using a design reserve² of 3. A design reserve of this magnitude is considered appropriate:

- On the basis of previous tank design work (Martinson, 2005);
- Quality control producing tanks in LEDCs will not be as high as that in industrialised countries. As MEDCs use values around 1.4–1.6 for loadings (the lower generally for static loads, the higher for dynamic

¹Characteristic strength: The value of strength below which 5% of all test results are expected to fall

²Design reserve: A factor, sometimes termed safety factor, representing the capability of a system over the requirements it will experience. This factor can be arrived at by combining a number of factors, including, cost of failure, statistical variation in material, effects of imperfection in construction etc.

loads), a higher design reserve was chosen to reflect this variability in quality control.

Wall thickness: As production of the tank will involve application of the mortar by hand plastering, the wall thickness should not be specified below 1cm.

Wall thickness variation: For global variations, constant wall thickness or linear wall thickness with height are achievable. In addition, local variations such as radii may be used.

4.6 Theory and Numerical Tools

A number of tools can assist with the analysis of thin-walled cementitious structures. Plate and shell analysis have some application, but for more complex shapes a numerical technique such as Finite Element Analysis (FEA) becomes necessary.

4.6.1 Plate theory

Plate theory considers an infinitesimal element subject to external loading, with direct and shear stresses, and bending moments acting, to develop a 4th order governing partial differential equation (Timoshenko & Woinowsky-Kreiger, 1959). Solutions for simple examples use a Fourier series approach (Jaeger, 1964). For more complex cases the direct application of plate theory is impractical, leading to design tables and figures. Experimental work by Paramasivam & Nathan (1984) has shown that numerical approaches can accurately be applied to rainwater harvesting tanks.

Irrespective of the difficulties in forming an analytical solution, plate theory provides some useful understanding for rainwater storage tanks: flat panels will resist the applied water loading by developing bending moments.

4.6.2 Shell theory

Shell theory uses the same approach as plate theory, but makes simplifying assumptions for thin sections, making a number of shapes amenable to direct analysis, including the constant wall thickness cylindrical tanks mentioned in section 4.3.2. The analysis, outlined in Flügge (1967), assumes the tank deforms by membrane action, i.e. with direct forces in the direction of the midsurface only, and then applies a bending moment at the joint between the tank wall and base to satisfy the boundary conditions for a built-in wall of zero deflection and slope. Thus the tank resists the load by developing a bending moment in the vertical direction, and a horizontal hoop stress. Section 5.3.1 covers the results from this in more detail, but several points of interest emerge from shell theory:

- Natural structures often achieve material efficiency through membrane action, as seen in examples including egg shells(Zingoni, 1997).
- Certain features in structures disrupt this membrane action and lead to bending moments. These include the “discontinuities” mentioned by Zingoni (1997) of:
 - curvature
 - loading
 - support
- The effect of bending moments caused by the discontinuities mentioned above attenuates rapidly with distance from the discontinuities.

However, when extending the designs of interest to double curvature tanks with variable wall thickness, numerical techniques become necessary.

4.6.3 Finite Element Analysis

Finite Element Analysis is a popular modelling method for simulating the behaviour of solids, particularly in cases not amenable to analytical techniques. The

FEA work covered in this Part used the SolidWorks package, with comments on the package in Section B.1 of Appendix B.

CHAPTER 5

Component Design: Datum Tank Design and Performance Measure

The previous chapter gave a classification of current tank designs by geometry, and a brief overview of the analytical tools available to simulate the behaviour of these designs. This chapter defines a datum measure, for use in comparing various modifications to tank designs. It takes this measure and:

- Optimises the datum design, to give dimensions that minimise material usage.
- Explores the benefits of other variations in thickness profile (different distributions of material) to give improved material economy.
- Identifies general features found during the analysis of the datum design, that could form rules of thumb for tank designs.

5.1 Performance measure

Searching for improved tank designs requires some criteria to quantify their performance. For the case of rainwater tanks, the majority of costs arise from

materials, in particular the cement used to produce the tank.

For each tank design to store a particular volume of water, using a particular sand and sand-cement ratio, we may define the *cement intensity* as the mass of cement used to produce the design. Whilst useful, a clearer comparison may be made by using normalised measures. For this purpose we define the measure: “relative cement intensity,” (RCI):

$$\text{Relative cement intensity (RCI)} = \frac{\text{Cement used in design}}{\text{Cement used in datum design}} \quad (5.1)$$

The lower the RCI, the better the tank design. RCIs <1 represent designs that make better use of materials than the datum design, and conversely RCIs >1 represent designs that make worse use of materials than the datum. For fair comparison between designs, the RCI should be based on designs produced with the same mortar, both in terms of sand-cement ratio and sand type.

5.2 Datum Tank Design

It is useful to have a datum with which to compare other designs and modifications. For this reason, we will first develop such a design, using cylindrical tanks of uniform wall thickness. These tanks are suitable as a reference, as:

- They represent reasonably simple geometry.
- Their shape is perceived as being efficient in terms of material usage.
- They are popular at present.

5.3 Analysis of datum design: Cylindrical tanks with constant wall thickness

The following section describes the analytical shell-theory solution for a uniform wall thickness cylinder. This is presented as:

- Cylindrical tanks are useful as a datum design.
- The analytical solution provides an opportunity to validate the FEA software used.
- The concepts used in forming this solution prove useful for generating improvements to the datum design, and for forming an understanding which can be applied to tanks with 2D curvature.

Note that for this solution, the character superscripts m and b are used to denote measures due to membrane and bending actions respectively, and do not indicate values raised to the power m or b , e.g. σ_{θ}^m denotes the membrane hoop stress, not hoop stress raised to the power m .

First, the membrane solution is found for the tank. The physical equivalent of this is a cylinder with its axis vertically aligned, resting on a flat frictionless surface. On filling with water, it will deform as shown in Figure 5.1.

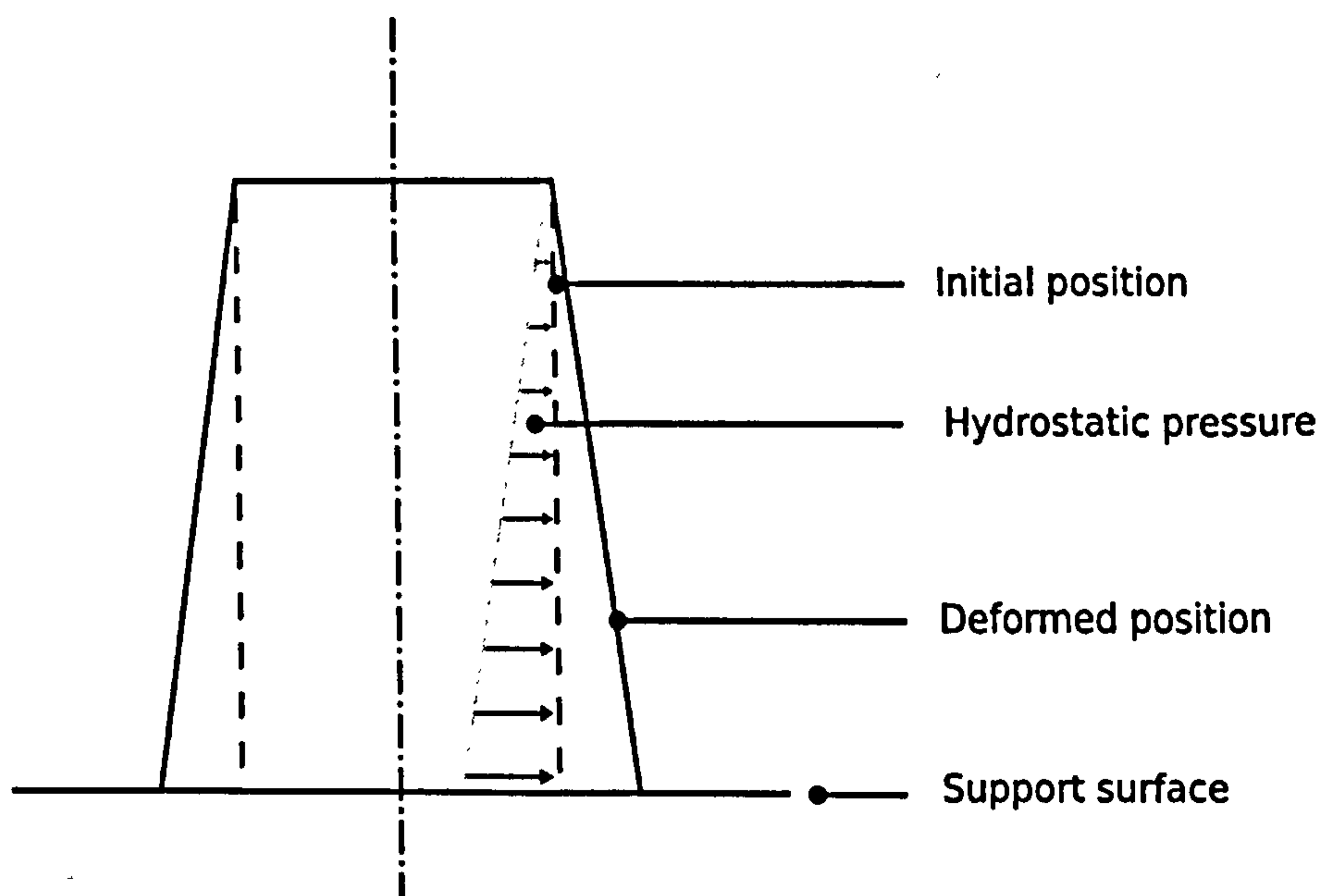


Figure 5.1: Membrane deformation of cylindrical tank under hydrostatic loading

The horizontal wall deformation, w^m , can be expressed in terms of the water loading, γ , the radius, a , Young's modulus of the mortar, E , wall thickness t ,

and distance from the top of the tank, x :

$$w^m = \frac{\gamma a^2}{Et} x \quad (5.2)$$

The slope of the deformed tank wall, V , is given by:

$$V = -\frac{\gamma a^2}{Et} \quad (5.3)$$

This will lead to a force per unit width in the hoop direction, N_θ :

$$N_\theta = \gamma a x \quad (5.4)$$

And a force per unit width in the x direction:

$$N_x^m = k \quad (5.5)$$

Where k is a constant. For the case of no lid, there will be no load at the top of the tank, so $N_x = 0$ throughout the cylinder.

This gives a complete solution, if the tank were resting on such a smooth support. However, the base of the tank will act as a restraint, effectively preventing displacement and rotation at the wall-base joint. This is particularly appropriate for rainwater tanks, as the base is generally designed to prevent damage from differential settlement, and so is significantly stiffer than the tank walls.

The effect of the base may be modelled as a shear force, and a bending moment, applied to the base of the tank. For the case where the lid of the tank may be considered relatively remote from the base (as applies for the long, thin-walled tanks of interest), a bending moment at the base will lead to a deflection, w^b , which may be expressed as:¹

$$w^b = e^{-\beta x} (B_1 \cos \beta x + B_2 \sin \beta x) \quad (5.6)$$

¹There is a more complete expression, with four unknowns, which is required for short cylinders. However, for the tanks of interest, the restraint at the base only has a relatively local effect, and this simpler form is appropriate.

β depends on Poisson's ratio, ν , cylinder radius, a , and wall thickness, t :

$$\beta = \left(\frac{3(1 - \nu^2)}{a^2 t^2} \right)^{1/4} \quad (5.7)$$

The bending moment in the x direction, M_x , and shear force normal to the x axis, H_x , may be obtained from:

$$(M_x)_{x=f} = D \left(\frac{d^2 w}{dx^2} \right)_{x=f} \quad (5.8)$$

$$(H_x)_{x=f} = D \left(\frac{d^3 w}{dx^3} \right)_{x=f} \quad (5.9)$$

Where D , the flexural rigidity of the cylinder, is given by:

$$D = \frac{Et^3}{12(1 - \nu^2)} \quad (5.10)$$

For the case of bending moment at the tank base, but no shear force, Equation 5.6 can be substituted into Equations 5.8 and 5.9, to give two simultaneous equations for the unknowns B_1 and B_2 . Solving these gives the deflection due to the axisymmetric edge moment M_e :

$$w_{M_e} = \frac{e^{-\beta x}}{2\beta^2 D} (\cos \beta x - \sin \beta x) M_e \quad (5.11)$$

Applying the same process for a shear force but no bending moment, gives an expression for the deflection due to an axisymmetric transverse force H_e :

$$w_{H_e} = \frac{e^{-\beta x}}{2\beta^3 D} (\cos \beta x) H_e \quad (5.12)$$

These expressions can both be differentiated to give the slope of the deflected tank wall. The deflection and slope can be used to give two boundary conditions:

- The total deflection at the base of the tank should be zero.
- The total slope at the base of the tank should be zero.

In which the two unknowns will be the bending moment, M_e , and the shear, H_e .

Solving these gives:

$$M_e = \frac{\gamma H}{2\beta^2} \left(1 - \frac{1}{\beta H} \right) \quad (5.13)$$

$$H_e = -\frac{\gamma H}{2\beta^2} \left(2\beta - \frac{1}{H} \right) \quad (5.14)$$

Once these two are calculated, the total bending deflection, w^b can be calculated ($w^b = w_{H_e}^b + w_{M_e}^b$), and combined with the membrane deflection to give the total tank deflection, w^T ($w^T = w^b + w^m$).

To find the stress at any point, in the x-direction (σ_x^T), or hoop-direction (σ_θ^T), the effect of the hoop and bending stresses can be combined, giving (with ν representing Poisson's ratio):

$$\sigma_x^T = \frac{N_x^m}{t} + \frac{N_x^b}{t} \pm \frac{6M_x}{t^2} = \frac{N_x^m}{t} \pm \frac{6M_x}{t^2} \quad (5.15)$$

$$\sigma_\theta^T = \frac{N_\theta^m}{t} + \frac{N_\theta^b}{t} \pm \frac{6M_\theta}{t^2} = \frac{N_\theta^m}{t} + \frac{N_\theta^b}{t} \pm \frac{6\nu M_x}{t^2} \quad (5.16)$$

These can be used in numerical code to evaluate the deflections, bending moments and stresses throughout the tank.

Figure 5.2 shows an example of the wall deflection of a cylindrical tank, indicating the effect of the base constraint, and the convergence to the deflection of a membrane-supported tank at some distance from the base.

Section B.2 of Appendix B outlines the approach for cylinders with an encastered lid.

5.3.1 Shell theory: Cylinders of constant wall thickness, no lid

Figure 5.3 shows the variation of peak stress with height for a cylinder of typical geometry (height of 2.0m, volume of 6.0m³, wall thickness of 3cm), indicating

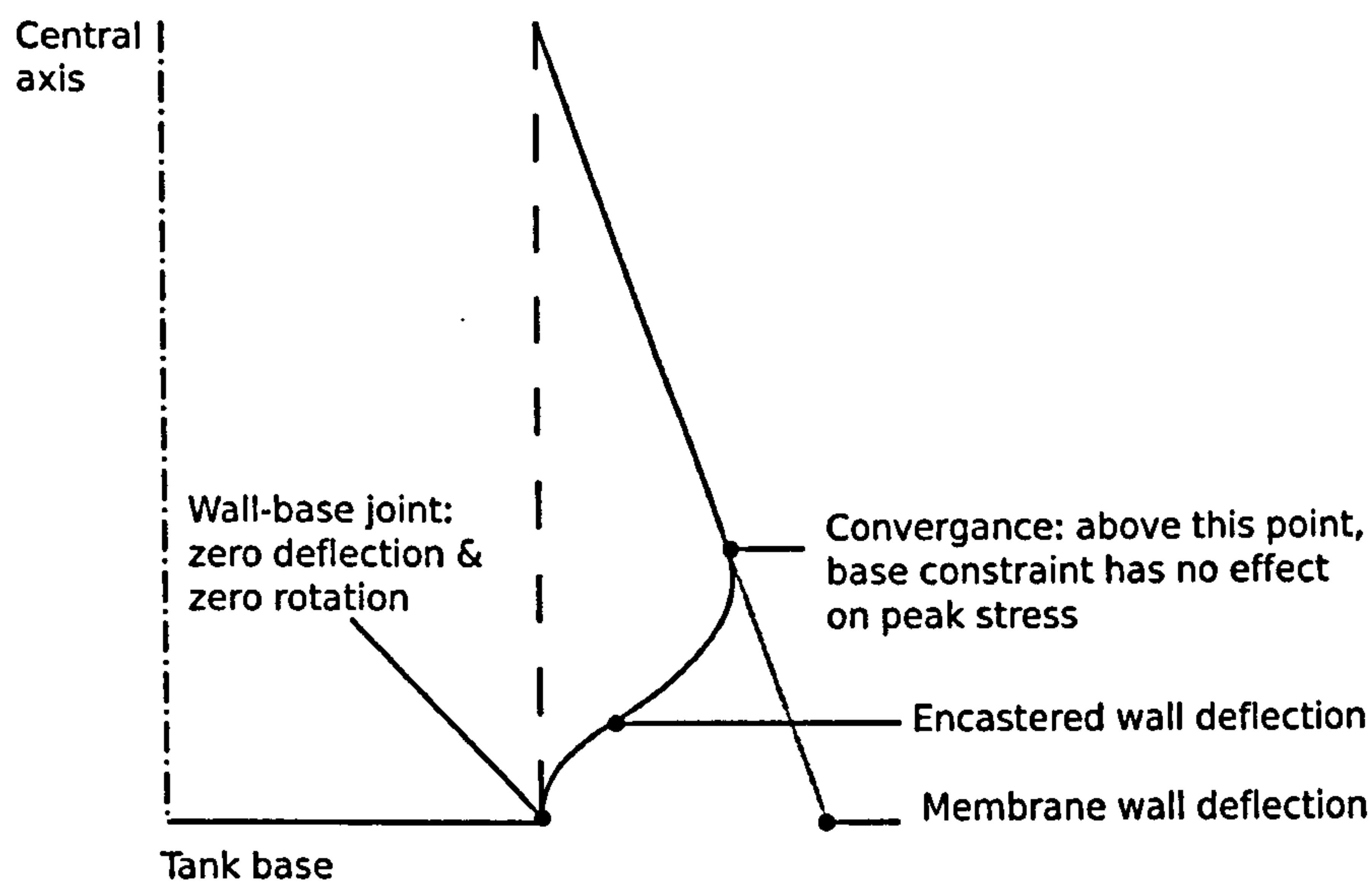


Figure 5.2: Wall deformation of uniform wall thickness cylindrical tank under hydrostatic loading

in which regions hoop and bending stresses dominate. This illustrates several features:

- There are two locations of peak stress: a hoop stress at around 30cm height, and a vertical bending stress at the very base. If thickening the bottom effectively reduced stress in the lower 5cm it could cheaply reduce the latter.
- The peak stress with the base restrained is around 1.5 times greater than the peak membrane stress, and this peak stress occurs at the base, due only to the bending moment action, and not hoop stresses.
- At a point a short height (in this case, around 8cm) above the base, the tensile stress reaches a minimum value and then rises. This minimum stress is significantly less than the bending stress at the wall-base joint.

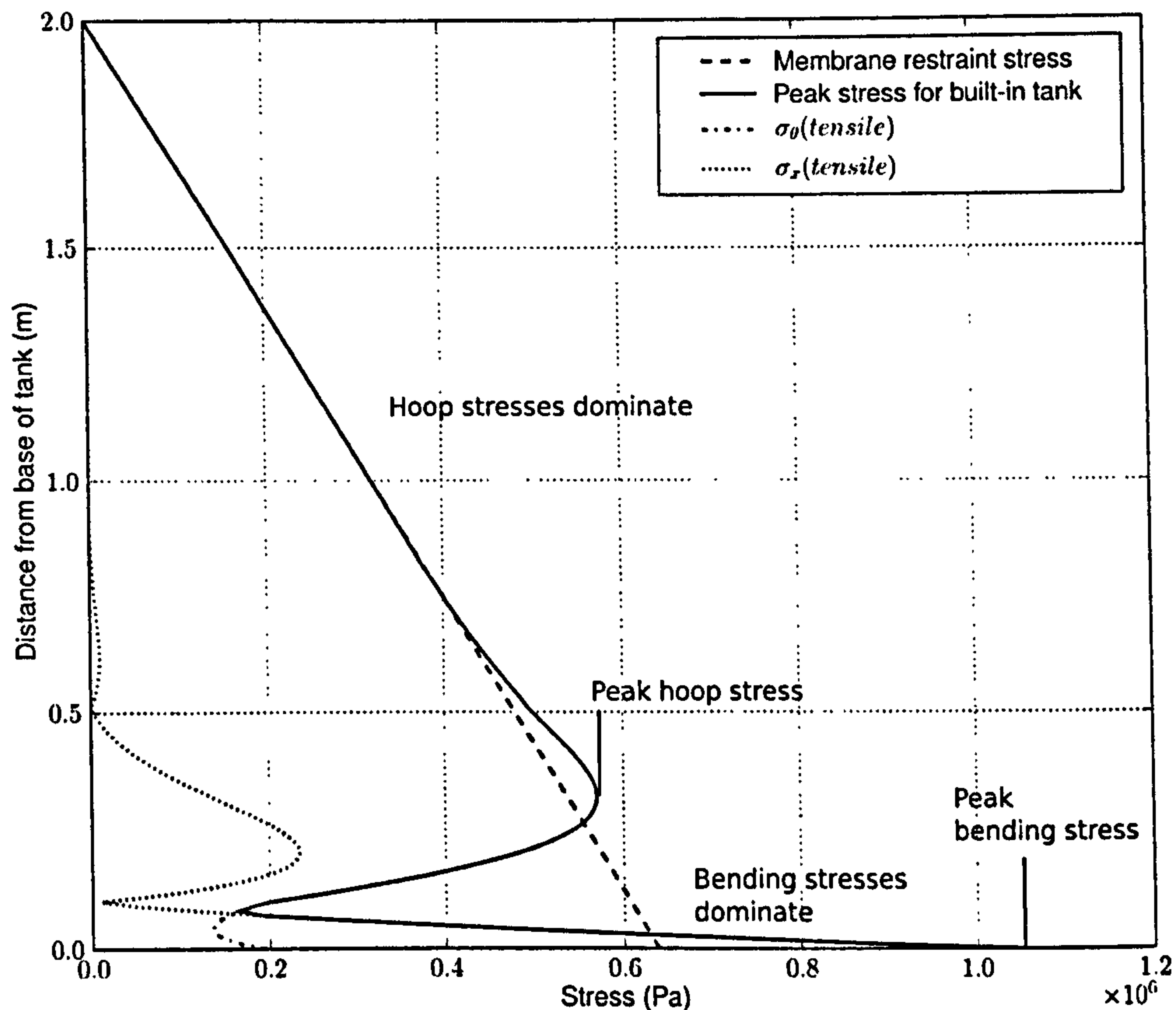


Figure 5.3: Variation in peak stress with height for a cylindrical tank of uniform wall thickness

5.3.2 Shell theory: Cylinders of constant wall thickness, encastered lid

Whether there is a lid or not, there will be no radial deflection due to water at the top of the tank. However, an encastered lid introduces a bending moment at the joint. Flügge (1967) covers the solution to this problem, treating it as a statically indeterminate structure. Figure 5.4 shows the bending moment in the x direction for a lid with a cantilevered lid. The bending moment at the lid-wall joint is significantly less than that at the wall-base joint.

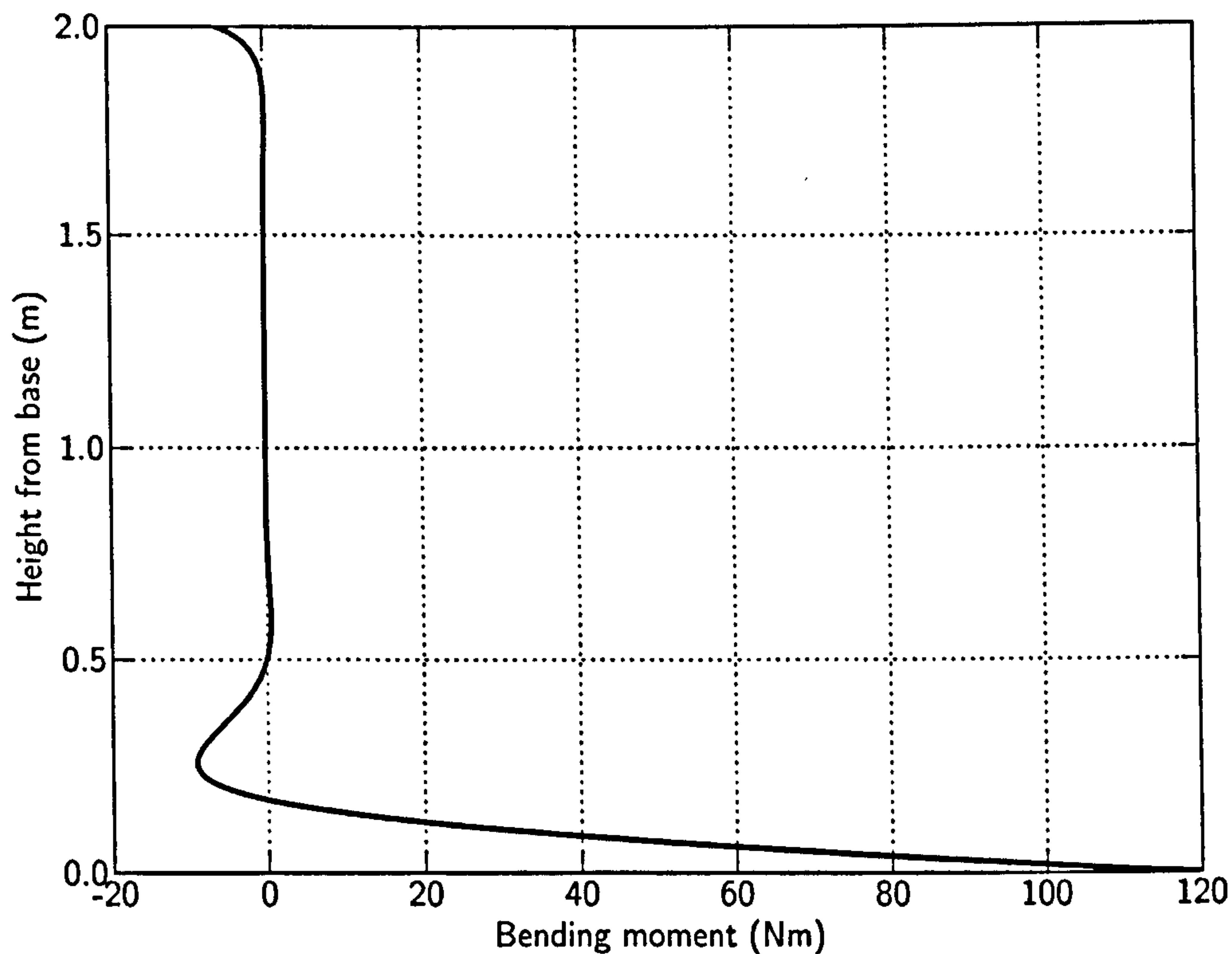


Figure 5.4: Variation in bending moment in x direction with height for cylindrical tank constant wall thickness, with encastered flat lid

5.3.3 Location of peak stress

The section above indicates that the bending moment arising from the lid has no effect on the peak stress, which section lid has no effect on the peak stress, which section 5.3.1 suggests will occur at the wall-base joint. The mass of the lid will generate an axial compressive force in the tank walls, but the stress arising from this is negligible compared to the bending moment stress²

whilst section 5.3.1 suggests that the peak stress will occur at the wall-base

²As an example, consider a tank with radius of 1m, wall and lid thickness of 2cm, bending stress at the base of 1MPa. Taking the density of the lid as 2000kg/m³, this gives a lid mass of $2000 \times \pi \times 1^2 \times 0.02 = 126\text{kg}$, and a compressive force of 1200N. The cross-sectional area of the tank will be approximately $2 \times \pi \times r \times 0.02 = 0.126\text{m}^2$, giving a stress of $\sigma = 1233/0.126 = 9.8e3\text{Pa} \simeq 1e4\text{Pa}$ i.e. 1% of the bending stress.

Table 5.1: Cylinder configurations used to test the thesis that bending moment at the base determines peak stress for cylindrical water tanks with uniform wall thickness

Height (m)	Radius (m)	Wall thick- ness (m)	Peak bending stress (MPa)	Peak hoop stress (MPa)
2.0	0.98	0.01	3.3	1.7
2.0	0.98	0.1	0.3	0.1
1.0	1.38	0.01	2.6	1.4
1.0	1.38	0.1	0.2	0.1

joint. To confirm this, a series of simulations used tanks with the configurations given in Table 5.1, which cover extremes of both height and wall thickness. For all cases the peak stress occurred at the wall-base joint.

5.3.4 Implications and possible generalisations from analysis of cylindrical tanks

Effect of lid on peak stress

For either an encastered lid, or a cylindrical tank without a lid, the peak stress arises from a bending moment at the base, and attenuates rapidly with distance from the base, hence the presence, absence, or particular design of the lid has no effect on the peak stress.

Variation in peak stress with wall thickness

Note that the peak stress does not vary inversely with the square of wall thickness. Such a relationship arises from the statics relationship between stress (σ), distance from neutral axis (y), bending moment (M) and second moment of area

(I): $\frac{\sigma}{y} = \frac{M}{I}$, where $y \propto t$ (t being component thickness) and $I \propto t^3$. However, this only holds for situations in which the moment, M , is independent of t , and this does not hold for cylindrical tanks. In fact, for cylindrical tanks, if bending stress at the wall-base joint dominates other stresses, then the peak stress is given by:

$$\sigma_p = \frac{6M_e}{t^2} \quad (5.17)$$

With the bending moment at the wall-base joint (M_e) depending on the relationship in Equation 5.13:

$$M_e = \frac{\gamma h}{2\beta^2} \left(1 - \frac{1}{\beta h}\right)$$

In this Equation, only β varies with t . For typical values, $\frac{1}{\beta h} \ll 1$, so $M_e \propto \frac{1}{\beta^2}$, and substituting from Equation 5.7 gives $M_e \propto t$. For this case, Equation 5.17 gives:

$$\sigma \propto \frac{M_e}{t^2} \propto \frac{1}{t} \quad (5.18)$$

This is in contrast to a number of other scenarios, such as bending of beams subject to external loads. This was confirmed by both analytical and numerical modelling of a representative tank, giving the results shown in Figure 5.5.

For this case, with $\sigma_p \propto 1/t$, there is less benefit to using a thicker wall than with bending of beams etc. where $\sigma_p \propto 1/t^2$. This implies lower optimal sand-cement ratios, as seen in Chapter 3.

Tanks with curvature in two dimensions will have some similar properties to their behaviour: a bending moment at the wall-base joint, and membrane action at locations away from this. If the same relationship between bending moment stress at the base and wall thickness holds for 2D-curvature tanks, this raises the possibility that the same relationship could apply for tanks with curvature in two dimensions, with peak stress inversely proportional to wall thickness. If this were the case, then from a single simulation of a wall thickness, one could

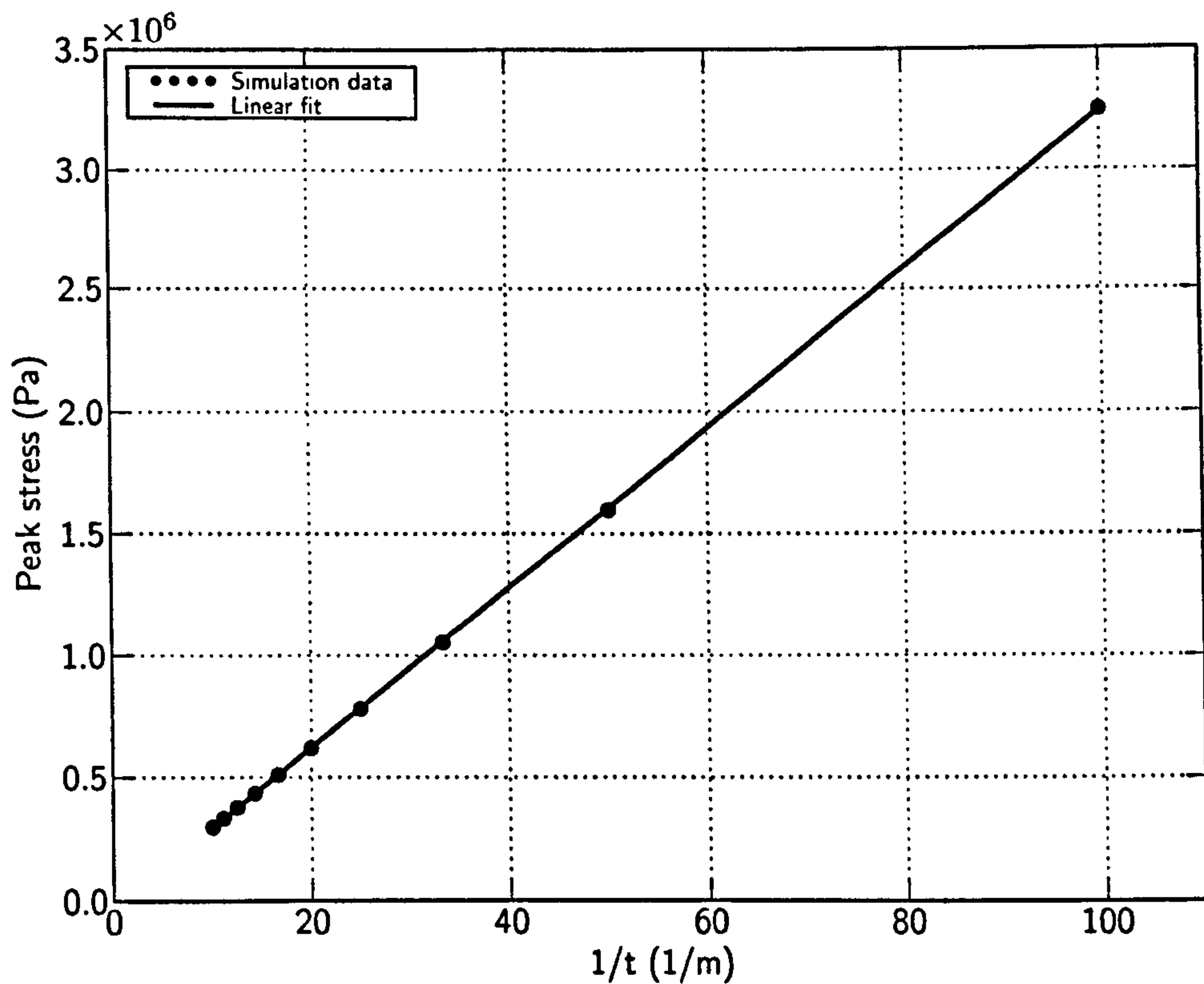


Figure 5.5: Variation in peak stress with inverse of wall thickness for cylindrical tank, showing linear relationship

determine the wall thickness required for a given design stress. In this case, with only one relationship between peak stress and wall thickness, regardless of bending or membrane stresses dominating, on the basis of the work in Part II, one could recommend a single sand type and sand-cement ratio for water tank construction.

Choice of sand type for datum configuration

At this point it appears that, at least for uniform wall thickness cylinders, one of two situations will hold:

- Peak stress arises from membrane action. In this case, peak stress ($\sigma_p \propto 1/t$).

- Peak stress arises from bending moment. For cylinders with constant wall thickness, we have shown that $\sigma_p \propto 1/t$.

For both of these cases we have a peak stress proportional to $1/t$. From the work in Chapter 3, this suggests that a high quality “imported” sand will prove more economical than “local” sand, that the optimum sand-cement ratio will be around 3:1, and that this will have a splitting tensile strength of around 3MPa. Taking a design reserve of 3, we then have a design stress of 1MPa. This also gives a simple single case to use for the majority of designs considered rather than having to change between a stronger, rich mix for tanks where membrane stresses dominate, and a weaker, lean mix for tanks where bending stresses dominate.

Location of wall-base joint

The sections above showed that the bending stresses at the wall-base joint dominate in cylindrical tanks, yet many designs produce a flat base and then mortar on to it. Producing a base with a small lip, of around 10cm, would lead to the joint between the two sections experiencing stresses around $1/3$ of those at the wall-base joint. Figure 5.6 shows a cross-section view of this proposed modification.

5.3.5 Optimisation of uniform thickness cylindrical tanks

As noted above, the localised effect of bending moments, and dominance of the bending moment at the wall-base joint, mean that cylinders of uniform wall thickness may be designed using the criteria of stress at the joint.

The code given in Appendix D.3 allows optimisation of cylindrical tanks, by creating instances of cylindrical tanks from a base class, and choosing the minimum wall thickness that gives an acceptable stress (the specified design stress). This leaves two variables, the height of the tank (with the radius a dependent variable to give the specified volume), and the combined thickness of the base and lid. Although, as the comments above indicated, the base and

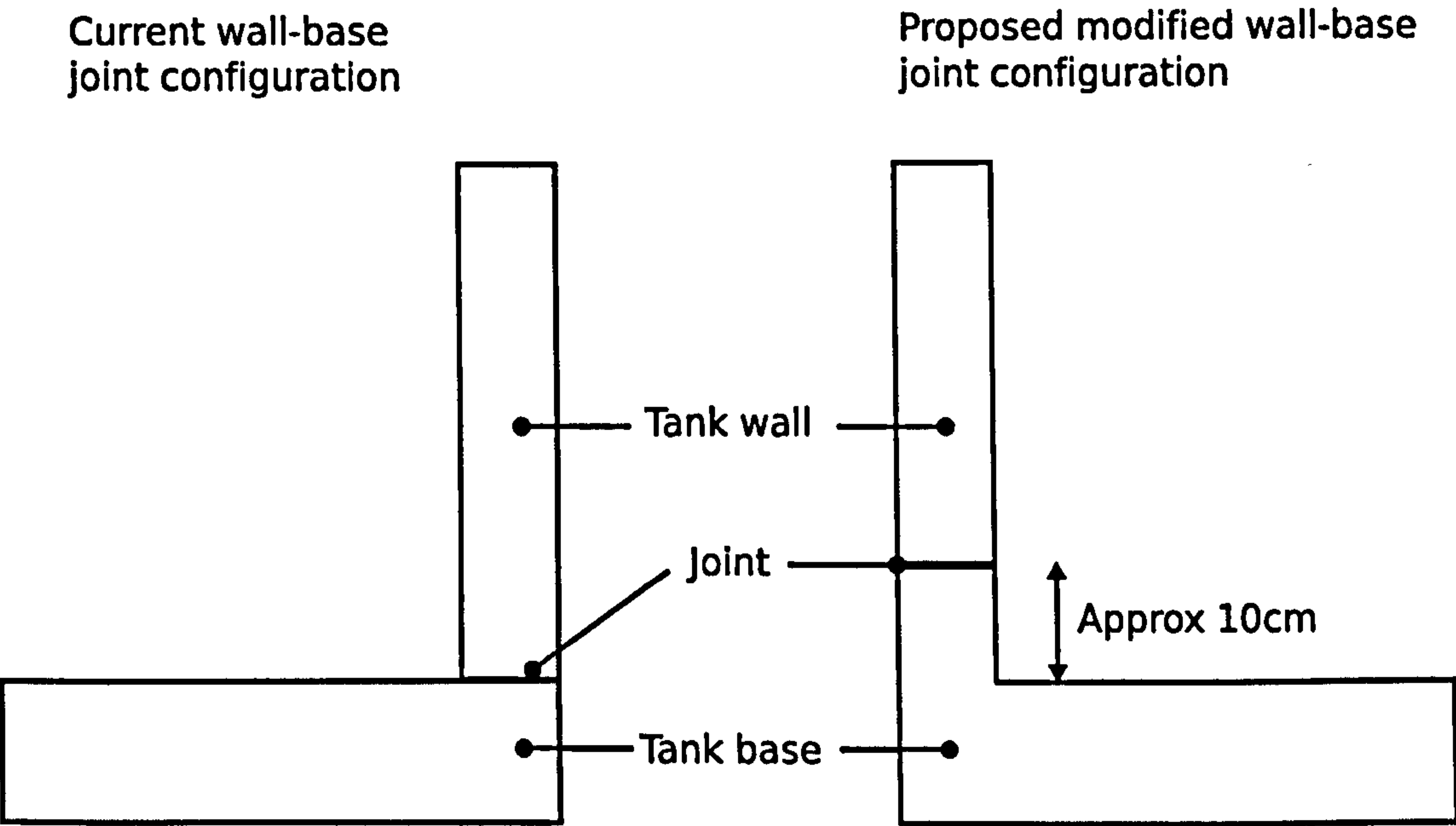


Figure 5.6: Cross-section of wall-base region of cylindrical tanks, showing proposed modification to provide a base with a small lip

lid thickness do not affect the wall stresses within the tank, they generally have minimum values for other reasons: the base to prevent differential settlement, and the lid to provide a protective cover.

Figure 5.7 shows the effect of changing the combined thickness of the covers on the optimum tank height, and the material penalty incurred by using a non-optimal tank height. Whilst the optimal tank height does vary significantly over a representative range of combined cover thicknesses (from 2 to 6cm), it remains relatively insensitive to changes around its optimum value, suggesting that a constant tank height would give acceptable performance. It also suggests that, for 6m³ cylinder rainwater tanks, the optimum height is generally limited by the gutter height of single-storey buildings (as discussed on page 101 in Section 4.5).

Generating the datum design

Table 5.2 shows the datum design parameters, which provides a reference with which to compare other designs. The remainder of the Chapter will explore designs of increasing geometric complexity, evaluating modifications to the general case, and evaluating them using relative cement intensity (RCI).

5.4 Modifications to improve the Relative Cement Index of cylindrical tanks

The previous section defined the datum design, using the best achievable combination of wall thickness and height to store the required volume of water. The remainder of the Chapter now addresses modifications to the datum, and examines the benefits offered by:

- Constant wall thickness, and local variation in thickness at the wall-base joint.
- Wall thickness varying linearly with height.

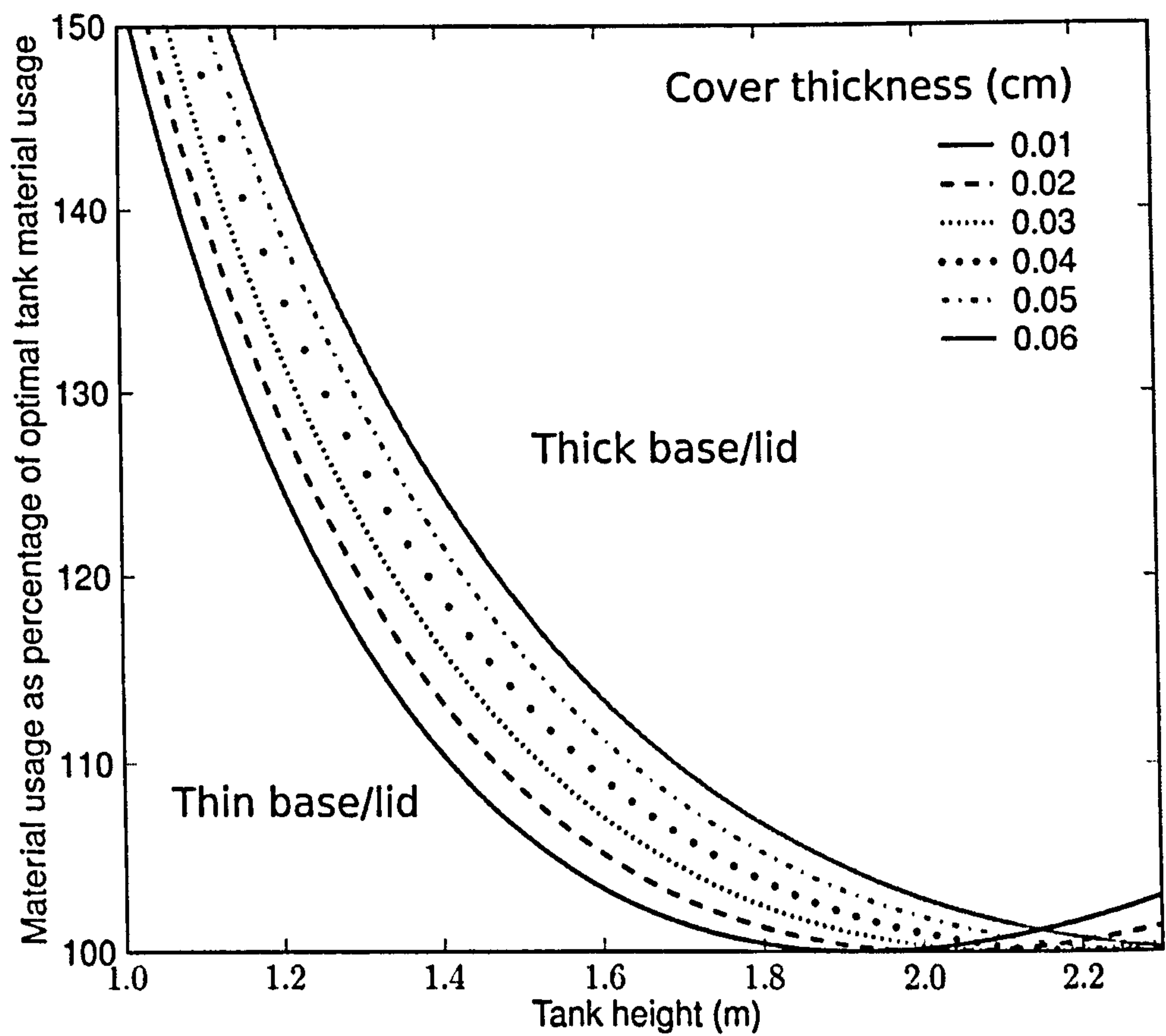


Figure 5.7: Effect of changing cover thickness on optimum tank height, and material penalty from using a non-optimal height, with lines of different total cover thickness (combined lid and base thickness)^a

^aThe measure for the ordinate axis is the amount of extra material used in the design, as a percentage of the amount of material that would have been used with an optimally-proportioned tank.

Table 5.2: Definition of the datum design: constant wall thickness cylinder to store 6m³ of water

Parameter	Value
Height	2m
Radius	0.98m
Storage volume	6m ³
Design tensile stress	1MPa
Base thickness	30mm
Cover thickness	10mm
Wall thickness	32mm
Mortar volume used	0.53m ³
Mass of cement used	230kg

- Wall thickness varying linearly with height, and local variation in wall thickness at the wall-base joint.

5.4.1 FEA modelling of cylindrical tanks

The software used for FEA modelling was CosmosWorks, part of the SolidWorks 3D modelling suite (Solidworks, 2006). The following section describes the FEA modelling of cylindrical tanks used in this Thesis. Whilst some aspects of this modelling change for other tank designs (0D and 2D curvature tanks), the majority, such as mesh generation, convergence criteria etc. remain the same.

Model generation

As part of an integrated set of modelling tools, the cylinder model was generated in SoldiWorks. To reduce computational effort, a section of the cylinder was used. This was deemed acceptable as both the structure and the loading were axisymmetric. Appropriate restraints, described below, were applied to ensure

the model maintained this axisymmetric behaviour.

Figure 5.8 shows the model geometry, with restraints applied. Two restraints were chosen:

1. A fixed restraint at the base of the tank. Tank foundation thicknesses are generally chosen to prevent problems from differential settlement of the soil beneath them, and may thus be considered as encastered.
2. Sliding restraints on the two side edges of the cylindrical section (labelled in Figure 5.8). These allow the faces exposed by cutting the tank to move radially and axially, but prevent any rotation around the axis. This ensures the section of the cylinder behaves as the entire cylinder would.

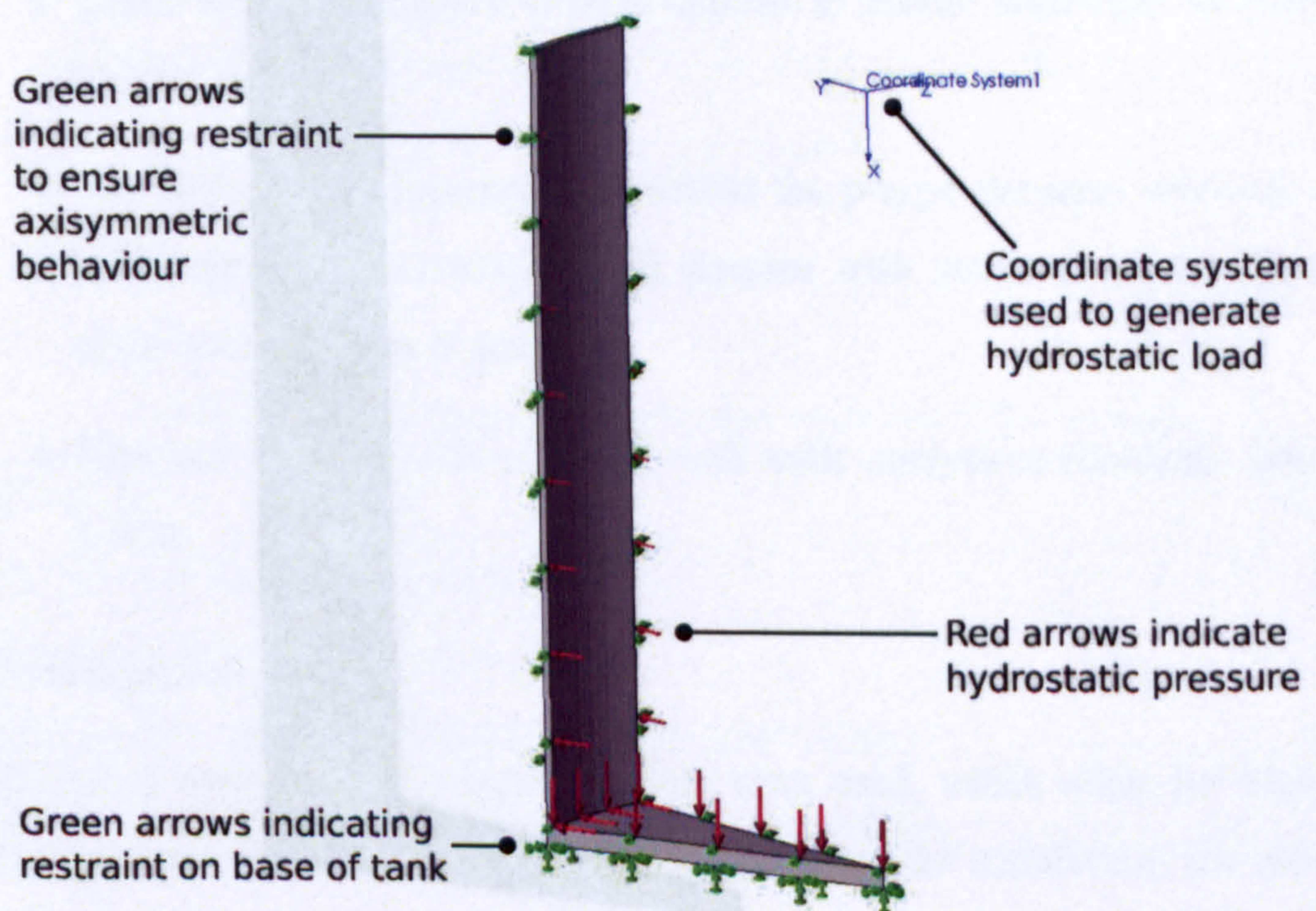


Figure 5.8: FEA model of cylindrical tank in SolidWorks, showing loads and restraints

Mesh generation

The mesh resolution was set to, at its coarsest, the wall thickness of the component, and in general was finer than this. In addition, ‘controls’—local, user-defined specifications for the mesh—were applied in areas of expected high stress-variation, such as the wall-base joint, and the joints between panels for 0D curvature tanks. These controls typically doubled the local mesh resolution. Figure 5.9 shows an example mesh, in this case for a cylindrical tank, and Figure 5.10 shows the increase in mesh resolution at the wall-base control.



Figure 5.9: Mesh applied to FEA model of section of a cylindrical tank

This choice of mesh resolution was considered adequate, as:

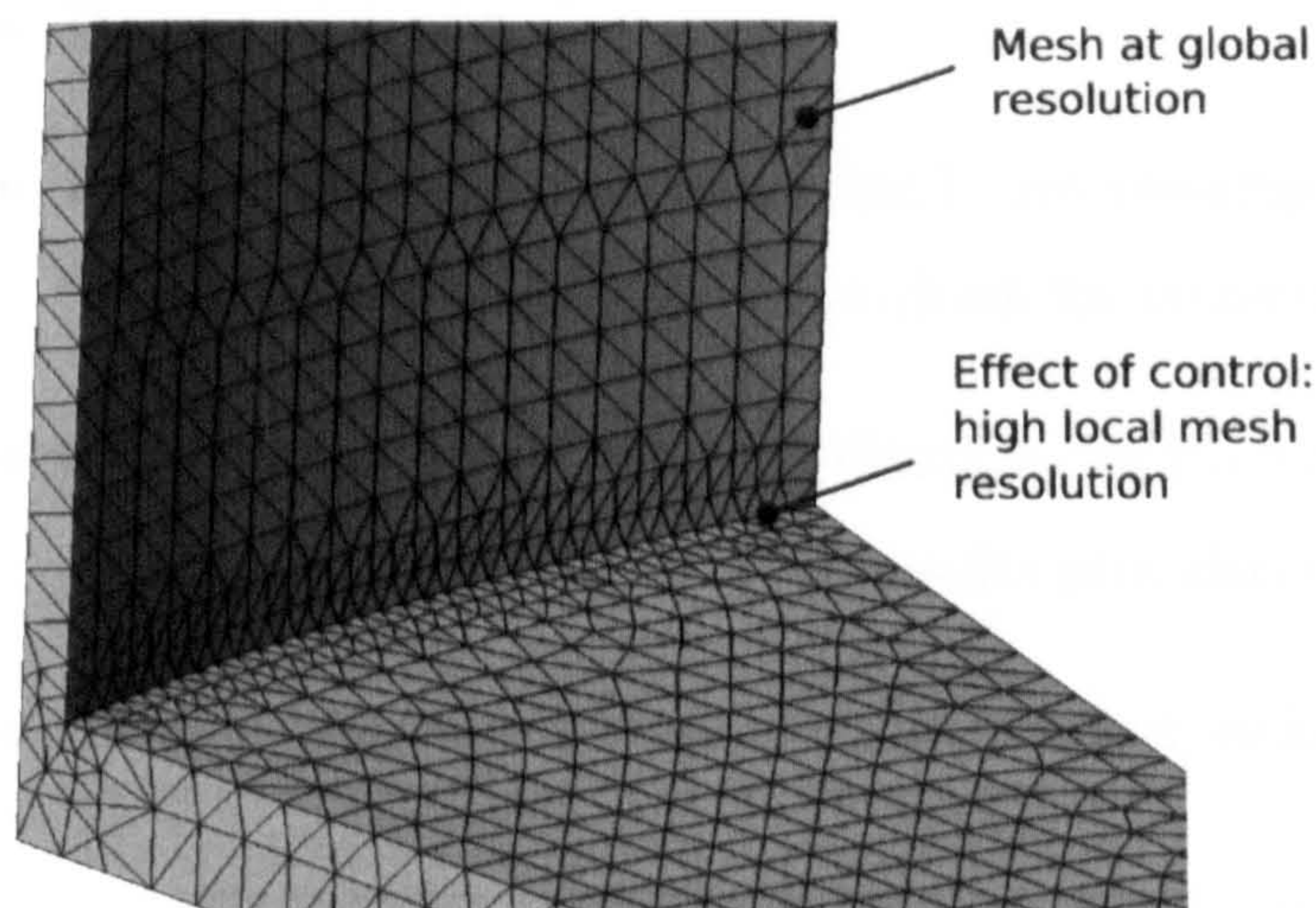


Figure 5.10: Section of mesh applied to cylindrical tank, showing increase in mesh resolution at “control”

- There were convergence criteria applied to ensure numerical stability (described below).
- The higher-order interpolation within the p-type elements used can model relatively complex variations in stresses with single elements (up to 5th order interpolation is possible).
- The use of this mesh matched well with analytical solutions, described below.

Convergence criteria

To ensure convergence, p-type elements were used, which allow for high-order interpolation within each element. For a single model simulation, the process is as follows:

- An initial run is conducted with the lowest order interpolation (e.g. 2nd order) interpolation within the elements.
- Measures such as strain energy are computed both for the individual elements and for the whole structure.

- The order of interpolation is increased.
- The model is re-run.
- The measures (strain energy etc.) are re-computed, and compared with those from the previous run, to check for convergence.
- If the change in convergence criteria is less than the specified threshold, the simulation is stopped, and the results provided to the user.
- If the convergence criteria are not satisfied, either:
 - If the order of interpolation is below the maximum, it is increased for selected elements (those elements whose local measure, such as strain energy, has changed by more than a threshold value between runs), and the model is re-run.
 - If the order of interpolation is the maximum available, the results are saved, and an error message is returned.

The settings in Table 5.3 were used.

Table 5.3: Criteria and settings used for FEA models

Measure	Value
Minimum interpolation order	2
Maximum interpolation order	5
Convergence threshold: change in total strain energy	1%
Update threshold for elements: relative strain energy	1%

Validation

The FEA package was validated for cylindrical tanks, with a built-in base, and free top edge. An example of the validation is presented below: Figure 5.11 shows

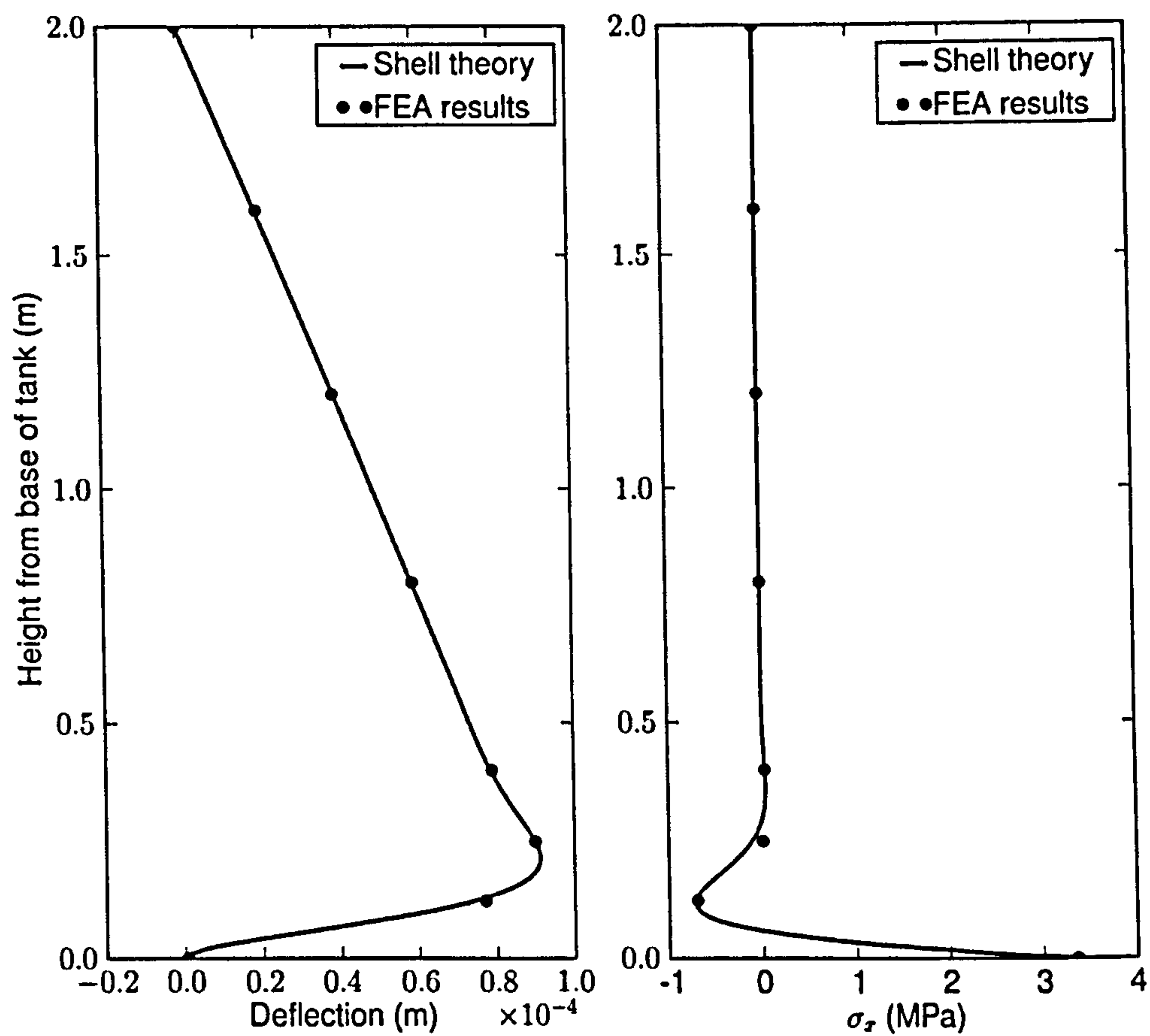


Figure 5.11: Example of FEA validation, comparing axial (x -direction) stresses and deflections of an FEA model and predictions from shell theory

a comparison of both the deflections and x -direction stresses for a cylindrical tank, 2m tall, with a wall thickness of 1cm.

The Figure indicates a small error (of the order of 2%) between the two, both in terms of deflection and stress. Table B.1 in Appendix B lists other comparisons between FEA results and those from shell theory. The approach of examining deflections as well as stresses also provides a useful visual qualitative check for simulations of more complex shapes, where an analytical solution is not possible: checking the simulation to see that the deflection seems reasonable, e.g. boundary conditions maintained, axisymmetric behaviour, deflections of the right sign.

5.4.2 Radial fillet at joint between tank wall and base

The features of cylindrical tanks, namely the highly localised bending stress at the wall-base joint, and its sensitivity to wall thickness, suggest that local modifications to the thickness could substantially reduce the bending stress, and hence the maximum global stress.

Figure 5.12 shows the cross-section and characteristic dimension of a radial fillet which could easily be applied to the wall-base joint of a cylindrical tank.

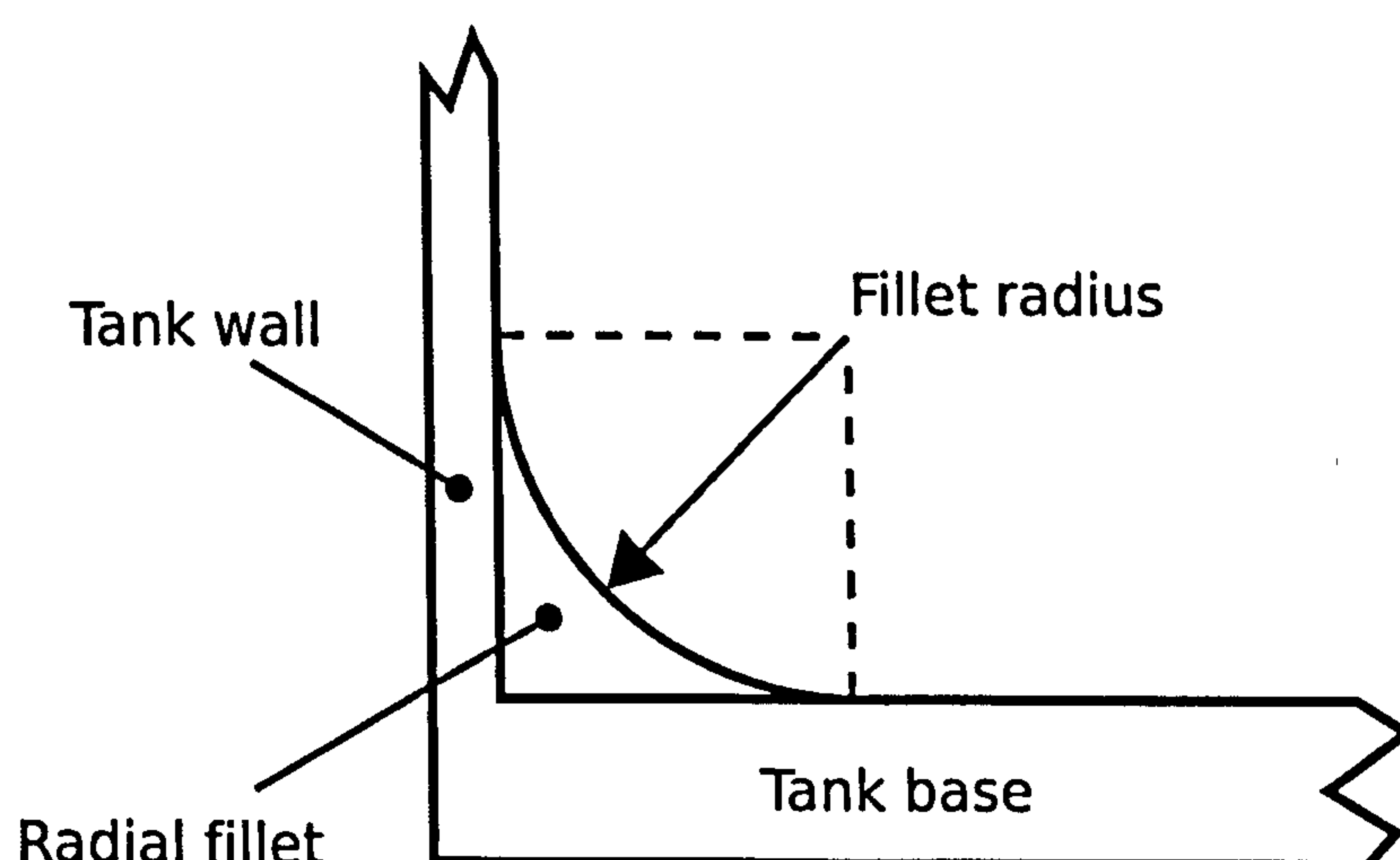


Figure 5.12: Cross section of wall-base joint of a cylindrical tank, showing radial fillet at joint

A number of runs using an FEA model assessed the effect of this radial fil-

let. Figure 5.13 shows a section of the FEA model, with the mesh used, and Figure 5.14 shows the variation in peak stress with fillet radius.



Figure 5.13: Section of FEA model for cylindrical tank with radial fillet, showing fine global mesh, and increased mesh resolution around fillet

Increasing the fillet dimension gives a significant reduction in stress. More interestingly, the amount of extra material required is small: a reduction of around 40% in stress is obtainable with only around 5% of the total material used to produce the tank. In addition to this, the FEA shows that, beyond a certain point, increasing the radial fillet at the base does not reduce the peak stress: initially peak stress occurs at the wall base joint, but once the radial fillet becomes sufficiently large, this stress falls below the greatest hoop stress higher in the tank, and no further benefit is obtained from increasing the fillet radius.

Approach: thickness to satisfy membrane constraint

The findings above suggest a simple method for optimising the design of constant thickness cylindrical tanks with fillets at the wall-base joint, as the radial fillet reduces the bending stress to less than the peak membrane stress with a negligible addition of material. Thus, to determine the optimum configuration:

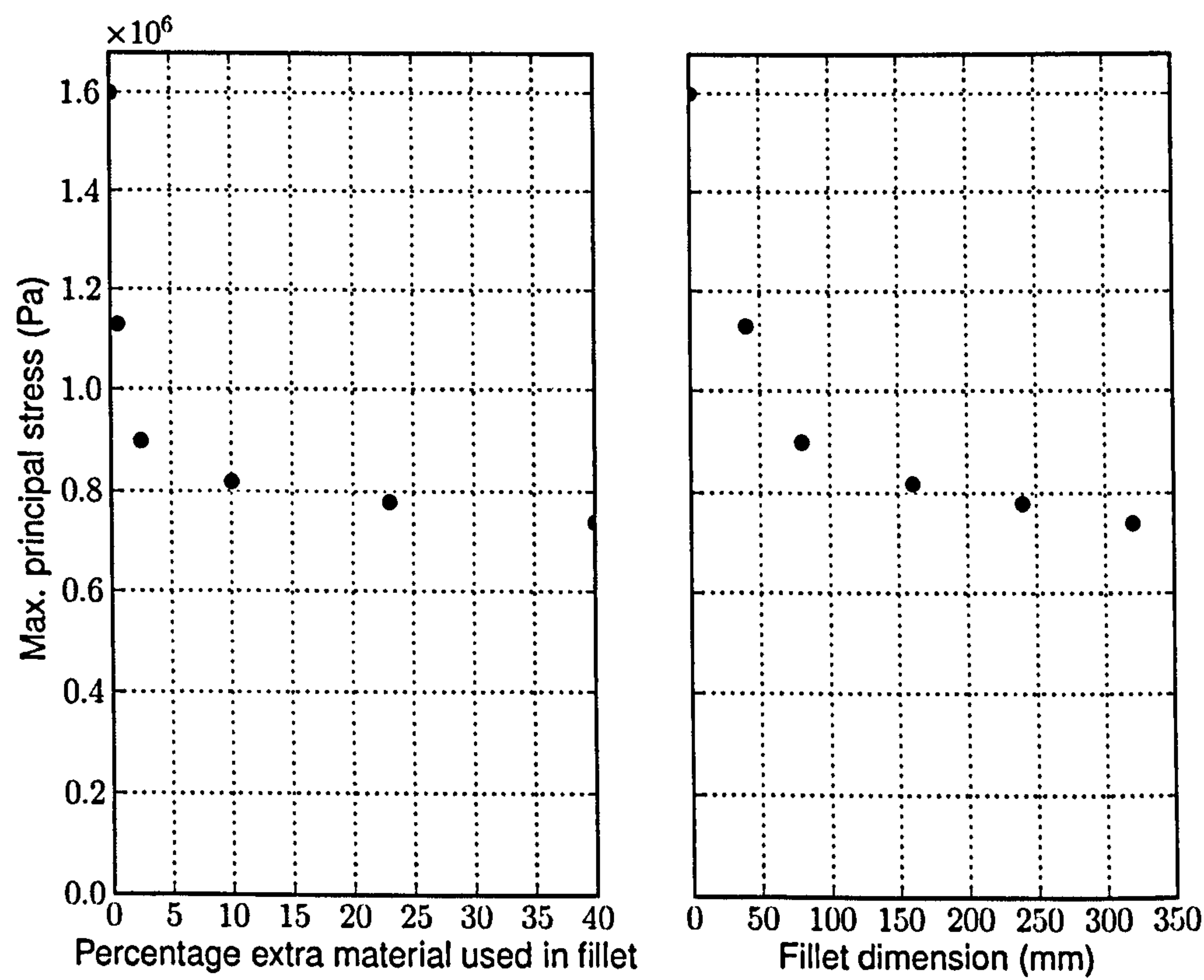


Figure 5.14: Variation in peak stress with radial fillet size for cylindrical tank

- Design the tank to give the minimum thickness to satisfy the hoop stress of the restrained shape
- Apply an internal radial fillet to reduce the bending stress to this level.

For this case we still have the limit of 10mm minimum wall thickness.

In this example, the optimum wall thickness falls to 18mm. Using this as a guide gives a total material volume of 0.35m^3 , plus the amount required to provide the radial fillet at the base. From a series of design scenarios in SolidWorks, this gives a total mortar volume of 0.37m^3 , which represents a 30% saving in materials and a relative cement intensity of 0.70: a significant saving.

Cement intensity of cylindrical tank, constant wall thickness and local thickness variation at base

For large (6m^3) tanks, a cylindrical tank with constant wall thickness will have a relative cement intensity of 0.70: the local thickness variation at the base gives a 30% reduction in materials usage.

5.4.3 Linear wall thickness variation with height

Several methods could provide a solution to the optimisation of this configuration: analytical, numerical based on solving the 4th order differential equation for a cylindrical tank, and numerical based on a solid model (FEA).

For this example we assume that the wall thickness can vary linearly with height, but that there is no radial fillet applied to the base. The same limitations for minimum wall thickness apply, as above.

In this case, the thickness of the wall at the wall-base joint, and height of the tank, must be chosen to give a bending stress below the design stress.

Using the minimum wall thickness of 1cm at the top, the base thickness must be 43mm, giving an average thickness of 26.5mm, and material saving of around

14% in total. This appears of similar magnitude to that reported by Thevendran & Thambiratnam (1987), working on cylindrical concrete tanks.

Cement intensity of cylindrical tank, linearly varying wall thickness, no fillet

For large (6m^3) tanks, a cylindrical tank with wall thickness that varies linearly with height will have a relative cement intensity of 0.86

5.4.4 Fillet at base and linearly varying wall thickness with height

This case represents the most difficult to achieve both practically and analytically. In fact, given the limitation that the top thickness cannot fall below 1cm, we could follow an approach similar to that of optimising tanks with constant wall thickness and a fillet at the wall-base joint:

- The constraint of the base limits the deflection locally; at some distance from the base, the deflection is the same whether the base is encastered or resting on a frictionless flat surface (the latter corresponding to the membrane solution). It is relatively straightforward to determine this point for a uniform wall thickness cylinder.
- We may assume that this height at which the base restraints have negligible effect is the same for cylindrical tanks with constant wall thickness and those with linearly-varying wall thickness.
- We can design the tank to have a local thickness sufficient to withstand hoop forces at this point.
- In addition to this thickness, and the minimum thickness at the lid of the tank, a radial fillet must be applied at the wall-base joint to alleviate high local bending stresses.

Using this approach gives a wall thickness of 18mm at a height of approx 0.5m, and a wall thickness at the base thickness of 21mm, giving an average wall thickness of 16mm. Combined with the addition of the radial fillet, this gives a material usage of 0.33m^3 , and an RCI of 0.62.

Cement intensity of cylindrical tank, linearly varying wall thickness, fillet at the wall-base joint

For large (6m^3) tanks, a cylindrical tank with wall thickness that varies linearly with height, and a fillet at the wall-base joint, will have a relative cement intensity of 0.62.

5.5 Summary

This Chapter has briefly covered the theory used to analyse cylindrical tanks. It has applied numerical and analytical tools to the optimisation of cylindrical tanks with increasingly complex cross-sections. The work indicates that the simple and easily achievable modification of applying a radial fillet at the joint between wall and base can give a significant reduction in either peak stress for negligible increase in materials, or a significant reduction in materials usage to satisfy a given design stress. The alternate modification, and more difficult to accurately produce by hand plastering, of varying wall thickness linearly with height, gives a significant, though smaller benefit, and would prove more difficult to achieve in practice. The combination of the two techniques; the most difficult to achieve in practice, would give the largest reduction in material usage.

5.5.1 Relative Cement Indices for cylindrical tanks

5.5.2 General implications for tank designs

Several features of cylindrical tanks may apply to other tank designs, including:

Table 5.4: Relative Cement Indices for cylindrical tanks of increasing thickness complexity

Design	Relative Cement Index
Uniform wall thickness cylinder	1
Uniform wall thickness, with fillet at base	0.70
Linearly varying wall thickness with height	0.86
Linear varying wall thickness with height, and fillet at base	0.62

- For constant wall thickness, peak stress may vary inversely with wall thickness ($\sigma_p \propto 1/t$) for both bending and membrane stresses.
- The discontinuity in both geometry and support at the wall-base joint may lead to high bending stresses, which can effectively be alleviated with a local increase in thickness.

These remain to be confirmed by further analysis, and are covered in the next Chapter.

CHAPTER 6

Component Design: Optimising Tank Designs

The previous Chapter addressed the datum design case, and modifications to improve the material economy. This Chapter considers the other two geometric classifications developed in Section 4.3 of Chapter 4, namely tanks with 0D curvature (prismatic tanks), and those with 2D curvature.

6.1 0D curvature: flat plates

As noted in the review in Chapter 4, flat plates have seen some use in water storage tanks. The smallest number of panels possible for a flat-panelled tank is three, but this has obvious inefficiencies in terms of ratio of enclosed area to perimeter. As the number of panels increases, this ratio improves, as the tank tends towards the limit, at an infinite number of panels, of a circular tank. However, increasing the number of panels has associated problems with the number of inter-panel joints required. Previous examples of flat panel tanks have used square plan tanks. For this section we will consider the case of hexagonal plan sections, as representing a balance between the benefit of a larger number of smaller panels, and the cost of having to join those panels.

Figure 6.1 shows an FEA model of a 0D curvature tank, with and without

radial fillets applied at the joints between panels and base.



Figure 6.1: Section of 0D curvature tank, with (a), and without (b) radial fillets at panel joints and wall-base joint

Finite element analysis of several tank configurations indicated that the high rigidity of the joints between adjacent panels, and between panels and the floor, gave the effect of a flat panel encastered on three edges and free on the top edge. Figure 6.2 shows the reduction in stress with increasing thickness of a typical plate.

Tanks with 0D curvature are attractive for the simplicity of manufacture they offer. However, this must be weighed against the poor material efficiency they offer. Even at significant thicknesses, substantially greater than those used for cylindrical tanks, the stress does not fall to a reasonable range for mortars in tension, as discussed in Chapter 4, i.e. even with an RCI of greater than 3, the flat panel tank does not satisfy the stress constraints.

Uniform wall thickness prismatic tanks

Uniform wall thickness prismatic tanks incur a significant penalty compared to the datum design, and are therefore unattractive.

The maximum stress develops at the joint between adjacent wall panels, part-way up the panels. As with the cylindrical tanks in the previous Chapter, this

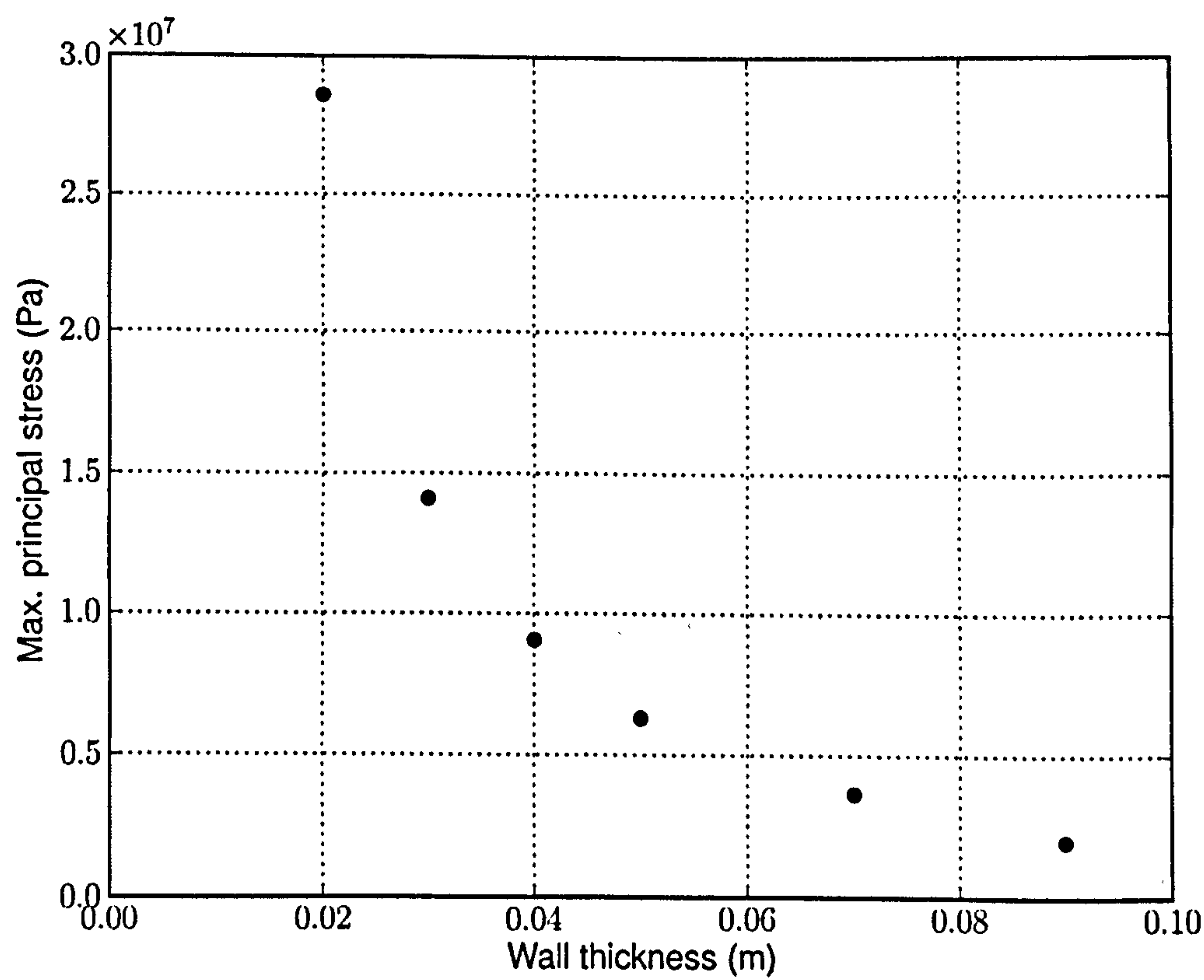


Figure 6.2: Variation in peak stress with wall thickness for panel tank with hexagonal plan, 2m tall and storing 6m³

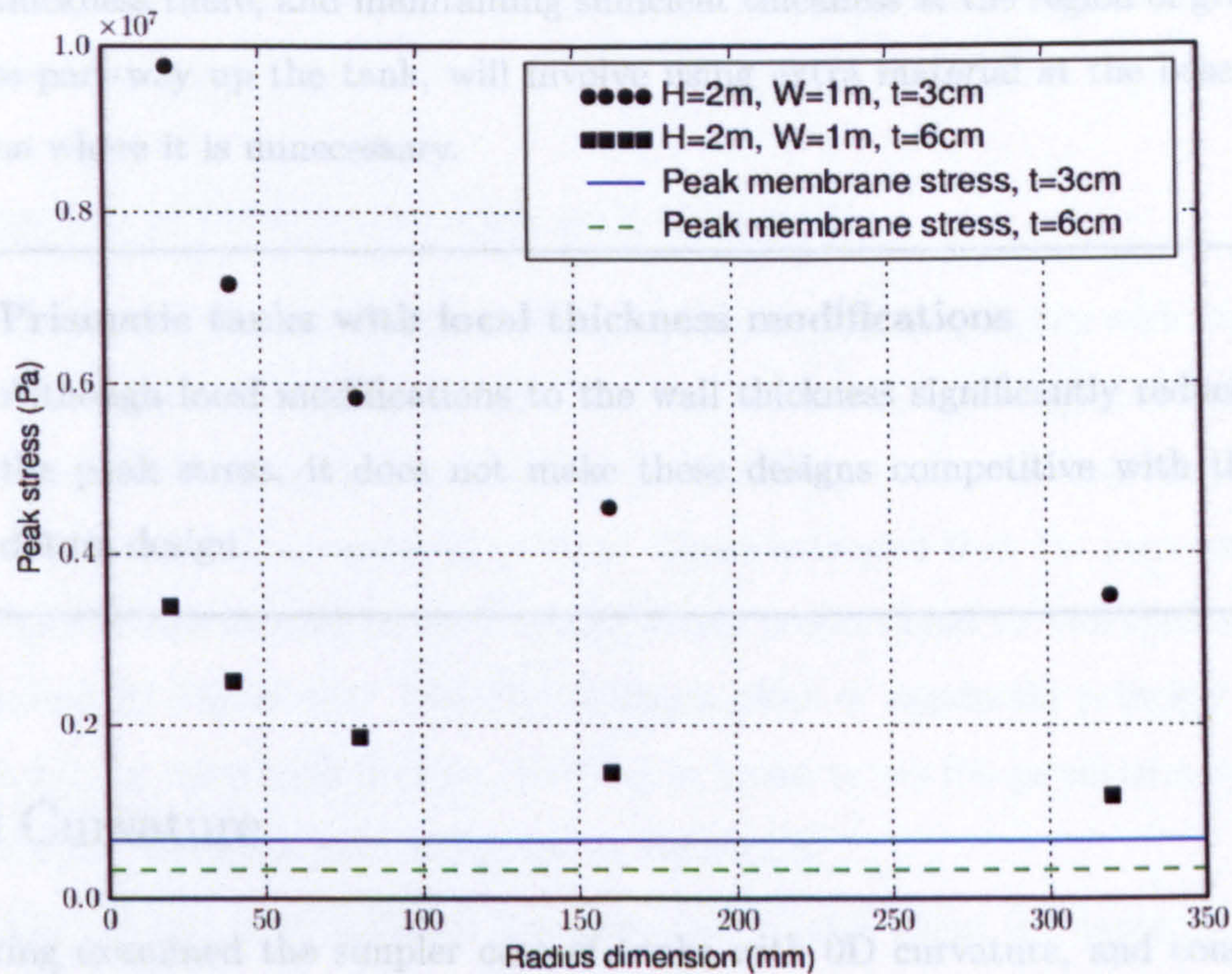


Figure 6.3: Effect of edge fillets on maximum principal stress for hexagonal plan prismatic tank, 2m high and storing 6m³ of water

suggests that applying radial fillets at these joints, and at the wall-base joint, could give an appreciable reduction in stress for little extra material. This does in fact hold, as shown in Figure 6.3, but again even a significant radial fillet does not reduce the stress to that of cylindrical tank.

The figure indicates that a wall thickness similar to the datum design will not give acceptable stresses, but that a greater thickness and large fillets will drop the stress to an acceptable level. However, in this case the volume of mortar used becomes significant: 6cm wall thicknesses and the less efficient shape (in terms of enclosed volume to surface area) give a mortar volume of around 0.91m³, and thus an RCI of 1.7, still considerably worse than the datum design.

The location of the peak stress some distance up the tank also indicates that varying the wall thickness linearly with height will give little benefit in terms of

stress reduction. Although there is little stress at the top of the tank, reducing the thickness there, and maintaining sufficient thickness at the region of greatest stress part-way up the tank, will involve using extra material at the base, in a region where it is unnecessary.

Prismatic tanks with local thickness modifications

Although local modifications to the wall thickness significantly reduces the peak stress, it does not make these designs competitive with the datum design

6.2 2D Curvature

Having examined the simpler case of tanks with 0D curvature, and concluded that they lead to a considerable penalty in terms of material use, we now turn to the more complex geometries of tanks with 2D curvature. Whilst some work has considered the use of membrane theory to generate efficient meridional shapes (Flügge, 1967), it used the criteria of constant stress throughout the entire structure, rather than the more useful, though more difficult to satisfy, criteria of minimising material usage for volume stored, with a given design strength. In addition, the membrane hypotheses break down at the wall-base joint (Timoshenko & Woinowsky-Kreiger, 1959), leading to the development of a non-trivial bending moment.

For these shapes, we consider the combination of linear wall thickness with height and 2D curvature too complex to produce in practice, leaving the two options of:

- Constant wall thickness.
- Constant wall thickness, and a fillet at the wall-base joint

Shell structures of the complexity of the designs in this section prove resistant to purely analytical methods, but amenable to numerical tools such as Finite Element Analysis.

6.2.1 Variation of peak stress with wall thickness

Section 5.3.4 of Chapter 5 indicated that the peak stress in cylinders with constant wall thickness varied inversely with the wall thickness, and suggested that this might apply to other tank geometries. To test this, a series of simulations were run for tanks with a variety of profiles. These indicated that the peak stress of constant thickness shell tanks is also inversely proportional to wall thickness, as indicated by Figure 6.4. The Figure shows plots of maximum principal stress with $1/t$ for three tank profiles, covering in broad terms the geometries possible with a 2D-curvature tank, indicated in Figure 6.5.

The top two lines in Figure 6.4 show some scatter about the linear fit, whilst the bottom line, representing the top-heavy tank, does not. The top-heavy tank differs from the other two, as the peak stress occurs in a region of membrane rather than bending action, and in this region stress does not vary rapidly with location. The other two designs (bottom heavy and equal radii) have peak stress occurring due to the bending moment action at the wall-base joint, and, as seen with the case of cylindrical tanks, in Figure 5.3 on page 113, this stress varies rapidly with location. It may be that this rapid variation makes the modelling more prone to artifacts in the mesh, so variations arise from the numerical modelling, and are not inherent to the solution of the governing equations.

The variation in peak stress with wall thickness has implications for materials selection, both in terms of sand type, for the situations discussed in Part II, where there is a choice between cheap, clay-contaminated local sand, or more expensive, uncontaminated imported sand, and sand-cement ratio.

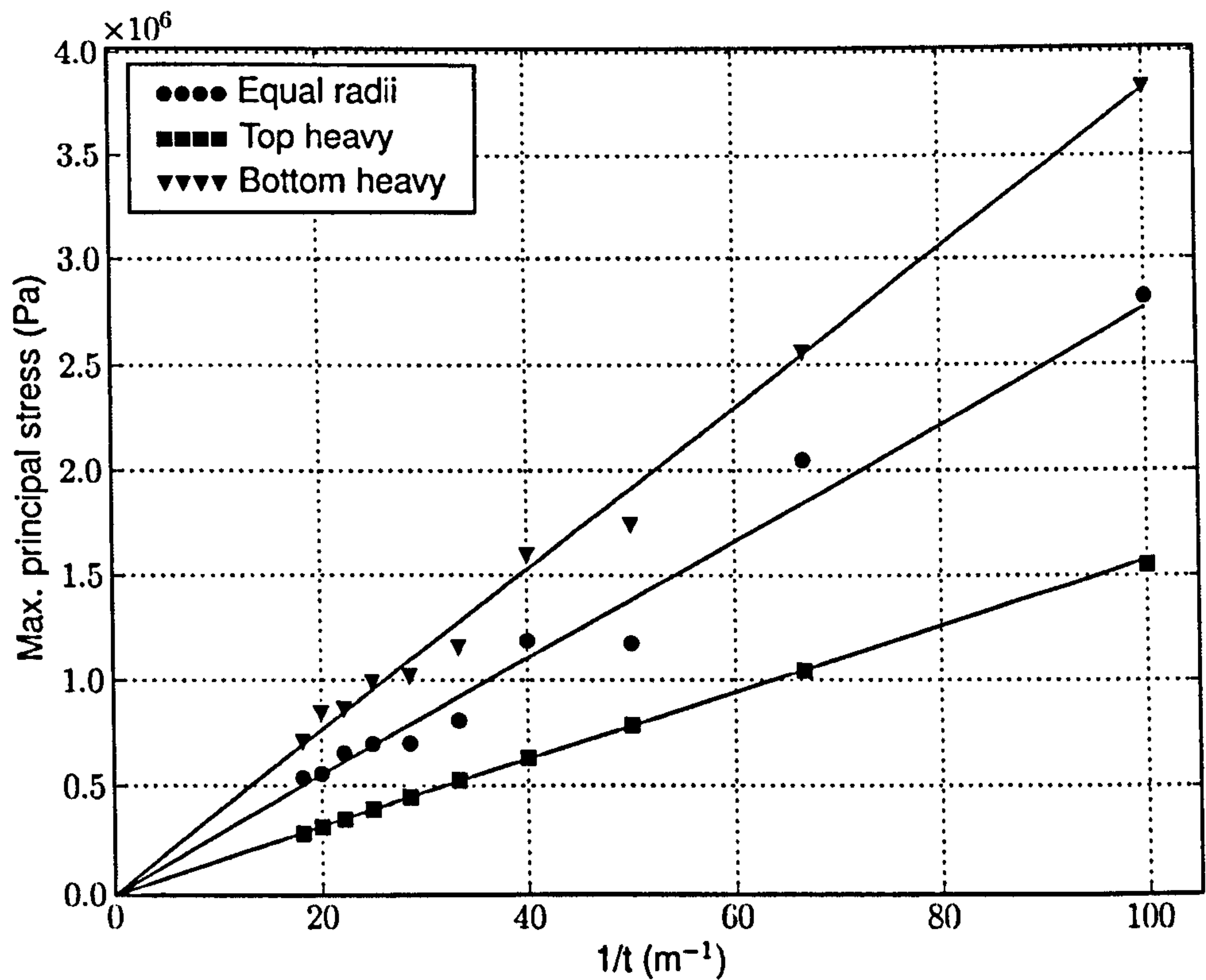


Figure 6.4: Variation in maximum principal stress with wall thickness for a variety of tank profiles, showing that peak stress is inversely proportional to wall thickness (solid lines indicate $\sigma \propto 1/t$ best fit).

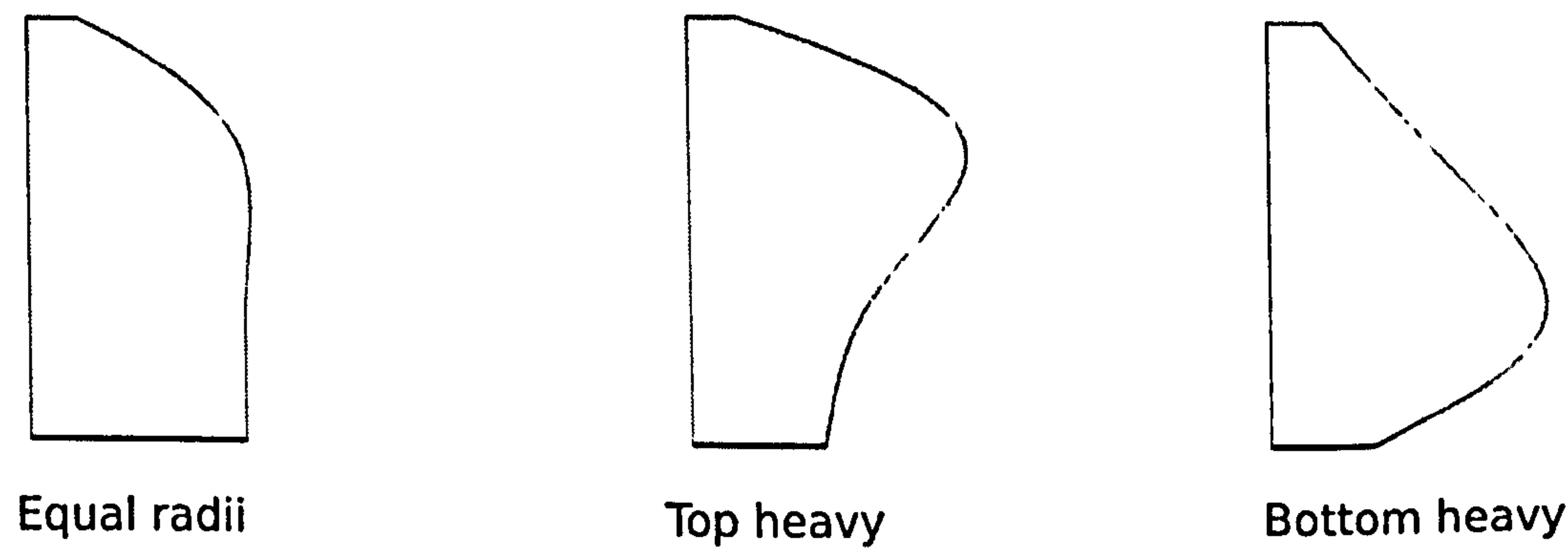


Figure 6.5: Examples of 2D profile types: top-heavy, equal radii and bottom heavy

Variation in peak stress with wall thickness

It appears that, for all attractive designs of constant wall thickness, the peak stress varies inversely with wall thickness. This suggests that a rich mix (sand-cement ratio of around 3:1) is the most economical, and that a more expensive, imported sand will perform better than a local, clay-contaminated sand.

6.2.2 Analysis of existing designs**Thai jar**

The Thai jar, a small tank of storage capacity around 2m^3 , has a design as shown in Figure 6.6.

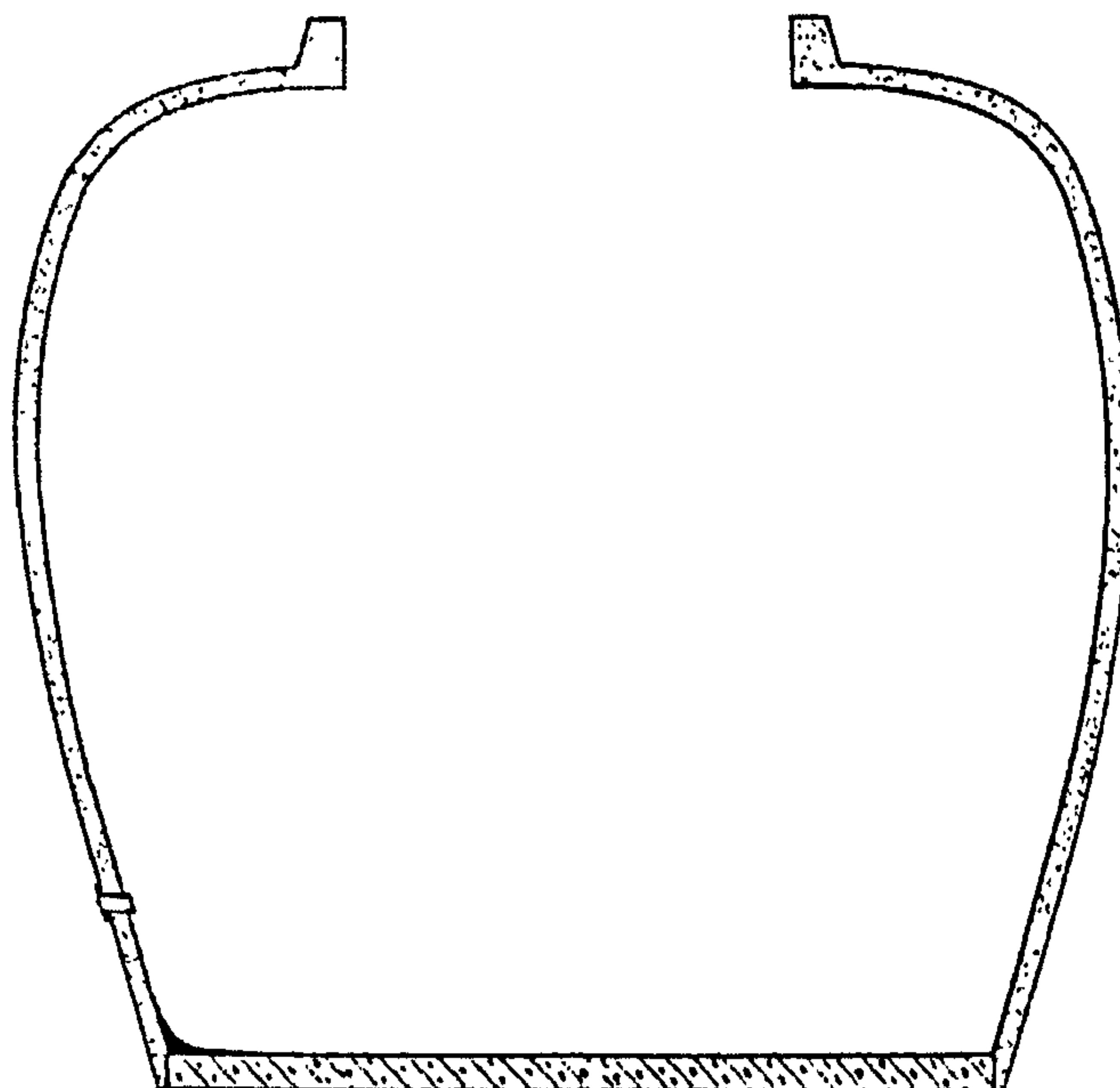


Figure 6.6: Thai jar profile

FEA simulations of the tank indicated that for the current design, the peak predicted stress is around 0.24MPa, significantly below the expected design stress. The design includes a small fillet at the wall base joint, and, providing this is greater than 60mm, the peak stress arises from membrane action, at a point above the base (about 0.3m above the base): Figure 6.7 shows this profile.

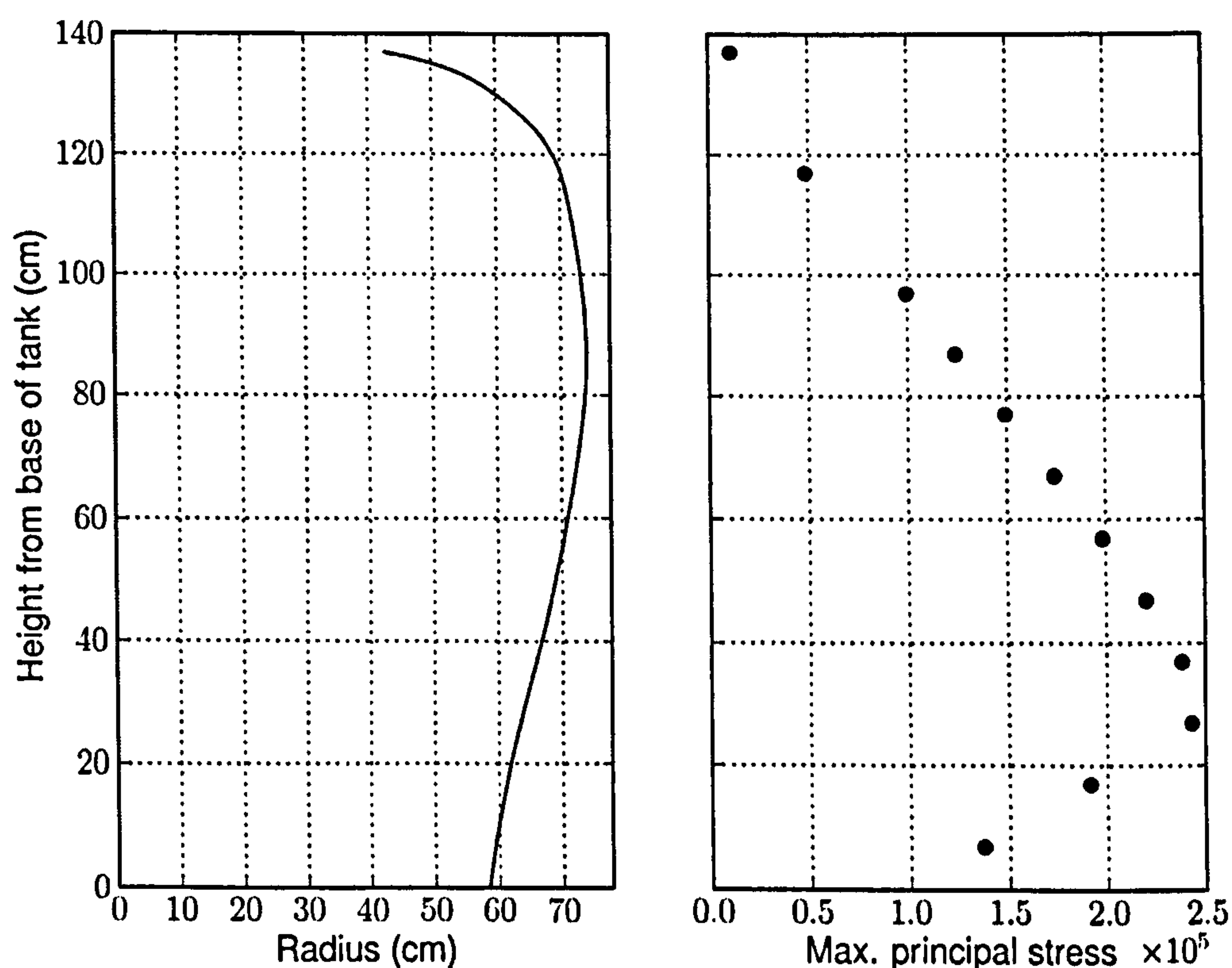


Figure 6.7: Variation in peak stress with height within Thai jar

In addition to this, reducing the wall thickness will give a stress closer to the design stress: if adequate filleting is used, the wall thickness can be reduced to 1cm without exceeding the design stress.

Sri Lankan pumpkin tank

The pumpkin tank has a larger storage volume, of around 5-5.5m³, and was designed to reduce bending stresses at the wall-base joint, by providing a smooth

transition between the two surfaces (as shown in Figure 6.8).

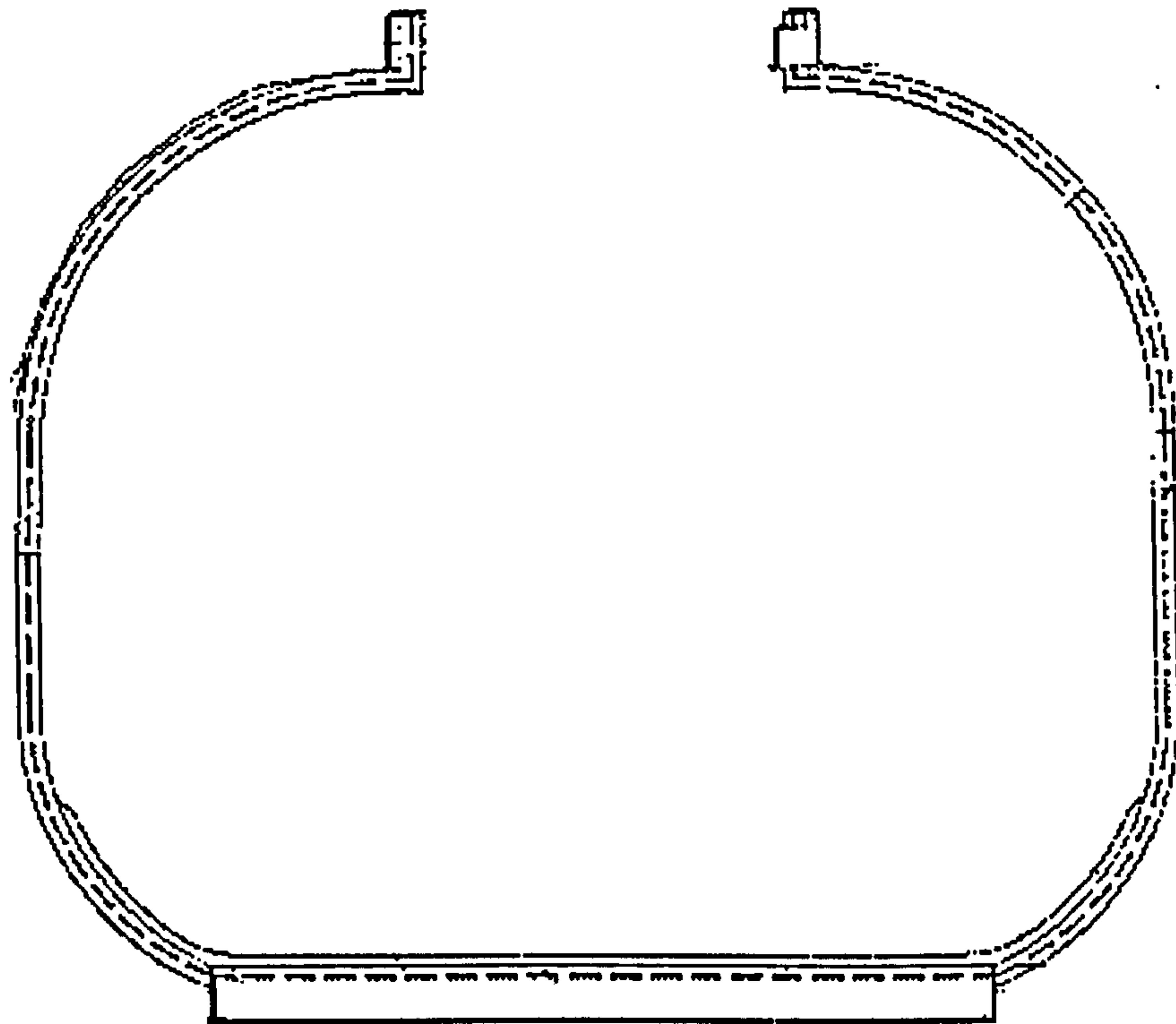


Figure 6.8: Profile of Sri Lankan Pumpkin tank, showing smooth wall-base joint, and extra layer of mortar at base

FEA modelling of this also indicated that the peak stress still occurred at the wall-base joint, and that the Pumpkin tank and the datum design use a similar amount of material. This suggests that modifications to approximate smooth curvatures at the wall-base joint are not sufficient to reduce the bending stress to lower than the peak membrane stress.

Summary of existing designs with 2D curvature

Both the popular designs examined have some degree of thickness modification at the wall-base joint, in an attempt to alleviate the stress there. Whilst the Thai jar does this effectively (providing the radial fillet at the wall-base joint is large enough), the modification on the Pumpkin tank does not appear effective.

6.2.3 Profile selection: constant wall thickness

To select the optimum geometry, a number of iterations were employed. A generic tank design was produced, using a spline with four control points. The top point was set to a radius of 0.25m, to provide a tank opening of sufficient width for access to maintain the tank, but small enough to be easy to span with a cover. The middle two radii were varied, and the base radius selected by an iterative routine to give the required storage volume. Figures 6.9 and 6.10 show an example model, including the defining geometry, and the shape of a meshed tank respectively.

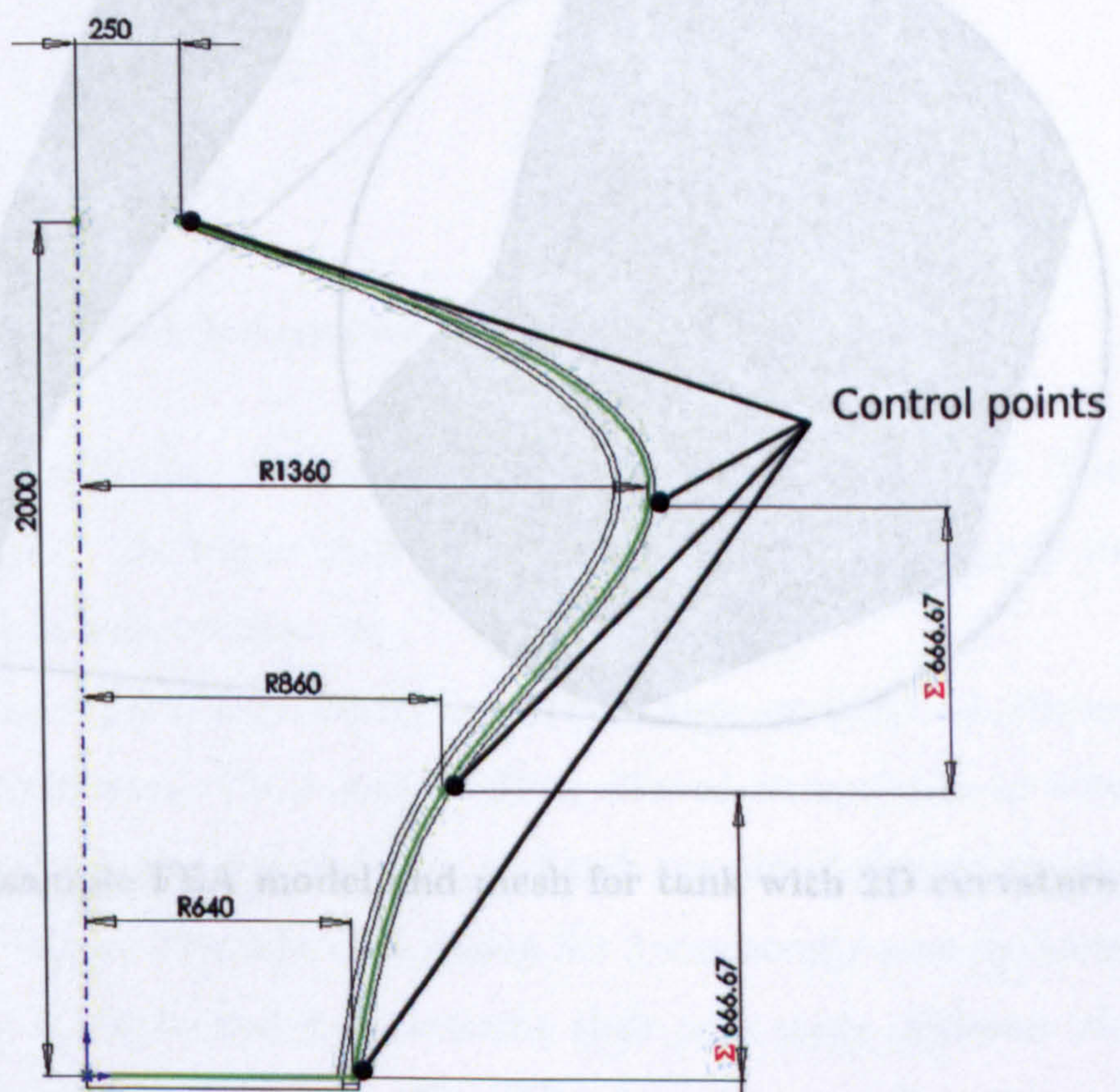


Figure 6.9: Example FEA model for tank with 2D curvature, showing spline with control points

A number of configurations were selected, shown in Figure 6.11 (Table B.2 in

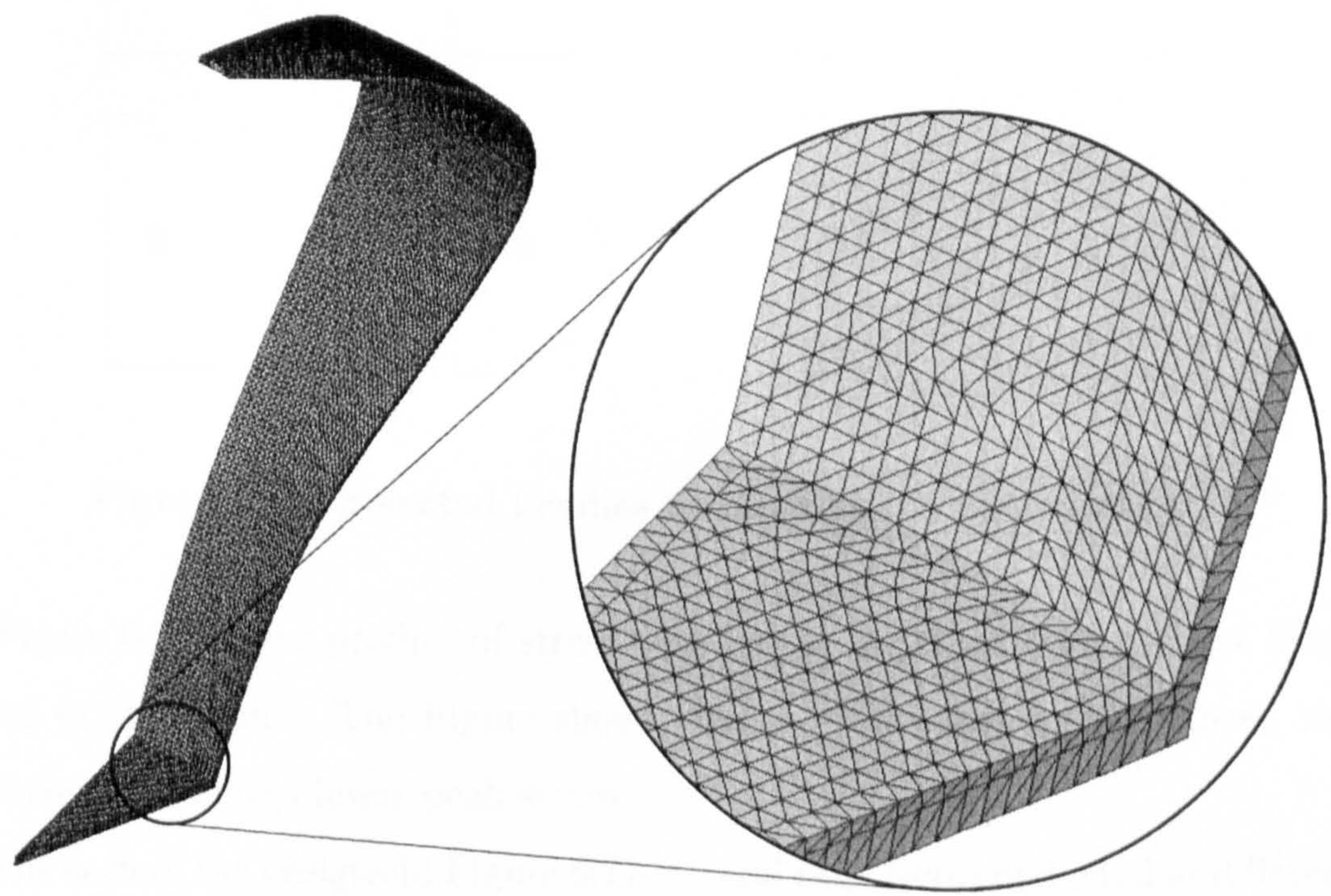


Figure 6.10: Example FEA model and mesh for tank with 2D curvature

Appendix B lists the configurations).

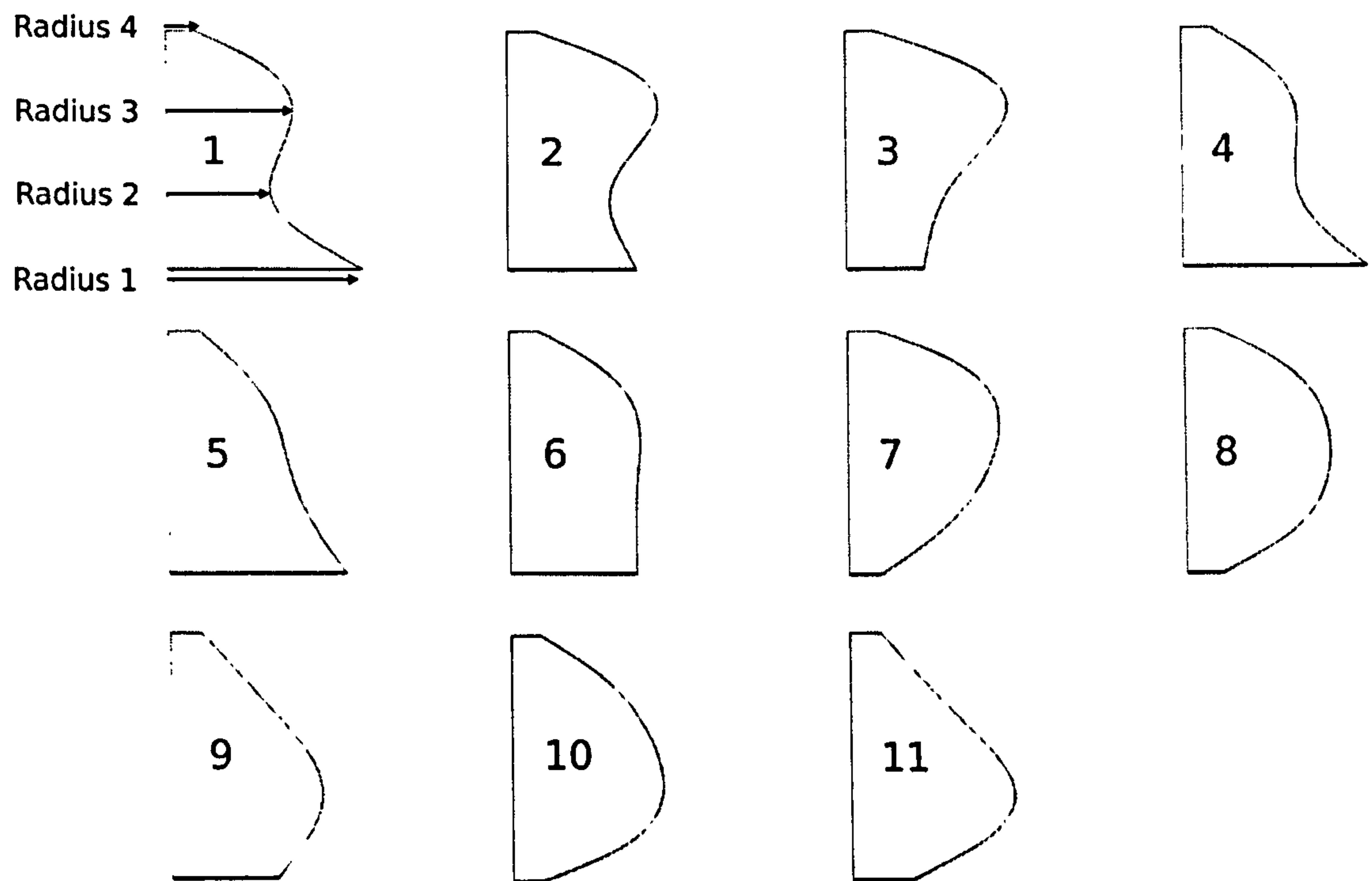


Figure 6.11: Selected profiles for tank shape optimisation

Figure 6.12 shows profiles of stress with height for three tank designs, illustrated in the Figure. The Figure shows that, for the same wall thickness, the top-heavy tank gives lower peak stress.

For each of the designs in Figure 6.11, several runs were conducted at different (constant) wall thicknesses. These configurations allowed interpolation to select the optimum wall thickness for each design, and each run provided some comparison between the designs. Over the runs, design Set 3 consistently gave the lowest stresses. Analysis of all the designs, combining their peak stress-thickness relationships, and their material usage, confirmed Set 3 as the most efficient (lowest material usage) design.

Choosing the minimum wall thickness to give a stress below 1MPa gives a mortar volume of 0.31m^3 , and hence an RCI of 0.58.

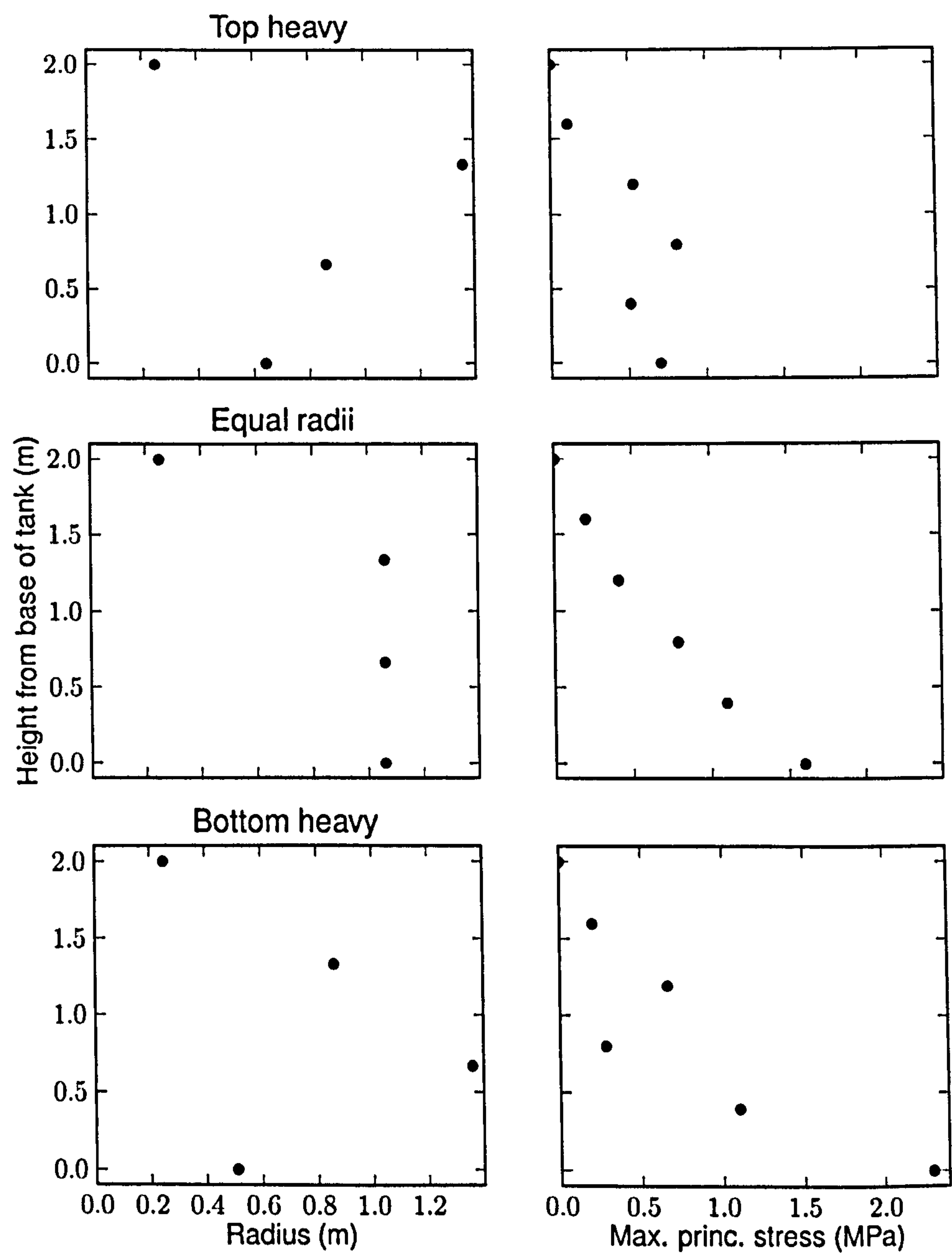


Figure 6.12: Example stress profiles for 2D curvature tanks, plotted with control points

Constant thickness tank with curvature in 2 dimensions

Choosing a “top-heavy” tank, with 2D curvature, gives a significant materials saving over the datum design

The good performance of the top-heavy tank design can be understood by using similar concepts to those involved in the modelling of cylindrical tanks. Without the wall-base joint, the tank base would be free to move, and this movement would lead to hoop stresses. In general, and as with the cylindrical tank, the larger the radius of the tank, the greater the hoop stress. In addition, the larger the pressure, the greater the hoop stress. The base constraint exerts a restraining force and moment at the joint between wall and base, giving rise to bending stresses. A smaller diameter at the base will lead to lower hoop stresses, and hence require a smaller “correction” action from the base. The section of the tank with larger diameter is higher up, and hence experiences lower hydrostatic pressure. In addition to this, as the tank base is thicker than the tank walls, designs that have a large base radius incur a materials penalty that will favour top-heavy designs, with their smaller base radius.

As well as leading to lower materials usage, the peak stress in the optimal constant thickness profile occurs some distance from the base of the tank. In this case, filleting the wall-base joint, assuming a good joint has been made during production, will give no stress reduction.

6.2.4 Optimisation of membrane action tanks

Previous sections of this chapter have noted that:

- The membrane solution for axisymmetric tanks is significantly simpler to obtain than a solution that involves the effects of bending.
- The disruption to the membrane solution occurs due to “discontinuities”

- For water storage tanks, the “discontinuity” that causes bending stress is the wall-base joint.
- The effect of the bending stress is localised.

We have seen, in the case of cylindrical tanks, that the addition of relatively little material in the region of peak bending stress can significantly reduce this stress, to the extent that the peak hoop stress elsewhere in the tank limits the minimum wall thickness. The same approach may be taken for tanks with curvature in two dimensions.

The code in Section D.4 of Appendix D creates a class that allows for the solution of any membrane tank, with the base point selected to give the required storage volume, and wall thickness varying linearly with height. The program also calculates the mass of mortar used to produce the tank, given the wall thickness at the base and top, and the plinth and cover thicknesses. As it is computationally quite cheap to find the solution to membrane-action tanks, a search can easily examine a large number of designs.

The simulations confirmed the choice of top-heavy tanks (with linear wall thickness) as the optimal design. This shape corresponds well with the FEA work in section 6.2.3. This is useful as a confirmation of the results from the FEA, but not, at present, as a stand-alone design tool. The restraint of the base makes the membrane solution inaccurate in that region, both in terms of the bending moment (not considered in this approach, for the reasons indicated above), and in terms of displacements, and hence stresses.

6.3 Summary

It appears that the simplicity of prismatic tanks comes with a considerable cost in terms of materials usage, whilst the increased complexity of curvature in 2 dimensions allows much more efficient shapes to be used.

CHAPTER 7

Component Design: Tank Prototype Design, Manufacture and Testing

Overview

The previous chapter used analytical and numerical modelling to generate improved tank designs. This chapter covers complementary experimental work producing a 2000l storage-capacity water tank. The work was intended to:

- Validate the practical use of the designs generated in chapter 6.
- Validate the numerical modelling (FEA) employed.
- Explore an alternative production method, using an external mould. Chapter 9 covers this.

The sections in this Chapter cover:

- Production of a prototype design.
- The testing of this design.

- Assessing the accuracy of the Finite Element Analysis modelling.
- Analysing the failure of the tank during testing, which occurred when filled to 1600l of the 2000l design capacity.

The production and testing indicate:

- The failure *mode* of the tank matches that predicted by the FEA modelling.
- The failure appears due to low local wall thickness and poor build quality.
- Whilst designs such as that described here, and those employed in the field (DTU, 2006b), can work effectively, the low wall thicknesses employed make good quality control imperative.

7.1 Design

7.1.1 Geometry

For a storage capacity of 2000l, the profile shown in Figure 7.1 (optimised using FE analysis for the criterion ‘constant wall thickness’) was chosen, with a wall thickness of 1cm, 8cm radius base fillet, and a stress safety factor of 3.

7.1.2 Materials and mix

As the work in Chapters 5 and 6 suggested the peak stress will vary inversely with wall thickness ($\sigma \propto 1/t$), and the results from Part II indicate that a high quality (“imported”) sand gives the lowest cost for this design, such sand was selected for the prototype. The sand used was similar to that in Chapter 3.

7.2 Method: Tank production

The basic process was: make the bottom 70% of the tank in one piece, and the top 30% as a basin, then invert the lid and place it on the bottom section. An

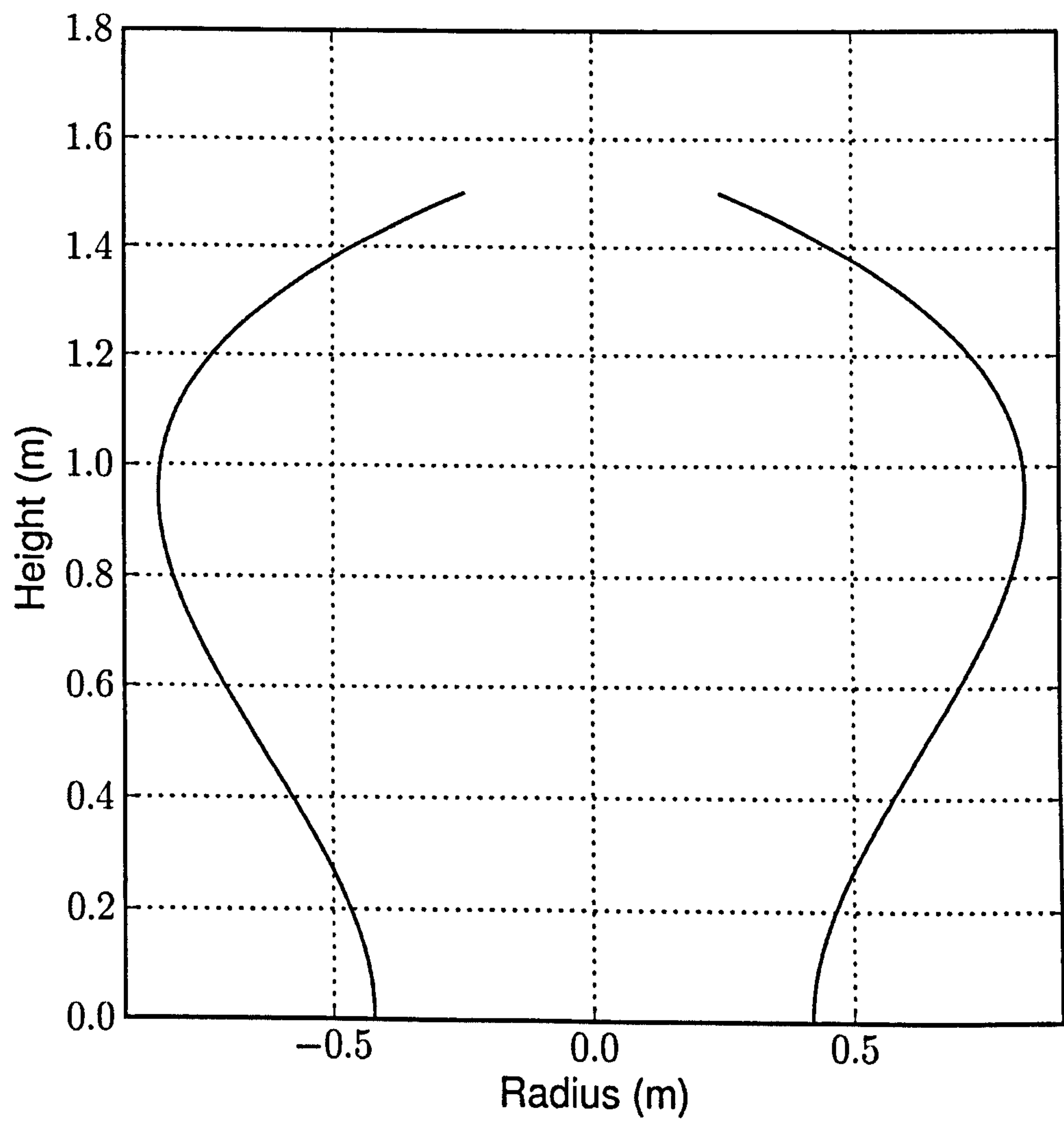


Figure 7.1: Profile selected for 2000l water tank

external mould was used, as discussed in Chapter 9.

7.2.1 Wooden mould construction

Section B.5 of Appendix B gives details of the mould construction, which involved the following stages:

- Cut thick (12mm) plywood to make profiles.
- Mount the profiles to make section frames.
- Drill these frames to join them to each other.
- Fix thin (5.5mm) strips of plywood on the sections.
- Varnish.

Figure 7.2 shows these stages.

7.2.2 Mould preparation: mud coating

Following production of the mould, a layer of “mud”¹ was applied, to give a smooth surface finish, and act as a release agent to aid demoulding the tank.

Mud was chosen as the release agent as:

- It has successfully been used for production of water storage tanks in LEDCs (DTU, 2006b).
- It is cheap and relatively readily available in LEDCs.
- It can be rendered to a smooth finish.
- It will lose strength with the addition of water, easing the process of demoulding.

¹Sand K was used, with a moisture content of approximately 17%, to produce a “mud” release agent in sufficient quantities.

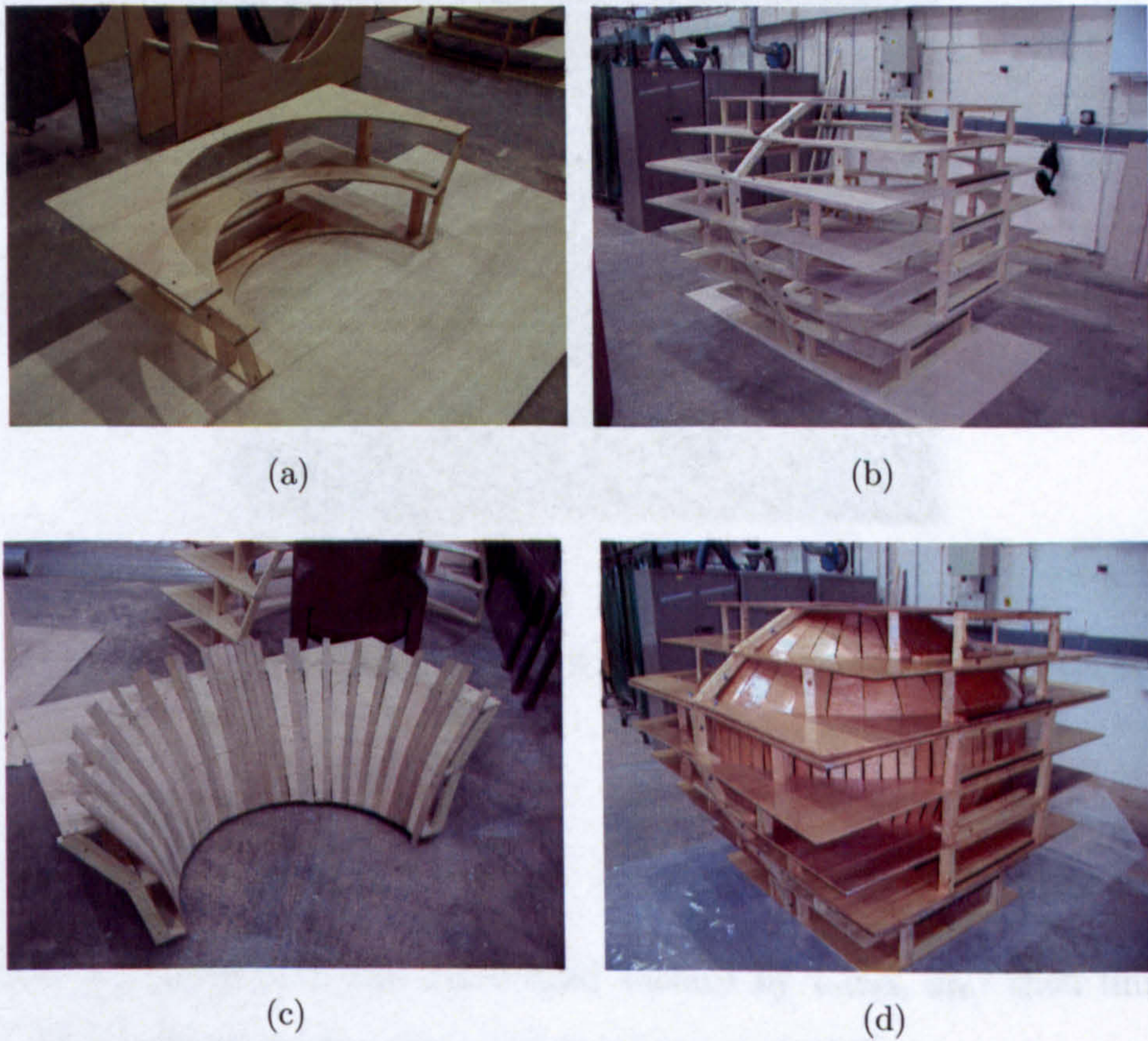


Figure 7.2: Phases in the construction of the wooden mould, from (a), a single wooden frame, to (b), the complete set of profiles as a frame, to (c), fixing ply strips to form the “coarse” surface, and finally (d), the completed mould coated with varnish.

- On sufficient drying, it can be reused.

The two sections that form the bottom layer of the mould, and one of the upper sections, were held together at this point, to minimise the number of joints between mould sections to be made during plastering of mortar on to the mould. Figure 7.3 shows this.

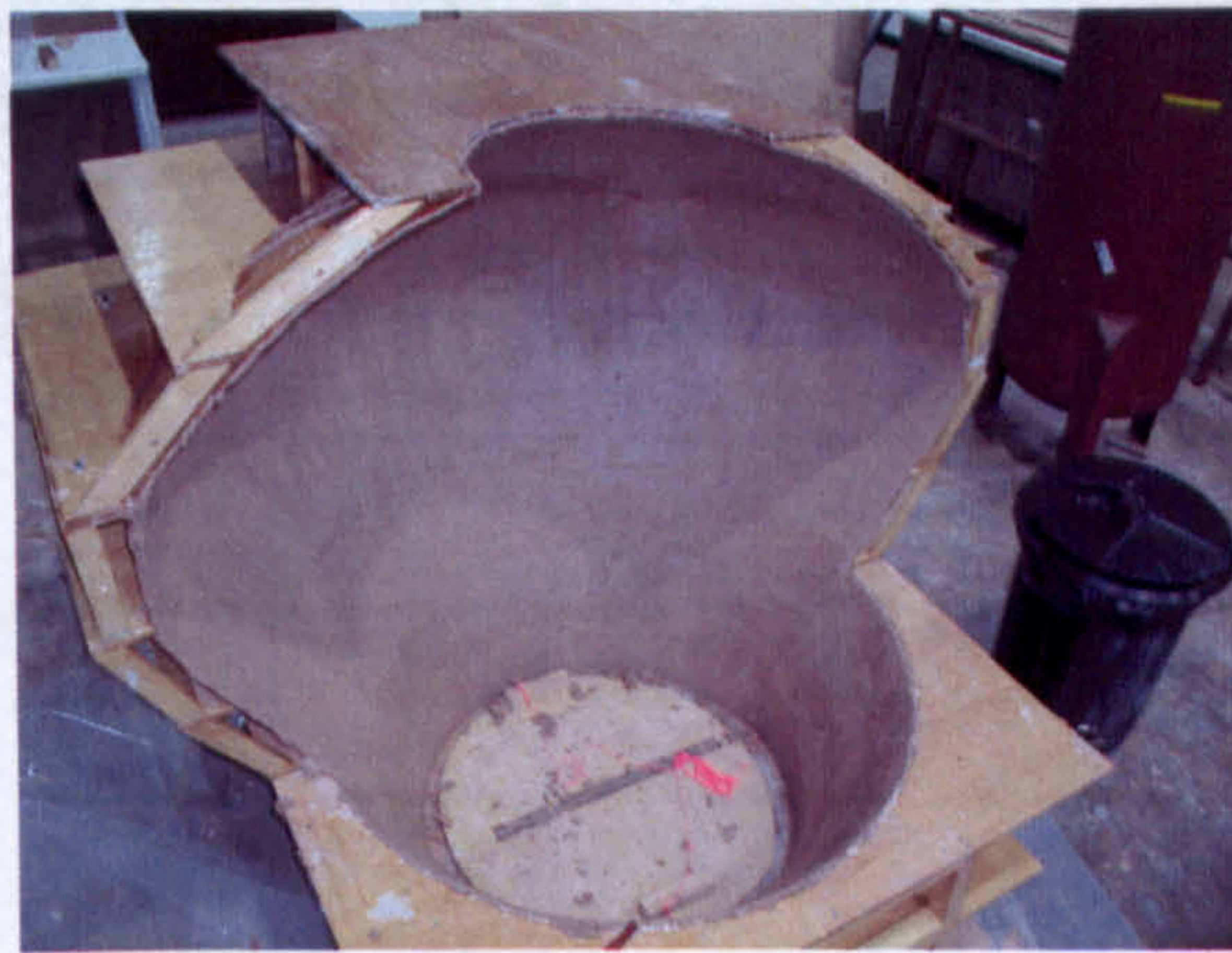


Figure 7.3: Application of mud coating to wooden tank mould

7.2.3 Application of mortar

Mortar was applied onto the dried mud surface by hand, and then finished by trowel. The internal surface did not appear very smooth.

7.2.4 Joining tank lid and base

The lid was cast inverted (i.e. as a basin shape), to avoid problems with mortar adhering on an overhanging surface, and plastering overhead, and then inverted, resting on several scaffolding planks. It was then lifted by these planks, and placed on the rim of the lower part of the tank. 50×50mm wooden spacers were placed around the circumference, and the scaffold planks removed. Mortar was placed between the wooden spacers, and the spacers then gradually removed, to leave the lid resting entirely on the mortar. The outside surface of the joint was

then mortared over, to give the completed tank. Figure 7.4 shows the lid being put in place, and the completed tank.



Figure 7.4: Placing the lid on the tank (a), to form the completed tank (b).

7.2.5 Curing

During curing the tank was covered with damp hessian, and then wrapped in polythene sheeting, similar to the curing conditions used for the mortar samples in Part II, and to that used in the field. Once the samples had cured for a day, water was placed in the bottom sections to ensure a moist environment for curing.

7.3 Method: Tank strain and strength testing

7.3.1 Instrumentation

To obtain data from the tank testing, a number of forms of instrumentation were used: two forms of strain measurement (demec gauges and strain gauges), and video recording.

Video recording

It was considered possible that the tank would fail at some point during the testing. Whilst workers in the field have experienced this, failure does not nor-

usually occur in situations where detailed analysis is possible. To obtain a greater understanding of the failure process, a video recording of the whole tank loading process was taken, using a Pulnix TM 250NIR video camera.

Strain measurements

For both the strain measurements, a number of properties were desirable:

- A number of data points to enable comparison with the FEA results.
- A number of points, at the same height and of the same orientation, on different meridians around the tank, to give data as to how axisymmetric the deformation was. In theory these equivalent points should deform by the same amount.

To allow for this, both sets of gauges were mounted at six points along a meridian, and on three meridians distributed axisymmetrically around the tank. At each point a pair of gauges were mounted for each form of measurement: one horizontally, to measure hoop strain, the other in a vertical plane along the meridian, to measure meridional strain.

Figure 7.5 shows an example mounting of strain and demec gauges. 50mm demec gauges were used, along with 30mm, 120 ohm strain gauges.

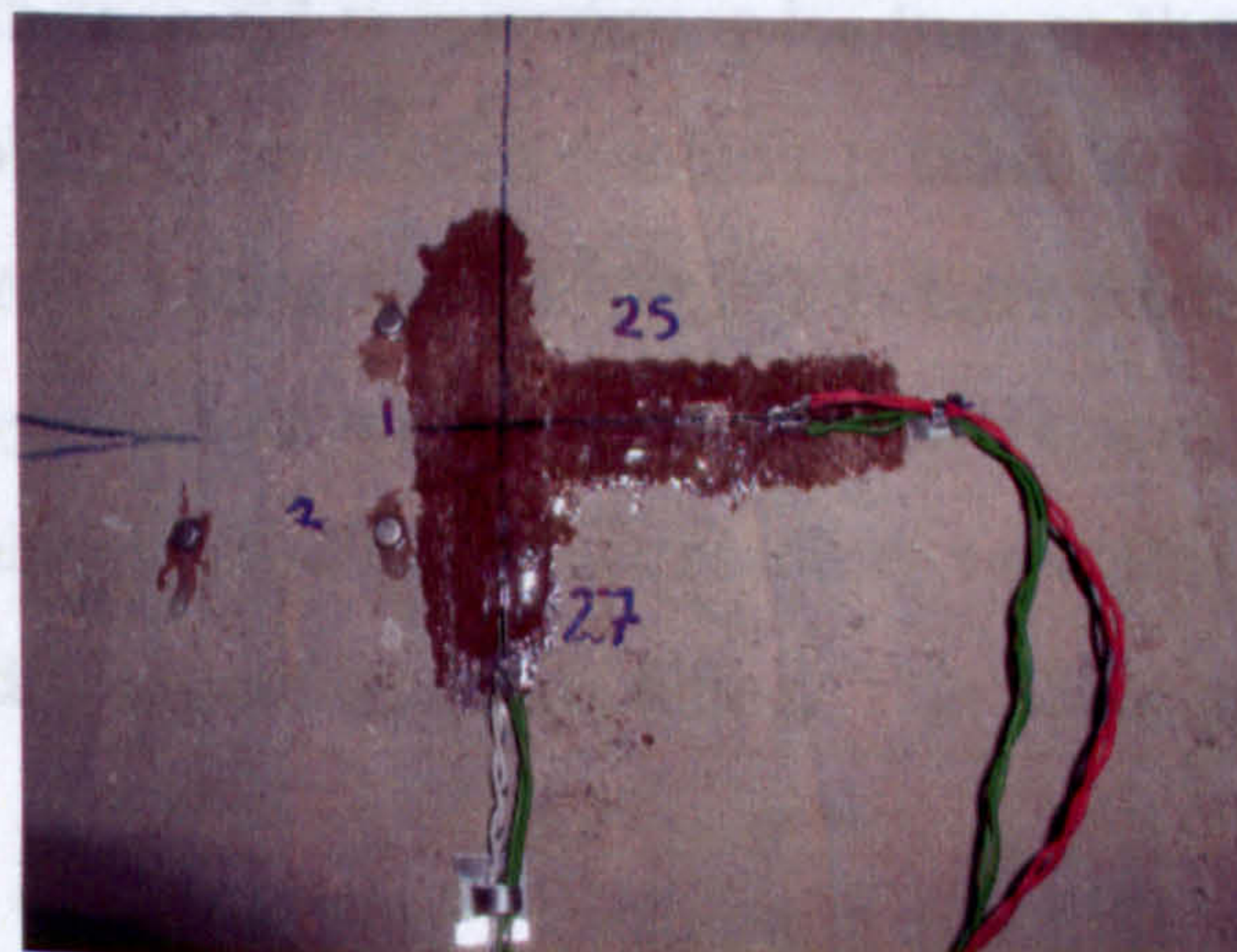


Figure 7.5: Orientation of Demec and strain gauges on the tank surface

The strain gauges were recorded using a Solartron 3531D data logger. For initial filling readings were taken every 10 seconds. During the later stages of filling, readings were taken every 5 seconds. The gauges were configured in a quarter-bridge arrangement. Whilst this would provide temperature compensation for variations in global temperature, it would not correct for local variations at the tank surface due to filling with cold water. However, the error in changing temperature from ambient levels of 19°C to mains water temperature, measured at 11°C, would not exceed 7%, based on the manufacturer's data.

Section B.6 of Appendix B shows the configuration of the gauges.

Figure 7.6 shows a sample video image during testing. The visible meridian is A (strain gauges in the range 1–23), with meridian B (strain gauge channels 25–47) 120° to the right, and meridian C (strain gauge channels 49–71) 120° to the left.

7.3.2 Loading process

Loading of the tank took place over several hours. To confirm the capacity of the tank, the flow rate from a mains water supply was measured as 21l/min, and filling occurred in discrete intervals of 5 minutes. When compared with the FEA model, the filling was consist around 20% less than that expected. The flow rate within the building may have varied over time (the sound pitch of water coming from the tap did change during loading, so the positive correlation between expected volume and measured volume is taken as an indication that the FEA model was correct, and is used in Table 7.1. Each filling session (of around 130l) was followed by observation of the tank, measurement of the water height, and after every 10 minutes of filling demec readings were also taken. Strain gauge readings were logged continually during filling. The filling process ran as shown in Table 7.1.

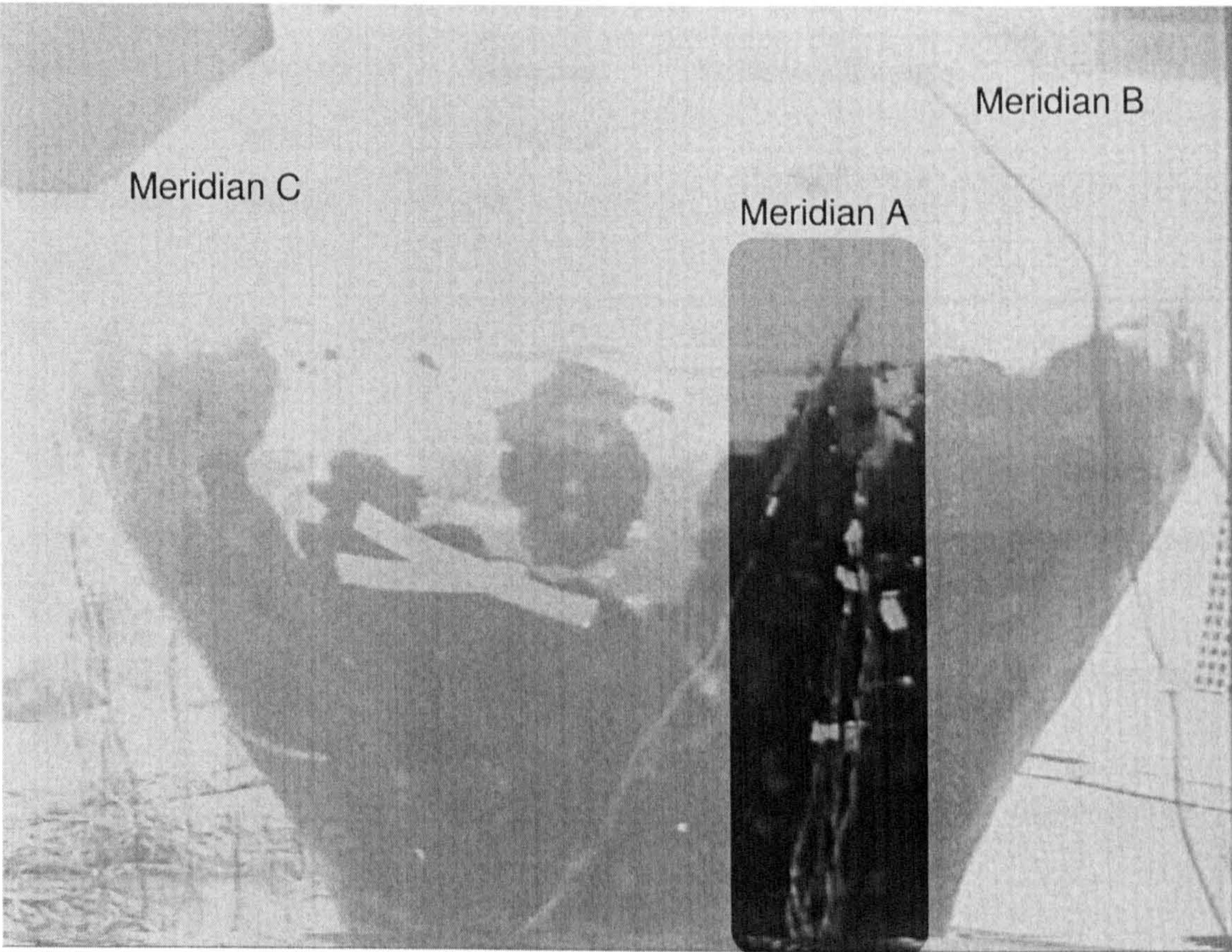


Figure 7.6: Sample video image, showing location of strain gauge meridians

Table 7.1: Filling process for tank testing

Total filling duration (min)	Depth of water (cm)	Volume of water (l)	Actions/Events
0	0	0	Initialize readings
5	33	190	Demec readings and observations
10	49	360	Demec readings and observations
15	58	480	Demec readings and observations
20	65	580	Observations
25	72	690	Demec readings and observations
30	79	830	Observations
35	84	940	Demec readings and observations
40	88	1020	Observations
45	97	1200	Demec readings and observations
50	101	1300	Observations
55	109	1470	Demec readings and observations
60	115	1580	Observations, tank failure

7.4 Results and Analysis

7.4.1 FEA results

FEA simulations were run using CosmosWorks, to provide data for comparison with the strain readings taken. The files for the model and the results are included in Section D.5 of the electronic resources in Appendix D.

Figure 7.7 shows the maximum principal stress over the height of the tank. The Figure clearly shows that the region from 0.4 to 0.6m above the base of the tank experiences the highest stresses. The FEA results indicate this as a hoop stress.

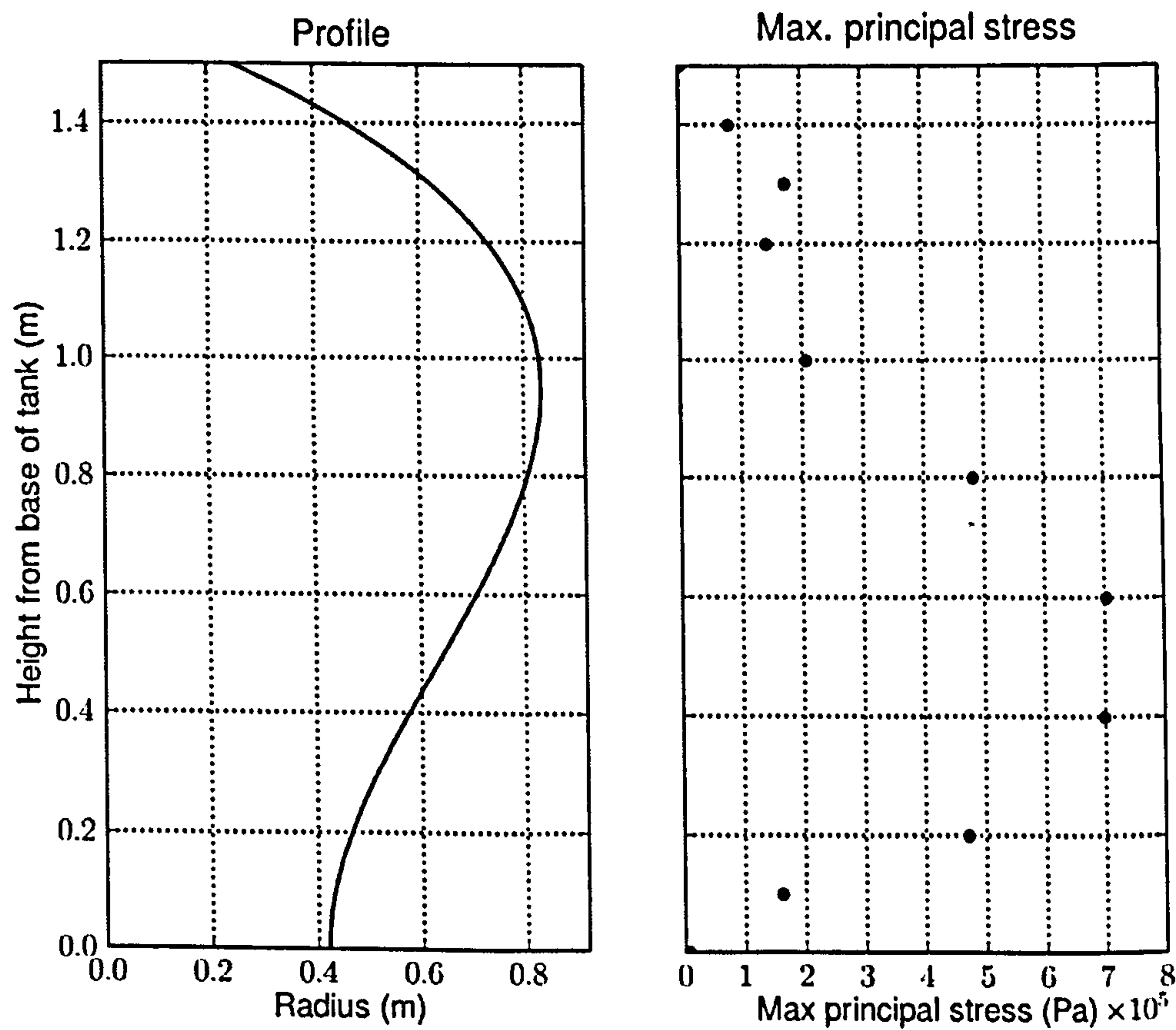


Figure 7.7: FEA results showing maximum principal stresses alongside the tank design used for the prototype

Figure 7.8 shows the expected strains, in both the meridional and hoop directions, for the 12 different locations, and over the range of filling depths.

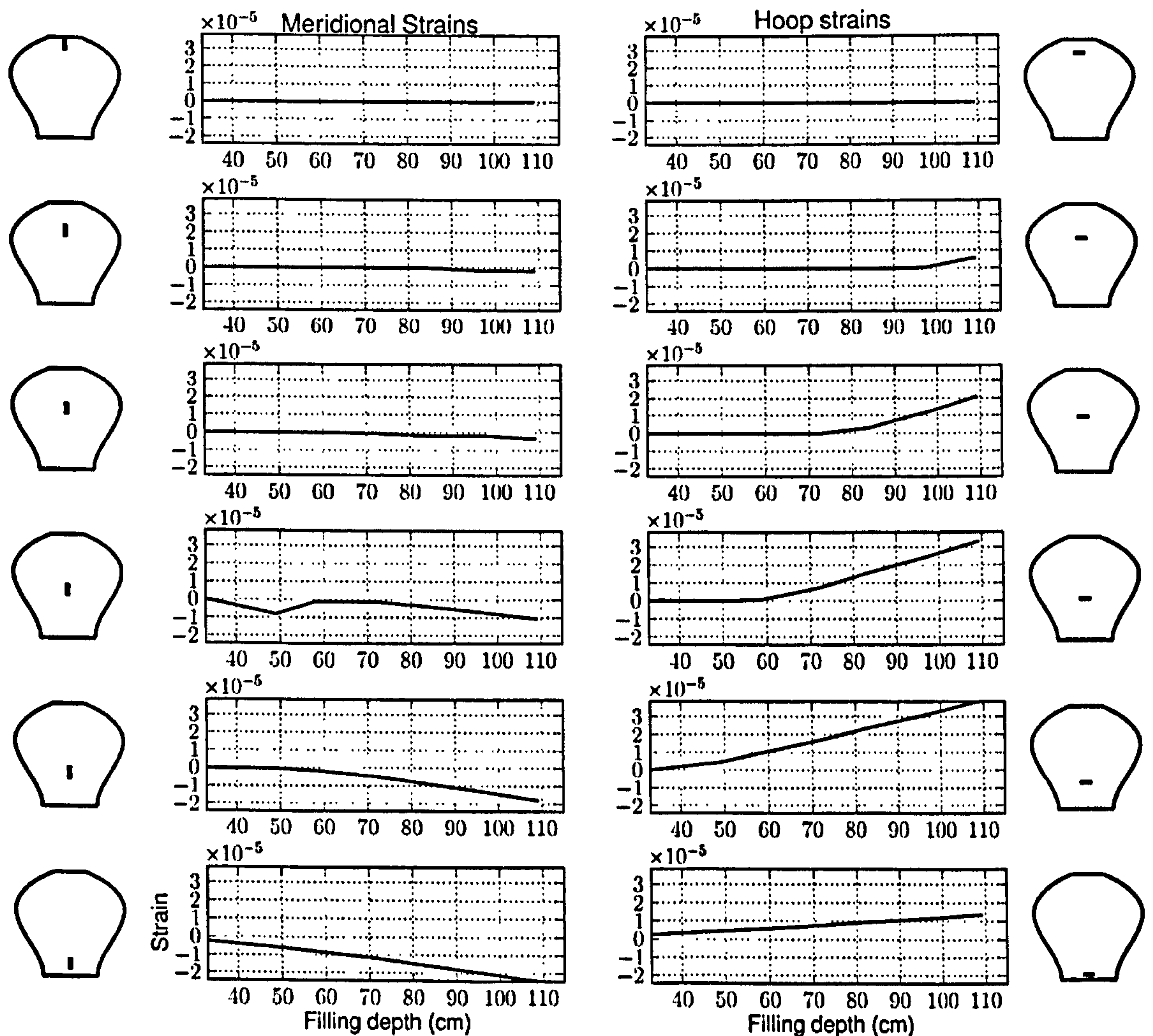


Figure 7.8: Predicted meridional and hoop strains within tank during filling

The Figure shows several features of interest:

- The strain for the top two positions never deviates significantly from zero.
- The meridional strains start from zero, and fall (i.e. become compressive) as the tank fills.

- The hoop strains start from zero, and rise (i.e. become tensile) as the tank fills.
- For both the hoop and meridional strains, significant deviation from zero occurs only when the water level reaches the position in question.
- The magnitude of the hoop strains is significantly greater than the meridional strains.
- The changes in strain, both meridional and hoop, appear linear with increasing water depth once the water level has reached the position.

7.4.2 Visual observations

Whilst curing, and during testing, small damp areas were visible on the outer surface of the tank²: Figure 7.9 shows an example of these. After 35 minutes of filling, two points on the tank developed visible leaks, with water running from them.



Figure 7.9: External surface of the tank during filling, with dark damp patches indicating locations of leaks

Although the visual observations indicated flaws in the structure, they gave no unique indication as to when the tank would fail.

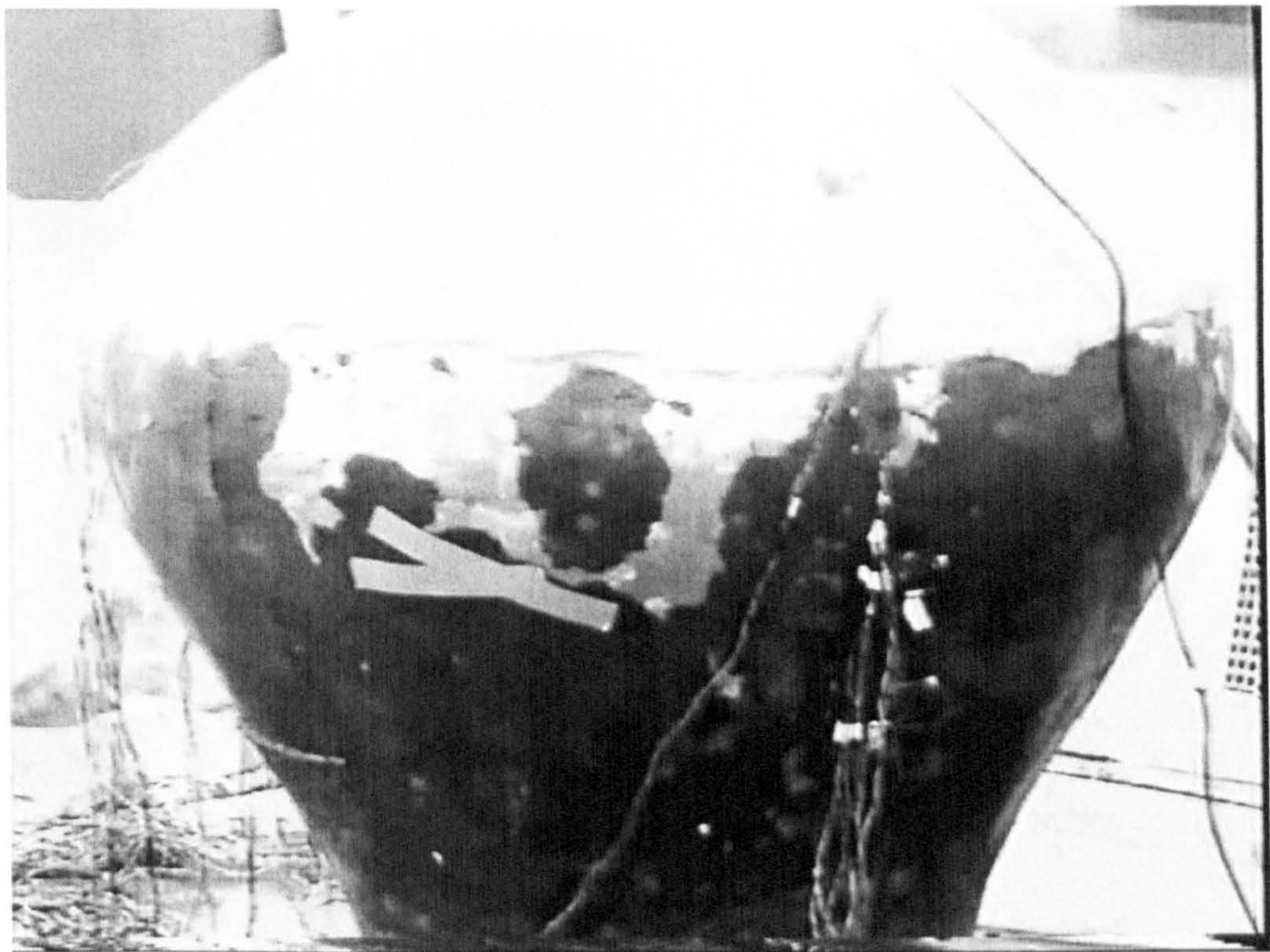
7.4.3 Video recording

The tank failure was captured on video. It took less than 2 seconds from the first visible failure in the tank wall to the lid of the tank impacting the ground. Section D.6 of Appendix D contains an electronic version of this failure. Figure 7.4.3 shows the failure occurring frame-by-frame. The frame interval was 40ms.

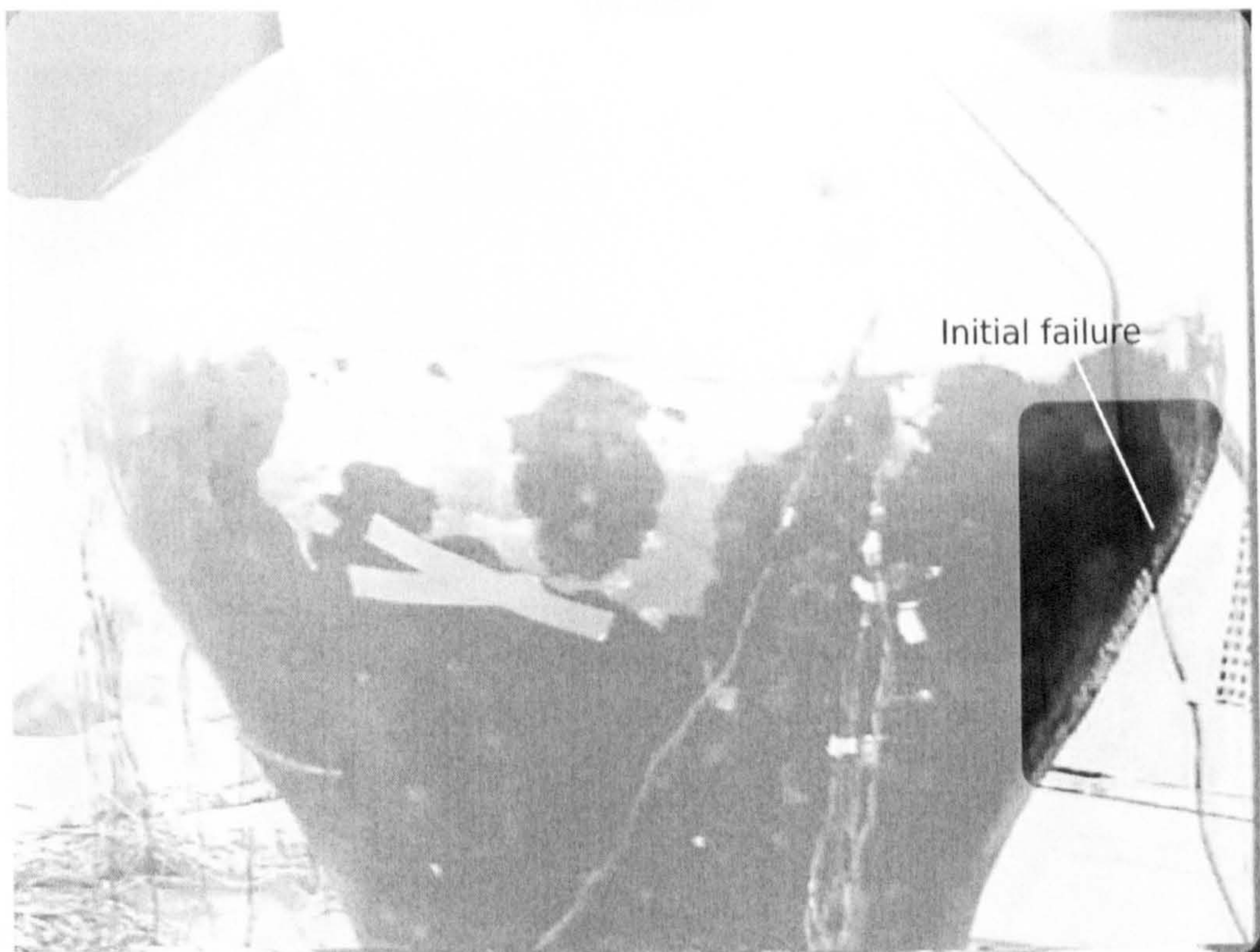
A number of comments may be made on the video footage:

²In normal field production a waterproofing agent is added to the mortar that closes off seepage after about 48 hours. In the laboratory no such agent was employed.

- The camera only viewed the tank from one side, which makes it difficult to be completely certain that the observed failure source was the original cause of failure. However, the development of the first visible fault (line of leakage) takes a number of frames (around 7 frames, or 280ms). The development of the secondary set of visible faults takes much less time (less than 1 frame). This difference in timescale suggests that the first visible fault is the first critical fault in the tank.
- The first visible fault develops vertically, and originates in the area that the FEA analysis predicted as that of greatest principal stress. Both of these features match the FEA: one would expect failure to occur at the point of greatest stress, and as this is a hoop stress, acting horizontally, the crack should propagate in a plane normal to this i.e. along a vertical meridian.
one would expect a failure in a region of hoop stress to propagate vertically.
- Once the first visible fault reaches the joint between the lower and upper sections of the tank, horizontal cracks, and cracks in other locations, develop rapidly.
- The time from initial evidence of failure to complete collapse is relatively short: of the order of 2 seconds.

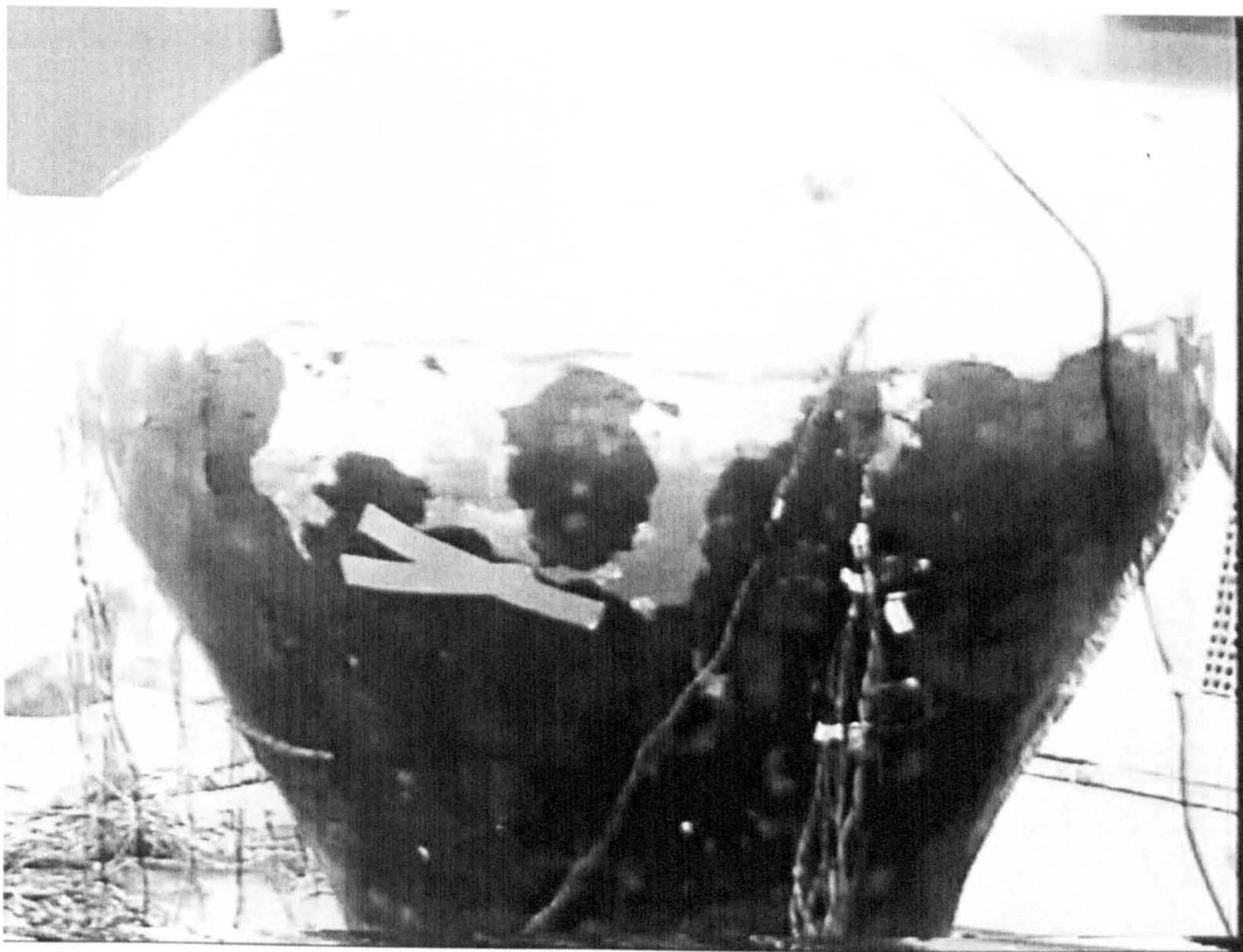


(a) 0ms

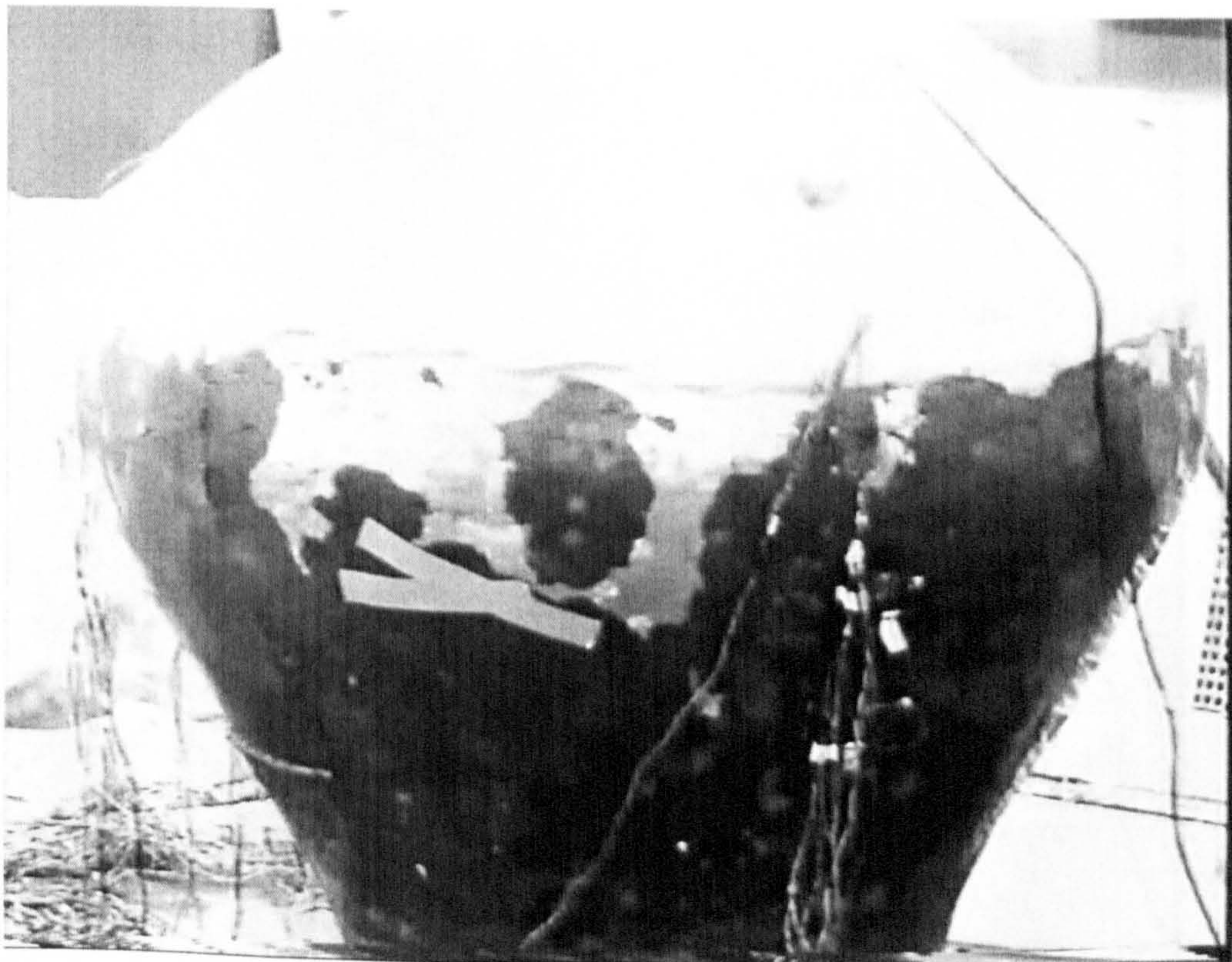


(b) 40ms

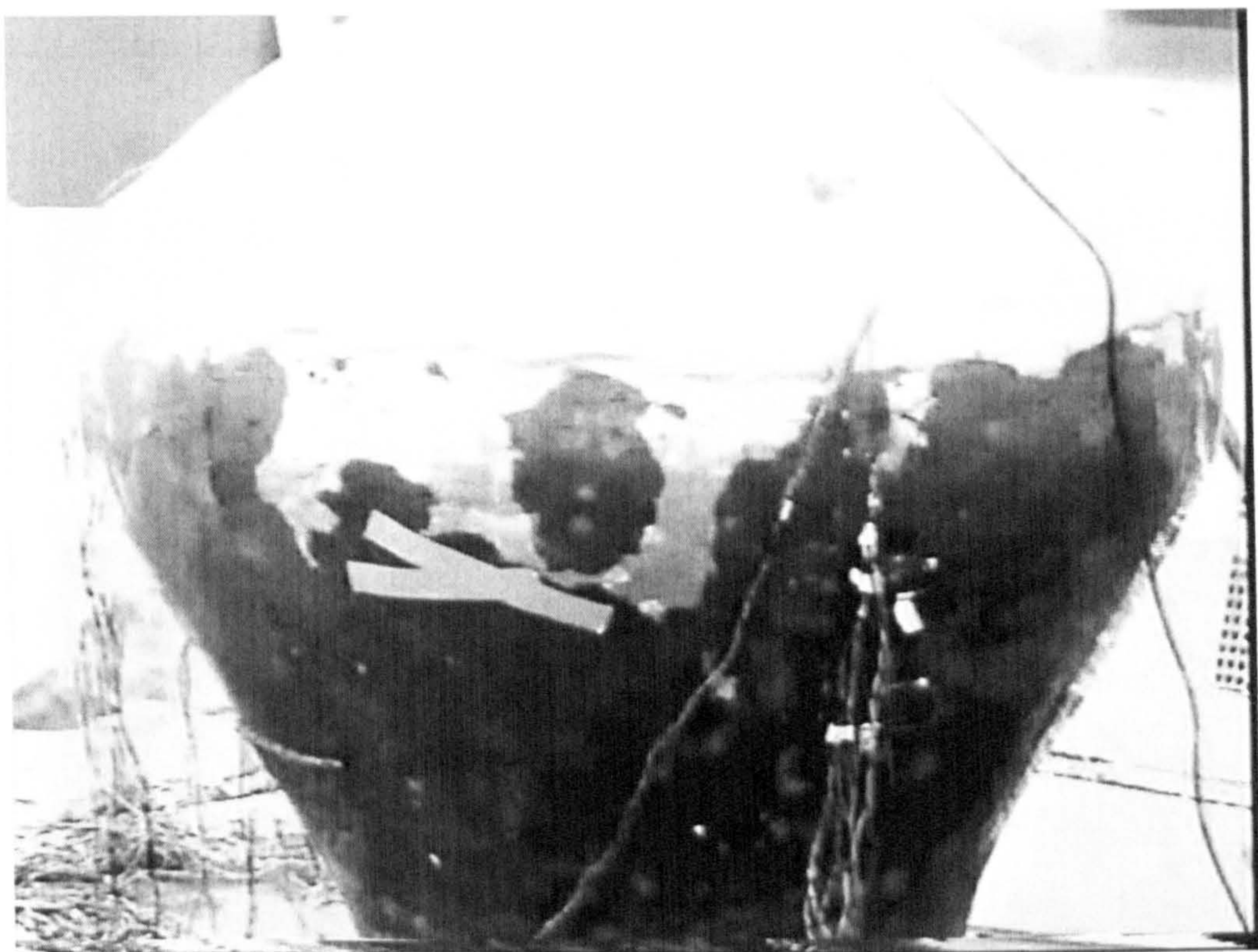
Figure 7.10: Frames from the video footage of the tank failure, showing the tank immediately before failure (a), initial failure (b), the crack propagating vertically ((c)–(f)), and rapid failure in other regions (g).



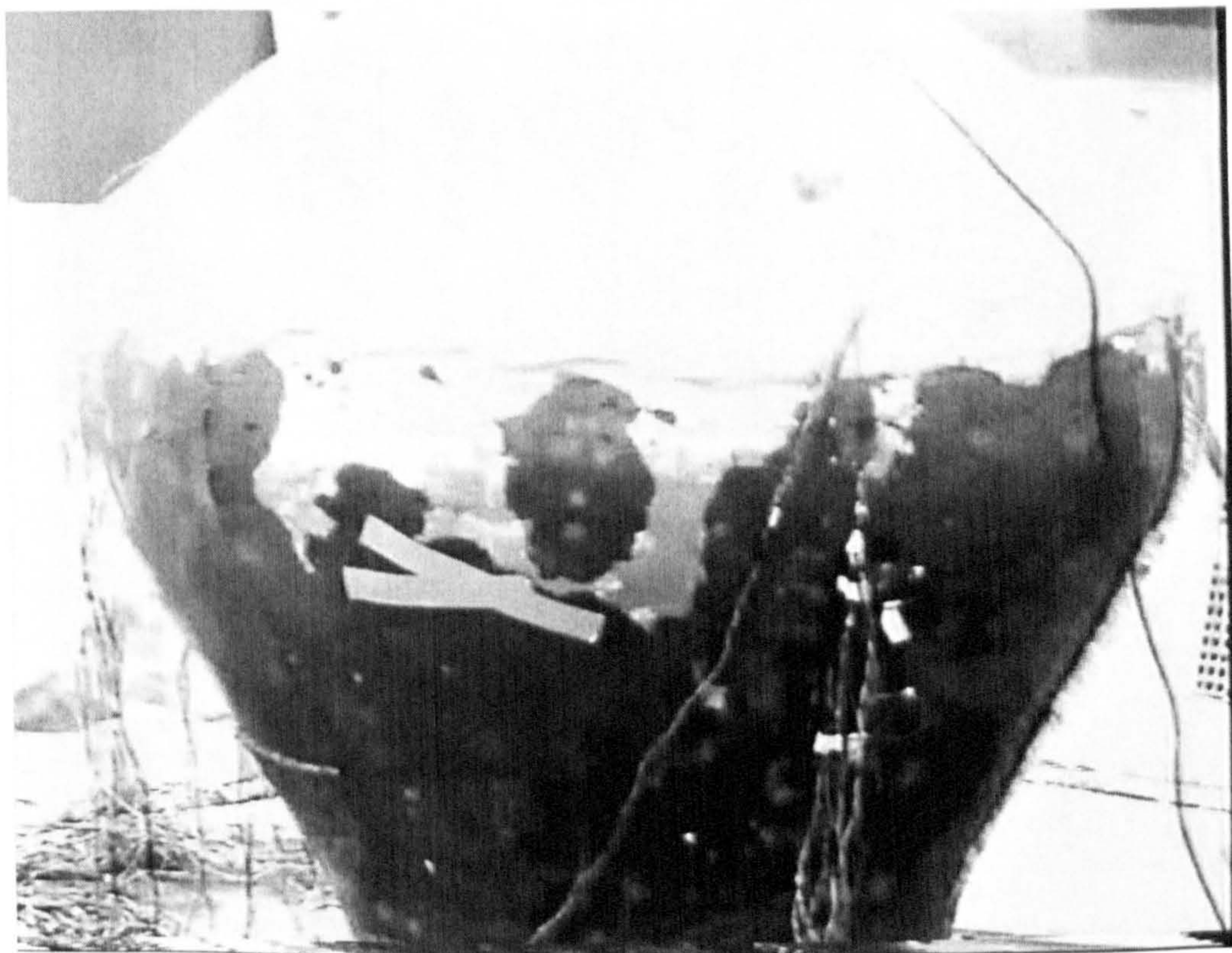
(c) 80ms



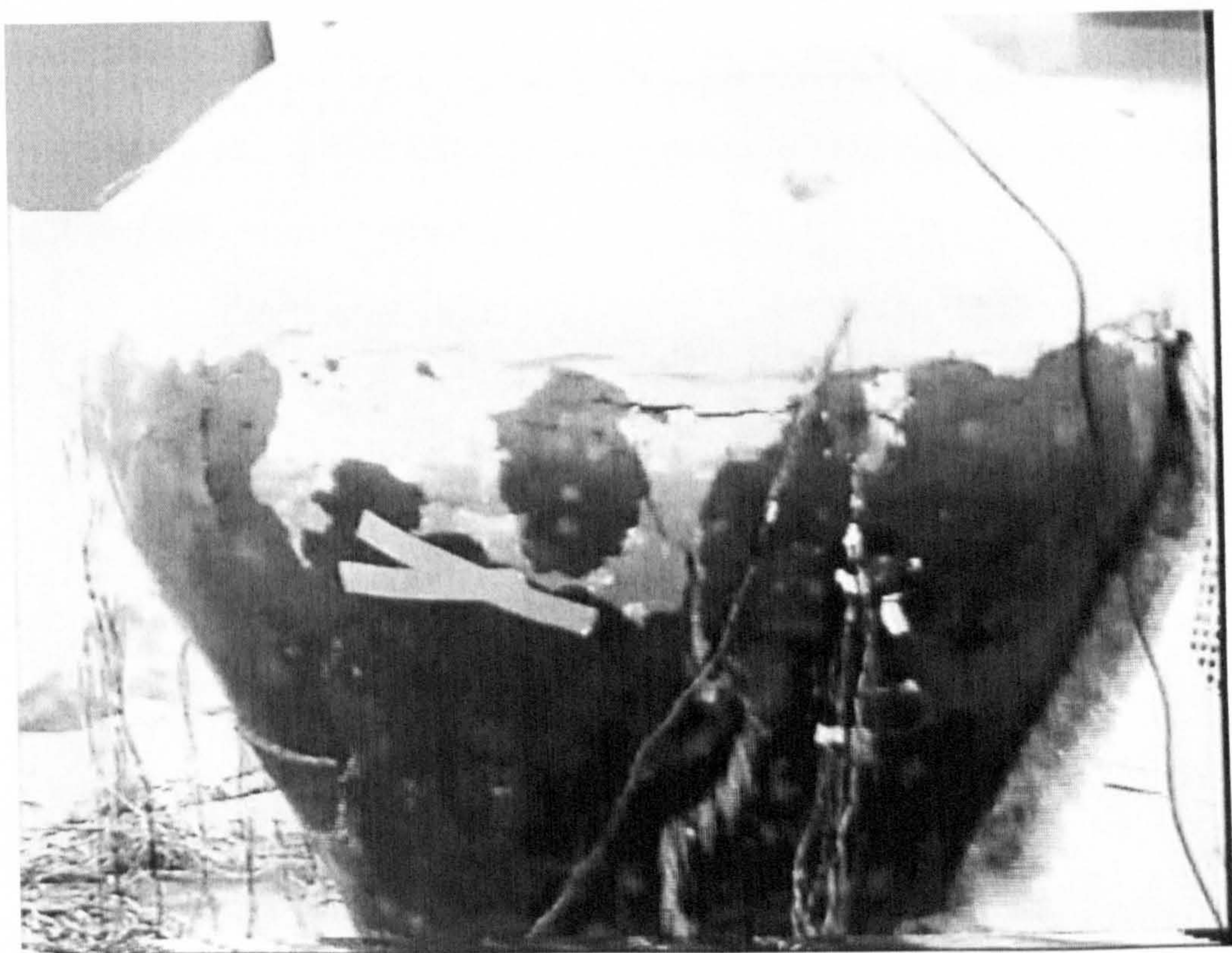
(d) 160ms



(e) 240ms



(f) 320ms



(g) 360ms

7.4.4 Post-failure material samples

The failure of the tank left pieces scattered over several metres, so identification of the section that failed first was not possible. However, pieces of the tank were examined after failure. They indicated several features of interest.

Joint between lid and base

As seen in the video footage in section 7.4.3, the failure of the tank appeared to spread horizontally along the lid-base joint, once the vertical initial crack reached the joint. This was confirmed by pieces of the tank that showed clean debonding along this point, as in Figure 7.11.



Figure 7.11: Section of prototype tank, indicating clean debonding at joint between lid and lower section of tank

Variable wall thickness

A number of the pieces indicated the production of the tank had not attained the constant wall thickness desired. Some of these showed sections with very low wall thicknesses, such as that in Figure 7.12.



Figure 7.12: Section of prototype tank showing thin wall section

Poor bonding

In addition to the variable wall thickness, some of the sections had visible flaws; sections where the mortar was not homogeneous, as shown in Figure 7.13. This suggests that the mortar had not bonded during plastering, probably due to insufficient force being applied and/or the mortar having started to cure, thus becoming less workable.

Summary of post-failure samples

The combination of low wall thickness, and evidence of flaws in the structure, suggest that these caused the initial tank failure, which then propagated vertically, as seen in Section 7.4.3. The presence of variable thickness and flaws throughout the samples examined after the tank failure, and the number of leaks developed during testing, suggest that there were a number of these features present in the tank.

Section D 7 of Appendix B contains the full set of device readings. Figure 7.14 gives a summary of the readings.

The device readings significantly differ from those predicted by the FEA, both in terms of magnitude (the devices being significantly greater), and, in the case of the axial strain, in terms of sign: the device readings indicate tensile strains,



Figure 7.13: Section of the tank, obtained after failure, showing a flaw due to poor plastering during construction

7.4.5 Demec readings

Section D.7 of Appendix D contains the full set of demec readings. Figure 7.14 gives a summary of the readings.

The demec readings significantly differ from those predicted by the FEA, both in terms of magnitude (the demecs being significantly greater), and, in the case of meridional strain, in terms of sign: the demec readings indicate tensile strains, whilst the FEA results indicate compressive strains.

A certain amount of the error can be explained by the instrumentation: an increment on the demec scale is equivalent to 20 micro-strain, so any reading errors are likely to be significant.

7.4.6 Strain gauge readings

Section D.8 of Appendix D contains the full strain gauge data.

A number of the strain gauges showed erratic readings, with several potential causes for this behaviour:

Incorrect mounting Gauges mounted over air pockets and voids will give erroneously high readings.

Wetting of the gauge During testing, sections of the tank started to leak. Given the expected contamination of the water, having seeped through a layer of mortar, and, due to an experimental oversight, the exposed terminal tags of the gauges, with little distance between them, water contact with the gauge could short them, causing incorrect readings.

The effect of wetting is relatively easy to identify: contact with water, and shorting across the terminal tags, will have the effect of reducing the resistance of the gauge, resulting in an abrupt drop in apparent strain. This change in strain gauge reading appears in some strain gauge readings: Figure 7.15 on page 177 shows this.

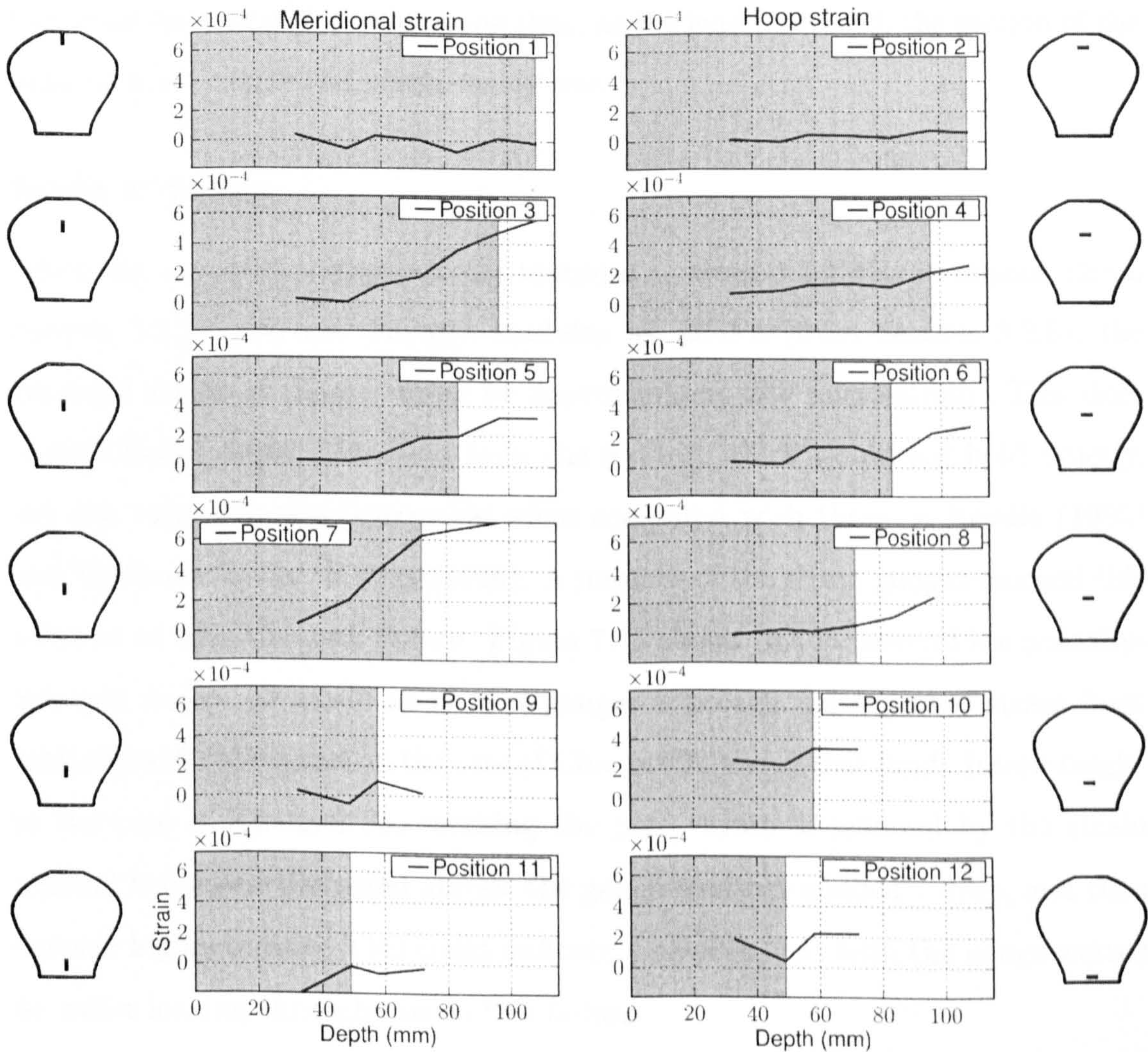


Figure 7.14: Summary of demec readings taken during tank testing. Each reading is the average of three around the tank. The grey shaded area indicates the region in which the water level was below the gauge.

Variation between meridians

The video footage showed the failure occurring at a section between lines A and B (i.e. channels in the ranges 1–23 and 25–47). The strains on line C (strain gauges with numbers between 49 and 71) show considerably lower values than those on the other two meridians, suggesting that, as the load increased, the section of the tank on line C deformed considerably less.

Strain at failure

Given the expected strength of the material as around 3.4MPa in tension (from Section 3.2.3), and the Young's modulus as 12GPa (from Section 3.2.5), the expected strain at failure would be approximately 280 micro-strain. This does assume linear elastic behaviour from the mortar, which would not hold exactly, but the value appears reasonable when compared with those in Neville (1995) and Tasdemir, Lydon & Barr (1996). A number of the strain gauges reached this value at or near the tank failure. Figure 7.15 shows this for several horizontally-oriented gauges on meridian B. The gauges approach the expected strain limit towards tank failure and, in the case of Channel 33, reach that limit. Interestingly, in the case of Channel 33, reaching the peak strain is followed by the strain reading behaviour discussed above: the gauge readings suddenly drop, and then become highly erratic. This could indicate a local failure, with the gauge wetted by water leaking through due to this failure.

7.4.7 Discrepancies between instrumentation and modelling

The sections above have provided a number of reasons for the lack of correlation between the predicted strains and the recorded data, including:

- Relative insensitivity of some instrumentation (demec gauges).
- Significance of noise (strain gauges).

- Imperfections in construction, both in terms of wall thickness and material homogeneity.
- Poor surface finish.

7.3 Conclusions

The tank did not perform as designed and the data does not allow for quantitative validation of the FEA prediction work. The mode of failure, and its location, do match those predicted by the model, giving some qualitative confidence in the modelling.

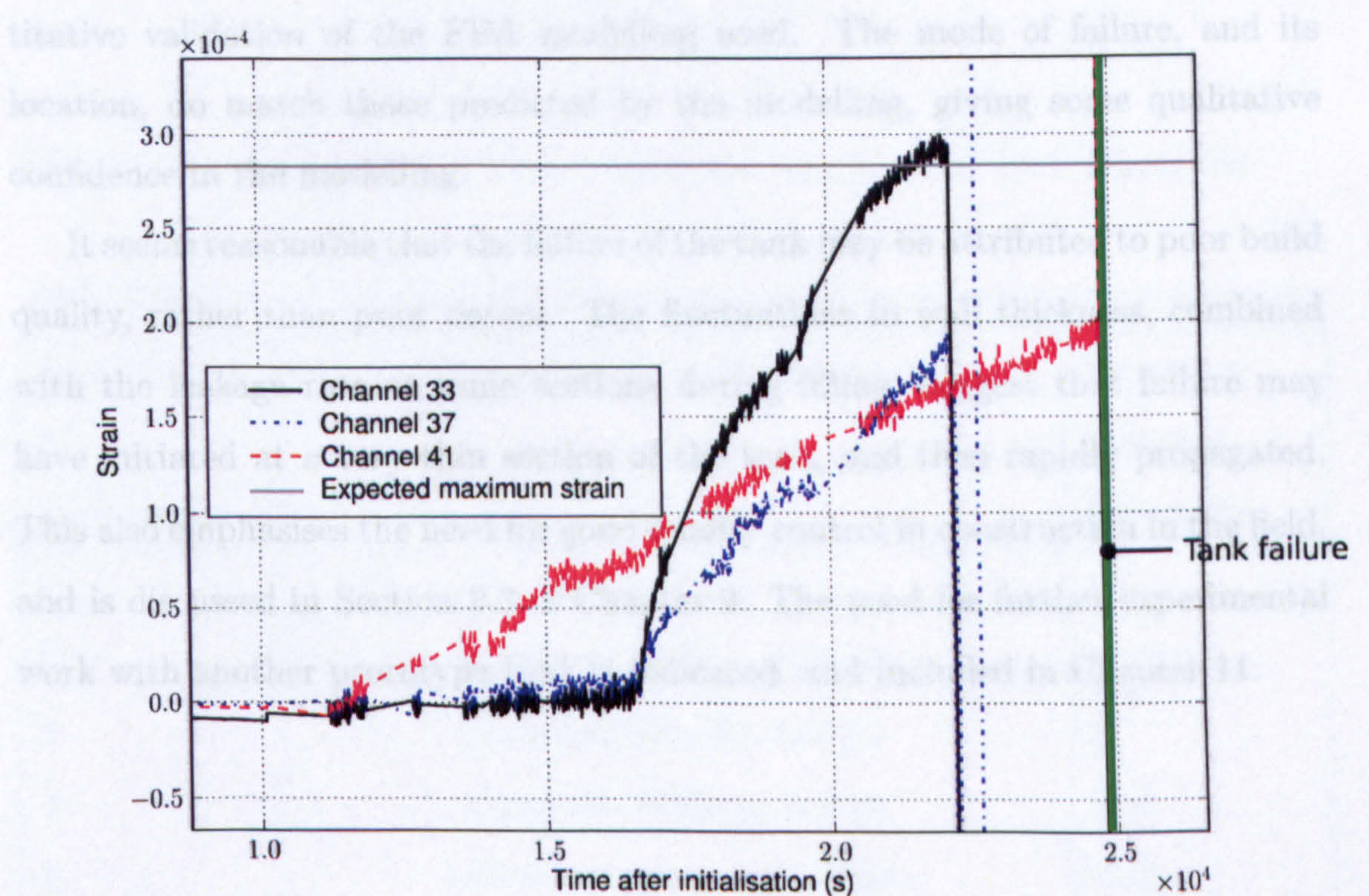


Figure 7.15: Sample strain gauge readings, showing high strain levels approaching material limit, and indicating effect of water leakage on gauge readings. Horizontal grey line indicates expected material strain limit.

- Imperfections in construction, both in terms of wall thickness and material homogeneity.
- Poor surface finish.

7.5 Conclusions

The tank did not perform as desired, and thus the data does not allow for quantitative validation of the FEA modelling used. The mode of failure, and its location, do match those predicted by the modelling, giving some qualitative confidence in the modelling.

It seems reasonable that the failure of the tank may be attributed to poor build quality, rather than poor design. The fluctuations in wall thickness, combined with the leakage rate at some sections during filling, suggest that failure may have initiated at a very thin section of the tank, and then rapidly propagated. This also emphasises the need for good quality control in construction in the field, and is discussed in Section 9.3 of Chapter 9. The need for further experimental work with another prototype tank is indicated, and included in Chapter 11.

Component Design:

Summary

Table 7.2 summarises the results of the shape optimisation work conducted.

Table 7.2: Relative Cement Indices of tank designs of increasing complexity

Dimensions of Curvature	Variations in wall thickness	Relative Cement Intensity
0	Constant	>3
0	Constant, filleting at joints	≈1.7
1	Constant (datum design)	1
1	Constant, filleting at base	0.70
1	Linearly varying with height	0.84
1	Linearly varying with height, filleting at base	0.62
2	Constant	0.58

Prismatic tanks (0D curvature) appear unattractive both with uniform wall thickness, and with filleting at the joints between panels. After the datum design, simple modifications give a substantial reduction in material usage, with the addition of a fillet at the wall-base joint lowering total material usage by 30%. Increasing the complexity of the tank by varying the wall thickness both locally and globally increases the material savings to 38%. After this, the increased complexity of 2D curvature offers additional benefits, and 42% reduction in material

usage.

The use of 2D curvature thus gives significant benefits over the datum case, but relatively small benefits compared to using a cylindrical tank of optimised wall profile. However, it does still offer the advantages of material saving, of not requiring a separate spanning structure to form the lid, and with which good quality control may be achieved.

For cases where local technology will allow it, the top-heavy tanks with 2D curvature should provide best practicable material economy. In cases where the materials or technology are not available, cylindrical tanks with a fillet at the wall-base joint still provide good material economy, and cylindrical tanks with a fillet at the wall-base joint and wall thickness that varies linearly with height gives very good material economy.

PART IV

Production Environment

Production Method and Environment: Overview

The Chapters in parts II and III considered materials selection and component design respectively as methods for reducing component cost. This Part considers another approach: altering the production environment and method.

Chapter 8 gives a brief summary of arguments for prefabrication, including those specific to LEDCs, and describes the three scenarios of interest: on-site, “knock-down” and factory-based.

Chapter 9 examines each scenario in the context of rainwater harvesting tank production, discussing their merits and disadvantages. It also covers the production of tanks using the novel method of external moulds, examining the experiences of Chapter 7 from the perspective of tank production rather than component design.

The Part concludes with a brief summary on page 202.

CHAPTER 8

Production Environment: Prefabrication Concepts and Scenarios

8.1 Introduction

The history of production of goods shows a significant trend towards specialisation and standardisation, with associated geographical concentration of manufacture, and benefits arising from economies of scale, including the use of more capital-intensive technologies. Certain industries, however, have to a large extent escaped this move to factory-based production, including housing. This chapter presents a (necessarily) broad overview of historical trends in housing production, and describes generic arguments for the pros and cons of off-site fabrication.

8.2 Trends and current situation in housing

The concept of prefabrication has not emerged suddenly. Accounts from the 1st century A.D. indicate Romans using wooden prefabrication in hospital construction (Gibb, 1999). However, despite some examples of the adoption of prefabrication, in large part we see construction taking place with the majority of work on-site. Recent work and the advocacy of modular building has led to some in-

crease in uptake of prefabrication, but others argue that conditions leading to failure in previous attempts persist (Ngowi, 1997). Early housing production, as noted by Ngowi (1997), focused on low energy techniques, relied on local materials, and involved communal participation with the end-users involved in the construction.

8.2.1 Industrialised Countries

As seen in industrialised countries, many building products have passed through several types of production, ranging from use of only local materials to importing of prefabricated items made from materials available elsewhere. In many housing situations we still see an intermediate technique of an on-site assembly using prefabricated elements.

8.2.2 Developing countries

Development has seen a move from very low performance housing requiring continual maintenance, to cleaner, more durable and lower maintenance materials. At present housing in developing countries remains technically fairly simple, with few services required (relative to industrialised countries).

8.3 Generic pros and cons for prefabrication

General arguments for prefabrication include:

- Control of production environment.
- Increases in scale allow the use of more capital-intensive and efficient machinery

Table 8.1: Factors affecting the extent of off-site fabrication (OSF), taken from Gibb (1999)

	Client characteristics	Project characteristics	Site location and characteristics	Labour considerations
Factors or scenarios leading to increase in OSF	Client who will benefit from early handover	Project with aim to minimise on-site duration	Geographically remote site yet where craneage and adequate access are achievable	Expensive labour at site location
	Client or team who has used OSF before	Project with high-quality specifications	Site away from centres of industry	Lack of skilled labour at site location
	Client prepared to fund initial off-site fabrication study	Project suitable for use of standard systems	City centre/congested site	Available manufacturing labour within economical transport distance
	Client who wants predictable project outcomes	Projects with significant repetition		

Continued on next page

Table 8.1 – continued from previous page

	Client characteristics	Project characteristics	Site location and characteristics	Labour considerations
	Client with significant repeat business opportunities Client who understands the manufacturing process	Project type that will be repeated elsewhere Project with time for off-site prototype testing Project where early construction/manufacturing expertise can be obtained		
Factors or scenarios leading to decrease in OSF	Client who concentrates on lowest initial cost alone	One-off project, with little repetition	Poor manufacturing base within economical transport distance	Cheap available on-site labour

Continued on next page

Table 8.2: Methods of production

Production method	Example
On-site building, maybe using some on-site material	Using adobe to make a wall
Factory-based production, of “knock-down” elements, generally employing more specialised raw materials, followed by on-site assembly	Brick and mortar construction of a wall
Factory-based production of large complete components, followed by transport to required location	Use of a precast concrete wall unit

Table 8.3: Comparison of “on-site” and “knock-down” manufacture

On-site	Knock-down
Low cost to set up	High cost to set up
Simple tools readily available	Specialist tools required
Series of one-off projects	Economies of scale achievable
Poor control of production environment hence some materials waste	Good control of production environment and hence product quality, leading to materials savings
Easy to transport materials to site	Potential difficulty in transporting elements

off-site fabrication can successfully apply to developing countries in which events conspire to encourage high labour utilisation (for reasons of cost or more general social and political objectives). In these cases choices of technology can:

- Reduce materials consumption, found in some cases to constitute around 70 to 90% of production cost (Mwamila & Karumuna, 1999; Erguden, 2001).
- Improve quality control.
- Increase construction speed.
- Allow an increased use of relatively unskilled labour (with some supervision) (Mwamila & Karumuna, 1999).

Previous work has noted that the concept of prefabrication has existed for some time (Gibb, 1999; Stallen, Chabannes & Steinberg, 1994), particularly in terms of modular construction, and has found successful application in a number of situations in developing countries. From a series of case studies, Stallen *et al.* (1994) suggest that a number of factors influence the successful uptake of prefabrication, particularly delivery capabilities, stating that:

“The capacity to organise this delivery system seems to override the technological difficulties involved in prefab.”

8.6 Summary

Historical experience shows that construction has often lagged behind other industries in the uptake of prefabrication and modularisation. Reported evidence suggests that, correctly applied, prefabrication can offer significant benefits to production in both industrialised and developing countries. Given the concerns noted in section 8.5, choice of components suitable for easy transport seems imperative to a viable prefabrication scheme.

CHAPTER 9

Production Environment: Production Process

9.1 On-site production of water tanks

On-site production currently takes place with some success, and can be used to produce large structures, including the Sri Lankan Pumpkin tank, and even tanks with higher storage capacities (up to and above 80m³). For the case of above-ground tanks, these generally require a ferrocement style construction, with the formwork embedded in the tank, and left in it after construction: Figure 9.1 shows an example of this for the Pumpkin tank.

There are several cases why we might prefer to avoid this technique:

Cost of reinforcement Steel mesh and rebar are both expensive, so avoiding their presence, if possible, is attractive.

Potential for corrosion Particularly given the relatively low wall thicknesses advocated, and the potential porosity of the mortar (given that it will be sealed on the inside, but not on the outside), there are concerns about carbonation of the mortar, and rapid corrosion of the reinforcement within the tank¹.

¹Carbonation reduces the pH of pore water. Steel in concrete has a thin layer of oxide on its



Figure 9.1: Applying mortar to the mesh and rebar formwork of the Pumpkin tank

Accuracy in construction The use of mesh on-site makes it more difficult to make the formwork, and hence the final structure, to the desired axisymmetric shape.

Clearly there are cases where on-site is attractive: it allows for construction of larger tanks than could be transported.

9.2 “Knock-down” production

The literature review and discussion in Section 8.3 identified reasons for considering “knock-down” production of cement-based building components. The vibro-profiling methods discussed in Chapter 2 appear well suited to flat panel surface, which acts as a barrier, preventing it from rusting. At lower pH levels (such as those produced by carbonation), this protective oxide layer is removed, and corrosion occurs (Neville, 1995)

tanks, and the few examples in the open literature quote improvements in material performance of around 20%. However, several problems remain with this option:

Fabrication of joints. For the simplest option for prefabrication, individual flat panels would be produced, and then joined to each other and the base to form the tank. In this case, the joints would be produced at the region of greatest stress. Even taking the alternative approach, shown in Figure 9.2, of producing V-shaped channels, and joining along mid-plate lines, the problem still remains of having to make joints that will act in tension, between cement-based components which have already set. As will be covered more in section 9.3.1, joints made between set and “green” concrete often do not perform as well as continuously cast material, and therefore are unattractive.

Efficiency of designs. The work in Chapter 6 addressed the efficiency of material use of flat-panel tanks, indicating that they perform significantly worse than the datum design, and much worse than “good” designs with curvature in 2 dimensions.

9.3 Factory-based production

The previous Sections addressed the current practice of on-site production, and the intermediate case of knock-down production. The on-site practise has some disadvantages, but the change to knock-down production does not appear attractive. This leads to the third option: factory-based production of complete items, followed by transport to site. The attractions of this method include:

Production environment It is easier to control the environment in an enclosed space such as a factory, rather than the exposed conditions of a building site.

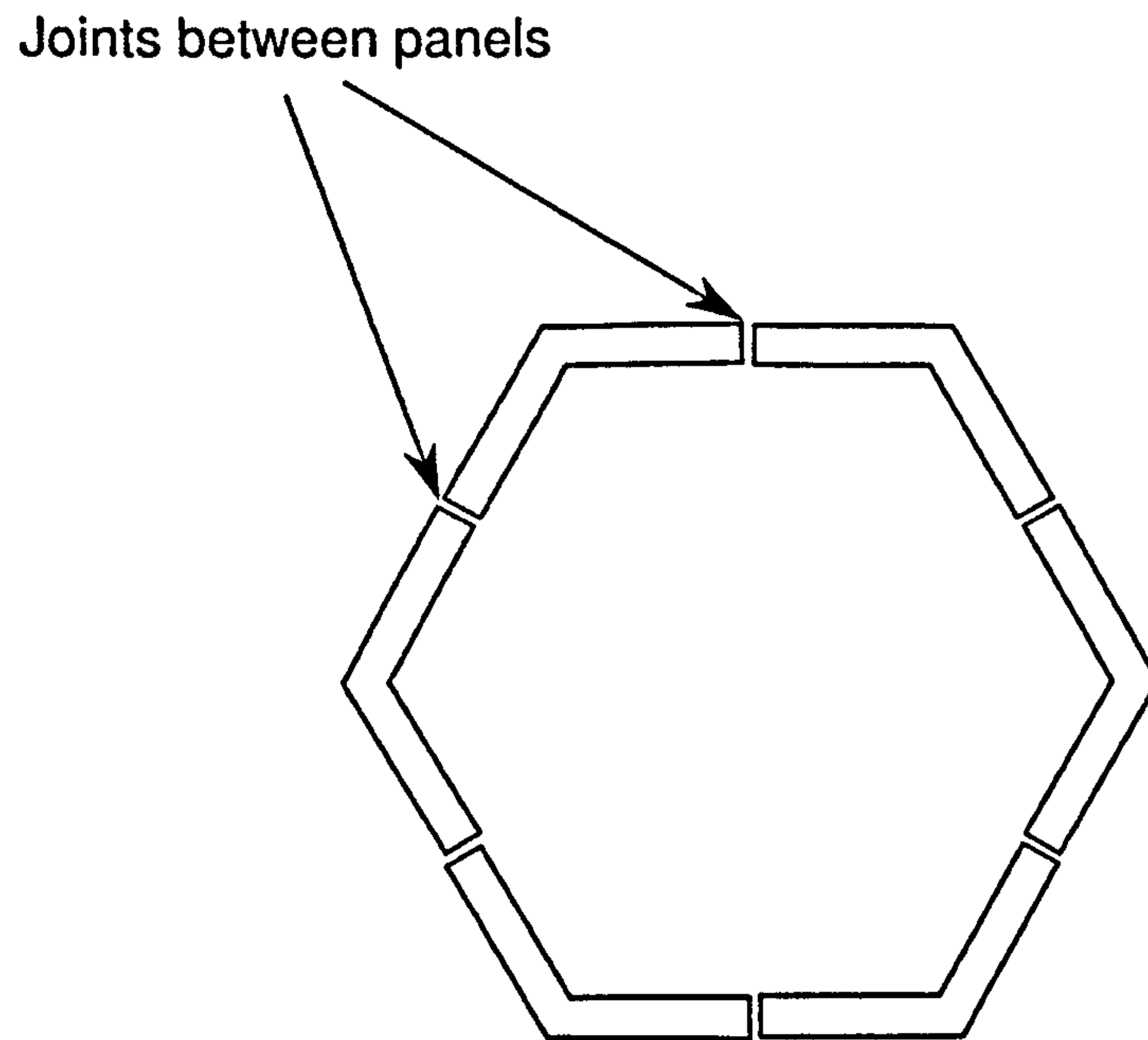


Figure 9.2: Plan view of hexagonal prismatic tank, showing alternative location for joints

Testing facilities Recent fieldwork in Uganda (Rennie, 2006a; DTU, 2006b), and the testing reported in Chapter 7 indicate that the significant material reductions make good quality-control imperative. Factory-based production allows for testing of each tank before shipping to the user. This has several benefits:

- It is easier to provide water for testing in the factory, and this water can be reused on a number of tanks.
- The user will have a significantly lower chance of encountering a failing tank. This is attractive, as there will be no loss of public confidence associated with a tank failing in the factory.

Labour productivity Production on-site requires transport of the materials to site, and then the labourer(s) presence there over a period of several days. This will reduce the productivity of the masons, compared to factory-based production in a single location, followed by a single journey to transport

the finished item for installation.

9.3.1 Alternative production method: external moulds

Previous tank production has used either mesh/rebar to provide a formwork (as in the Sri Lankan Pumpkin tank), or an internal mould (as in the production of the Thai Jar, and the small/low-volume tanks covered in the Development Technology Unit working paper TR-RWH10 (DTU, 2006b)). These each have their advantages, but there is a further alternative: external moulds.

It was decided to combine the testing of the prototype tank described in Chapter 7 with testing of tank production using an external mould.

Table 9.1 covers the predicted/considered pros and cons of external moulds. The main benefits centre around the possibility of “continuous” casting of the base and side walls, (avoiding joints between new and old mortar occurring at areas of high stress), and the lower number of components needed (hence greater ease of assembly and manufacture).

Table 9.1: Pros and cons of external moulds for producing rainwater tanks

Advantages
<ul style="list-style-type: none">• The base and (lower-half) walls can be plastered in one go — there is no ‘dry’ joint between base and wall.• Filleting the wall-base joint is easily done during the main plastering stage.• The moulds may encompass 1/3 or even 1/2 of the circumference, so there are fewer (but larger) external mould pieces than there would be internal ones. This has benefits:<ul style="list-style-type: none">– As soon as the mortar has hardened sufficiently, water can be poured inside the mortar cup to aid curing.– The mould acts as a moisture-retaining membrane during initial curing.– The moulds are easier to remove (than if they had to be extracted from inside the jar), so it may be possible to use them without a release agent but rely instead on a ‘peeling’ action to separate mould from partly-set mortar.
<i>Continued on next page</i>

Disadvantages

- The jar must be made in two parts (a) because the upper half is too near horizontal for mortar to stick to its underside and (b) the depth is too great to reach down to plaster inside (however moulds could be placed in two vertical stages and mortaring done one stage at a time).
 - The moulds must be much bigger — bigger than the jar rather than smaller.
 - The top half, once formed, must be somehow turned over, and lifted onto the second part. However this might be done at the final site, thereby reducing the transport weight of the largest part.
 - The combination of the two parts cannot be moved until the mortar used to join them has hardened, so we have had to wait for two periods of basic curing.
 - The surface finish of the mould, not the skill of the plasterer, determines the outside surface finish of the jar. Alternatively, if mud is used as a release agent, the inside finish of the mud layer determines the finish on the outside of the jar.
 - The mortar ‘cup’ is wide-mouthed. This mouth must be temporarily covered or sealed to aid curing.
 - Plastering on the inside of the tank requires a specialist tool, as the trowel should have some degree of dishing to produce the curved shapes required.
-
-

Choice of mould type

The main aim of the production was to test using an external mould: the technology did not have to match perfectly one that could be used in developing countries.

A three-level mould, with two layers for the base, and one for the lid, was chosen to allow for:

- Casting of the base and lower section in one piece.
- Access to the base section from the outside of the tank during casting (hence two layers for the bottom part of the mould).
- Separate casting of the overhanging (top) section, followed by joining on to the tank.

Results from testing: Base joint

As discussed in Chapter 7, the prototype tank failed catastrophically during testing. Tanks made during other experimental programs have also had this happen, but with a clearer separation of the wall-base joint, as shown in Figure 9.3.

This suggests that the continuous plastering of base and lower walls, without making a joint between set and green mortar at the point of maximum bending moment, does have the desired effect of giving greater strength in that region.

Results from testing: demoulding

Demoulding of the lower section of the tank was straightforward and quick, taking around 1/2 an hour. Demoulding the lid presented difficulties in inverting the lid without it cracking. For turning over the first lid two beams were bolted across the top of the mould, and the whole tank pivoted over one edge. During this process, a number of large cracks developed. For the second lid, a plywood support and more beams were used, and there were no problems with turning it over. This problem only arose as the lid was made separately: some of these



Figure 9.3: Base sections of two tanks after failure, showing (a) the joint debonding in the case of the tank produced with an internal mould and separate plastering of the base and walls, and (b) absence of such debonding in the case of the tank produced with an external mould and continuous plastering

constraints arose from health and safety issues that would not necessarily apply in LEDCs. If the lid were to be produced separately, an internal mould could be used for this part, and the lid lifted off it after a few days curing.

Results from production: mud coating and surface finish

The mud coating used during production (essentially sand K from Part II, with a moisture content of around 17%) cracked considerably during curing. This required:

- Repairs to achieve a smooth surface, before manufacture could start.
- Spraying of mud with water during production, to ensure adequate adhesion between the mortar and the mud.

Results from production: batch size

During production two people worked to produce the tank, using mortar mixes of 30 and 70kg. At several stages during the production, there was a noticeable

loss of workability towards the end of plastering with a batch — a situation exacerbated by the relatively dry mixes being used to obtain the peak strength. This experience, coupled with the flaws seen in Section 7.4.4, indicate the importance of:

- The use of smaller batches, such that low workability does not affect the compaction and placement of the mortar.
- The importance of continuous production, with the mason constantly supplied with mortar, rather than intermittent plastering, followed by mixing the next batch.

Results from production: thickness control

The production of the tank, and experience from producing tanks in Uganda, indicate the potential for unacceptable variations in wall thickness, such as that in Figure 9.4.

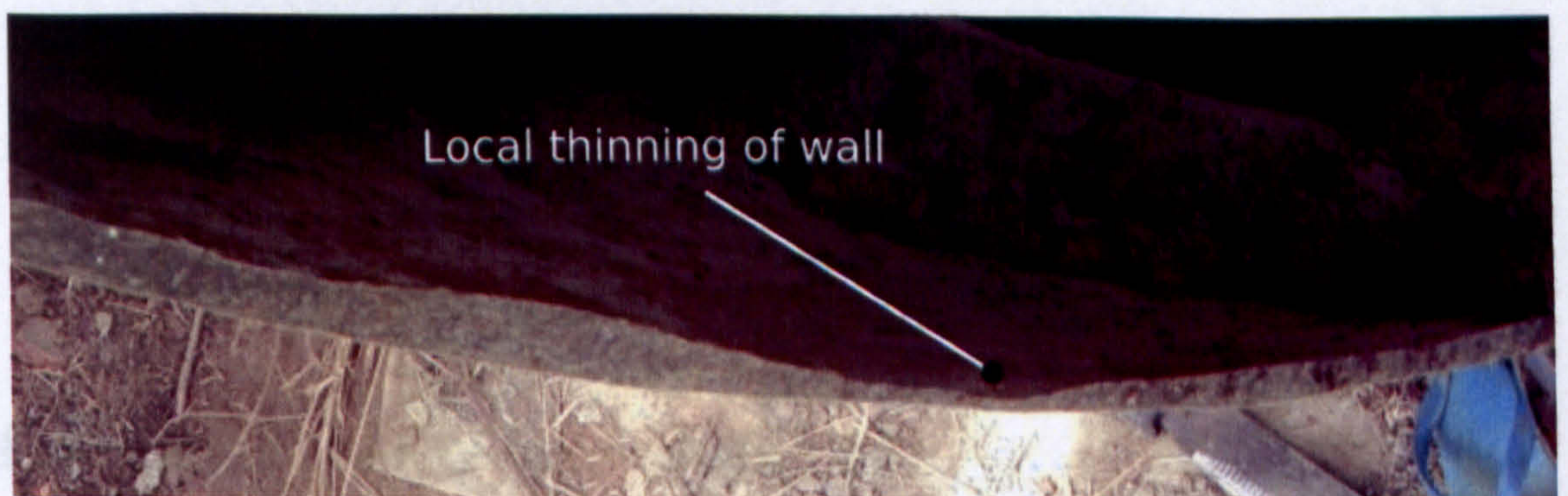


Figure 9.4: Section from broken tank in Uganda, indicating variable wall thickness produced by plastering (Rennie, 2006b)

These indicate the importance of quality control during production, particularly for the low wall thicknesses being used: any error becomes relatively more significant the lower the wall thickness.

Results from production: pre-sale testing

Manufacture of rainwater tanks in Uganda (DTU, 2006b) has used similar wall thicknesses, and successfully produced a number of operational tanks. However, even in these cases, some tanks have failed. This emphasises the need for testing before the tank is used, which is easier to achieve in a factory than on-site.

Pre-use testing has a number of advantages:

- It gives direct feedback to those producing the tank, allowing for more immediate monitoring of quality control.
- It gives the supplier greater confidence that their product will work.
- It allows for leak-seal compounds, where used, to take effect, and seal any minor imperfections in the tank, so the end-user does not experience a leaking tank.
- It allows for designs using lower design reserves: the cost to the producer of a tank failing in the factory is simply that of producing the tank, the material (water) to test it, and to remove the waste if the tank fails. However, if an installed tank fails, there is the additional cost of reinstalling a replacement tank, and a cost in terms of public perception, which may harm the reputation of those producing the tank.

9.3.2 Evaluation of factory-based production

The experiences of producing the tank described in Section 9.3.1, and those of fieldwork producing tanks in Uganda (DTU, 2006b), suggest the following:

- Factory-based production can effectively produce tanks using less materials than current practice.
- Use of external moulds, or production that allows for continuous plastering, rather than a “dry” joint between walls and base, can reduce the risk of failure at that highly-stressed location.

- The use of thin sections makes good quality control imperative, and makes pre-use testing of tanks important.

Production Environment:

Summary

The work within this Part differs from that in the previous two, as it does not provide a quantitative benefit of an alternative to existing practice. From the work discussed, it appears that:

- For small tanks, factory-based production, followed by transport to site is an attractive option, and makes it easier to access the more complex geometries discussed in Part III.
- For larger tanks, where factory-based production is not possible, on-site production is still the most attractive option.
- For scenarios of interest, the intermediate technology of “knock-down” production is not attractive.
- To push designs to their limit, using a safety factor as low as 3, high artisan skills, good quality control, and routine testing are all necessary.
- For components with high stress at the wall-base junction, the production method should be changed to avoid producing dry joints at this location.

PART V

Conclusions and Further Work

CHAPTER 10

Conclusions

10.1 Overview

One may argue that modern engineering has the potential to deliver considerable benefits in Less Economically Developed Countries. However, those who might benefit from these tools and techniques often do not have access to them. In line with this idea, this Thesis has examined three strategies to reduce the cost of cementitious building components in LEDCs:

- The use of local, cheap sands, with a degree of clay-contamination, instead of more expensive, uncontaminated, imported sands.
- The application of analytical and numerical tools to the design of components, in order to realise any potential reductions in material usage afforded by a more efficient structure.
- The use of alternative production environments, and the benefits they may offer such as better quality control, easier use of alternative production methods etc.

10.2 Material selection

Current literature on mortars predominantly concerns itself with high-quality sands. There is little work available on choosing the best water-cement ratio based on sand-cement ratio and grading; most work on grading and workability relates to self-compacting concrete, an area of practical import in industrialised nations, but unsuitable to Less Economically Developed Countries. The prevailing view within the literature, and in the concrete industry, is that the presence of clay in aggregates is deleterious to the strength of cementitious materials, and should thus be avoided.

Relationships between strength and water-cement ratio derived from data in the literature suggest sand-cement ratios to achieve best economy, but also contain some ambiguity, depending on which relationship is used. Research into materials conducted as part of this Thesis has resolved this ambiguity, indicating that the optimum sand-cement ratio depends on the relationship between peak stress and component thickness (i.e. the dominant loading of the component), but does not vary significantly with the presence or type of clay contamination in the sand used.

Abrams' parameters for representative LEDC sands are similar, regardless of clay content; at full compaction and with consistent curing, water-cement ratio is the primary strength-determining factor, and clay-contamination has little effect. However, clay-contamination, and the type of clay, have a significant effect on workability. This lower workability leads to higher water-cement ratios for optimum strength, and hence lower optimum strengths. The effect of this increased water-cement ratio is particularly marked at low sand-cement ratios. The additional water demand arising from clay contamination, rather than a cement-clay interaction, leads to the reduction in strength experienced on using clay-contaminated sands.

On an economic basis, the general approach of treating of clay as univer-

sally deleterious appears incorrect. Kaolin-contaminated sand may give adequate strengths for building components, even when present at 20% by mass. When the choice is between a cheaper, kaolin-contaminated local sand, and a more expensive, uncontaminated imported sand, the kaolin-contaminated sand is often of equivalent cost, or cheaper (by around 10%). By contrast, when the choice is between a cheaper, montmorillonite-contaminated (20% by mass) local sand, and a more expensive, uncontaminated, imported sand, the montmorillonite-contaminated sand incurs a prohibitive cost penalty.

10.3 Component Design

The literature on component design as applicable to LEDCs falls into two categories; those detailing theories, with relatively little content on practical design, and those detailing applications, with relatively little theoretical treatment. The work in this section of the Thesis sought to combine the two.

Current tank designs are field-tested, but have generally been produced either through a process of incremental changes by artisans, or by those with relatively little exposure to relevant fields of engineering. The literature at present shows some advocates for the use of flat panel prefabricated tanks, a number of supporters for cylindrical tanks, and a few variations of tanks with curvature in two dimensions (vase-shaped tanks). Clearly there is considerable cost associated with producing and testing prototypes of new designs. Conceptual, analytical and numerical tools allow for “cheap” testing of new designs, and thus better exploration of the problem space. There is a distinct benefit to using these tools in concert: a conceptual understanding is necessary to guide the search for improved designs, and numerical tools such as FEA are powerful for analysing more complex geometries.

The designs generated by this strategy of combining conceptual understanding with computational analytical use considerably less materials than the current popular design of uniform wall thickness cylinders. An understanding of the

behaviour of the structure, and stresses developed within it suggests the simple modification of a radial fillet at the wall-base joint, that gives considerable ($\simeq 30\%$) materials saving. Increasing the complexity of thickness profile of cylinders allows for a small additional reduction in materials usage, but reaches a state of diminishing returns, and the designs would be more difficult to manufacture. More complex shapes with 2D curvature were also explored, and allow for both a saving in terms of material ($\simeq 40\%$), and the additional benefit that they do not require a separate spanning structure to cover the tank. These top-heavy vase-shaped tank designs are recommended for field-testing and subsequent use.

The prototype testing within this section of the research, combined with field-work carried out at the same time by another researcher (Rennie, 2006a), also provides a cautionary note. Whilst these improved designs, and the use of a lower design reserve, are potentially effective in reducing materials usage, it increases the importance of good quality control, and requires practical testing of candidate designs to ensure their manufacture is practical.

10.4 Production environment

Whilst, as with many fields, there is more literature on prefabrication and the potential benefits of different production environments in the context of MEDCs, this research also shows that prefabrication has not previously been taken up extensively in construction (although there is a recent trend towards this). Less information is available for LEDC situations. Existing literature suggests benefits arising from increased use of prefabrication.

The literature reviewed in Chapter 8 suggested some improvements in material performance may be achieved through increased mechanisation of production via off-site prefabrication of parts followed by on-site assembly. However, the structural analysis in Section 6.1 of Chapter 6 indicates that the shapes favoured by this method are ill-suited to the purpose of water-storage; there are also associated problems with the production of load-bearing joints between sections of

mortar that have already set.

The combination of the factors above, an examination of current practice, and analysis of fieldwork recently conducted by others indicates a semi-prefabrication approach is not to be recommended in the case of rainwater storage tanks: one should adopt complete off-site production where resources and transport do not make this option impractical, and where off-site production is not possible, maintain the current practice of on-site production.

Factory-based production does allow benefits in terms of environmental control, makes the use of moulds easier, and pre-use testing cheaper and easier to perform. There is an upper limit, arising from available equipment, on the mass and volume of components that can be transported from factory to site, which should be considered for other construction components.

The work in this area suggests advocacy of off-site prefabrication should be guided by a sensible appreciation of potential products and uses. The body of research at present does not afford enough examples to provide guidelines as to which components will benefit from an off-site prefabrication approach.

10.5 Summary

All the strategies listed in 10.1 offer benefits over current practice. Of the first two, improved component design gives at least twice the material savings of using local materials, for the case study of rainwater harvesting tanks. A quantitative comparison with production environment was not conducted, but this strategy is valuable as it makes it easier to use the more complex, more efficient recommended tank designs.

The work in this thesis indicates that modern engineering can give considerable benefits when applied to LEDCS, particularly in the case of component design. It also shows that the received wisdom, both in related applications for MEDCs, and in current technologies for LEDCs, should be examined critically; the improvements made possible by this work would not have been achieved

without challenging widely accepted views.

In summary:

- Using local sand can reduce component cost.
- Improved component design significantly reduces component cost.
- Alternative production environments offer a number of benefits.

CHAPTER 11

Further Work

This Thesis has covered a number of different topics. Whilst it has presented some useful results from the research, there remains considerable scope for further work, outlined in the remainder of this Chapter.

11.1 Materials

11.1.1 Plasticisers

The work reported in Chapter 3 included a very brief examination of plasticisers, which may allow the reduction of water content in cementitious mixes and hence improved performance. Given the low quality of sands being considered, and the potential plasticising behaviour of waste products from industries such as sugar processing, further investigation of plasticisers is recommended.

11.1.2 Sand analysis

As discussed in Chapter 3, the laboratory work had to use synthesised sands, and locally available OPC. Ideally further sand samples from representative locations should be obtained, or fieldwork conducted using locally available materials.

11.1.3 Shrinkage and creep

The presence of clay can cause dimensional instability in cement-based products. Another research program, including work by V. Fernandes, has started to address the shrinkage behaviour of mortars containing clay.

11.1.4 Vibration compaction

The literature in Chapter 2 identified the potential of vibration for improving the workability of mixes. Whilst large devices are not likely to prove practicable, modified vibratory sanders etc. are used by ferrocement practitioners to give improved compaction. Further work should address the potential of these as an “intermediate technology” solution.

11.1.5 Curing conditions and strength

Section 3.2.4 on page 61 indicated that curing samples underwater did not give the expected increase in strength. Explanations for this phenomena include inadequate drying time at ambient conditions before testing, such that there was not a like-with-like comparison (wet strength being compared to dry strength). Further work should test a number of samples, and ensure that samples are in the same state at the time of testing.

11.1.6 Young's Modulus

The experimental work in Section 3.2.5, on page 62 indicated a difference between expected Young's modulus and that measured from mortar samples. A number of hypotheses could explain this behaviour, ranging from difficulties with the experimental method to a difference in material properties. Further work should record a range of stress-strain values, to resolve this matter.

11.2 Component Design

11.2.1 Prototype testing

The prototype testing in Chapter 7 gave some interesting findings, but still did not conclusively demonstrate the viability of the design. Another prototype tank should be made, and its performance tested.

11.2.2 Geometry optimisation using shell theory

There is scope for further optimisation of axisymmetric shell tanks, taking into account the variation in wall thickness with height, and effect of bending moments at the base. Authors such as Flügge (1967) cover the derivation of the 2nd order ODEs. Their solution should be possible, but is significantly less simple than the membrane solution. For the membrane case, only one boundary condition is required, which is known beforehand, so the solution may be obtained by stepping through the domain. For the case of tanks with bending moments acting, there are two unknowns: the shear, Q_ϕ , and the rotation, V . To solve over the domain, one has to use two known values at one boundary, estimate values for the other two (e.g. $\frac{dV}{ds}$ and $\frac{dQ_\phi}{ds}$ and then solve to find the resulting values at the other edge of the domain. The unknown boundary conditions at the first edge must be optimised to minimise the error of the two known boundary conditions at the other edge.

11.2.3 Membrane action panel tanks

A considerable amount of work covers the production of membrane structures, in which the forces are transmitted only in the direction of the mid-surface of the component, with notable examples such as those of the architect Isler (Chilton, 2000). A few examples in the literature cover the use of barrel vaults to produce water tanks, but these designs could possibly be taken to panels with curvature

in two dimensions. In the case of water tanks, a flat panel of polythene, clamped along its edges, would, under hydrostatic loading, deform to produce a shape such as that in Figure 11.1, with only tensile forces acting (similar to a 2D version of the catenary arch, but under hydrostatic instead of uniform load).

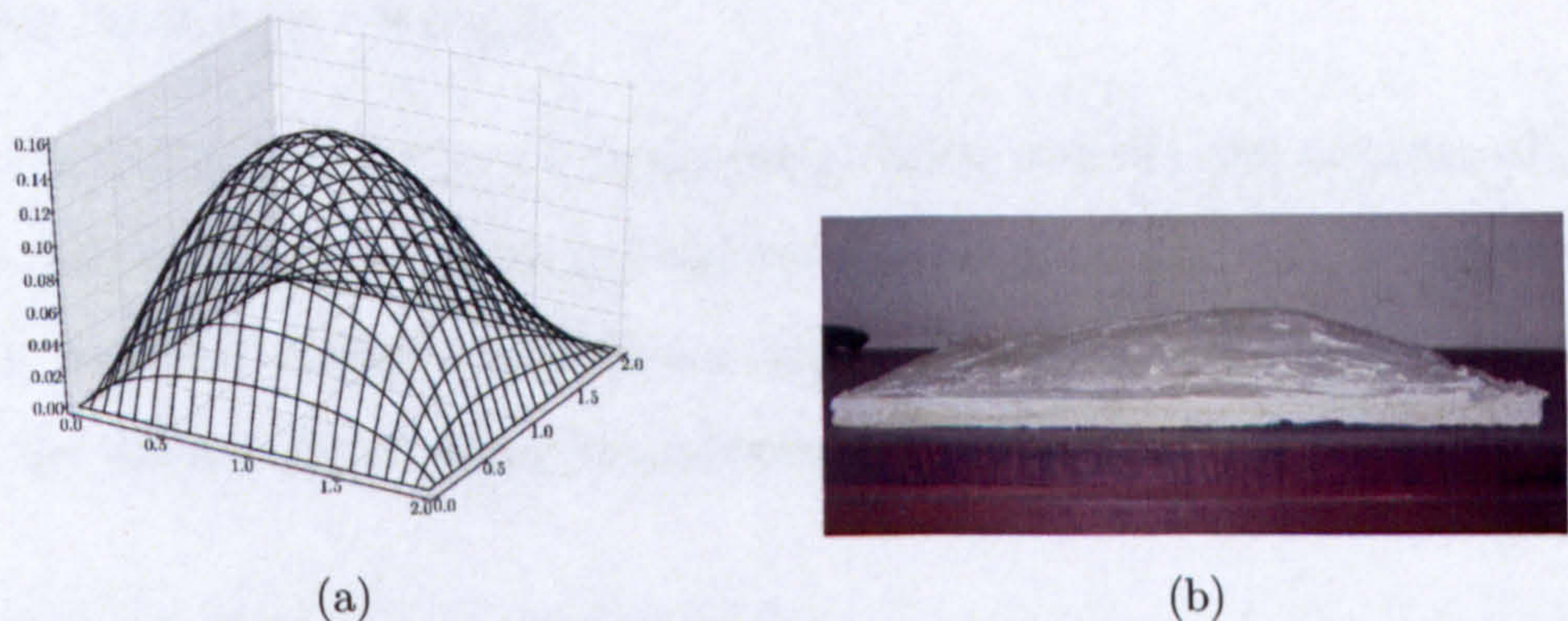


Figure 11.1: Examples of predicted membrane action panel shapes (a), obtained with data from Brew (2005), and cast membrane panel (b).

Inverting this shape should then give a structure acting only in compression. This should lead to arch thrusts at the joints between panels, which could conceivably be resisted by radial buttresses. These shapes would have the attraction of using the mortar in compression rather than tension, which might allow for better material economy. Initial experiments to generate such shapes were undertaken, and collaborative work involving computational generation of shapes has potential, but falls beyond the scope of this Thesis. These shapes might also prove useful for the more general case of cementitious components, the process being noted for material economy and relatively high labour content, both desirable in LEDCs.

11.2.4 Effect of imperfections

The design and modelling work included used a design reserve factor to take account of the presence of imperfections, both in the material used and the geometry of the design produced. The experimental work showed such imperfections to be

extensive, at least in the context of poor mason craftsmanship. A more complete understanding of the effect of geometric imperfections on the behaviour of tanks would benefit the design process, particularly if it included some description of the sensitivity of designs to different degrees of imperfection.

11.2.5 Stepwise thickness changes

Part III considered a number of thickness profiles, but did not exhaust all possibilities. Given the high stresses in the lower section of the tank, a stepwise, or relatively localised change in thickness might offer good material performance, without the difficulties of trying to produce a continually varying wall thickness.

11.2.6 Automation of design optimisation

The designs generated in the thesis often involved user interactions to generate new configurations of generic shapes, assess their performance, and then make modifications for the next set of iterations. Whilst some current FEA packages, such as CosmosWorks, do include optimisation facilities, these are limited in the constraints that they can handle. A more general framework would also help with examination of other components.

Some work was conducted, looking at using a Genetic Algorithm (GA), combined with an FEA package, to address this issue, and is discussed briefly in Appendix C. The algorithm was implemented in conjunction with an academic at the university, Dr. N. Evans, and used the same form as the Simple Genetic Algorithm described by Goldberg (1989). Some initial problems were found with both representing tank shapes efficiently, and with the nature of the problem: the initial handling of constraints (peak stress less than design stress) via a penalty function did not appear effective. Further work should improve the representation of tank designs, and implement an alternative constraint handling mechanism, such as lexographic ordering, as described by Deb (2000). The current version of the GA is included in Section D.9 of Appendix D, with the code to interface

with an open source FEA program, CalculiX.

11.3 Production Environment and Process

11.3.1 Post-construction testing of materials

Some brief laboratory experiments indicated that the strength of mortars produced by plastering or vibration compaction were the same. Further work should verify this, including testing mortar from a prototype tank.

11.3.2 Improved methods of quality control

As practical work both in laboratory conditions and in the field has indicated the importance of good quality control, including providing a consistent thickness, further work should address simple methods of implementing this.

11.3.3 Batch size and production

Similarly, as the practical work has indicated the value of continuously plastered components, and the potential problems with low workability mixes, further work should determine sensible batch sizes and production arrangements, and produce simple recommendations for publication and dissemination.

11.3.4 Alternative methods for producing external moulds

The method used to produce the external moulds discussed in Chapters 7 and 9 was not chosen as the best possible method for field implementation. A number of other methods have potential for improving performance, including making a half-tank of earth, and using this as the male part to form ferrocement mould panels. Further work should examine these options.

PART VI

Bibliography, Appendices and Index

Bibliography

- Akroyd, T. N. W. (1962). *Concrete: properties and manufacture*, 1 edn, Pergamon Press, Oxford; New York. 336 pages.
- Aldridge, E. (2005). The effect of plasticisers on clay-cement composites for use in developing countries. Unpublished 3rd year undergraduate thesis, University of Warwick.
- Bailey Buildbase (2006). Private correspondence.
- Banfill, P. F. G. (2003). The rheology of fresh cement and concrete — a review, in G. Grieve & G. Owens (eds), *Proceedings of the 11th International Cement Chemistry Congress*, Vol. 1, Durban, South Africa, pp. 50-62.
- Banfill, P. F. G. (2005). The rheology of fresh mortar - a review, in C. Fentiman (ed.), *Extended abstracts of the 25th cement and concrete science conference*, The Institute of Materials, Minerals and Mining, Egham, U.K.
- Banfill, P. F. G., Yongmo, X. & Domone, P. L. J. (1999). Relationship between the rheology of unvibrated fresh concrete and its flow under vibration in a vertical pipe apparatus, *Magazine of Concrete Research* 51(3): 181-190.
- Barnes, G. E. (2000). *Soil Mechanics: principles and practice*, 2 edn, MacMillan, Basingstoke, U.K. 493 pages.
- Bentz, D. P. (1999). Modelling cement microstructure: Pixels, particles, and property prediction, *Materials and Structures* 32: 187-195.

- Blyth, F. G. H. & de Freitas, M. H. (2006). *A Geology for Engineers*, 7 edn, Elsevier, Oxford, U.K. 325 pages.
- Brew, J. (2005). Private correspondence.
- Brouwers, H. J. H. & Radix, H. J. (2005). Self-compacting concrete: theoretical and experimental study, *Cement and Concrete Research* **35**: 2116-2136.
- BSI (1983a). Method for determination of static modulus of elasticity in compression, *BS 1881:121*, British Standards Institution.
- BSI (1983b). Method for making test beams from fresh concrete, *BS 1881:109*, British Standards Institution.
- BSI (1983c). Method for making test cubes from fresh concrete, *BS 1881:108*, British Standards Institution.
- BSI (1983d). Method for making test cylinders from fresh concrete, *BS 1881:110*, British Standards Institution.
- BSI (1992). Specification for aggregates from natural sources for concrete, *BS 882:1992*, British Standards Institution.
- BSI (2000a). Flexural strength of test specimens, *BS EN 12390-5:2000*, British Standards Institution.
- BSI (2000b). Slump test, *BS EN 12350-2*, British Standards Institution.
- BSI (2000c). Tensile splitting strength of test specimens, *BS EN 12390-6:2000*, British Standards Institution.
- BSI (2000d). Vebe test, *BS EN 12350-3*, British Standards Institution.
- BSI (2002). Compressive strength of test specimens, *BS EN 12398*, British Standards Institution.

- Building Materials and Technology Promotion Council (2001). Production of cost-effective building components, *Technical report*.
URL: "<http://www.bmtpc.org/machine.pdf>"
- Cebeci, O. Z., Al-Noury, S. I. & Mirza, W. H. (1989). Strength and drying shrinkage of masonry mortars in various temperature-humidity environments, *Cement & Concrete Research* 19: 53–62.
- Chandler, H. W. & Macphee, D. E. (2003). A model for the flow of cement pastes, *Cement and Concrete Research* 33(2): 265–270.
- Chang, D. Y. & Chan, S. Y. N. (1995). Straw pulp waste liquor as a water-reducing admixture, *Magazine of Concrete Research* 47(171): 113–118.
- Chilton, J. (2000). *The Engineer's Contribution to Contemporary Architecture: Heinz Isler*, Thomas Telford, London, U. K. 170 pages.
- Cyr, M., Legrand, C. & Mouret, M. (2000). Study of the shear thickening effect of superplasticizers on the rheological behaviour of cement pastes containing or not mineral additives, *Cement and Concrete Research* 30(9): 1477–1483.
- de Hanai, J. B., Martinelli, D. A. O., Montanari, I. & Debs, M. K. (1984). Ferrocement water tanks with precast barrel vault elements, *Journal of Ferrocement* 14(1): 37–44.
- De Schutter, G. & Poppe, A.-M. (2004). Quantification of the water demand of sand in mortar, *Construction and Building Materials* 18: 517–521.
- Deb, K. (2000). An efficient constraint handling method for genetic algorithms, *Computer methods in applied mechanics and engineering* 186: 311–338.
- Dewar, J. D. (1999). *Computer modelling of concrete mixtures*, Elsevier, London. 256 pages.

- DTU (2005). DTU publications on rainwater harvesting, *Technical report*, Development Technology Unit. <http://www.eng.warwick.ac.uk/dtu/pubs/rwh.html>.
- DTU (2006a). Case study 1: the Sri Lankan pumpkin tank, *Technical report*, Development Technology Unit. <http://www.eng.warwick.ac.uk/dtu/pubs/rwh.html>.
- DTU (2006b). Rain-jar handbook: Production and use of mortar rainwater jars, *Technical report*, Development Technology Unit. <http://www.eng.warwick.ac.uk/dtu/pubs/rwh.html>.
- Erguden, S. (2001). International conference on spatial information for sustainable development, *International conference on spatial information for sustainable development*, Housing Policy Section, UNCH, Nairobi, Kenya.
- Fernandes, V. (2002). The effect of fines in sand for the fabrication and application of concrete in developing countries. 3rd year undergraduate thesis, University of Warwick.
- Fernandes, V. A., Purnell, P., Still, G. T. & Thomas, T. H. (2006). The effect of clay content in sands used for cementitious materials in Developing Countries, *Cement and Concrete Research*. Accepted for publication October 2006.
- Flügge, W. (1967). *Stresses in shells*, Springer-Verlag, New York. 525 pages.
- Gibb, A. G. F. (1999). *Off-site fabrication: prefabrication, pre-assembly and modularisation*, Whittles, Caithness. 262 pages.
- Goldberg, D. E. (1989). *Genetic Algorithms in Search, Optimization & Machine Learning*, Addison-Wesley, Reading, Massachusetts.
- Gould, J. & Nissen-Petersen, E. (1999). *Rainwater catchment systems for domestic supply: design, construction and implementation*, Intermediate Technology, London. 335 pages.

- Gullered, K. & Cramer, S. (2002). Effect of aggregate coatings and films on concrete performance.
- Hotta, H. & Takiguchi, K. (1995). Influence of drying and water supplying after drying on tensile strength of cement mortar, *Nuclear Engineering and Design* 156: 219–228.
- Hu, C. & de Larrard, F. (1996). The rheology of fresh high-performance concrete, *Cement and Concrete Research* 26(2): 283–294.
- Hunter, J. (2005). Matplotlib: 2D plotting library for python.
URL: <http://matplotlib.sourceforge.net>
- Jaeger, L. G. (1964). *Elementary theory of elastic plates*, Pergamon: Macmillan, Oxford; New York. 118 pages.
- Jones, E., Oliphant, T., Peterson, P. *et al.* (2001–). SciPy: Open source scientific tools for Python.
URL: <http://www.scipy.org/>
- Kerali, A. G. & Thomas, T. H. (2002). Effect of mix retention and curing on low-cement walling blocks, *Building Research & Information* 30(5): 362–366.
- Khan, M. M. (1983). Construction of 400 gal capacity water tank with precast ferrocement elements, *Journal of Ferrocement* 13(3): 257–260.
- Kim, J.-K., Han, S. H. & Song, Y. C. (2002). Effect of temperature and aging on the mechanical properties of concrete. Part I. experimental results, *Cement and Concrete Research* 32: 1087–1094.
- Kintingu, S. (2005). Private correspondence.
- Kokobu, K., Cabrera, J. G. & Ueno, A. (1996). Compaction properties of roller compacted concrete, *Cement and Concrete Composites* 18(2): 109–117.

- Kumar, A., Irshad, M., Agarwal, S. K. & Kumar, A. (1995). Studies on paper mill effluent as a workability aid for cement mortars, *Building and Environment* 30(4): 579–582.
- Kumar, K. S., Sharma, P. C. & Robles-Austriaco, L. (1984). Review of design considerations and construction techniques for ferrocement water resources structures, *Journal of Ferrocement* 14(1): 49–63.
- Lydon, F. D. (1982). *Concrete Mix Design*, Vol. 1, Applied Science Publishers, London. 198 pages.
- Martinson, B. (2005). Private correspondence.
- Meek, J. L. (1982). Construction of a ferrocement water tank of novel design, *Journal of Ferrocement* 12(4): 385–389.
- Meier, G. M. & Rauch, J. E. (2000). *Leading issues in economic development*, 7th edn, Oxford University Press. 650 pages.
- Melis, L. M., Meyer, A. H. & Fowler, D. W. (1985). *An evaluation of tensile strength testing*, Research Report 4321-F, Center for Transportation Research, University of Texas, Austin, Texas.
- Moita, G. F., de Las Casas, E. B., Carrasco, E. V. M. & Bonifacio, S. N. (2003). Experimental and numerical analysis of large ferrocement water tanks, *Cement and Concrete Composites* 25.
- Montgomery, D. E. (2002a). *Dynamically-compacted cement stabilised soil blocks for low-cost walling*, PhD thesis, School of Engineering, University of Warwick.
- Montgomery, D. E. (2002b). Dynamically-compacted cement stabilized soil blocks for low-cost walling.
- Mwamila, B. L. M. & Karumuna, B. L. (1999). Semi-prefabrication concrete techniques in developing countries, *Building Research & Information* 27(3).

- Naaman, A. E. (2000). *Ferrocement and laminated cementitious composites*, Techno Press 3000, Michigan, USA. 372 pages.
- Nadif, A., Hunkeler, D. & Käuper, P. (2002). Sulfur-free lignins from alkaline pulping tested in mortar for use as mortar additives, *Bioresource Technology* 84: 49–55.
- Nelder, J. A. & Mead, R. (1965). A simplex method for function minimization, *The Computer Journal* 7: 303–333.
- Neville, A. M. (1995). *Properties of Concrete*, Longman, Harlow. 844 pages.
- Ngowi, A. B. (1997). A hybrid approach to house construction — a case study in botswana, *Building Research & Information* 25(3).
- Okamura, H. & Ouchi, M. (1998). Self-compacting high performance concrete, *Structural Engineering and Materials* 1(4): 378–383.
- Paramasivam, P. & Nathan, G. K. (1984). Prefabricated ferrocement water tank, *Journal of the American Concrete Institute* 81(6): 580–586.
- Paramasivam, P., Ong, K. C. G., Tan, K. H. & Lee, S. L. (1990). Rainwater storage using ferrocement tanks in developing countries, *Journal of Ferrocement* 20(4): 377–384.
- Popovics, S. (1998). *Strength and related properties of concrete: a quantitative approach*, John Wiley, New York; Chichester. 535 pages.
- Rao, G. A. (2001). Generalization of abram's law for cement mortars, *Cement and Concrete Research* 31(3): 495–502.
- Rennie, G. (2006a). Technology choice for the provision of rainwater storage for rural ugandan households. unpublished Masters thesis.
- Rennie, G. E. (2006b). Private correspondence.

- Ruthven, A. L. (2005). Microstructure of 'clay-contaminated' concrete and mortar. unpublished 3rd year undergraduate thesis, University of Warwick.
- Saak, A. W., Jennings, H. M. & Surenda, P. S. (2004). A generalized approach for the determination of yield stress by slump and slump flow, *Cement and Concrete Research* 34: 363–371.
- Sharma, P. C. (1983). A mechanized process for producing ferrocement roof and wall elements, *Journal of Ferrocement* 13(1): 13–26.
- Sharma, P. C. (2005). Ferrocement water storage tank for rain water harvesting in hills & islands, in D. K. Manavalan (ed.), *Proceedings of the XIIth International Rainwater Catchment Systems Association*, IRCSA, IRCSA, Delhi, India.
- Solidworks (2006). Solidworks 2006.
URL: <http://www.solidworks.com>
- Stallen, M., Chabannes, Y. & Steinberg, F. (1994). Potentials of prefabrication for self-help and mutual-aid housing in developing countries, *Habitat International* 18(2): 13–39.
- Still, G. T. & Thomas, T. H. (2004). Mix proportioning of mortars in tension, with particular reference to developing countries, in C. Fentiman (ed.), *Abstracts of the 24th conference on Cement and Concrete Science*, Institute of Materials, Minerals and Mining, University of Warwick.
- Still, G. T. & Thomas, T. H. (2005). Mix proportioning of mortars in tension, with particular reference to developing countries, in C. Fentiman (ed.), *Abstracts of the 25th conference on Cement and Concrete Science*, Institute of Materials, Minerals and Mining, Royal Holloway (University of London).
- Still, G. T. & Thomas, T. H. (2006). Mix proportioning of mortars in tension, with particular reference to developing countries, *Advances in Applied Ceramics* 105(4): 179–184.

- Still, G. T., Thomas, T. H., Fernandes, V. A. & Purnell, P. (2006). Selecting fine aggregate for cementitious building components in developing countries, *Building Research and Information* . submitted November 2006.
- Su, N., Hsu, K.-C. & Chai, H.-W. (2001). A simple mix design method for self-compacting concrete, *Cement and Concrete Research* **31**: 1799-1807.
- Su, N. & Miao, B. (2003). A new method for the mix design of medium strength flowing concrete with low cement content, *Cement and Concrete Composites* **25**: 215-222.
- Tarran, F. C. (1984). Ferrocement water tanks, *Journal of Ferrocement* **14**(1): 29-35.
- Tasdemir, M. A., Lydon, F. & Barr, B. I. G. (1996). The tensile strain capacity of concrete, *Magazine of Concrete Research* **48**(176): 211-218.
- Tattersall, G. H. (1992). *Workability and quality control of concrete*, E & FN Spon, London. 262 pages.
- Tattersall, G. H. & Banfill, P. F. G. (1983). *The rheology of fresh concrete*, Pitman, Boston (Mass.); London. 356 pages.
- Thanh, N. H. (1991). Optimal concrete composition based on paste content, *Journal of Ferrocement* **21**(4): 331-350.
- Thevendran, V. & Thambiratnam, D. P. (1987). Optimal shapes of cylindrical concrete water tanks, *Computers & Structures* **26**(5): 805-810.
- Thomas, T. H. (2007). Private correspondence.
- Timoshenko, S. P. & Woinowsky-Kreiger, S. (1959). *Theory of plates and shells*, McGraw-Hill, New York. 568 pages.
- Todaro, M. P. (2000). *Economic development*, 7th edn, Addison-Wesley, Massachusetts. 783 pages.

van Rossum, G. *et al.* (2005). Python.

URL: *http://www.python.org*

Venkatarama Reddy, B. V. & Gupta, A. (2005). Characteristics of cement-soil mortars, *Materials and Structures* **38**: 639-650.

Walker, A. W. (2002). *Special purpose concrete*, Master's thesis, School of Engineering, University of Warwick.

Walkus, B. R. & Malek, E. (1986). Prefabricated ferrocement roof elements in poland, *Journal of Ferrocement* **16**: 285-294.

Watt, S. B. (1978). *Ferrocement water tanks and their construction*, Intermediate Technology Publications, London, U. K. 118 pages.

Yool, A. I. G., Lees, T. P. & Fried, A. (1998). Improvements to the methylene blue dye test for harmful clay in aggregates for concrete and mortar, *Cement and Concrete Research* **28**(10): 1417-1428.

Zingoni, A. (1997). *Shell structures in civil and mechanical engineering: theory and closed-form analytical solutions*, Thomas Telford, London. 349 pages.

APPENDIX A

Materials Choice and Proportioning

A.1 Publications arising from materials research ratio



The effect of clay content in sands used for cementitious materials in developing countries

V.A. Fernandes, P. Purnell*, G.T. Still, T.H. Thomas

School of Engineering, University of Warwick, Coventry, CV4 7AL, UK

Received 16 December 2005; accepted 23 October 2006

Abstract

The cost of building materials in Less Economically Developed Countries (LEDCs) is one of the single largest contributing factors to housing costs. They are often transported over relatively large distances at considerable expense. Local sands may contain significant amounts of clay, considered by local artisans to be detrimental to concrete strength; however, in an LEDC context, there is little evidence to support this. In this study, the compressive strength and workability of representative LEDC clay-contaminated concrete was determined. Clay-cement interactions were studied using X-Ray Diffraction (XRD). Different clays appeared to have fundamentally different effects on both workability and strength. No chemical interactions were detected. It was concluded that satisfactory concrete could be made from clay-contaminated sand.

© 2007 Published by Elsevier Ltd.

Keywords: Workability; X-Ray diffraction; Compressive strength; Clay

1. Introduction

A significant demand exists for housing in Less Economically Developed Countries (LEDCs), where it has been estimated that more than 100 million people are homeless and about one billion people are inadequately housed [1]. Approximately twenty-one million new housing units are required each year [2].

The main costs of shelter provision are land purchase, building materials, machinery, man-power and loan interest payments [3]. Building materials are often the single largest component of housing cost in LEDCs; accounting for up to 70% of a standard low-cost housing unit [1]. By contrast, it is estimated that in the UK, only about 20% of the cost of a housing unit is for building materials, because the majority of costs are incurred for finishes, such as electricity, lighting and carpets; these are luxuries that the poor cannot afford. For the lack of more local suppliers, some 'quality' building materials in LEDCs are transported over relatively large distances (e.g. 50 km) and at considerable expense, despite natural resources

being available nearby that might be suitable for building materials production.

Building aggregate consists of two types; coarse (gravel or crushed stone) and fine (natural or manufactured sand). In the provincial areas of LEDCs countries, there is often an absence of a coarse-aggregate industry, so most cementitious products are made with only fine aggregates. Thus, with cement, sand is the major component needed for producing concrete and mortar for low-cost housing components. In LEDCs, for such reasons as the high cost of transport in relation to labour, cementitious components of low-cost housing use as aggregate either on-site soil or 'sand' from within 1 km of the site. In consequence there is a strong incentive to use sand that would not meet British Standards (BS EN12620:2002) with respect to grading and clay content. However, the effects of clay on concrete performance are poorly understood and specifications restricting their use tend to be vague [4,5]. If clay-containing local sand could be used, housing materials would be more cheaply and readily available.

Several different clays exist in soils and their characteristics are likely to have an effect on the properties of concrete containing them. The main clays found in tropical regions are kaolin and montmorillonite. Clay minerals have the ability to

* Corresponding author.

E-mail address: pp@eng.warwick.ac.uk (P. Purnell).

attract water molecules; a surface phenomenon called adsorption. Owing to their large surface areas and chemical structures, both clays have a great affinity for water and can also assimilate it into their microstructure. However they have different structures; the approximate specific surface area for kaolin is 10–20 m²/g and for montmorillonite, 800 m²/g [6]. This large specific surface, combined in the case of montmorillonite with the ability to absorb water into its microstructure, is reflected in the increased water content needed for adequate workability in fresh clay-contaminated concrete. The two essential functions of water in a mix are to hydrate the cement and to provide adequate workability. With clay in the mix, the amount of water needed for good workability can be considerably more than that needed for hydration (to a greater extent than in normal concrete). Therefore, once the concrete is cured and a portion of the water is chemically bound by hydration, a greater remainder than is usual evaporates leaving an increased content of voids (capillary porosity) in the hydrated assemblage, reducing the strength of the material [7].

The propensity of the clays to affect the normal storage and transport of water within cementitious matrices suggests that they can also affect the dimensional stability – shrinkage – of the resultant concrete; this is recognized by us and previous investigators [8]. Although not forming part of this report, a series of parallel experiments are ongoing to investigate the magnitude of this shrinkage, which will be reported in a companion paper.

In addition to the cementing reaction, the chemical interaction of cement and clay particles may have an effect on the properties of concrete and may explain why clay-contaminated concretes have different physical properties [9]. Very little analytical research has been undertaken on clay-contaminated sand for use in concrete production, especially in the context of use in low-cost housing. Parsons [10] concluded that clay is much more detrimental to the strength of concrete if present as a surface coating surrounding the sand grains, than if evenly distributed throughout the mass. When the clay forms such a surface coating, it is bound only by weak electrostatic forces, which led many researchers to suggest that clay particles interfere with the bond between the sand particles and cement paste matrix [11–14]. If the bond between either the clay coating and the sand, or the clay and the cement paste, is weaker than the normal cement–sand bond (which is thought likely) then *strength* and *durability* problems may result [14]. However, although many have concluded that clay surface coatings weaken the sand/cement paste bond, there is little experimental evidence that this reduces concrete strength and durability. Moreover, Parsons [10] suggested that if the clay is distributed *evenly* within the sand, there is no detrimental effect and it might increase the strength of the concrete by filling in the spaces between the larger particles. If both sand *and* clay could be regarded as chemically inert components, the cement would bind evenly-distributed sand and clay grains together during hardening, forming a roughly continuous matrix of a hard, strong material enclosing particles of sand and clay.

Sand is normally regarded as chemically inert and unlikely to affect any chemical changes taking place in resultant concretes.

Some work has however been published on clay–cement interactions [9,28,29].

According to Herzog & Mitchell [15] a clay–cement mixture cannot be regarded as a simple mixture of hydrated cement matrix bonding together unaltered clay particles, but should be considered as a system in which both clay and hydrating cement combine through secondary reactions. When the mixture is in its fresh state, cation exchange and flocculation effects occur causing structural stabilization of the clay [16]. During the hardening of the clay–cement mixture, the hydration of cement takes place, forming the usual cement hydration products; calcium silicate hydrates, calcium hydroxide Ca(OH)₂, and hydrated aluminates [17]. The calcium hydroxide formed in the primary phase, together with the soluble alkalis released during cement hydration which raise the pH of the pore solution to >13, could initiate attack of the clay particles and also cause a breakdown of amorphous alumina and silica, which then could combine with the calcium ions liberated from the hydrolysis of cement to form a secondary cementitious material [9]. This secondary reaction is known as the pozzolanic reaction [18], and could form products that are initially amorphous but may later become crystalline. X-ray investigations undertaken by Eades and Grim [19] of samples cured at 60 °C indicated a destruction of montmorillonite clay structure and moderate attack on kaolin clay in the presence of calcium hydroxide. This could be because of clay mineral structure breakdown and/or interaction with cement at the particle surfaces. However, any secondary cementitious material so formed remains unidentified.

Herzog and Mitchell [9] proposed a model of the resultant microstructure in which (using their terminology in quote marks) a “matrix” of sand and unreacted clay is surrounded by a “skeleton” of hydrated cement. They proposed that some of the clay reacts with (or is captured on the surface of) the skeleton, thereby strengthening it. The remainder of the clay stays in the clay–sand matrix. They did not, however, publish any micrographs or other evidence supporting this theory.

Thus there are two mechanisms by which clay might strengthen relatively weak concrete mixes: either pore-filling by the fine clay particles; or a chemical reaction between the clay and the hydrating cement and/or its hydration products producing further insoluble hydrates.

This paper presents the findings of experimental work on clay–cement–sand composites, the properties of which have not been well documented in the open literature. Despite clay being considered deleterious in normal concrete production, experimental evidence is offered to assess the use of clay-contaminated concrete blocks as a suitable building material for low-cost housing in LEDCs. An analytical research has been undertaken to try and identify whether the proposed secondary cementitious materials do actually form. While the primary context of this paper is assessing the use of clay-contaminated building materials in LEDCs, concrete aggregates in developed countries are also becoming increasingly scarce, so alternative sources also need to be found and proved; this research may also have applications in that regard.

2. Experimental methodology

2.1. Materials

The clay-free basic sand (sand 'S') used in experimentation was selected to be representative of concreting sands used in LEDCs [20]. XRD analysis of the sand used showed it to be a pure quartz sand with no significant impurities.

Two other sands were then synthesized by dry mixing, consisting of this Sand S with the substitution of either 20% of mass by kaolin (kaolin-contaminated sand, referred to as Sand K), or 20% by montmorillonite (montmorillonite-contaminated sand, referred to as Sand M). The composition of sands K and M were chosen to be as close as possible to a wide range of natural sands in LEDCs and were used for testing, as the quantities of samples needed were not practically obtainable directly from LEDCs.

The cement used during testing was Type 1 OPC. At present this cement (or its local analogue) is the most widely available and quality-consistent stabilizer in LEDCs, and is likely to remain so for at least the next ten years [21]. The water used was untreated laboratory tap water.

2.2. Methods of testing

100 mm concrete cubes were made using sand types S, K and M respectively. The data consists of sets of varying sand types, water/cement ratio and sand/cement ratio, with each sample consisting of 6 cubes. For every combination of each of the three sand types and for four sand/cement ratios (3, 5, 7, 10), the water/cement ratio was altered until an optimum compressive strength was achieved after 28 days curing in polyethylene bags. In general, fully compacted concrete has a monotonic strength relationship with w/c ratio; as the w/c decreases, strength increases. However, below a certain w/c ratio, the concrete will have insufficient workability for full compaction to be achieved, and the strength will then begin to decrease with decreasing w/c. Thus there is an optimum w/c ratio with regard to strength and an iterative process was adopted to find it. The workability of each iterative mix was also measured using slump and Vebe tests (but it is important to note that finding an 'optimum workability' was not an objective of this study).

The concrete mix was made starting with the selected (dry premixed) sand and clay, then adding the water, then adding the cement. Each mix was mixed in a pan mixer until a homogeneous mix was formed. Preliminary studies showed that seemingly adequate mixing could produce a highly uneven distribution of cement so extra care was taken to ensure homogeneity. The average mixing time was around 5 min.

The cubes were cast in lubricated steel moulds, being compacted using vibration, according to BS 1881: Part 108:1983. The manufactured cubes were placed under damp hessian overnight, and de-moulded the following morning. After the cubes were de-moulded, they were stored in sealed polyethylene bags. This prevented water from within the cube from escaping as surface evaporation was almost non-existent

in an environment of approximately 100% humidity. This was considered an appropriate optimal curing environment with regard to local practice. The temperature of the curing process, approximately 19°C, was determined by laboratory conditions.

After 28 days, the cubes were tested to failure using a compression test machine at 200 kN/min (BS 1881: Part 108: 1983), with maximum load and type of failure recorded. The total number of cubes tested in this study was 900.

In addition to the testing of the strength of cured blocks, X-Ray Diffraction (XRD) was used to detect any reactions between the clay and cement. A sample of each concrete block was taken and tested at 28 days and 1 year, from blocks manufactured with a sand/cement ratio of 5:1 at their respective optimum w/c ratios, (0.95 for sand S mix, 1.15 for sand K mix and 1.8 for the sand M mix). The samples were monitored using a BRUKER D5005 X-ray diffractometer machine over a period of eight hours, giving a range of 4° 2 θ to 70° 2 θ . The experimental data was examined to identify the peaks and relative intensities corresponding to the compounds of interest (as calibrated via the International Center for Diffraction Data [22]).

3. Results

3.1. Workability

Figs. 1 and 2 show slump and Vebe measurements (as a function of water/cement ratio) for all three sands at two different sand/cement ratios. These selected curves show the general trend but data is also available for the other sand/cement ratios. Since the lines are roughly parallel, we can summarize all the data by tabulating the 'extra' water required by a clay-contaminated mix (in terms of w/c) in order to restore its workability to that of the uncontaminated mix S. This data is given in Table 1. Note that the s/c=20:1 mixes are not included in this table as they have insufficient workability for slump to be measured or Vebe time to be recorded. In addition, for example, label (a) on Fig. 1 shows the 'extra' water mix K requires (in terms of w/c) with s/c of 3:1 in order to restore its workability to that of the uncontaminated mix S with s/c 3:1.

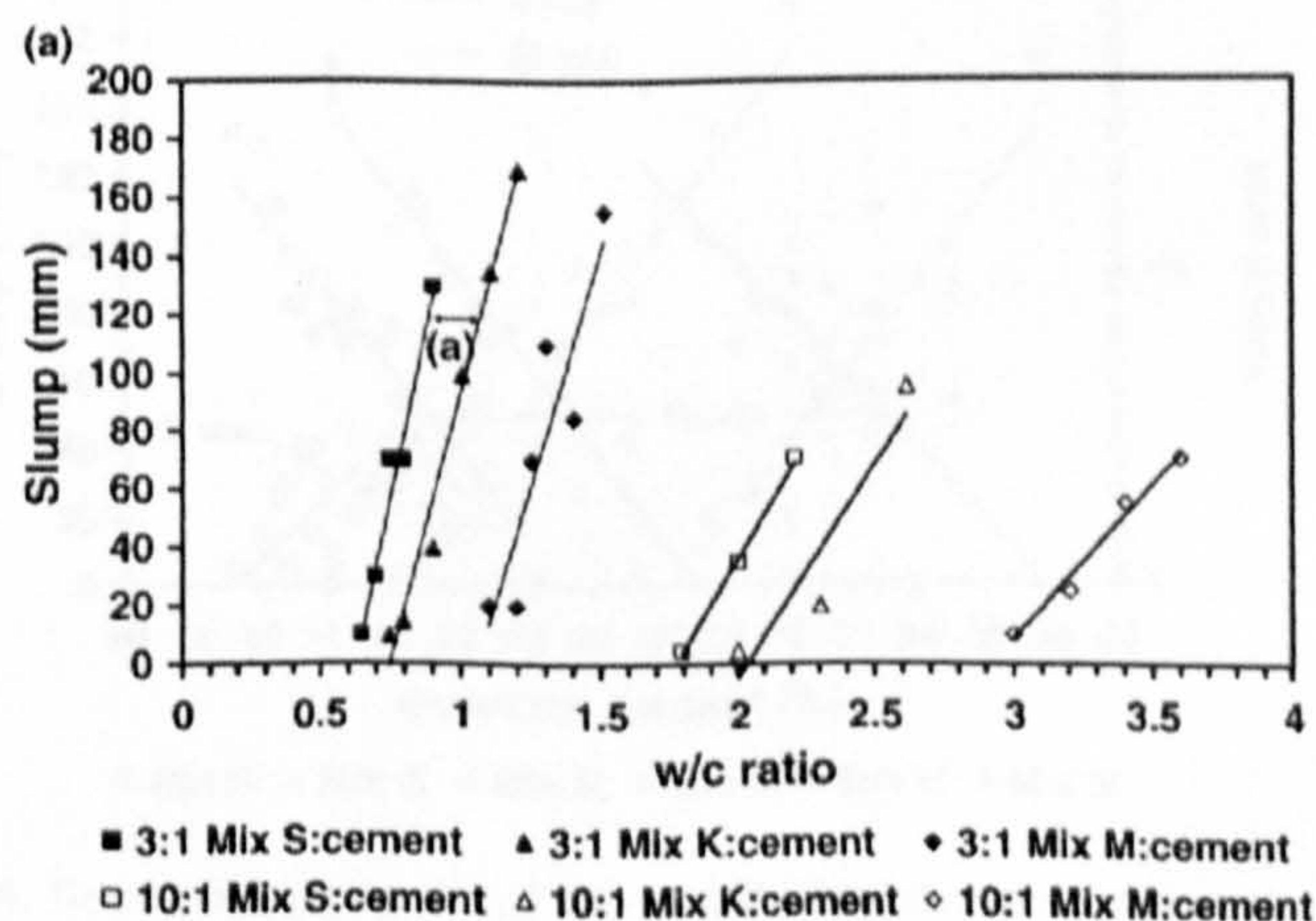


Fig. 1. Effect of sand type on slump for two sand/cement ratios.

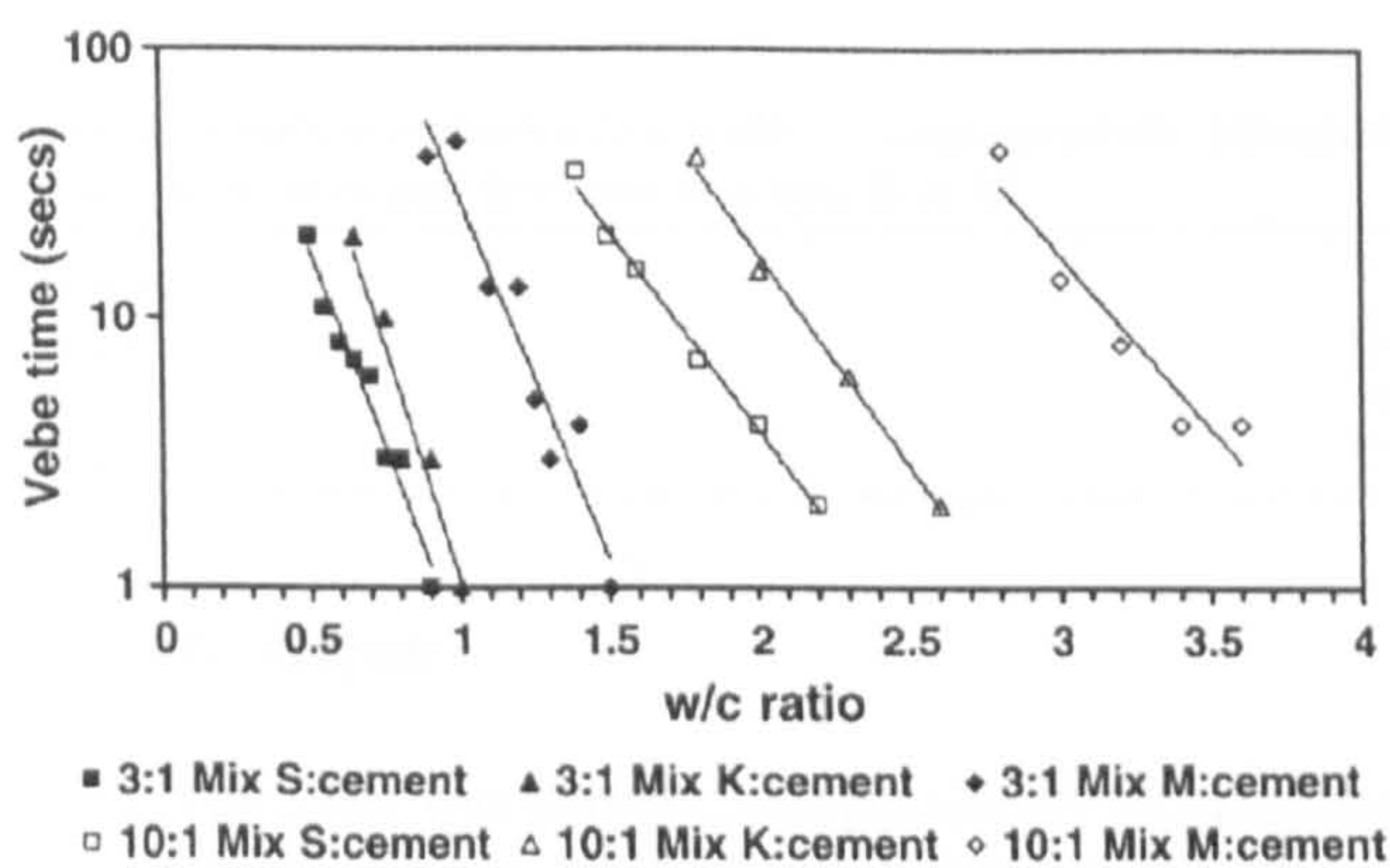


Fig. 2. Effect of sand type on Vebe for two sand/cement ratios.

For a given s/c ratio and w/c ratio, both clays significantly reduce the workability, montmorillonite having a greater effect than kaolin and therefore requiring the larger addition of water to restore required workability. As expected, for a given w/c ratio and sand type, increasing the s/c ratio reduces workability.

As w/c ratio (for a given workability) rises with s/c ratio, we might expect moisture content, λ (defined as the ratio by mass of water to solids), to correlate more simply with the workability measures than w/c ratio does. Fig. 3 plots slump and Vebe time against λ for a single sand type, S (note that Vebe time is on a logarithmic scale). The data for all four s/c ratios (3, 5, 7 and 10; data for s/c=20 is not included for the reasons outlined above) appear to follow a single linear relationship. This implies that workability for these mixes depends only on λ and not on s/c ratio. This also appears to apply for sands K and M, and all the relevant data is plotted on Fig. 4. The fit lines are approximately parallel, thus we can deduce a constant a that represents the additional moisture content needed to keep workability constant when switching from standard sand S to clay-contaminated sands K and M. For example, $a_{m, \text{Vebe}}$ and $a_{k, \text{Slump}}$ (as shown by the arrows on Fig. 4) represent the additional moisture content required to restore: the workability of a montmorillonite-contaminated mix (as measured using the Vebe test); and that required to restore workability of a kaolin-contaminated mix (as measured using the slump test) respectively. All values of a are given in Table 2. Note the

Table 1
Addition to w/c required to restore uncontaminated workability to clay-contaminated mixes

	s/c 3:1	s/c 5:1	s/c 7:1	s/c 10:1
Slump test				
Mix K	+0.14 ^a	+0.37	+0.46	+0.26
Mix M	+0.45	+0.79	+1.12	+1.05
Vebe test				
Mix K	+0.18	+0.24	−0.11	+0.36
Mix M	+0.62	+1.43	+0.68	+1.53
Average of both tests				
Mix K	+0.16	+0.31	+0.18	+0.31
Mix M	+0.54	+1.11	+0.90	+1.29

^a Marked (a) on Fig. 1.

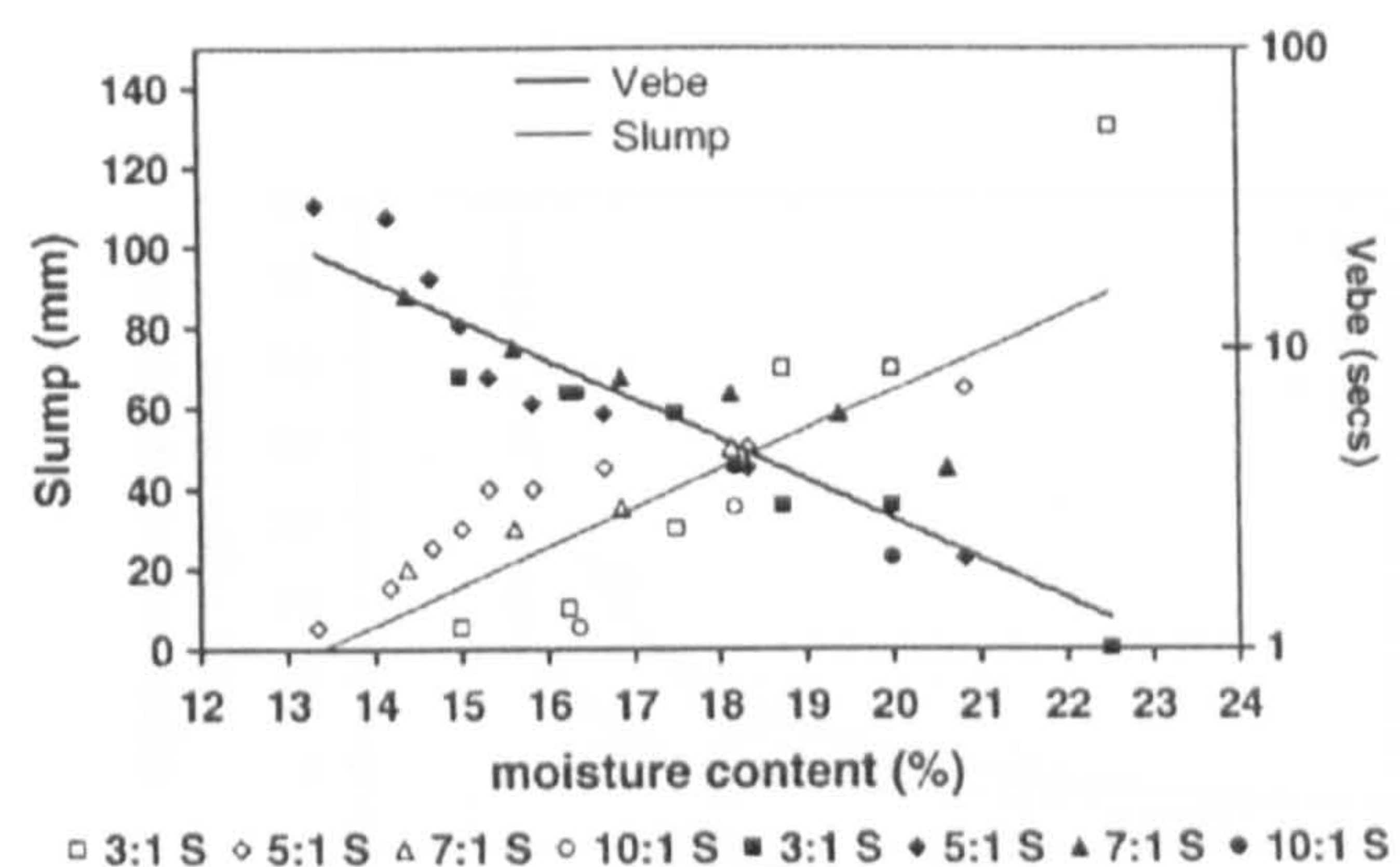


Fig. 3. Graph showing slump and Vebe vs. % moisture content relationship for mix S. Bold line/filled symbols denote Vebe results, light line/open symbols denote slump results. Legend numbers=s/c ratio.

similarities between values derived for both slump and Vebe tests, implying that either method may be used without affecting the results.

3.2. Compressive strength

Strength results are summarized in Figs. 5–7. It can be seen that in general, for each s/c ratio, the strength does indeed go through an optimum. For very lean samples, i.e. with s/c=20:1, this optimum is poorly defined (and indeed absent in sand M), as effects related to the cohesiveness of the clay tend to dominate over those related to hydration of the cement.

At low s/c ratios, the clay lowers the achievable optimum strength, the effect of montmorillonite being significantly greater than that of kaolin (Fig. 6). At higher s/c, the effect is indistinct and for sand K, may even be reversed; the clay may be marginally beneficial *vis a vis* strength. There is a good linear correlation between the s/c ratio and w/c ratio at optimum strength (Fig. 7). Note that the sand S and K lines virtually coincide, while that for sand M is rather different.

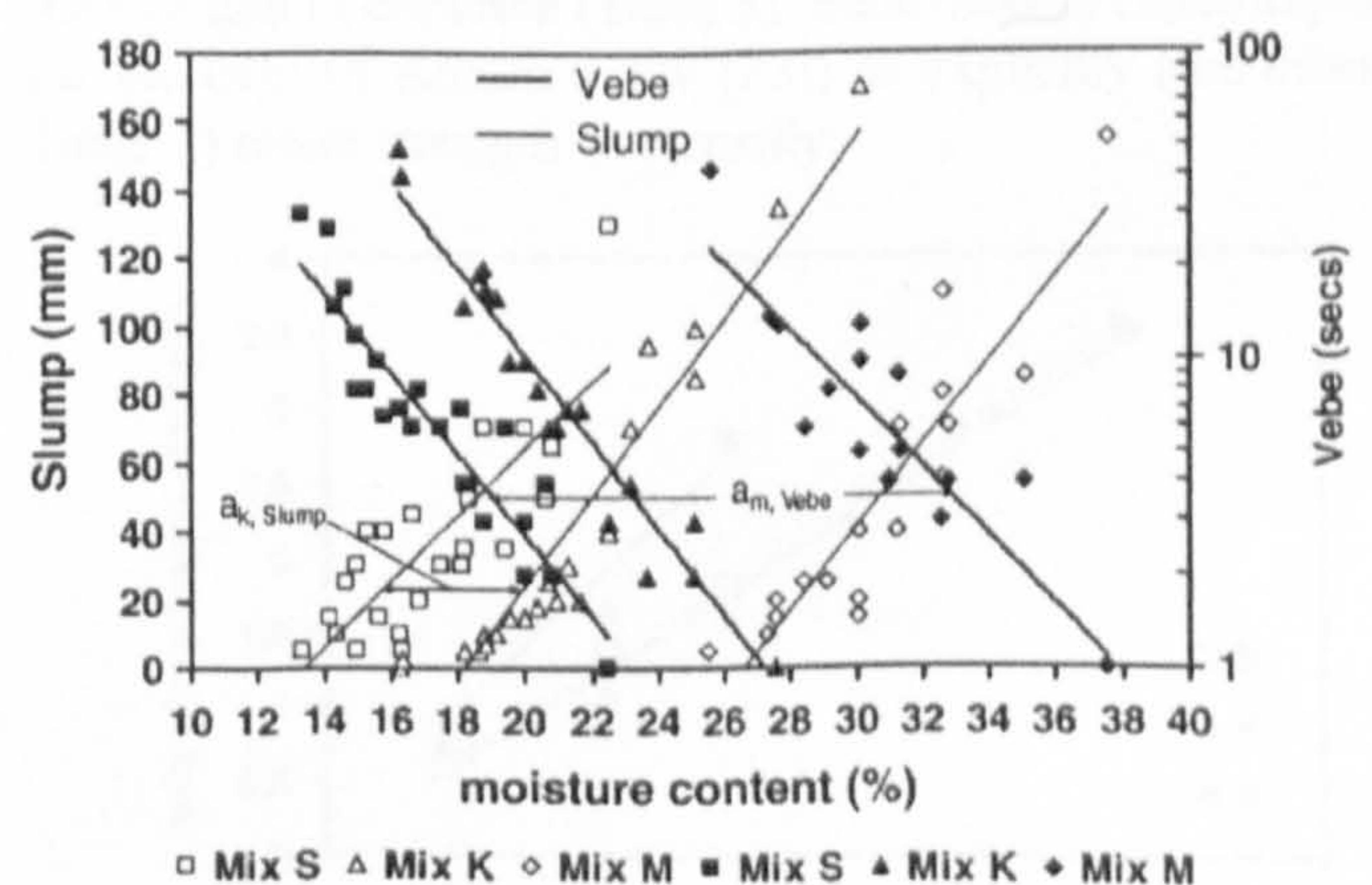


Fig. 4. Graph showing combined Slump and Vebe vs. % moisture content relationships for all mixes at s/c of 3:1–10:1. Bold line/filled symbols denote Vebe results, light line/open symbols denote slump results.

t2.1	Table 2	
t2.2	Additional moisture contents a (%) needed to keep workability (slump or Vebe)	
t2.2	constant when switching from mix S to mix K or M	
t2.3	a_k , slump	3.5 ± 0.8
t2.4	a_k , slump	12.2 ± 0.6
t2.5	a_k , Vebe	4.4 ± 0.2
t2.6	a_m , Vebe	13.0 ± 0.9

3.3. XRD analysis

XRD analysis was undertaken on a variety of samples at 1, 7 and 28 days, 9 months and one year. The results showed that there is no change in peaks for the different sand types after cement hydration, apart from the formation of Gypsum in the sand K after 1 year. No unusual chemical reactions have taken

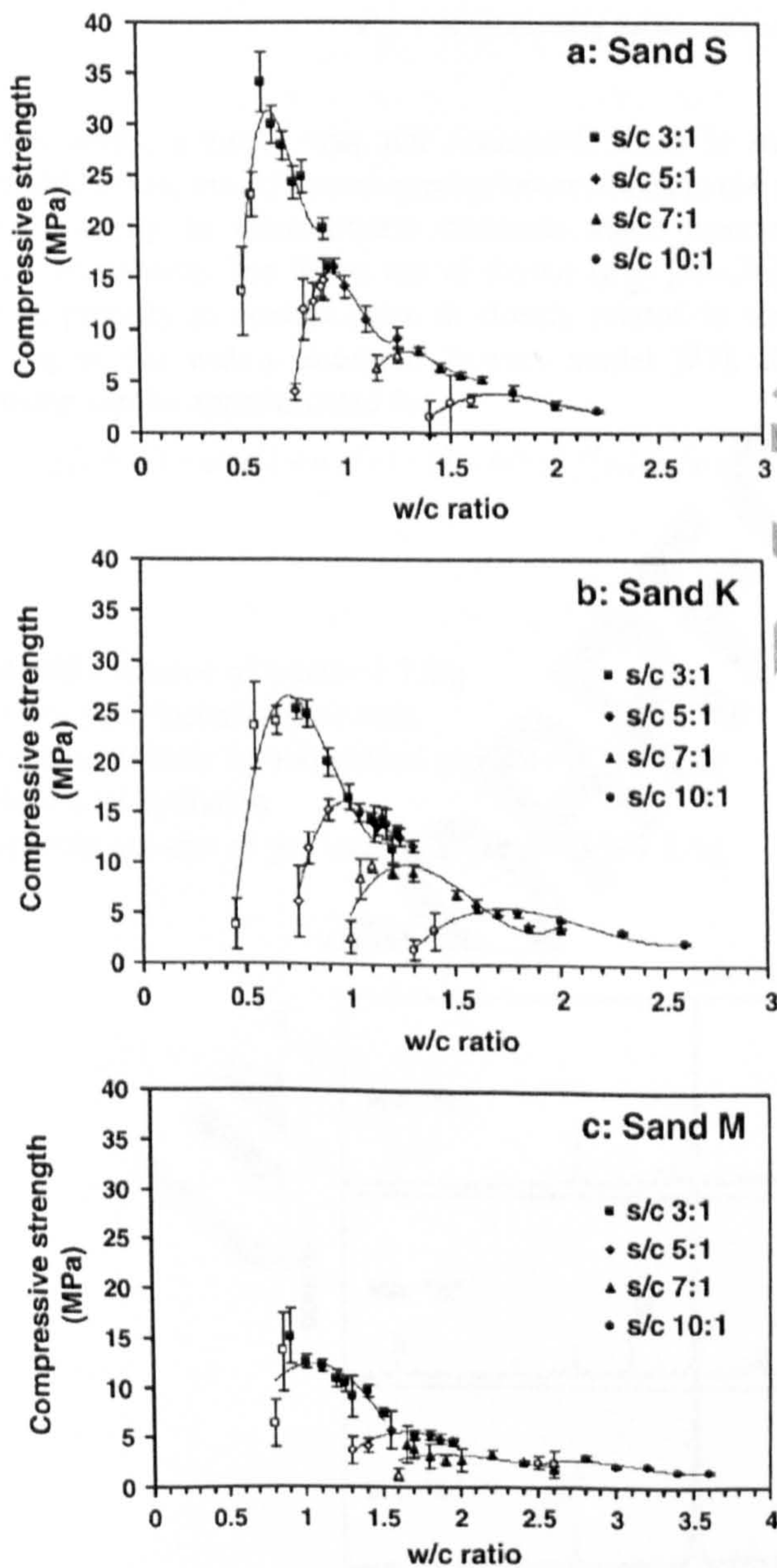


Fig. 5. Compressive strength vs. w/c ratio. Legends refer to sand/cement ratios. Where applicable, open symbols denote incomplete compaction; closed symbols, complete compaction. Error bars are ± 1 standard deviation (6 replicates). Lines are cubic fits to group data, not intended as analytical.

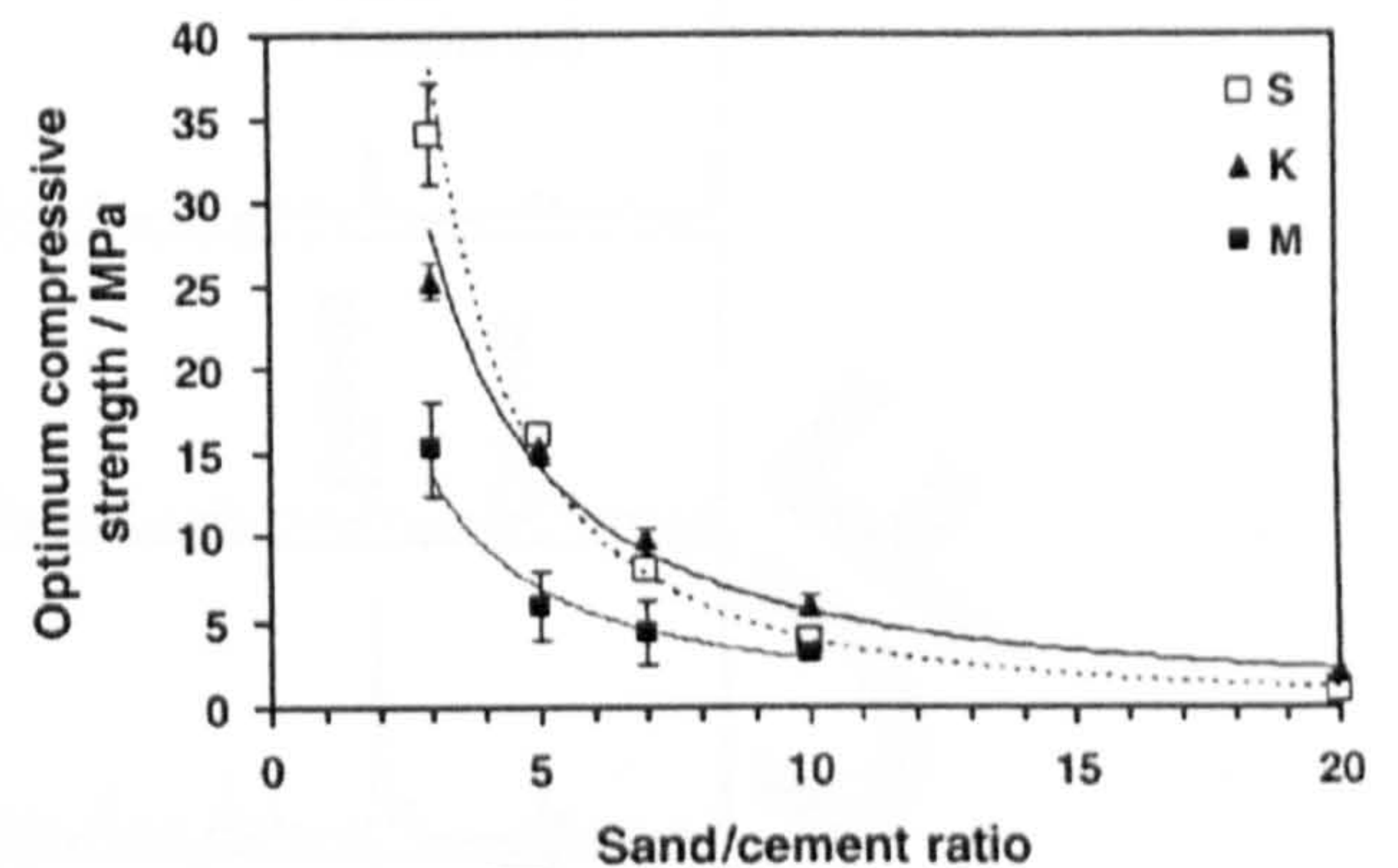


Fig. 6. Optimum compressive strength vs. sand/cement ratio. Error bars = ± 1 standard deviation. Lines are power law fits to the data.

place. Figs. 8 and 9 show examples of the results obtained for the three mixes at 28 days and at 1 year.

4. Discussion

Addition of clays in concreting aggregates significantly reduces their workability. As both types of clays examined have large specific surface areas and great ability to absorb water, an increased amount of water was needed to ensure adequate workability of the mix. Montmorillonite has a higher specific surface area ($800 \text{ m}^2/\text{g}$), along with a chemical structure more suited to absorbing water than silica or kaolin, so montmorillonite-contaminated mixes require a higher w/c ratio for a given workability than do kaolin-contaminated or uncontaminated-sand mixes. Increasing s/c ratio has a similar effect (of reducing workability) as it increases the surface of aggregate to be water-coated relative to the amount of cement.

If the falling branches of the curves in Fig. 5 (i.e. those mixes with sub-optimal strength owing to insufficient workability and compaction) are excluded, the data for all the s/c ratios can be considered together.

There are a number of relationships that can be used to model the strength of concrete (Table 3). Such models either implicitly (in the case of Abram's law [23]) or explicitly (the others in Table 3) relate strength to porosity.

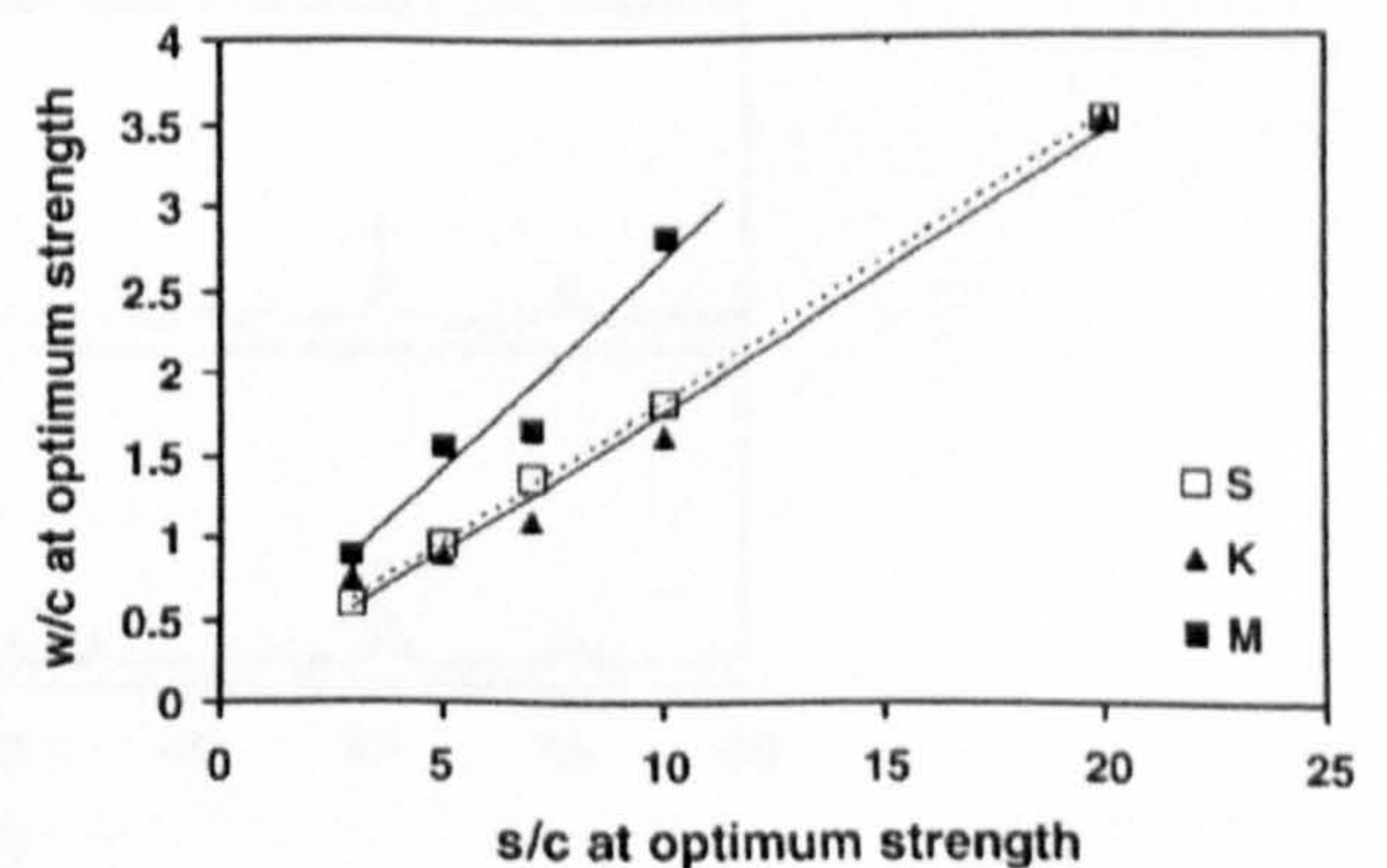


Fig. 7. w/c at optimum strength vs. s/c at optimum strength.

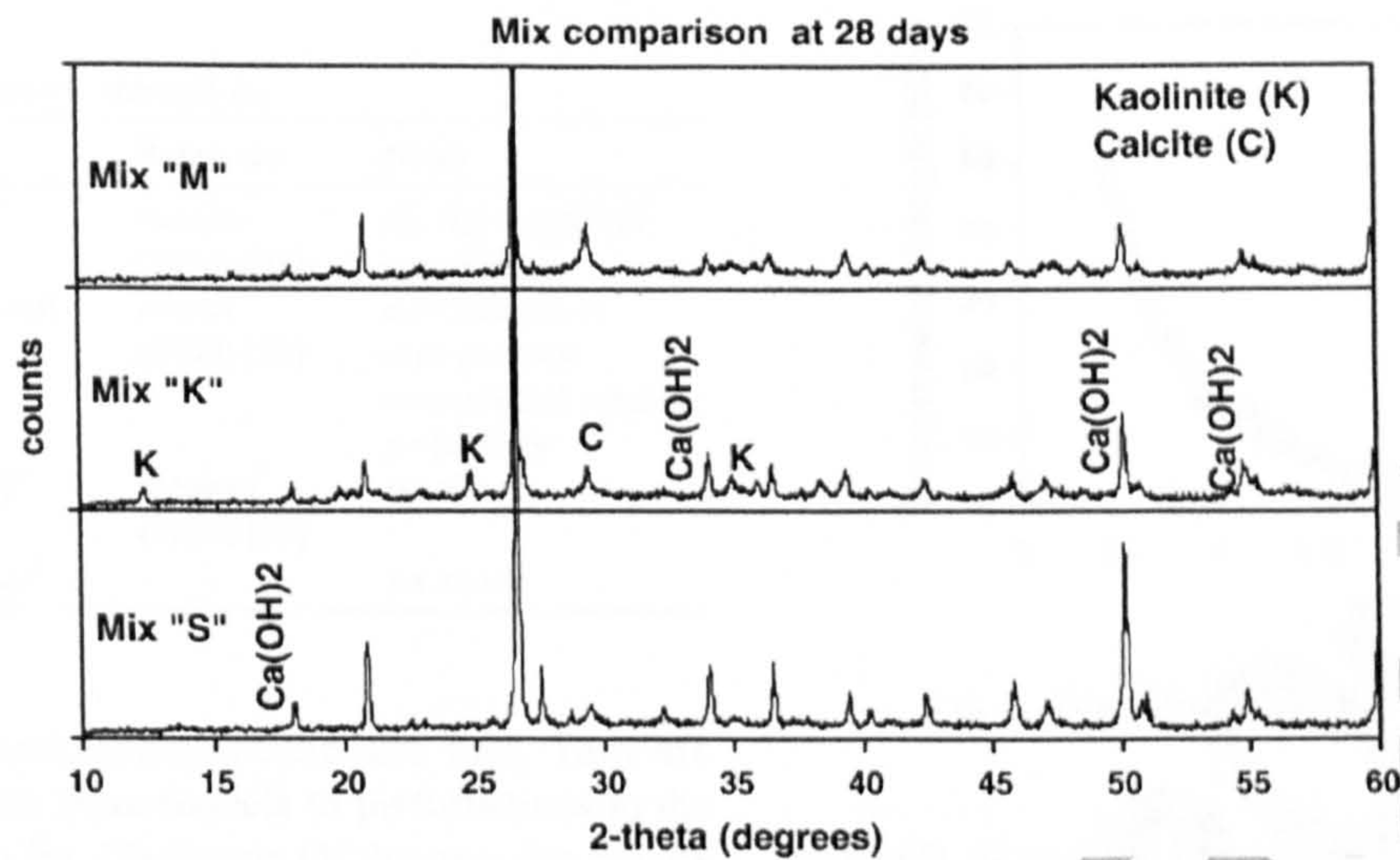


Fig. 8. XRD showing the comparisons between different the sand mixes at 28 days.

In this study, porosity was not measured; there is still considerable debate over the most appropriate methods to use to measure porosity in cementitious materials since mercury intrusion porosimetry has fallen out of favour (e.g. [24–26]). However, porosity in cement paste is closely related to w/c . According to the widely accepted Powers model [27], the relationship can be approximated to:

$$p = \frac{(v_w w_0/c + v_c) - m v_g (1 + w_n/c) - (1 - m) v_c}{(v_w w_0/c + v_c)} \quad (1)$$

where:

v_w = specific volume of water = 1 L/kg

w_0/c = w/c (free water/cement ratio)

v_c = specific volume of unhydrated cement = 0.315 L/kg

m = degree of hydration

v_g = specific volume of gel including pores = 0.567 L/kg

w_n/c = constant = 0.23; w_n is the weight of the combined water, c is the weight of the cement with which it combines

Using an appropriate value for degree of hydration at 28 days (80%) and treating the clay as aggregate, this simplifies to:

$$p = (w/c - 0.325)/(w/c + 0.315) \quad (2)$$

(We are aware of the limitations of this relationship but consider that it is of sufficient accuracy for the purposes of comparing different models).

This was substituted for porosity in the relations in Table 3 and fitted to the strength– w/c data. (Note: since the strength of the concrete is overwhelmingly dominated by the strength of the paste, we need not consider the porosity of the aggregate). The results are given in Table 4.

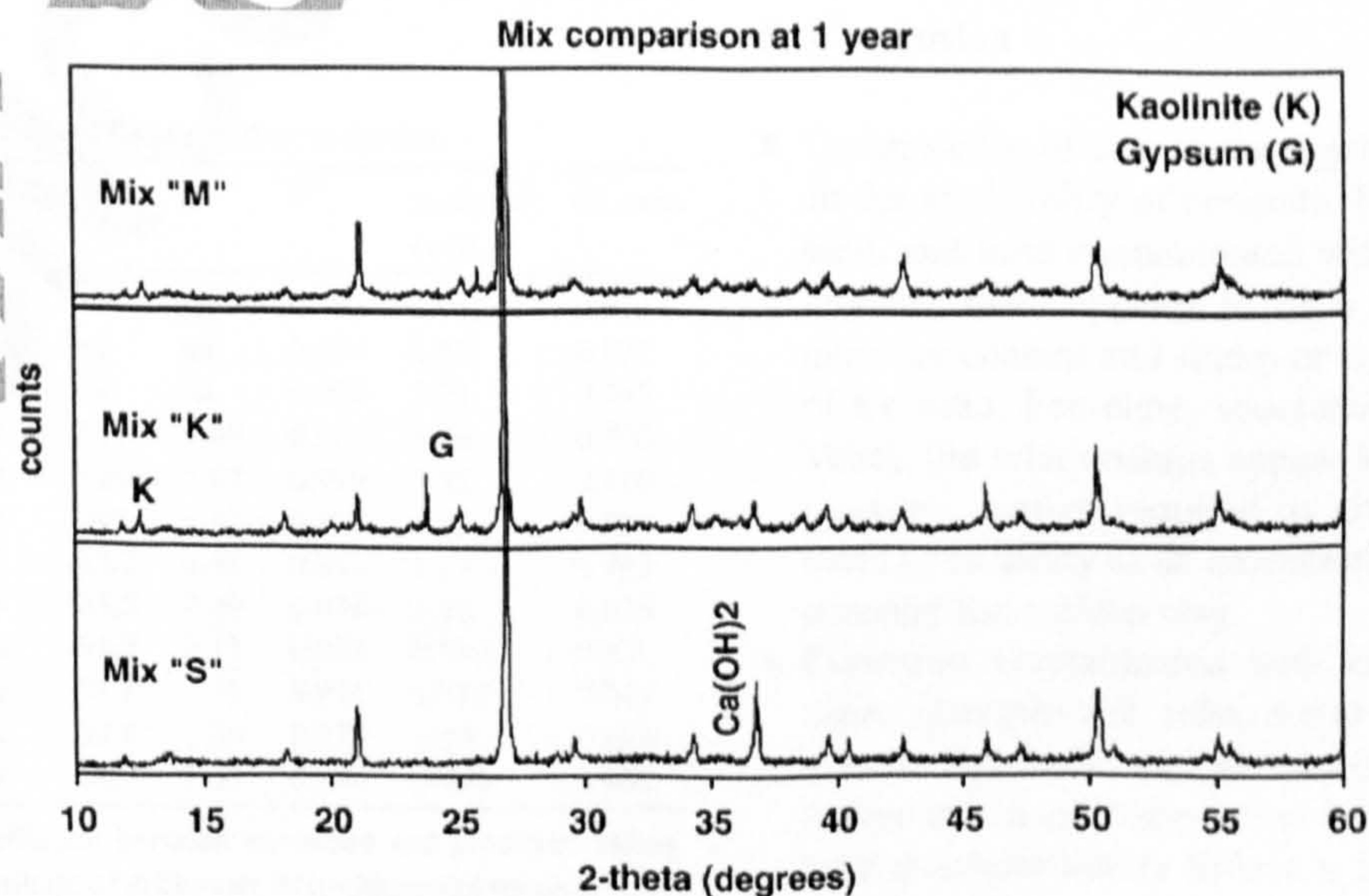


Fig. 9. XRD showing the comparisons between different the sand mixes at 1 year.

t3.1 Table 3

t3.2 Relationships for modelling concrete strength σ_c

t3.3	Author	Law	Reference	Notes
t3.4	Abrams	$\sigma_c = K_1 K_2^{w/c}$	Neville (1995) [23]	K_1, K_2 = empirical constants
t3.5	Ryshkewitch	$\sigma_c = \sigma_0 \exp(-np)$	Aldera (1969) [32]	σ_0 = strength at zero porosity; n = empirical constant; p = porosity
t3.6	Balshin	$\sigma_c = \sigma_0 (1 - p)^n$	Salmoni (1937) [33]	As above
t3.7	Square	$\sigma_c = \sigma_0 (1 - np)^2$	–	As above

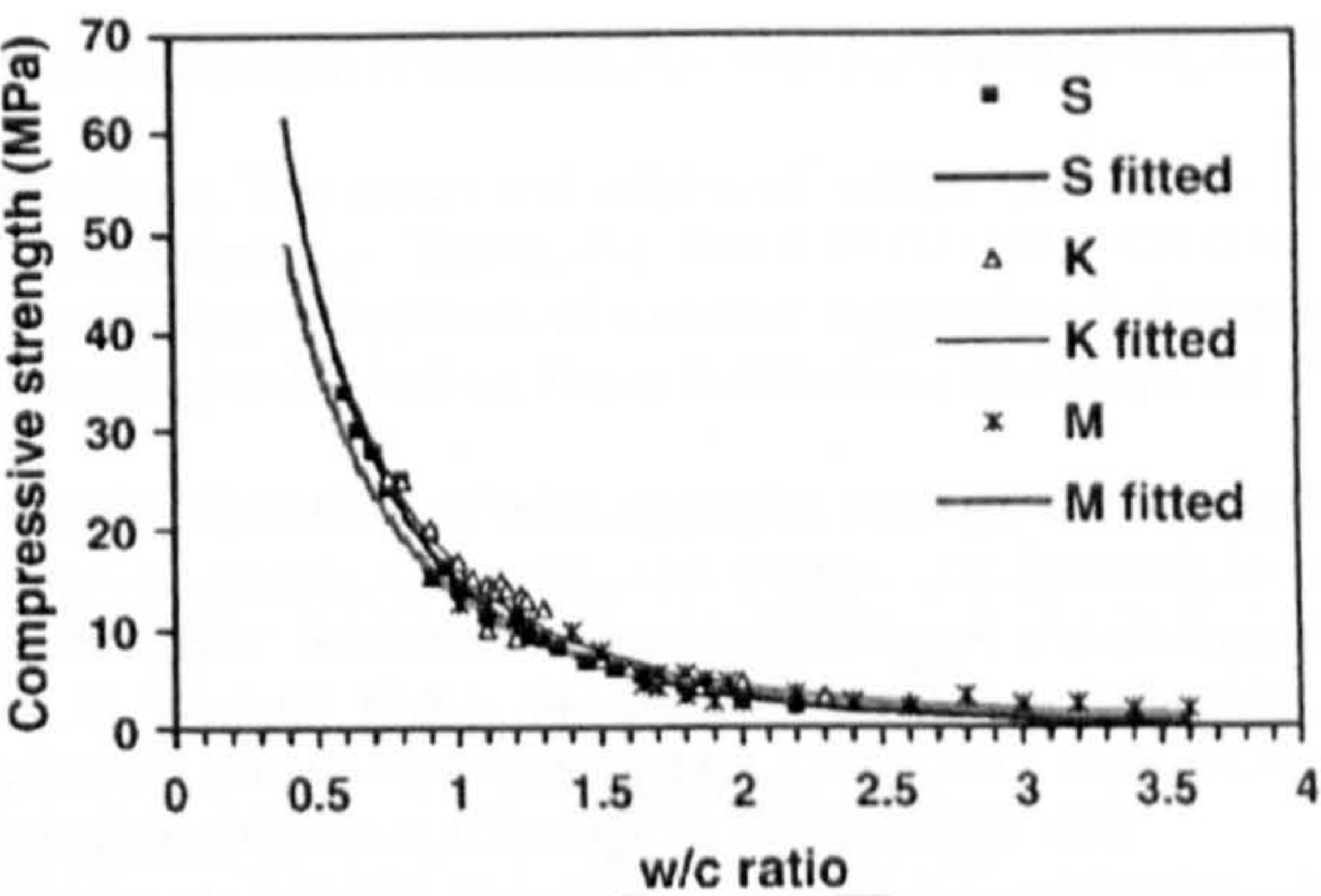


Fig. 10. Fits of Square model to compressive strength data.

372 The Balshin and Square models fit the data best. They are
373 also far less sensitive than other models to perturbations in the
374 numerical values used in Eq. (2) above. Of the two, the Square
375 model is preferred. A fit of the Square model to the three data
376 sets is given in Fig. 10. It can be seen that at $w/c < 0.8$, the S and
377 K fitted lines converge, while at $w/c > 1.6$, the K and M fitted
378 lines converge. Analysis of variance suggests that over the
379 range of w/c used in this study, the S and K data can be
380 represented by a single relationship while the M data is
381 different. This correlates with Figs. 6 and 7, where the K and S
382 data are almost coincident, while the M data follows a different
383 trend. Looking at the Square and Balshin model data in Table 4,
384 we can also see that the ‘baseline’ strength (i.e. the predicted
385 strength at zero porosity) of the S and K mortars is similar,
386 ~80 MPa, while that for the M mortar is lower, ~60 MPa. This
387 suggests that in K mortars, the clay is acting as ‘inert’ aggregate
388 and any effect of the kaolin on the strength of a concrete/mortar
389 mix is simply due to increased water demand and/or insufficient
390 compaction; whereas in a M mortar the effect of montmor-
391 illonite is more fundamental, actually causing a weaker
392 hydrated matrix to be formed during curing. Thus the effect
393 of clay contamination of aggregate on the properties of a
394 concrete are strongly dependent on the type of clay involved.
395 The XRD analysis (Figs. 8 and 9) shows results undertaken
396 on samples at 28 days and 1 year. The normal crystalline

products of cement hydration, i.e. portlandite, could be seen 397
in all mixes. There is no evidence of any pozzolanic reaction, 398
i.e. no depletion of either portlandite or clay mineral peaks, 399
nor formation of new crystalline compounds, between 400
28 days and 1 year of curing. This contradicts previous 401
work [28,29]. 402

These results suggest that the effect of clay contamination 403
on strength is more likely caused by physical mechanisms, 404
such as increased water demand for a given workability owing 405
to increased specific surface area, than chemical reactions. 406
However, there is still a possibility that non-crystalline 407
products have formed, which would not have shown on the 408
XRD traces. The question of how the montmorillonite affects 409
the hydrated assemblage in a different manner to kaolin 410
remains unresolved. 411

According to Montgomery and Orton [30,31] a compressive 412
strength of 3–7 MPa is common to building materials in LEDCs 413
and is referred to in building standards for masonry including 414
walls, columns and lintels. Therefore, satisfactory concretes can 415
be made from clay-contaminated aggregate, permitting these 416
building materials to be used and removing the necessity to 417
transport sand over long distances. 418

5. Conclusion 419

- The presence of clay in the aggregate has a significant effect 420
on the workability of concrete. For each sand type (i.e. pure 421
sand, and sand contaminated with either kaolin or montmor- 422
illonite), there appears to be a linear relationship between 423
moisture content and slump or log(vebe), that is independent 424
of s/c ratio. For either measurement method (i.e. slump or 425
vebe), the relationships appear to be parallel; thus the extra 426
moisture content required to give a contaminated mix the 427
same workability as an uncontaminated mix is approximately 428
constant for a given clay. 429
- Concretes contaminated with kaolin appear to follow the 430
same strength– w/c relationship as normal concrete, with 431
lower strengths simply attributed to increased water demand 432
and/or increased compaction difficulty. Those contaminated 433
with montmorillonite follow a different relationship, imply- 434
ing that it has an effect on the fundamental strength of the 435
hydrated phases. 436

t4.1 Table 4

t4.2 Fit parameters and analysis of fit quality for different models

t4.3	Model and sand	K_1	K_2	σ_0	n	r^2	Residual error	Fit ratio
t4.4	Abrams: S	109	7.13	na	na	0.992	0.913	0.913
t4.5	Abrams: K	80.5	4.88	na	na	0.934	1.57	0.871
t4.6	Abrams: M	47.6	3.57	na	na	0.936	1.01	0.745
t4.7	Ryshkewitch: S	na	na	151	4.69	0.966	1.94	0.760
t4.8	Ryshkewitch: K	na	na	202	5.02	0.914	1.82	0.790
t4.9	Ryshkewitch: M	na	na	247	5.67	0.914	1.15	0.781
t4.10	Balshin: S	na	na	85.2	2.46	0.988	1.13	0.902
t4.11	Balshin: K	na	na	83.5	2.29	0.935	1.56	0.876
t4.12	Balshin: M	na	na	64.5	2.17	0.938	0.962	0.811
t4.13	Square: S	na	na	78.9	1.11	0.991	0.989	0.943
t4.14	Square: K	na	na	77.8	1.06	0.936	1.54	0.886
t4.15	Square: M	na	na	60.7	1.03	0.938	0.960	0.805

r^2 = Pearson’s correlation coefficient between measured and predicted values.
Residual error = average magnitude of difference between model prediction and
measured value at a given point. Fit ratio = r.m.s. of ratio between predicted and
measured value (1 = perfect fit).

- At high w/c ratios, i.e. ≥ 1.7 , montmorillonite-contaminated mixes perform as well as the other materials with respect to strength.
- XRD investigations show no indication of any unusual secondary cementitious material forming in the presence of clay.
- Over the range of w/c and strengths common to building materials in LEDCs, satisfactory concrete components not requiring coarse aggregate, such as mortar and blocks, can be made from clay-contaminated sand but the effect of the clay type is significant. Structural concrete made with such materials would need to be investigated with regard to durability, particularly dimensional stability, which is the subject of current research by this group to be reported later.
- It is not necessary to transport 'quality' sand from long distances because local sands can usually perform as an adequate building material. Concrete blocks of sufficient integrity for low-cost housing may be made from lean mixes of cement with such sands by artisanal builders.

Acknowledgements

This paper is dedicated to the memory of PhD student Vicky Fernandes, who sadly passed away during the review stages of this article based on her work. A poster pre-cursor version of this work also won the Best Student Poster at the 25th Cement and Concrete Science Conference, Royal Holloway College, UK in September 2005.

References

- [1] S. Erguden, Low-cost Housing: Policies and Constraints in Developing Countries International Conference on Spatial Information for Sustainable Development, Housing Policy Section, Nairobi, Kenya, UNCH, 2001, 11 pp.
- [2] UNHCS, Global Report on Human Settlements, United Nations Centre for Human Settlements, Oxford University Press, 2004, 310 pp.
- [3] A. Ashworth, Cost Studies of Buildings, 2nd Edition, Longman Scientific and Technical, 1994, 330 pp.
- [4] A.I.G. Yool, T.P. Lees, A. Fried, Improvements to the Methylene blue test for harmful clay in aggregates for concrete and mortar, *Cem. Concr. Res.* 28 (10) (1998) 1417–1428.
- [5] K. Gullered, S. Cramer, Effect of Aggregate Coatings and Films on Concrete Performance, Wisconsin Highway Research Program #0092–00–07, 2002, p. 1.
- [6] T.N.W. Akroyd, Concrete: Properties and Manufacture, 1st Edition, Pergamon Press, Oxford; New York, 1962, 336 pp.
- [7] A.M. Neville, J.J. Brooks, Concrete Technology, 1st Edition, Longman Group Ltd, 1987, 438 pp.
- [8] D.E. Montgomery, Physical characteristics of soils that encourage SSB breakdown during moisture attack, University of Warwick working paper SSPR03, (Nov 1998), 29 pp.
- [9] A. Herzog, J.K. Mitchell, X-ray evidence for cement–clay interaction, *Nature* 4845 (195) (1962) 989–990.
- [10] D.A. Parsons, Strength of Concrete, Res. Natn Bur Standard, vol. 10, 1933, p. 257.
- [11] A.T. Goldbeck, The nature and effects of surface coatings on coarse aggregates, proceedings, Highw. Res. Board 12 (1) (1932) 305–319.
- [12] L. Dolar-Mantuani, Handbook of Concrete Aggregates: A Petrographic and Technological Evaluation, Noyes Publications, Park ridge, NJ, 1983, 345 pp.
- [13] J.W. Schmitt, The effects of mica, aggregate coatings, and water-soluble impurities on concrete, *Concr. Int., Des. Constr.* 12 (12) (1990) 54–58.
- [14] S.W. Forster, S.W. Soundness, deleterious substances and coatings, in: P. Kiegler, J. Lamond (Eds.), Significance of Tests and Properties of Concrete and Concrete-Making Materials, ASTM 169C, American Society for Testing and Materials, Philadelphia, 1994, pp. 415–426.
- [15] J.K. Herzog, A. Mitchell, Reactions accompanying stabilization of clay with cement, Committee on Soil-Portland Cement Stabilization, 1963, p. 144.
- [16] S. Bhattacharja, et al., Stabilization of Clay Soils by Portland Cement or Lime—A Critical Review, Portland Cement Association, PCA R&D Serial No. 2066, 2003, p. 3.
- [17] M.S. Morsy, El-Enein Abo, G.B. Hanna, Microstructure and hydration characteristics of artificial pozzolana-cement pastes containing burnt kaolinite clay, *Cem. Concr. Res.* 27 (9) (1997) 1307–1312.
- [18] S. Bhattacharja, J.I. Bhatta, H.A. Todres, Stabilization of Clay Soils by Portland Cement or Lime — A critical Review of Literature, Portland Cement Association, PCA R&D, Serial no. 2066, 2003.
- [19] J.L. Eades, R.E. Grim, Reaction of hydrated lime with pure clay minerals in soil stabilization, *HRB Bull.* 262 (1960) 51–63.
- [20] D.E. Montgomery, Dynamically-compacted cement stabilized soil blocks for low-cost walling, 2002, PhD Thesis, 280 pp.
- [21] D. Gooding, T. Thomas, The potential of cement-stabilized building blocks as an urban building material in Developing Countries, ODA Report, University of Warwick, UK, 1995, 22 pp.
- [22] PDF 2, The powder diffraction file, International Centre for Diffraction Data, 2005–2006.
- [23] A.M. Neville, Properties of Concrete, 4th Edition, Longman Group Ltd, 1995, 844 pp.
- [24] H.S. Wong, N.R. Buenfeld, Patch microstructure in cement-based materials: fact or artefact? *Cem. Concr. Res.* 36 (5) (2006) 990–997.
- [25] S. Diamond, A Discussion of Paper "Patch Microstructure in Cement-Based Materials: Fact or Artefact?", in: H.S. Wong, N.R. Buenfeld (Eds.), *Cem. Concr. Res.*, vol. 36 (5), 2006, pp. 998–1001.
- [26] H.S. Wong, N.R. Buenfeld, Reply to the discussion by Sidney Diamond of the paper "Patch microstructure in cement-based materials: fact or artefact?", *Cem. Concr. Res.* 36 (5) (2006) 1002–1003.
- [27] J.M. Illston, J.M. Dinwoodie, A.A. Smith, Concrete, Timber and Metals, Van Nostrand Reinhold Co. Ltd, 1979, 663 pp.
- [28] T.W. Lambe, A.S. Michaels, Z.C. Moh, Highw. Res. Board Bull. 241 (1960) (as cited in [9]).
- [29] A. Herzog, J.K. Mitchell, X-ray evidence for cement–clay interaction, *Nature* (1962) 989–990 (Sept).
- [30] D.E. Montgomery, Minimising the cement requirement of stabilized soil block walling, Stabilized Soil Research Progress Report SSRPR8, Development Technology Unit, School of Engineering, University of Warwick, 2001, p. 14.
- [31] A. Orton, Structural Design of Masonry, 2nd Edition, Longman, London, 1992, 159 pp.
- [32] R. Salmoni, Verfahren zur Verurzung der Abb indezeit von Tonerdeze-menten, Deutsches Patent 648851, 1937.
- [33] A. Aldera, Fluidized Molding Material for Manufacturing Cores and Molds and a Method Therefore, U.S. Patent 3,600.203, 1969.

Mix proportioning of mortars in tension, with particular reference to developing countries

G. T. Still* and T. H. Thomas

Production of cement based rainwater harvesting tanks in developing countries differs from the situation in industrialised nations, with low aggregate quality, negligible labour costs relative to material cost and use of unreinforced mortar in tension. The present paper details an experimental programme undertaken on mortars made with representative materials to determine their tensile performance. It appears that in lean mortars a synthesised sand, containing 20 wt-% kaolin clay (representative of local sands, often used in construction in Africa) gives higher strengths than clay free (standard) sand, while the same level of montmorillonite lowers the strength for rich or lean mortars. Economic modelling indicates that, for *bending* loading (maximum stress inversely proportional to thickness squared), using kaolin contaminated sand is preferable to using standard sand. However, the montmorillonite contaminated sand must cost around 2/3 less than the imported sand to become competitive. For *membrane* loading (maximum stress inversely proportional to thickness), kaolin contaminated sand is preferable only when it is considerably cheaper than standard sand, and montmorillonite contaminated sand is never preferable in practical situations.

Keywords: Aggregate, Clay, Cement, Developing countries, Sand

Introduction

Production scenario

Domestic rainwater harvesting in developing countries provides an affordable, autonomous supply of high quality water in many instances.¹ As water storage tanks constitute the component of greatest cost in a system,¹ there is significant interest in reducing this cost. Production takes place by hand application of the chosen material, often cement based. In the present article, 'concrete' refers to a composite of cement, coarse aggregate, fine aggregate, water and optional admixtures, while 'mortar' refers to cement, fine aggregate, water and optional admixtures. Concrete tanks, with greater cost of coarse aggregate and thicker sections required in production, generally prove too costly. However, tanks using a cement based mortar, allowing the use of thin sections, low cost materials and simple manufacturing technologies, provide an affordable solution. At the household level, tanks with capacities between 1500 L and 6 m³ are popular, typically up to 2 m tall with wall thicknesses of 1~4 cm.¹ Figure 1 shows a typical 1500 L capacity water jar.

Reinforcement in such tanks often has significant cost and suffers from corrosion, leading to the use of unreinforced mortar, with significantly lower strength in tension than compression. Hydrostatic loading, combined

with the design of tanks, leads to tensile and compressive stresses of similar magnitude, therefore, tensile failure forms the limiting design criteria. Tanks either have a leak seal admixture used with the mortar, or a cement slurry applied after manufacture, therefore, porosity is not a design concern. Those producing tanks have a choice between using locally available aggregates, often with a high fines content² and importing higher quality sands, with associated transport expense. Plasticiser and cement generally cost more relative to aggregates than they do in industrialised countries, while labour has such a low cost relative to materials that its contribution to overall cost may be neglected. All these factors contribute to a distinctive situation, characterised by:

- (i) choice between cheap, 'poor quality' (high fines content) locally available sand, or more expensive imported 'high quality' sand
- (ii) use of unreinforced mortar in situations where tensile failure from bending or membrane action dominates
- (iii) relative costs significantly different from those in industrialised countries, with negligible labour cost component.

Concrete theory

Strength, water/cement ratio and Abram's law

The presence of voids in concrete, as with any other ceramic, acts to weaken it. The volume ratio of hydrated products of reaction to the space available for such products (gel/space ratio) accurately predicts strength once calibrated for a given cement, and takes into

Development Technology Unit, School of Engineering, University of Warwick, CV4 7AL, UK

*Corresponding author, email g.t.still@warwick.ac.uk



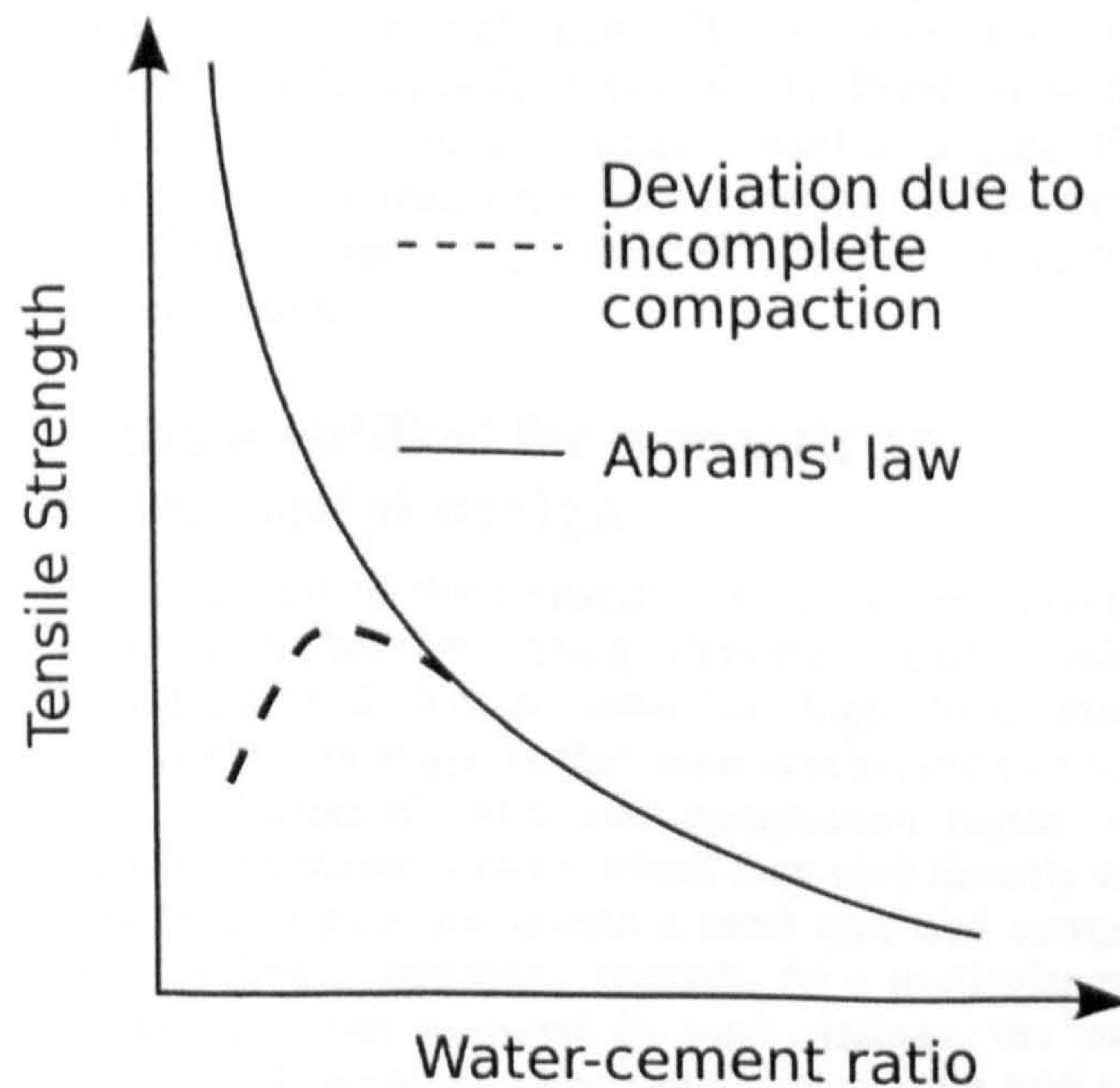
1 1500 L water storage jar, 10 mm wall thickness, during transport to site in Uganda

account the presence of air voids, excess water and the degree of hydration.³ However, it is difficult to measure this ratio, therefore, other relationships are often used.

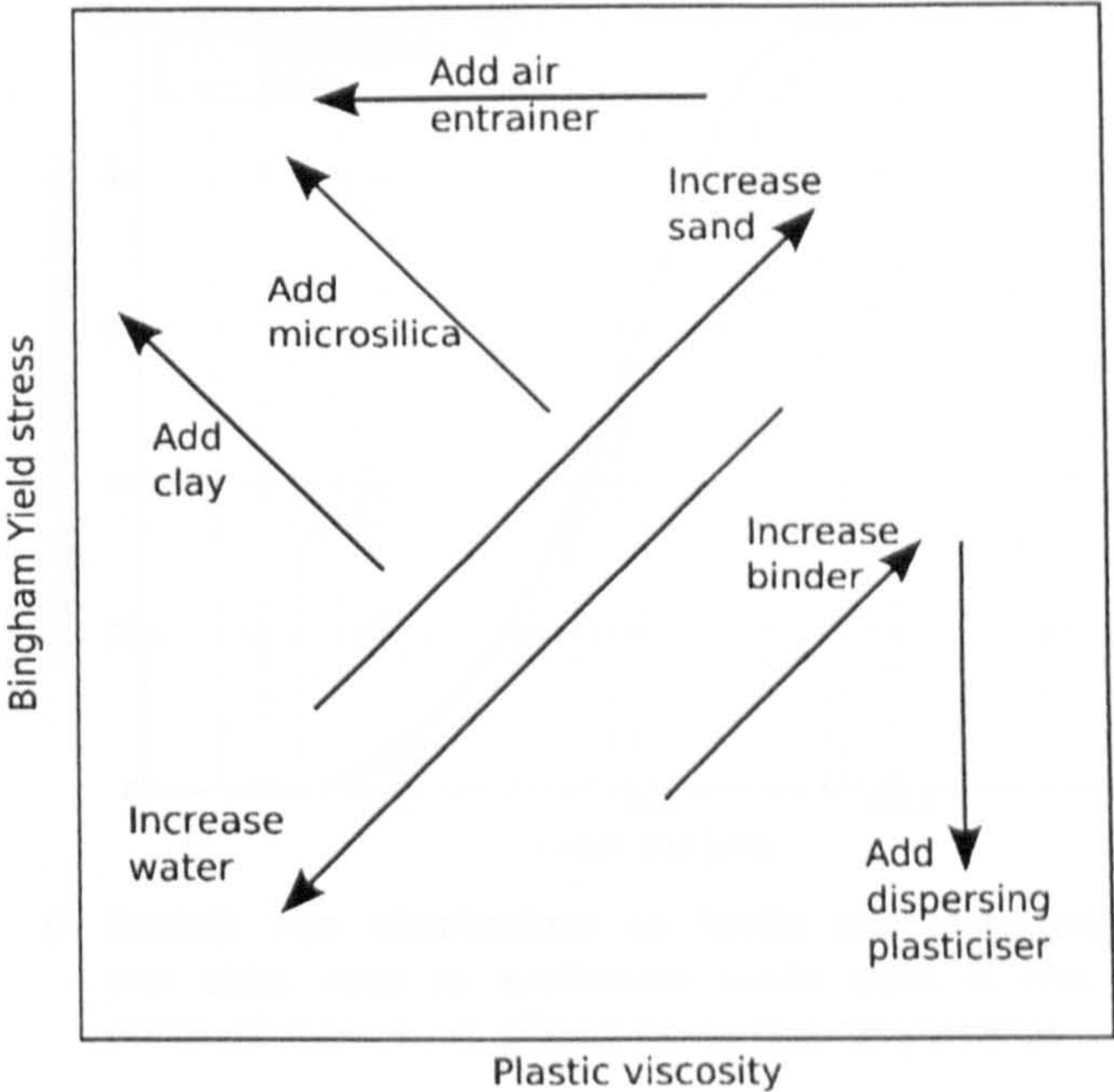
Abram's law⁴ states that water/cement ratio w/c dominates strength f , developed by concretes, as shown in equation (1)

$$f = A/B^{w/c} \tag{1}$$

where A and B are constants. Abram's law requires a number of conditions to hold, including comparable compaction;⁵ mixes normally have water contents in excess of that required for hydration, to ensure adequate workability. If the water/cement ratio is too low to allow for full compaction, air voids will be present, which have a deleterious effect on strength, causing it to fall below that predicted by Abram's law. Each mix and compaction method should give increasing strength with falling water content, as predicted by Abram's law, until strength loss from low workability outweighs the strength benefits of reducing water content and the strength falls as shown in Fig. 2. A given sand type and



2 Typical variation in strength with water content for mortar, showing Abram's law behaviour and loss in strength from incomplete compaction



3 Effect of modifications to mix on its Bingham properties, from Banfill⁶

sand/cement ratio mix should therefore have an optimum water/cement ratio that leads to peak strength for the method of compaction used.

Sand types and workability

The rheology of cementitious materials is complex, as they behave as non-Newtonian fluids. The simplest model to capture their behaviour is that of a Bingham fluid, which has a finite yield shear stress, below which no plastic deformation occurs (i.e. only recoverable elastic deformation takes place), and above which shear strain rate varies linearly with shear stress, with a constant coefficient of plastic viscosity, as shown in equation (2)

$$\dot{\gamma} = \begin{cases} 0 & \tau \leq \tau_0 \\ (\tau - \tau_0)/\mu & \tau > \tau_0 \end{cases} \tag{2}$$

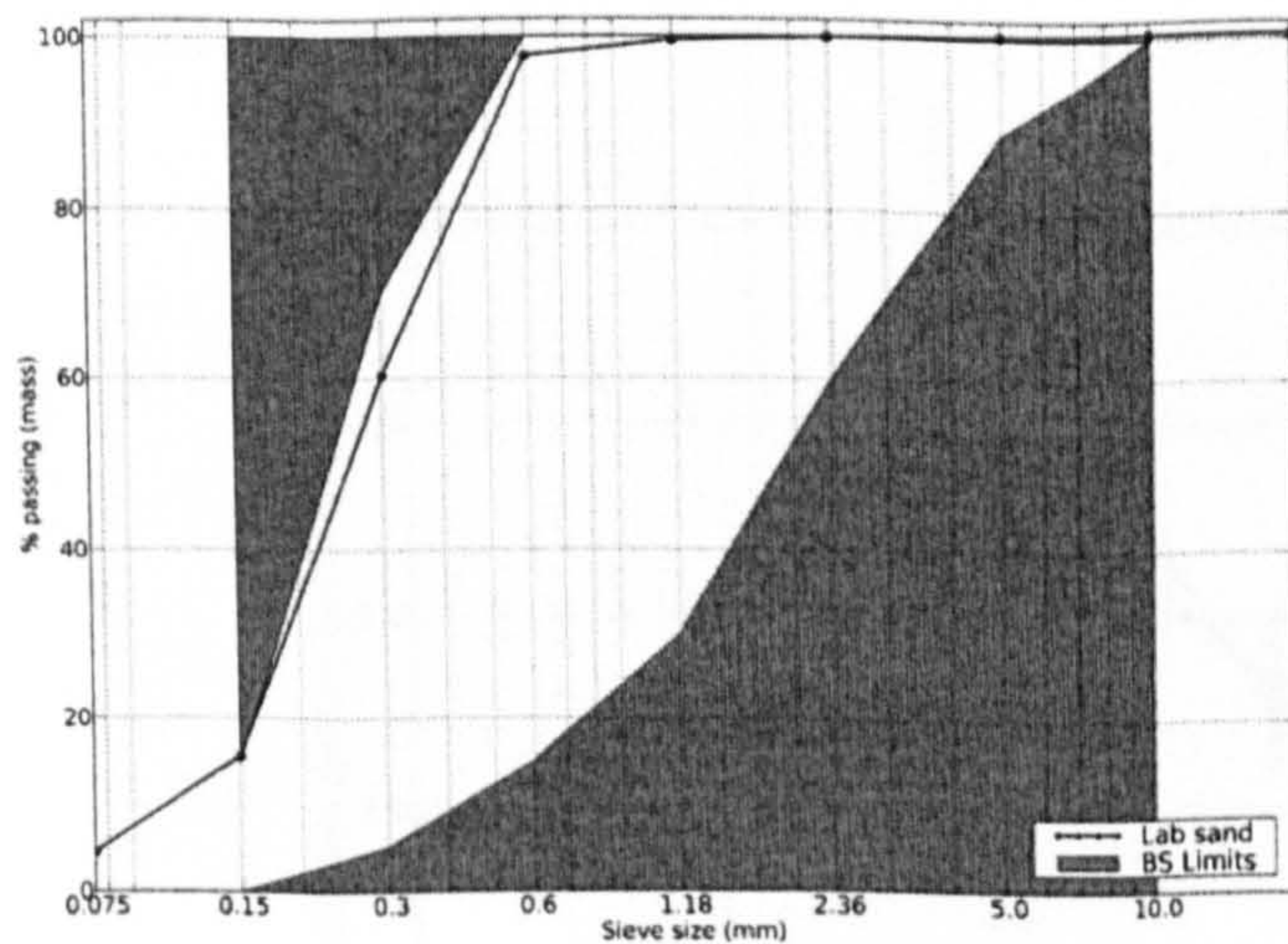
where $\dot{\gamma}$ represents shear strain rate, μ is plastic viscosity, τ is shear stress and τ_0 is Bingham yield shear stress.

Figure 3 shows the general effects of changing mix properties, adding admixtures to the concrete, etc.

The increase aggregate fineness raises both plastic viscosity and Bingham yield stress, as expected: a larger aggregate surface requires more water to coat and lubricate it. This would lead to a higher optimum water/cement ratio and therefore lower peak strength. However, as shown in Fig. 3, increasing clay content raises Bingham yield stress but can lower Bingham plastic viscosity, raising the issue of whether increased clay content could have a neutral or beneficial effect on workability. Banfill⁶ states that yield stress dominates workability, which suggests that the presence of clay should reduce workability.

Different clays have different structures: the two considered in the present paper (kaolin and montmorillonite) both have the ability to adsorb water on their surface, but montmorillonite can also absorb water within its platelike structure.⁷

The relationship between peak strength and sand/cement ratio will play a role in determining the most economical sand/cement ratio to withstand the load



4 Grading of sand type S used

imposed by the water stored within a tank. Thanh⁸ suggests that the water demand of a mix for a given workability varies linearly with mass of cement and sand

$$m_w = m_c k_c + m_s k_s$$

where m represents mass, k represents a constant and the subscripts w , c and s refer to water, cement and sand respectively. This implies that water/cement ratio should vary linearly with sand/cement ratio as shown in equation (3), and that at high sand/cement ratios, the optimum moisture content (mass ratio of water to solids) tends to a constant, which agrees with the suggestion of Lydon⁹ that moisture content should be used for proportioning lean mixes

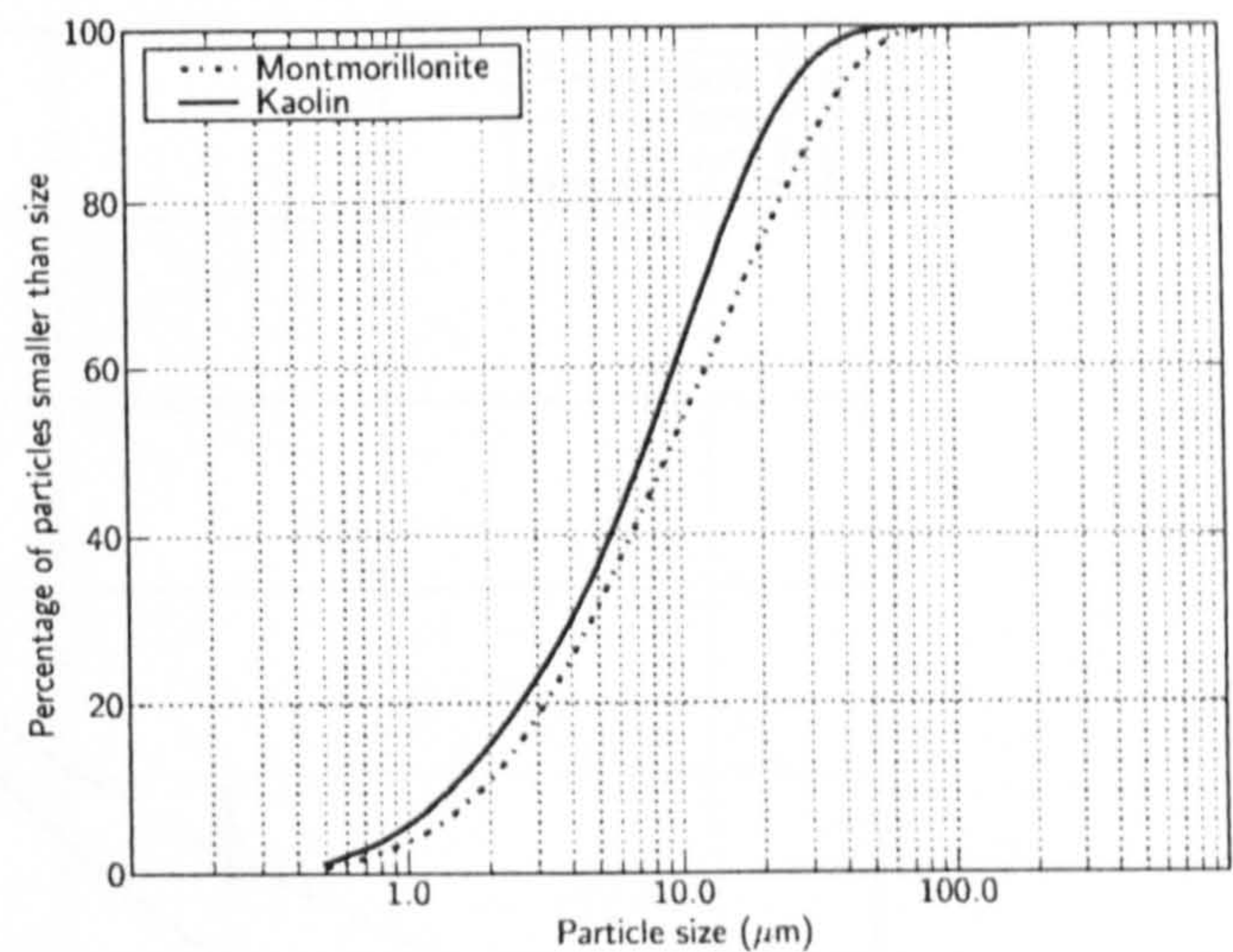
$$m_w/m_c = k_s(m_s/m_c) + k_c$$

$$\frac{m_w}{m_c + m_s} = \frac{m_c k_c + m_s k_s}{m_c + m_s} = \frac{m_c k_c + m_c R_{s/c} k_s}{m_c + R_{s/c} m_c} = \frac{k_c + R_{s/c} k_s}{1 + R_{s/c}} \rightarrow k_s \quad (3)$$

where $R_{s/c}$ represents sand/cement ratio by mass. m_s increases with fineness of aggregates, suggesting that sands with low particle size will have a greater water demand to achieve desired workability. Previous work¹⁰ and the lack of enforced quality control suggest that sands used for construction in developing countries may have higher fines content than those used in industrialised countries.

Areas identified for research and experimental design

The final aim of the research is to allow an economic comparison between using imported 'high quality' aggregates and locally available high fines sands. Existing theory suggests that each combination of sand type, sand/cement ratio and compaction regime will have a water/cement ratio, which may vary linearly with sand/cement ratio for constant sand type and compaction, leading to optimum strength. As a particular wall thickness is not required in tank designs, the most economical combination of sand/cement ratio and wall thickness should be chosen for a given sand type. Quantitative knowledge of the variation in strength with sand/cement ratio is required to do this. Therefore,



5 Particle size distributions of kaolin and montmorillonite clays used to synthesise sands types K and M, obtained from laser diffraction in isopropylalcohol

optimum tensile strengths of mortars over a range of sand/cement ratios are required, using low and high fines sands, produced with a representative compaction method. Experimental work to obtain such optima must involve varying water/cement ratio to ensure a turning point in strength.

To simulate materials from developing countries, the following laboratory materials were used:

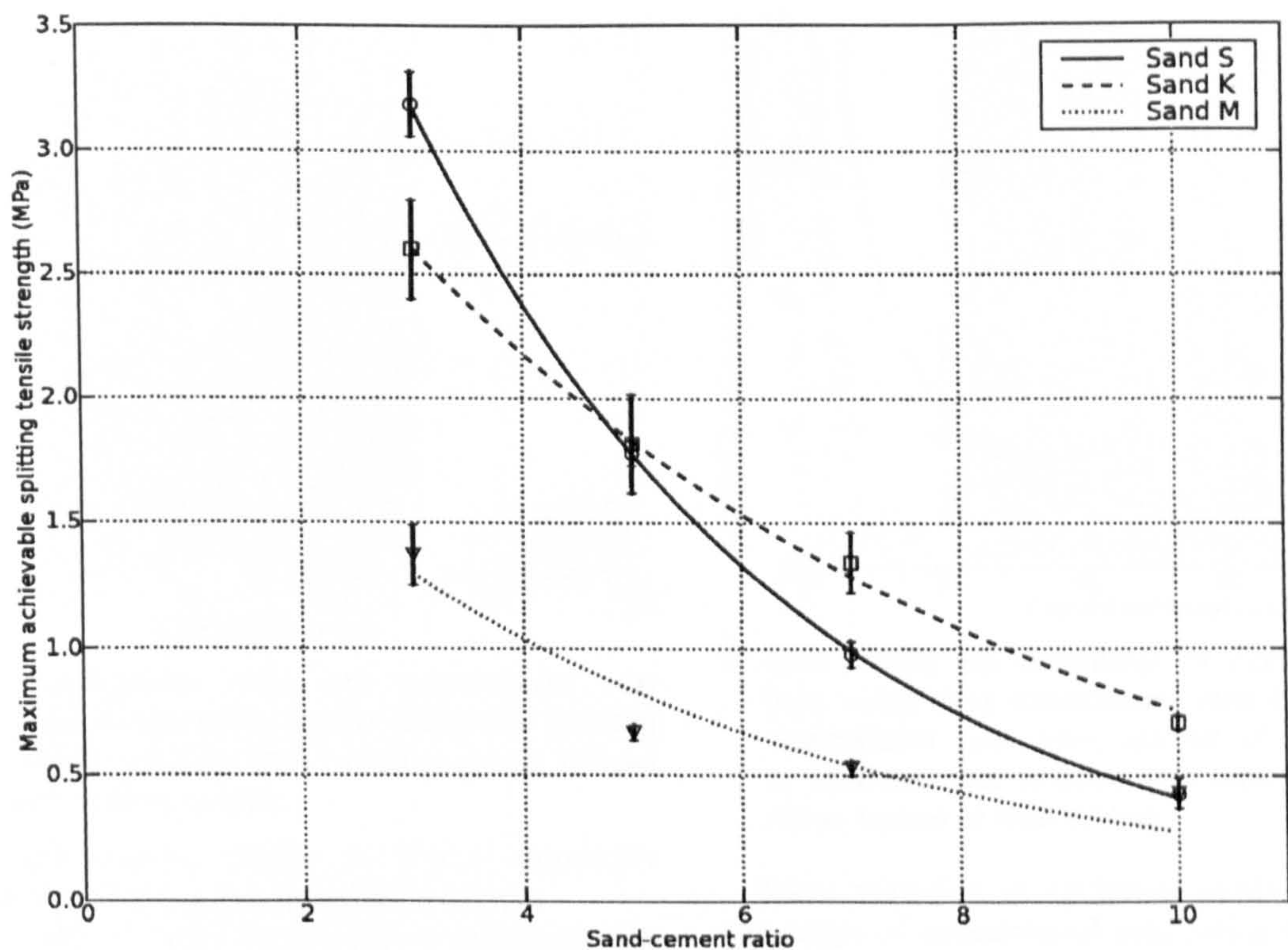
- sand only aggregate (sand type 'S'), considered representative of developing countries from previous research¹¹ and at the fine end of BS882
- kaolin sand aggregate (sand type 'K'), a mixture of 80 wt-% of sand type S and 20 wt-% of kaolin clay
- montmorillonite sand aggregate (sand type 'M'), a mixture of 80 wt-% of sand type S and 20 wt-% of montmorillonite clay
- type I OPC
- potable water.

Figures 4 and 5 show the grading of sand type S and the particle size distributions of the two clays used.

As previous research showed that curing conditions have a significant effect on strength developed,¹² the curing method was chosen to be representative of that in developing countries.

Experimental method

Sand was premixed dry with the clay (where used) to form sand type S, K or M, and then remixed with water. A final mix was conducted after addition of the cement. Once the mix had become homogenous, slump and Vebe tests were conducted. The mortar was cast into greased steel moulds and compacted by vibration on a British standard table, and the samples were cured overnight beneath damp hessian. Following demoulding the next day, the samples were cured sealed in polyethylene bags at ambient temperature of $\sim 23^\circ\text{C}$ until testing at 28 days. Testing used a Denison 7231 3000 kN hydraulic servo controlled compression testing machine, according to British standard BS EN 12398-3-2002. Mixes used the three sand types described in section 5, with four sand/cement ratios: 3, 5, 7 and 10:1. Each test set consisted of six cubes (100 mm side length) and three cylinders (100 mm diameter and 200 mm length). For



6 Splitting tensile strengths at optimum water/cement ratios versus sand/cement ratio for three sand types, and fitted Abram type curves, with error bars of ±1 standard deviation

each sand type and sand/cement ratio, repeated mixes at varying water/cement ratios established the optimum water content that gave peak strength by an iterative process.

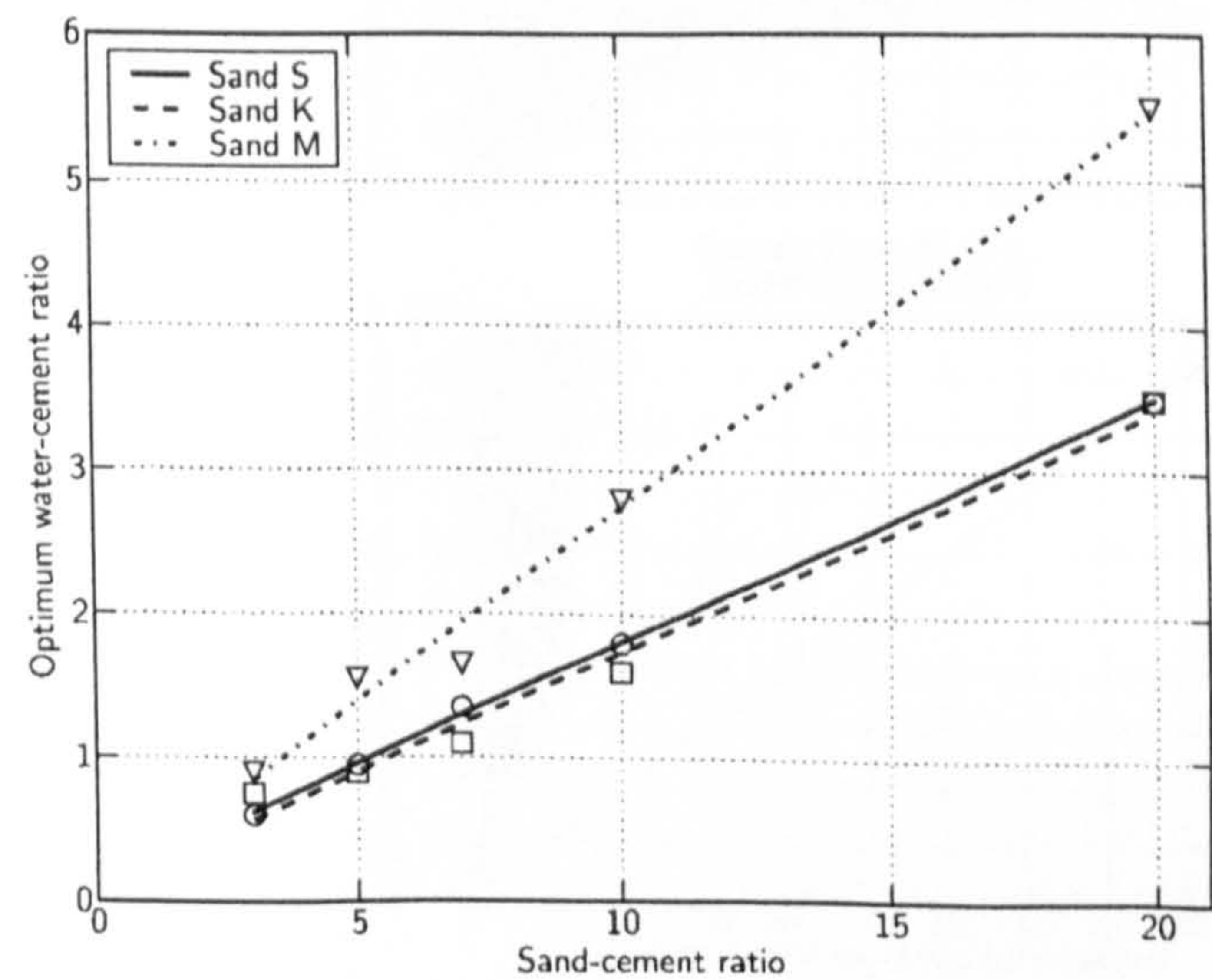
Results

Figure 6 shows optimum tensile strengths against sand/cement ratio, with fitted Abram type curves

$$f = K_1 / K_2^{s/c}$$

where K_1 and K_2 are constants.

The optimum water/cement ratios were found to vary linearly with sand/cement ratio for each of the sand types as shown in Fig. 7.



7 Relationship between optimum water/cement ratio and sand/cement ratio for mortars made with three sand types

Analysis and discussion

Strength, water/cement ratio and sand/cement ratio

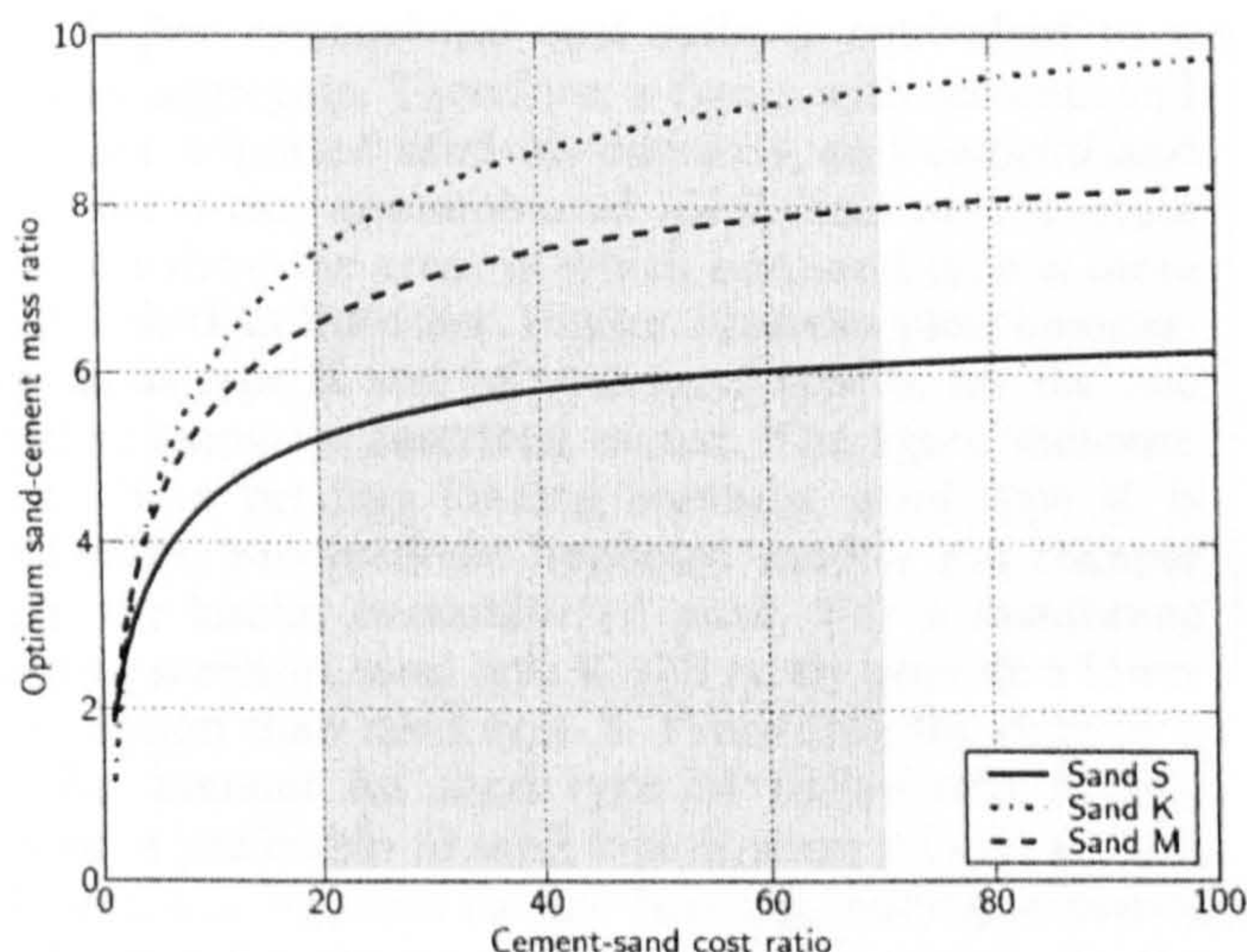
Figure 6 shows that for *rich* (low sand/cement ratio) mixes, standard sand type S performs considerably better than sand type K, which in turn develops substantially higher strengths than sand type M. At *lean* (high sand/cement ratio) mixes, the order changes, with sand type K the strongest, followed by sand type S and then sand type M. In all cases the low workability of the mixes led to the use of higher than conventional water/cement ratios (often in excess of 1), which explains the relatively low tensile strengths shown above. This low workability and high water demand can be explained by the relatively fine grading of the standard sand type S.

The linear correlation between optimum water/cement ratio and sand/cement ratio (Fig. 7), and power law relationship between sand/cement ratio and splitting tensile strength, suggest both peak strength and the required water/cement ratio can be accurately determined to give peak strength for any given sand/cement ratio.

Economic comparison of sands

The results mentioned above indicate that for high sand/cement ratios the clay contaminated sands develop strengths similar to each other, but that at low sand/cement ratios the uncontaminated sand type S gives higher peak strengths. Of more interest for practical applications is an economic comparison between the performances of these materials, so that it can be ascertained in which situations using locally available (contaminated) sand will cost the user less. To this end a simple model was developed, assuming:

- optimum water/cement ratio varies linearly with sand/cement ratio

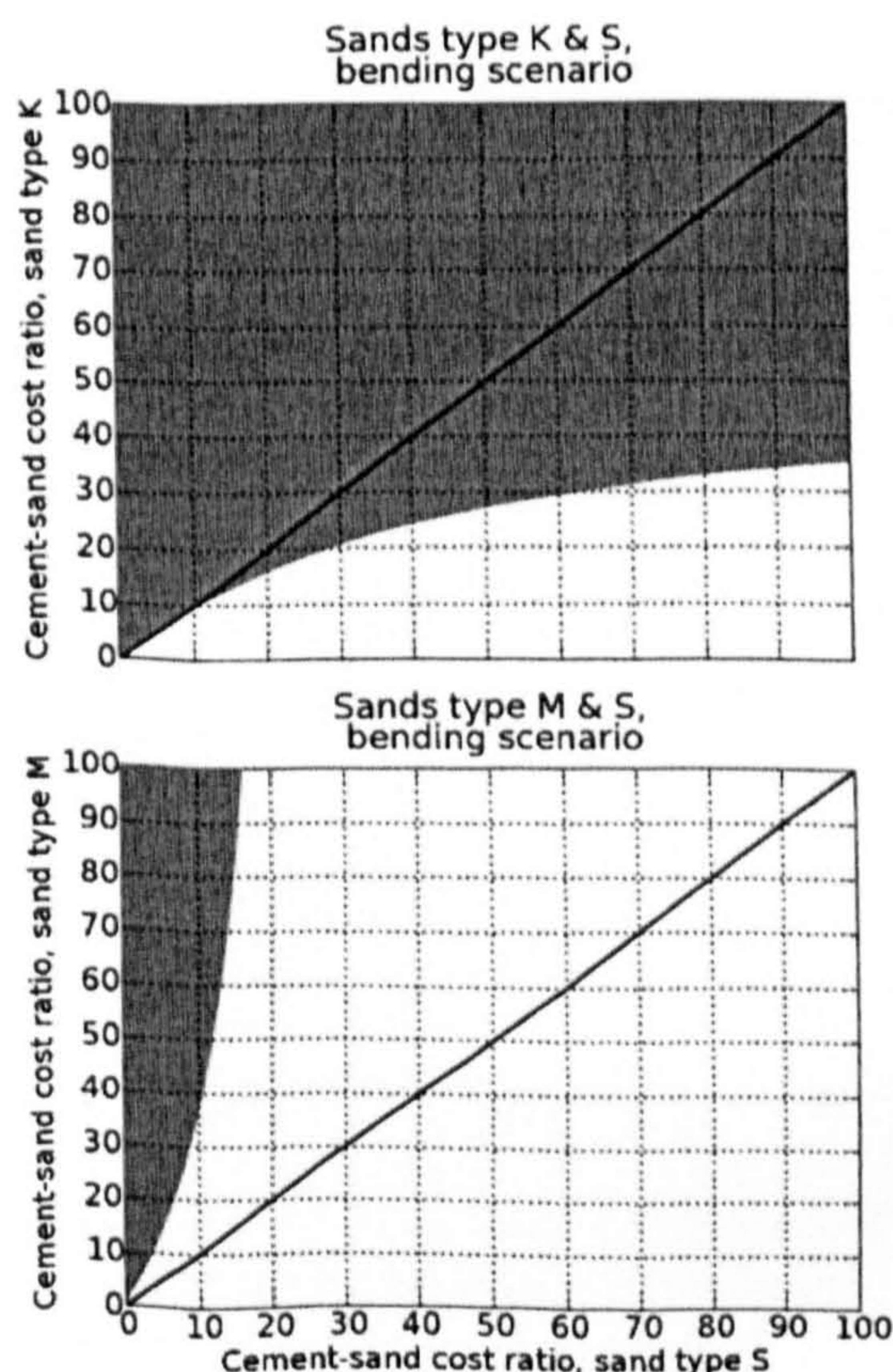


8 Optimum sand/cement ratio with cement/sand cost ratio for mixes designed for tensile failure and bending loading scenario (shaded area indicates range of cost ratios typical of East Africa)

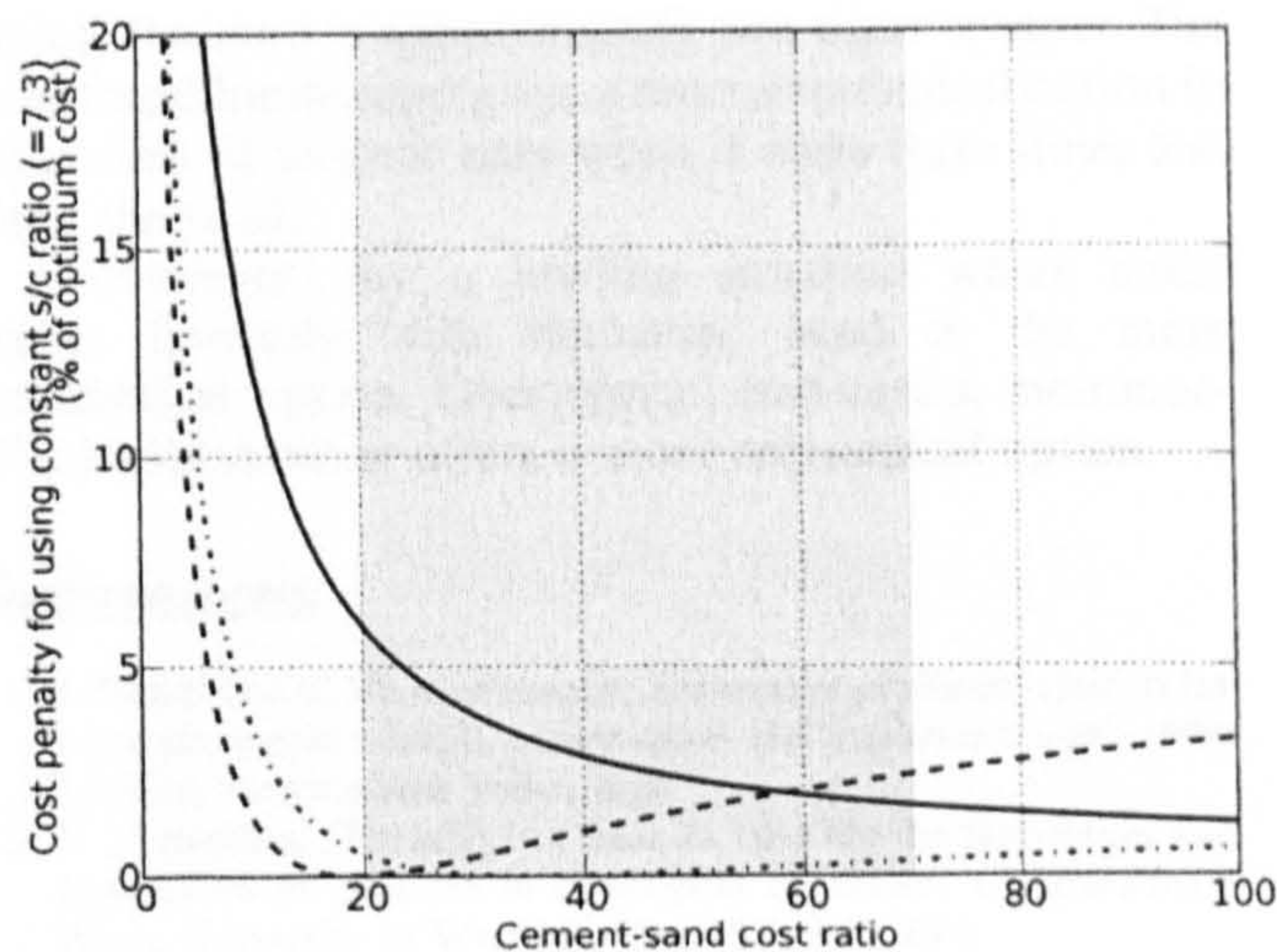
- (ii) the relationships shown in Fig. 6 accurately predict strength given sand/cement ratio
- (iii) the design of water tanks leads to tensile stresses forming the limiting design criteria, with maximum stress varying either inversely with the square of wall thickness: $J\alpha_{t_2}^{-1}$ (bending stress scenario) or inversely with wall thickness: $J\alpha_t^{-1}$ (membrane stress scenario).

Modelling proceeded by selecting a particular cement/sand cost ratio (by mass), then optimising sand/cement ratio and thickness to minimise cost, based on the assumptions above and constants obtained from the experimental work described above.

Figure 8 shows the variation in optimum sand/cement ratio with cement/sand cost ratio.



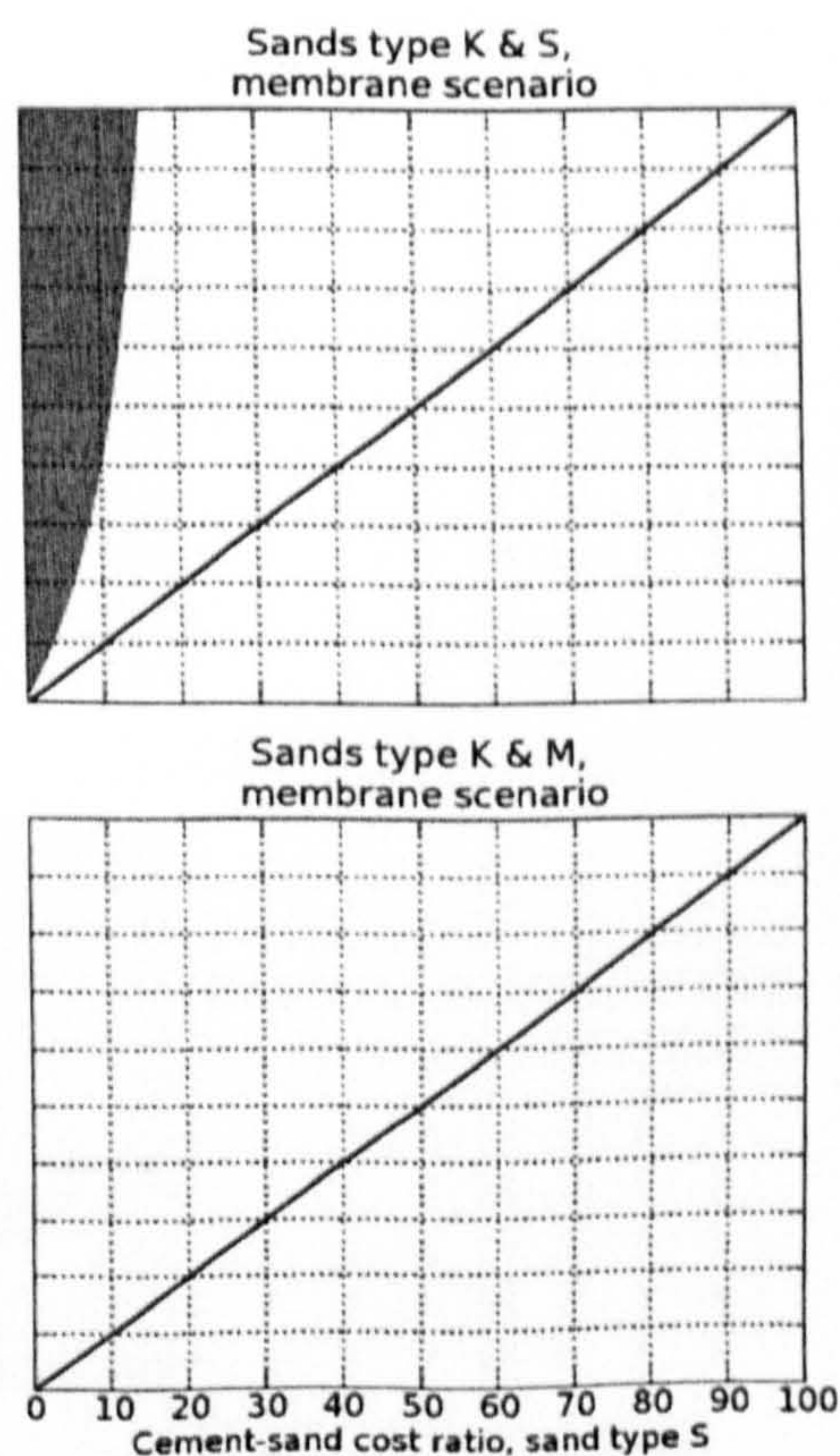
10 Cement/sand cost ratios at which sand types K (sand contaminated with 20 wt-% kaolin clay) or M (sand contaminated with 20 wt-% montmorillonite clay) is more economical than sand type S (imported uncontaminated sand) for bending loading, for wall thickness and sand/cement ratio jointly manipulated to minimise cost



9 Cost penalty (as percentage of optimum cost) arising from using fixed sand/cement ratio (7.3) irrespective of cement/sand cost ratio, instead of sand/cement ratio to minimise cost (shaded area indicates range of cost ratios typical of East Africa)

Some variation in optimum sand/cement ratio over the range of cement/sand cost ratios used (these ratios typically fall in the range of 20:1–70:1) can be seen. For practical use in the field it would be more helpful to have a rule of thumb recommending a constant sand/cement ratio. Averaging the optimum sand/cement mass ratio gave 5.8, 8.7 and 7.5 for sands S, K and M respectively, and an overall average of 7.3 over typical cement/sand cost ratios. Comparing the cost of a wall using this averaged sand/cement ratio at all sand/cement cost ratios with the cost of a wall using the optimum sand/cement ratio gives the results shown in Fig. 9.

Figure 9 shows that the constant sand/cement ratio approach incurs a negligible penalty for typical values.



A higher cement/sand cost ratio is equivalent to a cheaper aggregate. Therefore, a figure with cement/sand ratio for imported sand on one axis, and cement/sand ratio for a clay contaminated local sand on the other axis can show the areas in which one sand type is more economic than the other. Figure 10 shows plots comparing sands type K and M with sand type S, for the two loading scenarios described earlier. The figure indicates that, for a bending loading scenario, sand type K is preferable, provided the imported sand is not cheaper than the kaolin contaminated sand. For a membrane loading scenario, sand type K will rarely provide a lower cost option than sand type S. Processing the data in a similar manner for sand type M shows that it only becomes preferable to sand type S when it costs around 1/3 as much by mass for the bending loading scenario, and never for the membrane loading scenario. In the membrane loading scenario, increasing wall thickness gives a smaller stress reduction. This leads to lower optimum sand/cement ratios, therefore favouring the sand only aggregate.

Conclusions

1. The presence of kaolin or montmorillonite at 20 wt-% significantly reduces the peak strength obtainable in rich mixes.
2. At higher sand/cement ratios the two clays do not have a detrimental effect on peak strength, and the kaolin contaminated sand generally develops higher strengths.
3. Given an external load leading to bending stresses, kaolin sand gives a more economical option than sand,

unless the sand is approximately two times cheaper. The montmorillonite sand gives a more economical option in situations of interest only when it costs three times less than the sand.

4. However, for a loading situation where stress varies inversely with thickness, sand is the more economical option. Over typical cost ratios, montmorillonite sand never offers a more economical option.

References

1. J. Gould and E. Nissen-Petersen: 'Rainwater catchment systems for domestic supply: design, construction and implementation'; 1999, London, Intermediate Technology.
2. V. Fernandes: 'The effect of fines in sand for the fabrication and application of concrete in developing countries', Undergraduate thesis, University of Warwick, Coventry, UK, 2002.
3. H. F. W. Taylor: 'Cement chemistry'; 1997, London, Thomas Telford.
4. A. M. Neville: 'Properties of concrete', 269–273; 1995, Harlow, Longman.
5. S. Popovics: 'Strength and related properties of concrete: a quantitative approach'; 1998, New York, John Wiley.
6. P. Banfill: Proc. 25th Cement and Concrete Science Conf., London, UK, September 2005, Royal Holloway, University of London.
7. J. K. Mitchell: 'Fundamentals of soil behaviour', 2nd edn; 1993, New York, John Wiley & Sons.
8. N. H. Thanh: *J. Ferrocem.*, 1991, **21**, (4), 331–350.
9. F. D. Lydon: 'Concrete mix design'; 1982, London, Applied Science Publishers.
10. A. W. Walker: 'Special purpose concrete', Master's thesis, 2002, University of Warwick, Coventry, UK.
11. D. E. Montgomery: 'Dynamically-compacted cement stabilised soil blocks for low-cost walling', PhD thesis, School of Engineering, University of Warwick, Coventry, UK, 2002.
12. A. G. Kerali and T. H. Thomas: *Build. Res. Inf.*, 2002, **30**, (5), 362–366.

A.2 Relationships between strength and sand-cement ratio

Thanh (1991) suggests a linear relationship between water-cement ratio, w/c , and sand-cement ratio, s/c :

$$w/c = w_s(s/c) + w_c$$

With w_s and w_c representing constants. If this relationship holds, and peak strength f_p , occurs at a constant fraction of that predicted by Abram's law for a given water-cement ratio: $f_p = k \frac{A}{B(s/c)}$, then we can reach Equation A.5, suggesting that an Abrams-type relationship between strength and sand-cement ratio should hold:

$$s = k \frac{A}{B^{w/c}} \quad (\text{A.1})$$

$$s = k \frac{A}{B^{w_s(s/c) + w_c}} \quad (\text{A.2})$$

$$s = k \frac{A}{B^{w/c} B^{w_s(s/c)}} \quad (\text{A.3})$$

$$s = \frac{k_1}{k_2 B^{w_s(s/c)}} \quad (\text{A.4})$$

$$s = \frac{k_{1/2}}{B^{w_s(s/c)}} \quad (\text{A.5})$$

A.3 Curing and Strength

A.3.1 Data from Kim et al.

Kim *et al.* (2002) produced mixes with Type I cement, water-cement ratio of 0.40 and 0.50, and a range of curing temperatures (10, 23, 35 and 50°C). The aggregates used are shown in Table A.1, and the mix ratios are shown in Table A.2. Both mixes used an air-entraining agent at 0.005% of cement mass, and a superplasticiser at 0.5% of cement mass.

Table A.1: Aggregate properties for mixes produced by Kim *et al.* (2002)

Aggregate type	Aggregate description	Specific gravity	Fineness modulus
Fine sand	River sand	2.55	2.95
Coarse aggregate	crushed stone (granite), maximum size 19mm	2.58	7.23

Table A.2: Proportions for mixes produced by Kim *et al.* (2002)

Water-cement ratio	Aggregate-cement ratio	Sand-aggregate ratio ^a
0.40	3.58	0.39
0.50	4.69	0.42

^aRatio of mass of sand to combined masses of sand and coarse aggregate

Table A.3 shows the data, including compressive and tensile strength developed. Whilst relating to concretes, this is of interest as it shows that, even given a relatively wide range of curing temperatures, the 28-day strengths show, at most, a 10% variation.

Table A.3: Compressive and splitting tensile strengths of concretes cured at four temperatures, with two water-cement ratios. Data from Kim *et al.* (2002)

	Compressive strength (MPa)				Splitting tensile strength (MPa)			
	1 day	3 days	7 days	28	1 day	3 days	7 days	28
	days				days			
<i>w/c=0.40</i>								
10°C	5.4	22.1	36.0	51.3	1.2	2.6	4.0	5.1
23°C	20.9	31.6	41.5	50.8	3.0	3.4	4.2	5.0
35°C	22.8	34.6	39.2	49.4	2.9	3.9	4.2	4.5
50°C	31.7	35.8	43.6	48.7	3.5	4.1	4.5	4.9
<i>w/c=0.50</i>								
10°C	3.5	14.3	24.7	36.9	0.6	2.2	3.1	4.2
23°C	9.4	23.4	31.5	42.4	1.8	2.9	3.8	4.7
35°C	17.1	24.2	33.1	41.3	2.5	3.4	3.9	4.2
50°C	19.8	28.1	34.6	39.3	2.6	3.5	3.9	4.4

A.3.2 Data from Cebeci

The mixes used three cement types, two with considerable lime content.

Table A.4: Strength of mortars cured in lime-saturated water, data from (Cebeci *et al.*, 1989)

Curing pe- riod (days)	Strength (standard deviation) MPa					
	20°C		35°C		50°C	
	Compressive	Flexural	Compressive	Flexural	Compressive	Flexural
1	3.4 (0.1)	1.3 (0)	11.9 (0.3)	3 (0.1)	15.6 (0.3)	3.3 (0.2)
3	13.8 (0.2)	3.5 (0.3)	18.7 (1.1)	4.1 (0.2)	21 (0.7)	4.1 (0.1)
7	23.3 (0.5)	4.9 (0.1)	24.3 (0.8)	4.4 (0.1)	26.5 (0.6)	4.5 (0.2)
28	33.1 (0.9)	5.6 (0.1)	29.7 (0.2)	5.1 (0.1)	27.2 (0.8)	4.9 (0.2)
90	39.5 (0.9)	6.1 (0.1)	33.8 (0.7)	5.9 (0.6)	29.9 (1.1)	5.1 (0.1)
360	42.3 (0.9)	6.5 (0.2)	34.9 (1.1)	6.3 (0.4)	29.6 (1.6)	5.7 (0.2)

A.4 Workability

Figure A.1 shows the variation in slump distance with moisture content for the three sand types used in the experimental work described in Chapter 3. As the data from each sand type appears part of a single relationship, this suggests that one may relate slump and moisture content for a given sand type, regardless of sand-cement ratio. The Figure also indicates the difference in workability between the three sand types, with sand S giving the highest slump for a given moisture content, followed by Sand K, and finally Sand M.

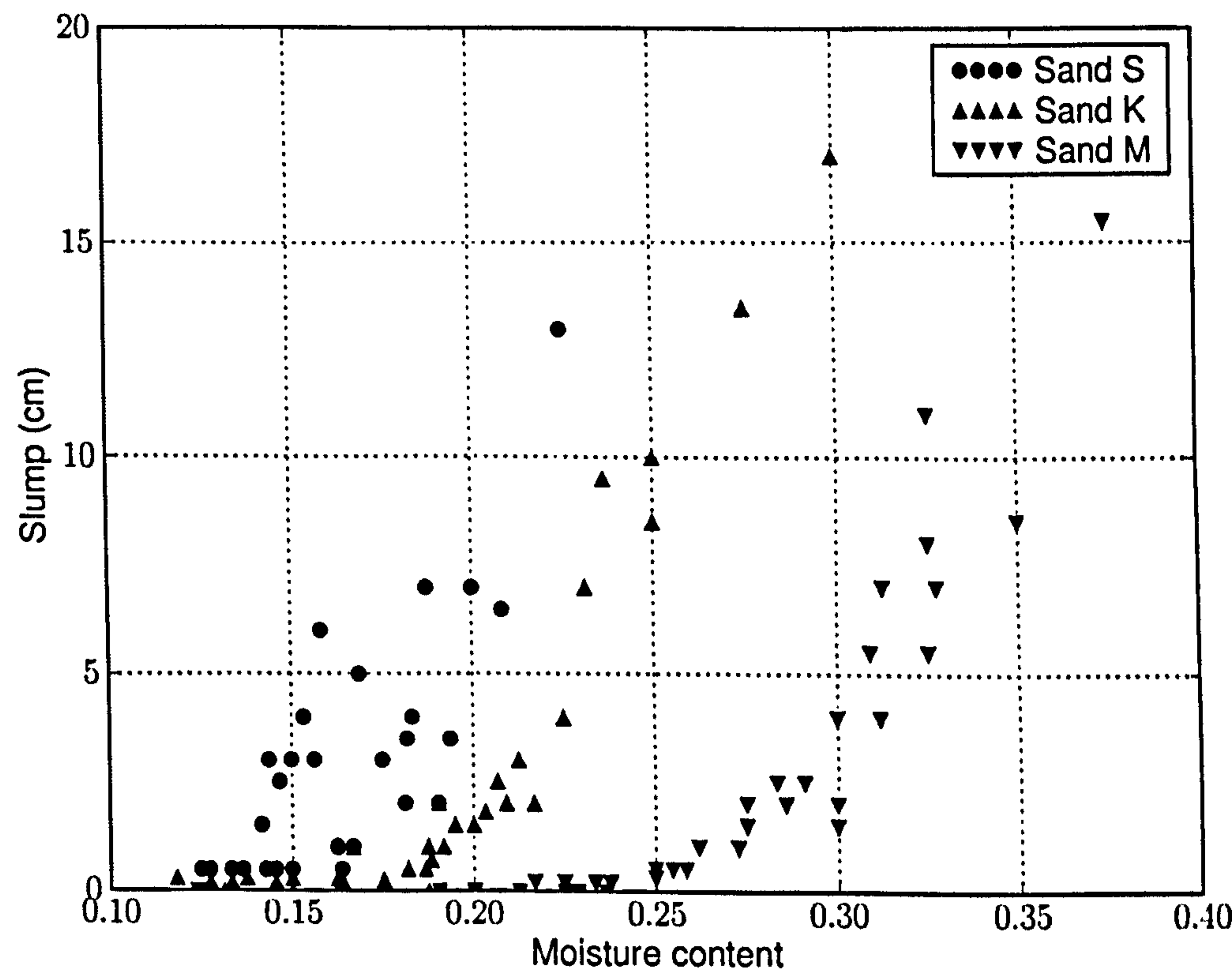


Figure A.1: Variation in slump distance with moisture content for sands S, K and M

A.5 Optimum moisture content

$$omc = \frac{wc}{1 + sc} \quad (A.6)$$

$$omc = \frac{C + D(sc)}{1 + sc} \quad (A.7)$$

$$omc = \frac{C(1 + sc)}{1 + sc} \quad (A.8)$$

$$omc = C \quad (A.9)$$

From Figure 3.12 the ratio of D/C for the three aggregate types is 1.9, 1.3 and 1.5 respectively, so C does not equal D , but the two are of similar magnitude.

In addition, as $omc = \frac{C+D(s/c)}{1+s/c}$, if $D(s/c) \gg C$ and $s/c \gg 1$, then $omc \rightarrow \frac{D(s/c)}{s/c} = D$, again, a constant.

A.6 Workability Data from Aldridge

The Table on the following page shows the strength data obtained by Aldridge (2005), including:

- Type of admixture used:
 - WL: washing-up liquid;
 - P: plasticiser;
 - SP: superplasticiser.
- Workability measures: slump distance and vebe time;
- Average sound velocity through 100mm cube;
- Average compressive strength of 100mm cube.

Admixture w/c ratio		Average slump (cm)	Average Vebe (s)	Average Density (kg/m ³)	Average Velocity (m/s)	Average Com- pressive Strength (MPa)
None	0.9	0.3	40	2160.17	3596.07	17.043
None	0.99	0.7	23	2143.33	3532.66	16.545
None	1.07	1	11	2123.83	3407.27	13.827
None	1.15	1.8	8.2	2106.5	3323.2	13.125
	(second time)					
None	1.15	1.5	7	2081	3205.24	11.063
None	1.24	3.8	4	2067	3168.77	10.878
WL	0.9	0.3	37.5	2121.33	3478.44	14.852
WL	0.99	1	14	2065.83	3274.34	12.725
WL	1.07	1.3	7.3	2027.67	3138.28	9.945
WL	1.15	2.3	3.3	1974.5	3003.84	8.498
WL	1.24	6.5	1.5	1847.33	2755.67	6.652
	(second time)					
WL	1.24	5.5	1.5	1893	2785.68	6.192
P	0.9	0.5	18	2185.17	3527.54	17.197
P	0.99	1	12.2	2131.67	3472.26	15.795
P	1.07	2.2	7.3	2116.33	3330.72	13.302
P	1.15	2.7	4.2	2100.33	3240.74	11.325
P	1.24	6.5	2.8	2071.83	3071.49	9.548
SP	0.9	0.3	27.5	2177.17	3512.01	15.402
SP	0.99	1.3	13.3	2135	3472.32	15.948
SP	1.07	1.2	7.7	2124.5	3342.74	12.052
SP	1.15	1.8	4.8	2112.5	3207.87	10.955
SP	1.24	4.7	3.3	2063	3133.99	10.29

A.7 Optimal sand-cement ratios

A.7.1 Example calculations toward determining optimum sand-cement ratio

For optimising water content, we are interested in relative costs between different mixes (combinations of sand type and sand-cement ratio). For this reason, whilst cost *ratios* are of interest, actual values (e.g. “this particular component will cost £3”) are not, and may be arbitrarily chosen, providing they are used consistently.

As an example calculation, assume that the cement-sand cost ratio is 30:1, the sand type is Sand S, and the membrane stress-thickness relationship ($\sigma_p \propto 1/t$) holds. As an initial estimate, the optimal sand-cement ratio will be taken as 4:1.

The water-cement ratio for this optimal mix may be calculated from the linear relationship between water-cement ratio and sand-cement ratio:

$$w/c = a + b \times s/c$$

Where the constants a and b are 0.173 and 0.094 respectively for Sand S, giving:

$$w/c = 0.173 + 0.094 \times 4 = 0.549$$

We may then use the Abrams-type relationship between strength and sand-cement ratio:

$$f_t = \frac{K_1}{K_2^{s/c}}$$

With K_1 and K_2 representing constants, equal to 7.65MPa and 1.34 respectively for tensile strength of sand S, giving f_t in MPa. In this case:

$$f_t = \frac{7.65}{1.34^4} = 2.37 \text{ MPa}$$

As we are using the case of membrane stress-thickness relationship, the required thickness for this design stress will be given by:

$$t = \frac{K}{f_t}$$

Where K would be a constant, depending on design reserve and component geometry. As these calculations relate to relative costs only, an arbitrary value can be assigned to K , providing it is maintained for all calculations. For this case, we will use $K = 1\text{mMPa}$, giving:

$$t = \frac{1}{2.37} = 0.42\text{m}$$

The values of density for the sand (ρ_s), cement (ρ_c), and water (ρ_w) in the mix are used, with ρ_s depending on sand type:

$$\rho_s = 2360\text{kg/m}^3, \rho_c = 3200\text{kg/m}^3, \rho_w = 1000\text{kg/m}^3$$

The mass of cement, m_c , used in the wall is then calculated, assuming the component has dimensions of $1 \times 1 \times t$:

$$m_c = \frac{t}{\frac{s/c}{\rho_s} + \frac{1}{\rho_c} + \frac{w/c}{\rho_w}}$$

Using the appropriate sand-cement ratio, water-cement ratio, and densities:

$$m_c = \frac{0.42}{\frac{4}{2360} + \frac{1}{3200} + \frac{0.55}{1000}} = 164\text{kg}$$

And the mass of sand, m_s , found from the sand-cement ratio:

$$m_s = m_c \times s/c = 164 \times 4 = 656\text{kg}$$

The unit cost (£/kg) of the cement, uc_c , is fixed for all calculations (taken as 0.2 in the code given). The unit cost of the sand, uc_s , is found by dividing the unit cost of the cement by the cement-sand cost ratio, 30 in this case, giving $0.2/30 = 0.0067\text{£/kg}$. The total cost of the component is then found by combining the masses and unit costs of both the sand and the cement:

$$\text{cost} = uc_c \times m_c + uc_s \times m_s = 0.2 \times 164 + 0.0067 \times 656 = \text{£}37.20$$

This gives a method of calculating a nominal component cost, starting with only sand-cement ratio and sand type. When implemented in code, this calculation of cost is a function that takes as its arguments the sand type and the cement-sand cost ratio. This is then used with the Nelder-Mead simplex algorithm¹ (Nelder & Mead, 1965) implemented in the Python software Scipy, to select the optimal sand-cement ratio, and determine the cost. This process is then repeated for a number of cement-sand cost ratios, and the optimal costs and sand-cement ratios stored. Repeating this process for the different sand types provides sufficient data for comparison between the sand types, at identical and different cement-sand cost ratios, and thus at different relative sand costs.

¹Nelder-Mead simplex algorithm: A commonly used optimisation algorithm for smoothly-varying functions, that generates a new combination of parameters by extrapolating from previous results using simplexes (polytopes of $n + 1$ dimensions for n parameters, e.g. a line for $n = 1$, and a triangle for $n = 2$)

A.7.2 Example of optimum sand-cement ratio for membrane loading

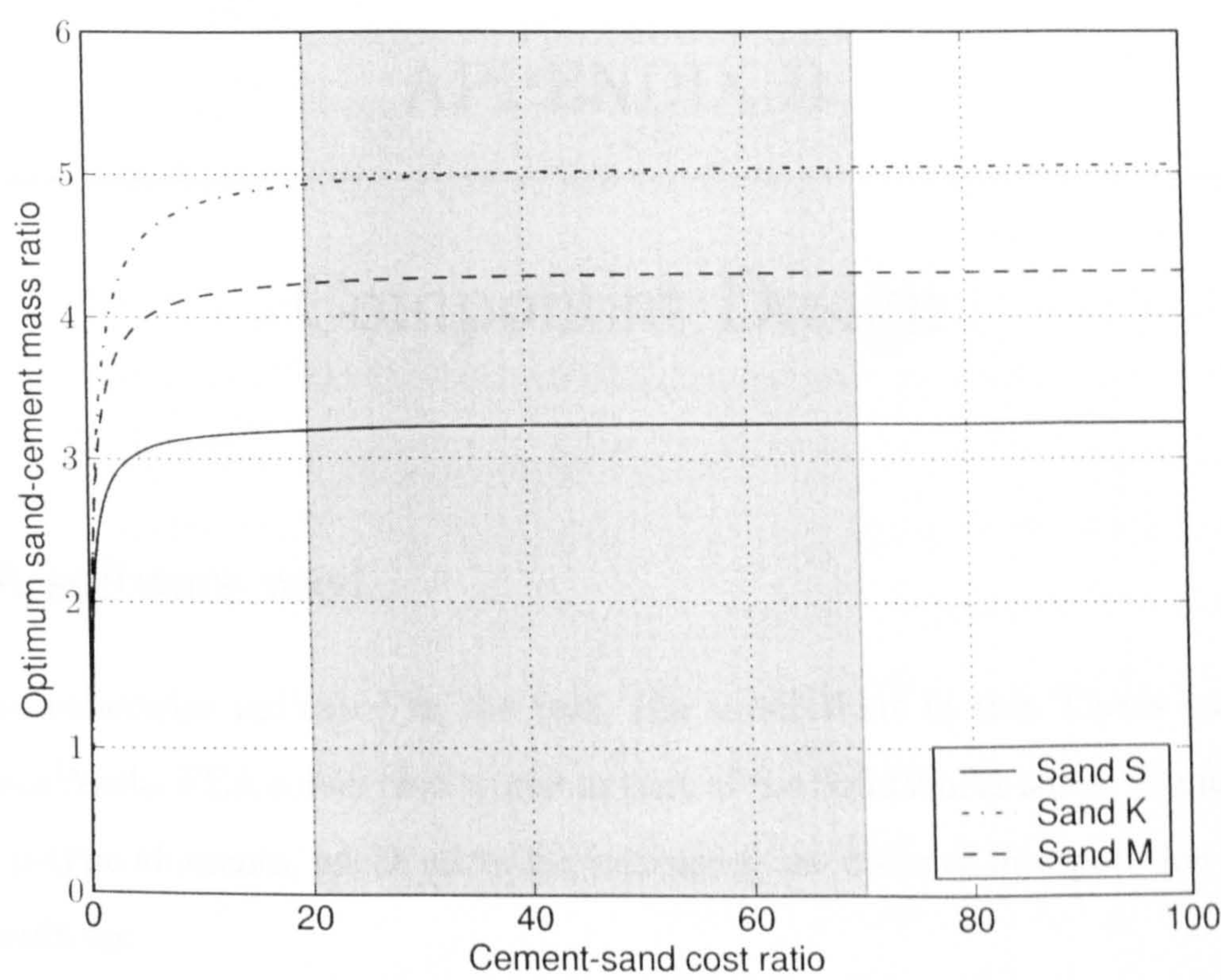


Figure A.2: Optimum sand-cement ratio with cement-sand const ratio for sands S, K and M. The shaded area indicates the typical range of cement-sand cost ratios

APPENDIX B

Component Design

B.1 FEA software used

Unless otherwise indicated in the text, the simulations in this Thesis used the CosmosWorks FEA solver that works as part of the SolidWorks suite. Simulations used p-type elements, which allow for increasing the order of interpolation within elements to:

- Increase the accuracy of the simulation.
- Test for convergence to an acceptable level of accuracy.

The software was validated against the test case of cylindrical tanks, using analytical solutions. For the majority of simulations, the mesh was refined in the region of the wall-base joint, to better capture the rapid changes in stress levels there. A maximum element size of the wall thickness was used, with 2nd to 5th order interpolation within the elements, subject to a 1% change in stress measures between runs.

In addition to this, other checks were applied after simulations e.g. confirming that the deformed structure did satisfy the boundary conditions, and that the stress patterns appeared sensible i.e. tended towards zero at the top of the tank.

To reduce run times, the axisymmetric nature of the problems was utilised, so a representative segment of the tank was analysed, with appropriate boundary conditions (faces constrained to allow for radial movement, but not rotation about the axis of symmetry).

B.2 Analytical Solution: Effect of Roof

A lid on the tank changes the boundary condition at the top from one of zero bending moment to a finite moment, without changing the deflection at the top (zero in both cases). Flügge (1967) covers the solution to this problem, treating it as a statically indeterminate structure. The top of the shell will not deform significantly radially, so the deflection (w) is zero. This leaves the clamping moment, M_x at the lid-wall joint as the redundant quantity. The relative rotation between shell and slab can be expressed in terms of that arising from external loads: the self-weight of the lid, and the pressure loading of the water), and that from the redundant moment. These can then be equated and solved to find the redundant moment, and from this the deflection, moments and stresses within the tank.

B.3 FEA Validation

Table B.1: Data for validation of FEA software, comparing maximum stress of uniform wall thickness cylinder with built-in base and free top edge obtained with CosmosWorks with that obtained from shell theory

Radius (m)	Height (m)	Wall thickness (cm)	Maximum σ_x (MPa)		% error
			Shell theory	FEA model	
1	1	1	1.60	1.59	0.6
1	2	1	3.33	3.36	0.9
2	1	1	3.08	3.20	3.9
2	2	1	6.54	6.55	0.2

B.4 Tank configurations for 2D tank optimisation

Figure B.1 shows the location of the four defining radii on the tank. Table B.2 shows the configurations used for simulation.

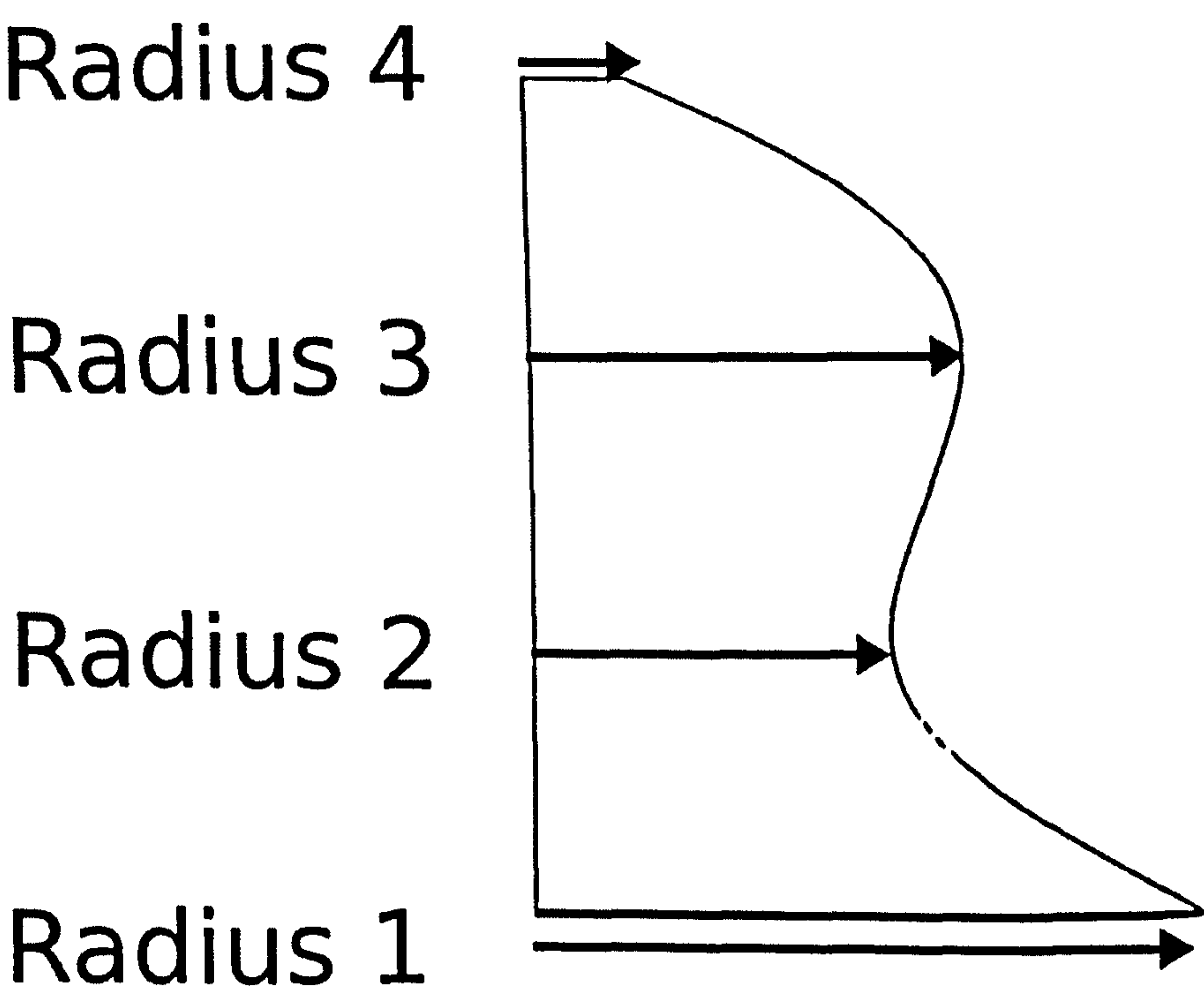


Figure B.1: Example profile of 2D curvature tank, with locations of 4 defining radii

Table B.2: Tank configurations for constant thickness shape optimisation

Set number	Radii (mm)			
	Base (1)	2	3	4
Set 1	1550	860	1060	250
Set 2	1050	860	1260	250
Set 3	640	860	1360	250
Set 4	1510	960	960	250
Set 5	1450	1060	860	250
Set 6	1060	1060	1060	250
Set 7	280	1060	1260	250
Set 8	320	1160	1160	250
Set 9	900	1260	860	250
Set 10	270	1260	1060	250
Set 11	510	1360	860	250

B.5 Wooden mould construction

The first stage of constructing the prototype tank involved creating the wooden framework. A set of wooden templates, in 12mm ply, were cut to shape, each consisting of two quarter-circle pieces, and fixed together, as shown in Figure B.2.

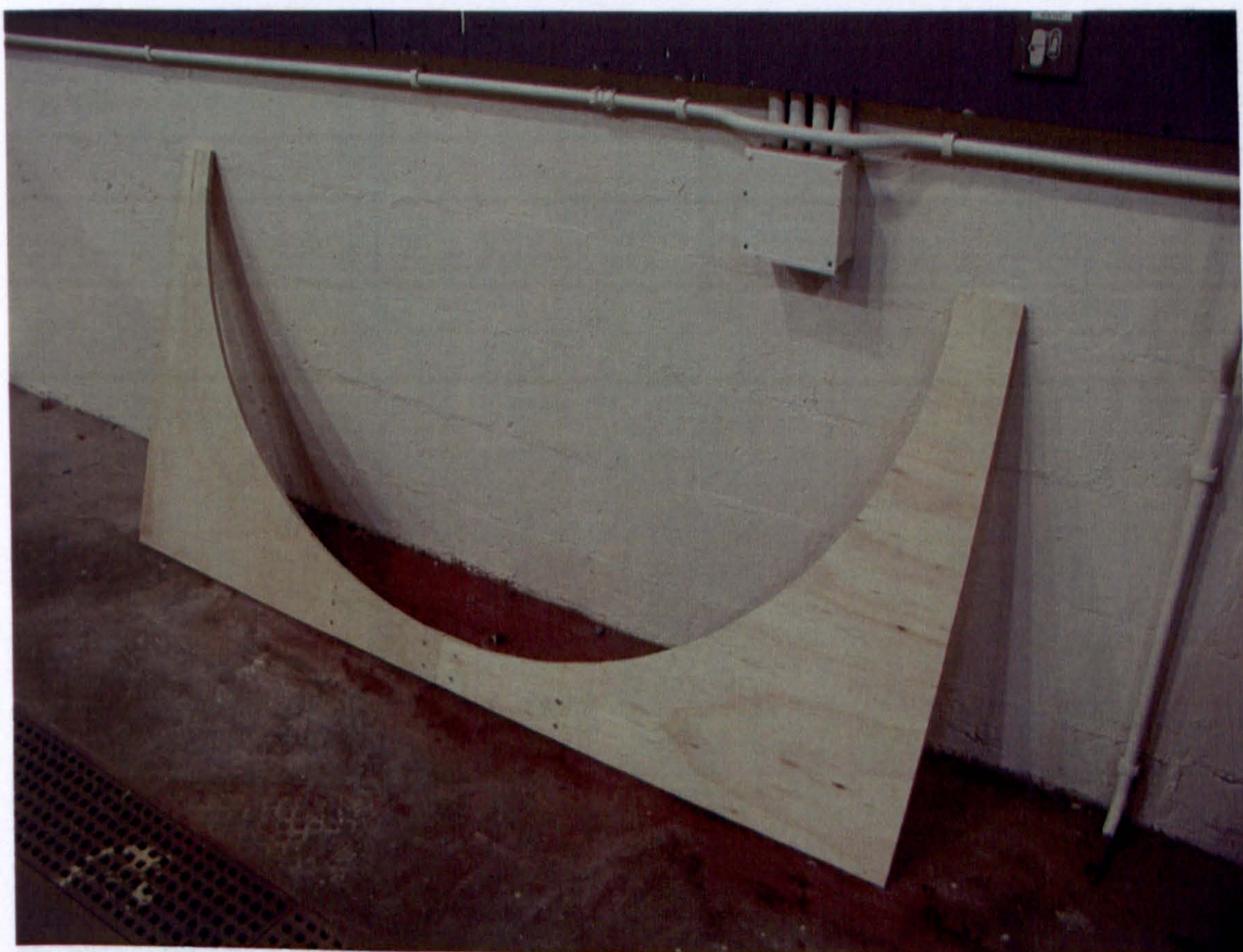


Figure B.2: Wooden template forming semicircular profile of tank

Once these profiles were assembled, they were mounted on separating 2" \times 2" wooden struts, to make individual frames, as in Figure B.3.

Individual frames were made in pairs, to match each other, bolt-holes drilled through them, and joined together, then the next layer made and mounted on top. These gave a final set of frames, as shown in Figure B.4

Having created the entire frame, sections of 5.5mm plywood were cut to ap-



Figure B.3: Single frame of wooden mould (1/2 bottom section of mould)

appropriate shapes, and nailed to the frame. Some of the strips of ply had to have non-rectangular shapes, as the change in radius with height of the tank would otherwise lead to unacceptable spaces between the tanks. This gave a fitted mould section, as shown in Figure B.3.



Figure B.4: Complete frame (assembled)

Note that, for the middle section, the ply would not have been dry, so it required soaking in water for at least 1/2 an hour, before forming to the required curvature.

Once the frames had ply strips attached, several coats of varnish were applied. Repeating this process for all of the sections gave the entire mould, as shown in Figure B.5.

At this point the mould was ready for casting with sand.

appropriate shapes, and nailed to the frame. Some of the strips of ply had to have non-rectangular shapes, as the change in radius with height of the tank would otherwise lead to unacceptable spaces between the tanks. This gave a filled mould section, as shown in Figure B.5.



Figure B.5: Frame section, with ply strips attached

Note that, for the middle section, the ply would not bend to the frame when dry, so it required soaking in water for at least 1/2 an hour, before forming to the required curvature.

Once the frames had ply strips attached, several coats of varnish were applied. Repeating this process for all of the sections gave the entire mould, as shown in Figure B.6.

At this point the mould was ready for coating with mud.



Figure B.6: Assembled frame, with two coats of varnish applied

B.6 Configuration of instrumentation for strain gauge testing

Figure B.7 shows the layout of the instrumentation. The three meridians A, B and C all lie in vertical planes, and are axisymmetrically distributed around the tank, at 120° intervals. The even channel numbers were not used.

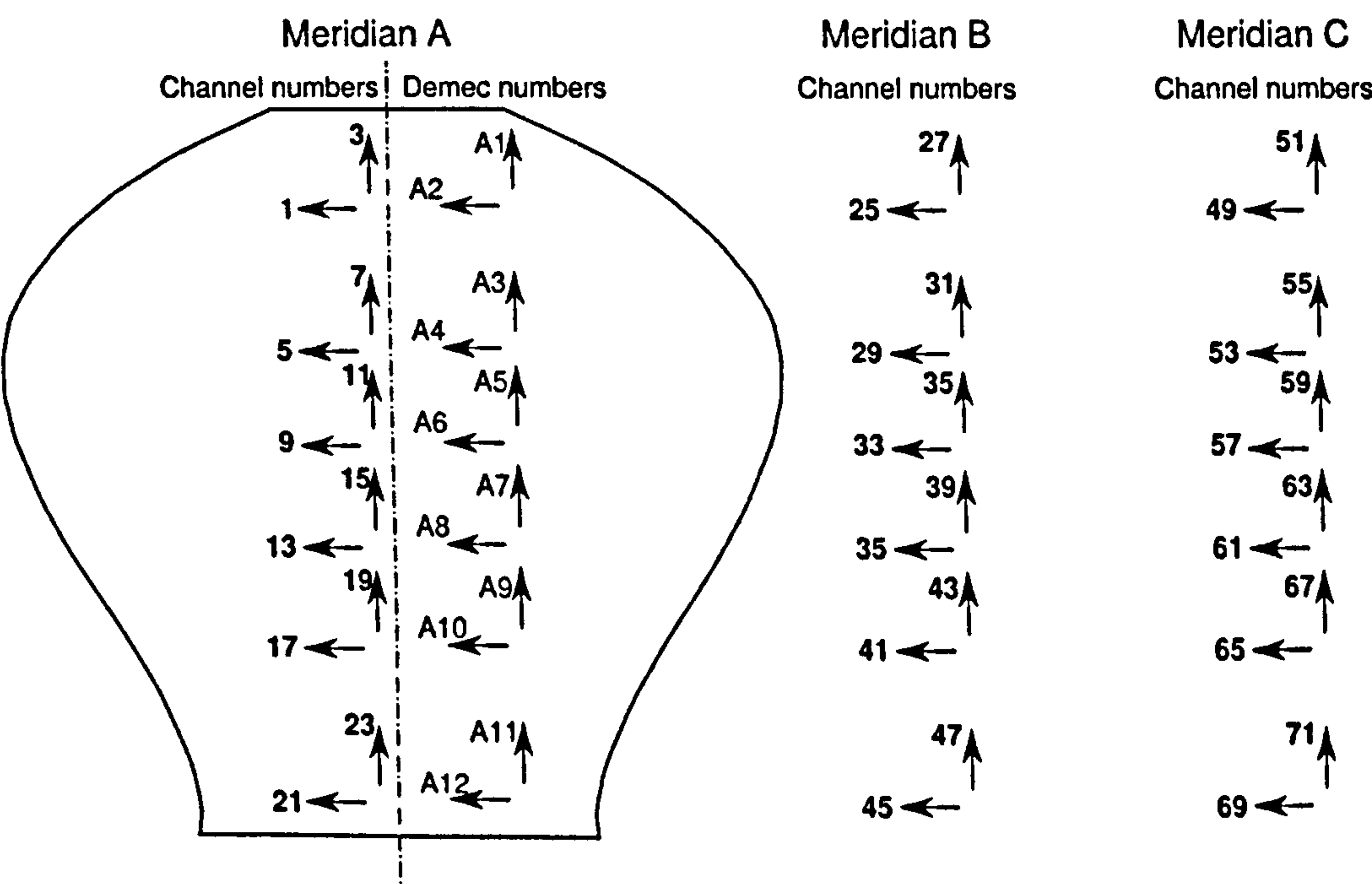


Figure B.7: Configuration of instrumentation on tank

APPENDIX C

Automating Component Design: Genetic Algorithm Optimisation of Tank Designs

C.1 Overview

Optimisation of tank designs is well suited to numerical methods. Genetic Algorithms present an optimisation approach suited to tank designs. This chapter details the development of a Genetic Algorithm, used in combination with a Finite Element Analysis package, to optimise tank designs. The sections within it:

- Describe the problem being considered, explaining why it favours a numerical approach, and why Genetic Algorithms seem a reasonable choice.
- Give an outline description of GAs.
- Covers the implementation of a GA in Python.
- Outlines validation of the GA, using typical test cases.
- Details validation of the FEA package used (CalculiX).

- Covers the configuration of the GA for use with this particular problem.
- Reports results obtained from simulation runs.

C.2 Introduction

C.2.1 Genetic Algorithms

Basic principles

Genetic algorithms mimic the natural process of evolution. Many conventional search methods evaluate an individual combination of parameters, and use derivatives etc. to determine the next combination of parameters to be tested. GAs consider a number of possible solutions, considered a population of solutions, evaluate these, and use a number of mechanisms to create the next generation of solutions. In their simplest form, they employ three mechanisms:

Selection The members of the population are assessed, and a number of parents created for the next generation. Those that perform best are reproduced a number of times, whilst poorer-performing individuals are reproduced less frequently, or are not reproduced.

Crossover Pairs of individuals have their information exchanged in various ways, to produce new chromosomes.

Mutation The chromosome of any individual undergoes random permutations.

C.2.2 Problem description and suitability of GAs

The optimisation of a component with a complex geometry, such as a rainwater storage tank, lends itself to numerical techniques. Brute force approaches will take too much computational effort to run, while manual optimisation becomes tedious for the user, will not necessarily find an optimal design, and may have to be repeated for designing tanks of different storage volumes.

A list of parameters can describe a tank design. For example, a 5-item list can fully describe the geometry of a uniform thickness tank: height, radius, base thickness, wall thickness and lid thickness. Limits will apply to each of these, for various reasons, including:

Geometry The radius of the tank cannot fall to or below zero at any height above the ground, as this would produce a sealed container.

Manufacture For application by hand, the wall thickness cannot fall below 1cm.

Application The tank height cannot exceed 2m, as water must run downhill from the roof of a single-storey building into the tank.

Together with these, sensible bounds apply to all parameters. A wall thickness greater than that used in competitive designs will not lead to designs of interest.

We can then consider the optimisation of tanks as a multiple-parameter, bounded optimisation. Genetic Algorithms provide a method of optimising such functions.

C.3 Implementation

C.3.1 Interfacing with Finite Element Analysis program

The FEA package used in Chapters 5 and 6, CosmosWorks, is well suited to manual operations, but a program that stored input and output files in clear text was chosen for easy interface generation.¹ The program selected was CalculiX, an open source FEA program that has a scriptable GUI and uses a similar input file format to Abaqus.

The code generated performs the following actions:

¹An alternative would be to use the SolidWorks programming API and write code in C++ or Visual Basic.

- Takes a set of configuration options, with sensible defaults, including radii and heights that determine the profile of the tank.
- Changes the base radius to give the desired storage volume, provided the resultant base radius falls within preset limits.
- Writes an output file that generates the geometry of the tank, and applies a hydrostatic loading to its surface.
- Runs the pre- and post- processor program, cgx, to produce a series of output files detailing the mesh and loadings.
- Compiles the output files to give an input file for the FEA solver, ccx.
- Runs the ccx solver.
- Reads the output file from ccx, and:
 - Extracts the stress components at each node.
 - Converts these to give maximum principal stresses.
 - Stores the maximum tensile and compressive stress for the entire structure.
- Stores data about the design, including the maximum stresses, and volume of mortar required to produce the design.

Section D.9 of Appendix D contains the code that performs these operations.

C.3.2 PySGA: Python Simple Genetic Algorithm

The genetic algorithm PySGA uses the object-oriented programming language Python. Section D.9 of Appendix D contains the source code, and provides copies of the ccx and cgx executables (version 1.5) for compatibility. The program defines four classes:

SGAOptions The configuration for the GA, allowing the user to specify parameters such as crossover probability.

Individual An individual, representing a single trial solution to the problem in question.

GA The Genetic Algorithm class, that controls the operation.

Population An individual, representing a single trial solution to the problem in question.

APPENDIX D

Electronic Data

The CD attached contains the following sections:

D.1 Material Selection: Mortar results

Full data of the experimental results obtained during laboratory work, reported in Chapter 3.

D.2 Material Selection: Sand-cement ratio and component thickness

Source code for the optimisation of component thickness and sand-cement ratio. The code for this program is written to run on machines using Python 2.4 (van Rossum *et al.*, 2005). It uses the standard modules, and two additional sets: SciPy (Jones, Oliphant, Peterson *et al.*, 2001–), a set of scientific modules, and Matplotlib (Hunter, 2005), a set of plotting tools that emulate the plotting interface of Matlab. If the user only wants to run the program, and look at the results in numeric form, they need not have Matplotlib.

D.3 Component Design: Cylindrical tank optimisation

D.4 Component Design: Membrane tank optimisation

D.5 Component Design: Tank prototyping—FEA models

Cosmosworks models used to generate the FEA results for the tank prototyping.

D.6 Component Design: Tank protoyping—Video recording

An electronic version of the video recording captured as the tank failed.

D.7 Component Design: Tank prototyping—Demec readings

D.8 Component Design: Tank prototyping—Strain gauge readings

D.9 Component Design: Automating Tank Optimisation—Genetic Algorithms and FEA

Includes PySGA, a Simple Genetic Algorithm written in Python, and python code to interface with CalculiX, an FEA package.

Index

- Aldridge (2005), 61, 170
BSI (1983), 38, 170
BSI (1992), 35, 170
BSI (2000a), 37, 170
BSI (2000b), 37, 170
BSI (2000c), 38, 171
BSI (2000d), 38, 171
BSI (2002), 37, 171
Banfill *et al.* (1999), 22, 170
Banfill (2003), 21, 170
Banfill (2005), 22, 23, 170
Bentz (1999), 31, 170
Brew (2005), 165, 170
Cebeci *et al.* (1989), 30, 47, 171, 180
Chandler & Macphee (2003), 21, 171
Chang & Chan (1995), 30, 171
Chilton (2000), 165, 171
DTU (2005), 77, 171
DTU (2006), 113, 152, 157, 172
Deb (2000), 167, 171
Dewar (1999), 25, 171
De Schutter & Poppe (2004), 24-26, 171
Erguden (2001), 6, 147, 172
Fernandes *et al.* (2005), 13, 172
Fernandes (2002), 17, 35, 172
Flügge (1967), 83, 88, 164, 172, 188
Gibb (1999), 8, 141, 143, 145, 147, 172
Goldberg (1989), 167, 172
Gould & Nissen-Petersen (1999), 10, 76, 78, 172
Hotta & Takiguchi (1995), 30, 172
Hu & de Larrard (1996), 22, 172
Hunter (2005), 173, 201
Jaeger (1964), 83, 173
Jones *et al.* (2001-), 173, 201
Kerali & Thomas (2002), 30, 173
Khan (1983), 77, 173
Kim *et al.* (2002), 30, 173, 179
Kokobu *et al.* (1996), 22, 173
Kumar *et al.* (1984), 77, 78, 173
Kumar *et al.* (1995), 30, 173
Lydon (1982), 27, 173
Meek (1982), 78, 173
Meier & Rauch (2000), 7, 174
Moita *et al.* (2003), 78, 174
Montgomery (2002), 35, 174

- Mwamila & Karumuna (1999), 147, 174
 Naaman (2000), 78, 174
 Nadif *et al.* (2002), 30, 174
 Neville (1995), 18, 29, 135, 174
 Ngowi (1997), 142, 174
 Paramasivam & Nathan (1984), xvi, 77, 78, 83, 174
 Paramasivam *et al.* (1990), 78, 174
 Popovics (1998), 20, 174
 Rao (2001), 20, 32, 175
 Ruthven (2005), 59, 175
 Saak *et al.* (2004), 22, 175
 Sharma (1983), 23, 24, 175
 Sharma (2005), 78, 175
 Stallen *et al.* (1994), 147, 175
 Still & Thomas (2004), 13, 175
 Still & Thomas (2005), 13, 175
 Still & Thomas (2006), 13, 175
 Still *et al.* (2005), 13, 175
 Tarran (1984), 78, 176
 Tasdemir *et al.* (1996), 135, 176
 Tattersall & Banfill (1983), 21, 22, 176
 Tattersall (1992), 22, 176
 Thanh (1991), 18–20, 24, 25, 27–29, 32, 176, 178
 Thevendran & Thambiratnam (1987), 98, 176
 Timoshenko & Woinowsky-Kreiger (1959), 83, 176
 Todaro (2000), 7, 176
 Walker (2002), 18, 176
 Walkus & Malek (1986), 23, 24, 176
 Watt (1978), 78, 176
 Zingoni (1997), 84, 90, 177
 van Rossum *et al.* (2005), 176, 201
 de Hanai *et al.* (1984), 78, 171
- Abrams' Law
 Limits & poor compaction, 21
 Typical values, 20
 Values, 44
- Abrams' law, 20, 43
- Bingham fluid, 22
- Compaction, 23
- Curing, 29
- Cylindrical tanks, 86
- FEA, 84
- Housing
 demand, 6
- Moisture content, 27
- Mortar
 Aggregate choice, 17
 s/c ratio, 18
 Tests, 36
 PSD, 36
 Sieve analysis, 36
 Slump, 37
 Splitting tensile strength, 38

Tensile flexural, 38
 Vebe, 37
 Young's modulus, 38
 Optimum water content, 48
 Optimum water-cement ratio, 21
 Plate theory, 83
 Prefabrication, 141
 history, 141
 pros & cons, 142
 Production
 capital-labour cost ratio, 8
 Cementitious building components,
 8
 development, 7
 in developing countries, 6
 technologies, 7
 PSD, 36, 58
 Rainwater Harvesting, 76
 system components, 76
 Relative Cement Index, 86
 Research & Development, 7
 Sand
 grading, 35
 Water demand, 25
 Sand-cement ratio
 Optimum, 62
 Shell theory, 83
 Sieve analysis, 36, 61

Strength
 Abrams' Law, 20
 Abrams' law, 40
 curing conditions, 29
 Effect of cement type, 58
 effect of curing, 47
 effect of sand type, 46
 effect of sand-cement ratio, 46
 Peak, 46
 s/c ratio, 27
 Splitting tensile, 38
 Tensile flexural, 38
 tensile-compressive, 18
 tensile-compressive relationship, 39
 tensile-flexural relationship, 40
 Water-cement ratio, 40
 Tanks
 0D curvature, 77
 1D Curvature, 104
 1D curvature, 78, 86
 Summary of modifications & im-
 provements, 100
 2D curvature, 79
 Choice of sand type, 92
 classification, 77
 Datum design, 86
 Definition, 93
 Effect of lid, 89
 materials usage, 79

OD curvature, 101

Peak stress and wall thickness, 90

Performance measure, 85

Production, 113

Simulation tools, 82

Specification, 81

Water demand

 calculating, 24

Workability, 21

 Admixtures, 61

 admixtures, 30

 Bingham fluid, 22

 Fineness modulus, 27

 Slump test, 37

 Specific surface, 25

 Vebe test, 37

 Vebe time, 44

 Vibration, 22

 Water demand, 25

Young's modulus, 48